THE DEVELOPMENT OF A PROCESS AND QUALITY CONTROL METHODS FOR A CONJUGATE VACCINE AGAINST *STREPTOCOCCUS PNEUMONIAE* SEROTYPE 1

By

Cesarina Edmonds – Smith

Thesis Presented for the Degree of

DOCTOR OF PHILOSOPHY

In the Department of Chemistry

UNIVERSITY OF CAPE TOWN

June 2013

Supervisors: Associate Professor Neil Ravenscroft
Doctor Seanette Wilson

Declaration

I declare that “The development of a process and quality control methods for a conjugate vaccine against *Streptococcus pneumoniae* serotype 1” is my own work and that all sources that I have used or quoted have been indicated and acknowledged by means of complete references.

_____

Cesarina Edmonds-Smith

Abstract

Pneumonia is the leading cause of death in children worldwide and is estimated to kill 1.6 million children every year. Pneumonia affects children and families everywhere, but is most prevalent in sub–Saharan Africa and South–east Asia. Serotype 1 is responsible for up to 20 % of invasive pneumococcal diseases (IPD) in developing countries and has been the cause of several outbreaks in the African meningitis belt. Conjugate vaccines are effective in young children, induce immunological memory and reduce carriage. A conjugate vaccine against 7 serotypes (PCV7) was licensed in 2000 which resulted in a dramatic reduction of IPD. An increase in the number of cases due to non–vaccine serotypes (serotype replacement) led to the recent development and licensure of 10– and 13– valent conjugate vaccines that provide broader coverage.

This thesis describes the development of purification and conjugation processes and associated analytical methods for the preparation of a *Streptococcus pneumoniae* serotype 1 polysaccharide (Pn1) conjugate vaccine.

The Pn1 polysaccharide was purified following a two–step process utilising a differential filtration with ethanol. Analytical tests including size analysis, uronic acid composition, *O*–acetylation and purity (nucleic acids and protein) were optimized and performed on Pn 1 lots. The purified polysaccharide was found to meet World Health Organisation (WHO) specifications.

The purified polysaccharide is viscous with a rigid structure that hampers full conjugation reactions and detailed characterisation. Size–reduction was performed and shown to have no impact on the structural integrity of the generated saccharide. The *O*–acetylated size–reduced polysaccharide was amenable to full nuclear magnetic resonance (NMR) characterisation to confirm the structural identity of Pn1 and determine the percentage of cell wall polysaccharide (CWPS) and the degree and position of *O*–acetylation present.

Composition analysis was performed using published hydrolysis methods, however, they resulted in low recoveries and therefore alternative microwave assisted conditions were investigated followed by chromatographic separation and analysis.

The size–reduced polysaccharide was conjugated to hydrazide–derivatized protein carriers via the polysaccharide carboxyl groups. The conjugates prepared using different activators were evaluated in mice and the immunogenicity data showed that they were non–inferior to two commercially available conjugate vaccines.

Acknowledgments

All the work behind this thesis could not have been possible without the help and support of many people. I would like to thank the following people for their contribution to the preparation of this thesis:

Foremost, my principal supervisor Associate Professor Neil Ravenscroft for his patience, guidance, motivation, enthusiasm and expertise in all things vaccine related and for his many hours in front of the NMR machine.

To my second supervisor Doctor Seanette Wilson whose insights, valued comment and suggestions have been of great benefit for the improvement of my work and in writing my thesis.

Doctor Ebrahim Mohammed for all your help and guidance in and out of the laboratory and everyone else involved in the pneumococcal project at The Biovac Institute especially Dr. Nelius Swart, Dr. Ike James, Shantal Dorasamy, Francisca Theunissen, Margaret Lennon, Rochelle Hendricks, Charlie Nemugumoni, Lizelle Gordon, Daria Kow, Dr. Melinda Scanlen, Charmaine Steggink and Patrick Tippoo.

Past and present members of the Bioanalytical and Vaccine Research group including Tanith Curtin, Dr. Meredith Hearshaw and Taigh Anderson.

A special thank you to Ms. Astrid Trimmel for her great assistance and friendship and wonderful talks and encouragement.

The Biovac Institute and Program for Appropriate Technology for Health (PATH) for the opportunity to work on such an interesting and engaging project and for their financial assistance.

The National Research Foundation (NRF) for their financial assistance.

And finally, to my family and friends, for their love, support and constant patience during the course of this PhD.

Contents

Declaration i

Abstract ii

Acknowledgments iii

Contents iv

Abbreviations ix

Chapter 1. Introduction 1

1.1 Early history of *Streptococcus pneumoniae* 2
1.2 Surface components of *Streptococcus pneumoniae* 3
1.3 Pneumococcal disease 4
1.3.1 Non-invasive pneumococcal disease 5
1.3.2 Invasive pneumococcal disease 5
1.4 Serogroup distribution of *Streptococcus pneumoniae* in Africa 6
1.5 Immune response to polysaccharide and conjugate vaccines 9
1.6 Pneumococcal vaccines 13
1.6.1 Whole cell vaccines 13
1.6.2 Pneumococcal polysaccharide vaccines 14
1.6.3 Conjugate vaccines 16
1.6.3.1 Prevnar7 17
1.6.3.2 Vaccine trials incorporating more serotypes 20
1.6.3.3 Synflorix 22
1.6.3.4 Prevnar13 25
1.6.4 Pneumococcal vaccines in development 28
1.6.5 Pneumococcal serotype 1 29
1.7 Aim and objectives 30

Chapter 2. General Methods 31

2.1 Fermentation of Pn1 31
2.2 Purification of Pn1 32
2.3 Colorimetric assays 33
2.3.1 Uronic acid assay 34
2.3.2 *O*-Acetyl Assay 35
2.3.3 UV protein assay 36

2.3.4 Bradford (Coomassie) protein assay 37
2.3.5 Trinitrobenzenesulfonic acid assay 37
2.4 Immunological Assays 39
2.4.1 ELISA 39
2.4.2 Nephelometry 40
2.5 Electrophoresis 41
2.5.1 SDS Page 42
2.5.2 Western blot 43
2.6 Chromatographic methods 44
2.6.1 Liquid Chromatography 45
2.6.1.1 Size exclusion chromatography 46
2.6.1.2 Anion exchange chromatography 48
2.6.2 Gas chromatography 51
2.7 Nuclear magnetic resonance spectroscopy 53
2.8 Conjugation of Pn1 to protein carrier 54
2.8.1 Protein derivatization 55
2.8.2 Polysaccharide size reduction 55
2.8.2.1 Sonication 55
2.8.2.2 Microfluidization 55
2.8.3 HOBt mediated EDC conjugation 56
2.8.4 Triazine mediated conjugation 56
2.8.5 Conjugate purification 57
2.8.5.1 Gel filtration liquid chromatography 57
2.8.5.2 Hydrophobic interaction chromatography 57
2.8.5.3 Ammonium sulfate precipitation 58
2.8.5.4 Deoxycholate precipitation 59
2.8.6 Formulation 59

Chapter 3. Structural Characterisation of Pn1 PS 61

3.1 Introduction 61
3.2 The structure of Pn1 polysaccharide 61
3.3 Colorimetric assays 64
3.3.1 Uronic acid assay 65
3.3.1.1 Assay optimisation 66
3.3.1.2 Correction factor 67
3.3.1.3 Assay validation 68
3.3.2 *O*-Acetyl assay 70

3.3.2.1 Assay optimisation 70
3.3.2.2 Assay validation 71
3.3.3 Summary of colorimetric methods 73
3.4 Polysaccharide hydrolysis 74
3.4.1 Microwaves 80
3.4.2 Chromatographic methods 82
3.4.2.1 HPAEC-PAD 82
3.4.2.2 GC-FID 83
3.4.3 TFA hydrolysis of Pn1 84
3.4.4 Methanolysis of Pn1 PS 87
3.4.5 Combination of methanolysis and TFA hydrolysis 91
3.4.5.1 HPAEC-PAD 91
3.4.5.2 GC-FID 93
3.4.6 Summary 94
3.5 Nuclear magnetic resonance spectroscopy 95
3.5.1 Cell wall polysaccharide contaminant 98
3.5.2 Extent of *O*-acetylation 100
3.5.3 NMR structural analysis of Pn1 polysaccharide 101
3.5.3.1 De-O-acetylated Pn1 polysaccharide 102
3.5.3.2 O-acetylated Pn1 polysaccharide 105
3.5.4 Summary 110

Chapter 4. Purification of Pn1 Polysaccharide 112

4.1 Purification methodology 112
4.1.1 Purification optimisation 116
4.1.1.1 Establishment of process parameters 116
4.1.1.2 Inactivation strategies 119
4.1.2 Large scale fermentation batches 126
4.1.3 Summary 129
4.2 Polysaccharide size reduction 132
4.2.1 Mechanical size reduction 134
4.2.2 Sonication 136
4.2.3 Microfluidization 142
4.2.3.1 Pn6B 142
4.2.3.2 Pn14 145
4.2.3.3 Pn1 148
4.2.4 Consistency 149

4.2.5 Summary 150

Chapter 5. Protein Derivatization For Conjugation 152

5.1 Background to derivatization strategies 152
5.2 Protein carriers in conjugate vaccines 157
5.2.1 Hib vaccines 157
5.2.1.1 Native protein carriers 157
5.2.1.2 Derivatized protein carriers 157
5.2.2 Meningococcal vaccines 159
5.2.2.1 Native protein carriers 159
5.2.2.2 Derivatized protein carriers 160
5.2.3 Pneumococcal vaccines 160
5.2.3.1 Native protein carriers 160
5.2.3.2 Derivatized protein carriers 161
5.2.4 Immune response interference among carrier proteins 161
5.3 Bovine Serum Albumin 162
5.3.1 Derivatization of BSA 164
5.4 Tetanus Toxoid 165
5.4.1 Derivatization of TT 167
5.5 CRM_{197} 168
5.5.1 Derivatization of CRM_{197} 169
5.6 Pneumolysoid 171
5.6.1 Derivatization of PLD 172
5.7 Electrophoretic comparison of protein carriers 173
5.8 Summary 174

Chapter 6. Conjugation 176

6.1 Introduction 176
6.2 EDC Chemistry 182
6.2.1 EDC conjugations to BSA 187
6.2.2 EDC conjugations to TT 191
6.3 Activator chemistry 193
6.3.1 HOBt activator chemistry 194
6.3.1.1 HOBt mediated conjugations to TT 197
6.3.1.2 Summary of HOBt conjugations with TT 207
6.3.1.3 HOBt mediated conjugations to CRM_{197} 208
6.3.1.4 Summary of HOBt conjugations to CRM_{197} 212

6.3.2 Triazine activator conjugations 213
6.4 Formulation with adjuvant 218
6.4.1 Formulation study 220
6.5 Animal studies 222
6.5.1 Animal study design 222
6.5.2 Immunoassays 223
6.5.2.1 ELISA 224
6.5.2.2 OPA 224
6.5.3 Body weight profiles 225
6.5.4 Round I results 225
6.5.5 Round II 226
6.5.5.1 Western blot analysis of conjugates 226
6.5.5.2 Animal results 227
6.5.6 Summary of animal results 229

Chapter 7. Conclusions 231

Conferences and Presentations 234

Appendix 1: Purification Results 235

References 236

Abbreviations

AAT	2–acetamido–4–amino–2,4,6–trideoxygalactose
ADH	Adipic acid dihydrazide
BSA	Bovine serum albumin
BSL	Biological safety level
°C	Celsius
CDAP	1–cyano–4–dimethylaminopyridinium tetrafluoroborate
CDC	Centre for Disease Control
CDIBP	Chengdu Institute of Biological Products
CDMT	2–chloro–4,6–dimethoxy–1,3,5–triazine
CNBr	Cyanogen bromide
COSY	Correlation spectroscopy
CTAB	Cetyltrimethylammonium bromide
CTEA	Cyanotriethylammonium
CTLs	Cytotoxic T lymphocytes
CRM_{197}	Cross–reactive material 197
CWPS	Cell wall polysaccharide
D_2O	Deuterium oxide
DAD	Diode array detector
DEPT	Distortion enhancement by polarization transfer
DOC	Deoxycholate
DMSO	Dimethylsulfoxide
DMTMM	4–(4,6–dimethoxy–1,3,5–triazin–2–yl)–4–methylmorpholinium chloride
DT	Diphtheria toxin
ECD	Electron capture detector
EDC	1–[3–(dimethylamino)propyl]–3–ethyl carbodiimide hydrochloride
ELISA	Enzyme linked immunosorbent assays
EtOH	Ethanol
$FeCl_3$	Ferric chloride
FID	Flame ionisation detector
Gal	Galactose
GalA	Galacturonic acid
GC	Gas chromatography
GlcA	Glucuronic acid
GlcN	Glucosamine
GlcNAc	*N*–acetyl glucosamine
Glc	Glucose
GMC	Geometric mean concentration

GMP	Good manufacturing practice
GSK	GlaxoSmithKline
HA	Hyaluronic acid
HCl	Hydrochloric acid
HF	Hydrofluoric acid
Hib	*Haemophilus influenzae* type b
HIC	Hydrophobic interaction chromatography
HIV	Human immunodeficiency virus
HMBC	Heteronuclear multiple bond correlations
HMF	Hydroxymethylfurfural
HOBt	1–Hydroxybenzotriazole
HPAEC–PAD	High performance anion exchange chromatography with pulsed amperometric detection
HPLC	High performance liquid chromatography
hr.	Hour
HRP	Horse radish peroxidase
HSA	Human serum albumin
HSQC	Heteronuclear single–quantum correlation
Hz	Hertz
Ig	Immunoglobulin
IPD	Invasive pneumococcal diseases
KH_2PO_4	Potassium dihydrogen phosphate
LOD	Limit of detection
LOQ	Limit of quantitation
m/z	Mass to charge ratio
M	Molar
MBC	Memory B cells
Men	Meningococcal group
MeOH	Methanol
MES	2–(*N*–morpholino)ethanesulfonic acid
MHC	Major histocompatibility complex
µg	Microgram(s)
µl	Microlitre(s)
mg	Milligram
ml	Millilitre(s)
min	Minute
mM	millimolar
MS	Mass spectrometry
Mw	Molecular weight

MWCO	Molecular weight cut off
NaCl	Sodium chloride
Na_2CO_3	Sodium carbonate
NaOH	Sodium hydroxide
NHLS	National Health Laboratory Services
NHS	*N*–hydroxysuccinimide
NICD	National Institute of Communicable Diseases
NMM	*N*–methylmorpholine
NMR	Nuclear magnetic resonance
OM	Otitis media
OMPC	Outer membrane complex C
OPA	Opsonophagocytic activity
PATH	Program for Appropriate Technology for Health
PBS	Phosphate buffered saline
PCV	Pneumococcal conjugate vaccine
PEG	Polyethylene glycol
PHID–CV	Synflorix
pI	Isoelectric point
PLD	Pneumolysoid
PLY	Pneumolysin
Pn	Pneumococcal
Pn1	Pneumococcal serotype 1
PPV	Pneumococcal polysaccharide vaccine
PRP	Polyribosyl–ribitol–phosphate
PS	Polysaccharide
PsaA	Pneumococcal adhesion protein
PVDF	Polyvinylidene difluoride
R^2	Correlation coefficient
Rha	Rhamnose
RID	Refractive index detector
RT	Room temperature
S. pneumoniae	*Streptococcus pneumoniae*
S–NHS	Sulfo–*N*–hydroxysuccinimide
SDS–PAGE	Sodium dodecyl sulphate polyacrylamide gel electrophoresis
SEC	Size exclusion chromatography
SIIL	Serum Institute of India Limited
TD	Thymus dependent
TEA	Triethylamine
TFA	Trifluoroacetic acid

Th	Helper T cells
TI	Thymus independent
TMS	Trimethylsilyl–
TNBS	Trinitrobenzenesufonic acid
TOCSY	Total correlation spectroscopy
TT	Tetanus toxoid
UV	Ultraviolet
W	Watts
WHO	World Health Organization
w/w	Weight by weight
ZPS	Zwitterionic polysaccharide

CHAPTER 1. INTRODUCTION

Streptococcus pneumoniae (also known as pneumococcus) is a major cause of serious diseases such as pneumonia, meningitis, bacteraemia and sepsis as well as more common illnesses including otitis media and sinusitis [1]. The majority of these disease outbreaks, in developed and developing countries, occur in children under the age of two as well as in the elderly. In 2002, the World Health Organization (WHO) estimated that 1.6 million childhood deaths were attributed to pneumococcal disease (Figure 1.1) [2].

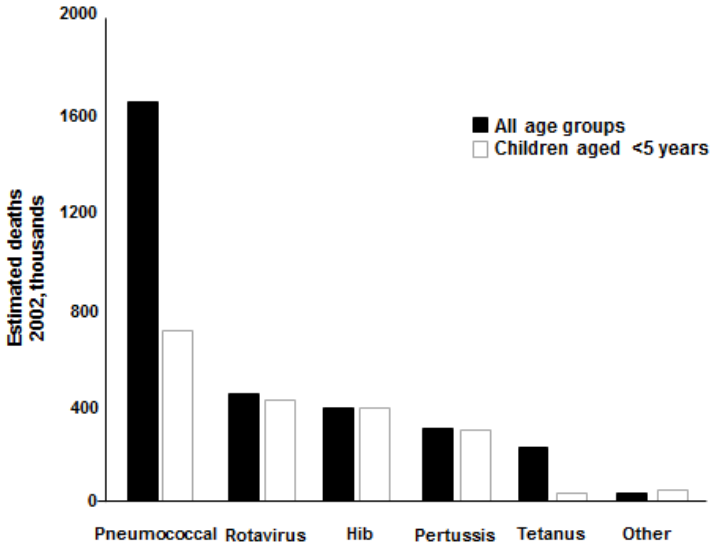

Figure 1.1. Comparison of estimated deaths in 2005 from various bacterial diseases [2].

In 2008, the WHO estimated 476 000 of the 8.8 million deaths of children under 5 years of age were caused by pneumococcal infections [2], 99 % of these deaths occurred in Africa and Asia as shown in Figure 1.2 [3], and in 2010 pneumonia accounted for 18 % of childhood mortality (Figure 1.3) [4].

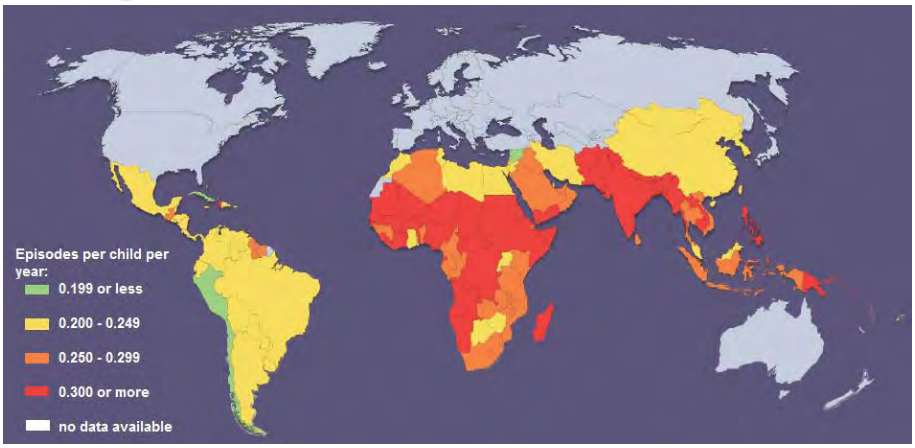

Figure 1.2. Estimated incidence of childhood pneumonia worldwide (2004) [5].

Pneumonia is the most common form of invasive pneumococcal disease (IPD) and it accounts for one in every four deaths amongst young children. It is also the leading cause of non–invasive diseases such as otitis media [6]. Pneumonia has a bi–modal incidence rate that peaks twice; the first occurs in children under 2 years of age and the second peak arises in adults over 65 years of age (Figure 1.4) [7].

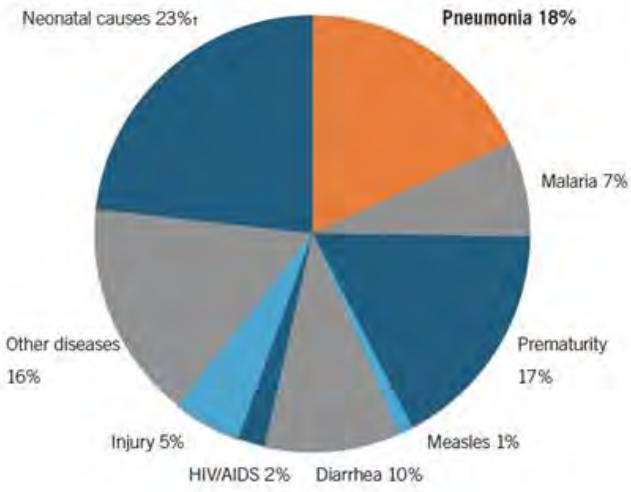

Figure 1.3. Global causes of childhood mortality in 2010 [4].

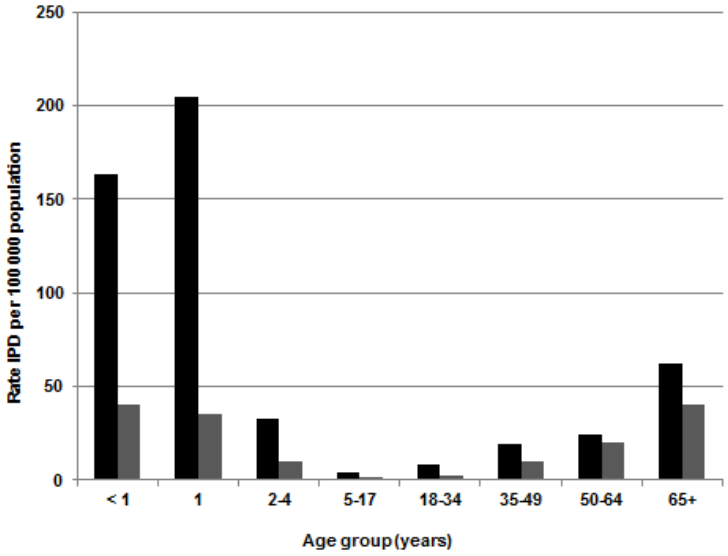

Figure 1.4. Incidence rate of pneumococcal infection by age group in 1998 [7].

1.1 Early history of *Streptococcus pneumoniae*

The discovery of pneumonia is largely associated with two men, Sternberg and Pasteur, who both, independently, isolated the bacteria in 1880 [8]. While Pasteur named the isolate "microbe septicemique du saliva", Sternberg called his *Micrococcus pasteri* in honour of Pasteur who had published his results a mere three months earlier [8]. The term "pneumoniekokke" was first used in 1883 by Matray, followed in 1886 by the more well–

known name “pneumokokkus” by Fraenkel. The bacteria was renamed *Diplococcus pneumoniae* in 1920 as the morphology was more associated with the diplococcal group, but in 1974 it was reclassified as *Streptococcus pneumoniae (S. pneumoniae)* due to its growth in chains in liquid media and other similarities to the streptococci bacterial group [8-10]. Neufeld is credited with the identification of characteristics that separate *S. pneumoniae* from other bacteria, namely the bile solubility test and the Quellung reaction that results in the swelling of the capsule of the pneumococcus [11].

1.2 Surface components of *Streptococcus pneumoniae*

S. pneumoniae are Gram positive, lancet–shaped, encapsulated organisms that commonly exist in pairs (diplococci) but can present in short chains or as single cells (Figure 1.5a) [12]. *S. pneumoniae* is an aerotolerant anaerobe and is fastidious in that it has complex nutritional requirements [9, 13, 14]. The bacteria grow readily on blood agar plates and display alpha haemolysis unless grown anaerobically, where they show beta haemolysis. The bacteria are sensitive to bile salts which break down the cell wall with the presence of the cell’s own enzyme, autolysin. Three major surface layers are recognisable; the plasma membrane, the cell wall and the capsule (Figure 1.5b) [15].

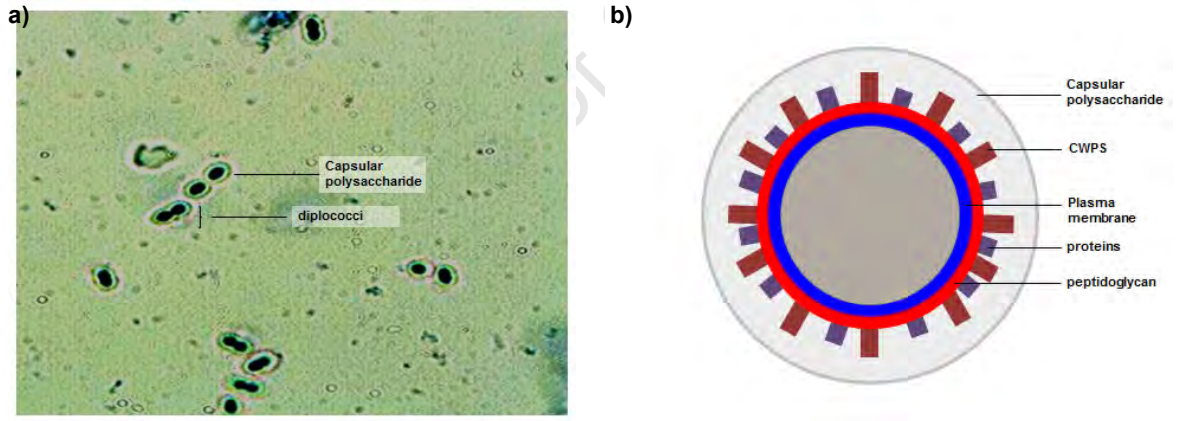

Figure 1.5. a) Pneumococcal cell showing diplococcal formation as well as the outer capsular polysaccharide b) Idealised schematic of the surface components of a pneumococcal cell, modified from AlonsoDeVelasco *et al.* [15].

A common characteristic of Gram positive bacteria is the presence of a thick cell wall. This wall consists mainly of peptidoglycans which are repeating units of *N*–acetylglucosamine and *N*–acetylmuramic acid. Attached to the *N*–acetylmuramic is a five amino acid peptide chain which is cross–linked over the bacterial cell [16]. The peptidoglycan serves as an anchor for the capsular polysaccharides (PS) as well as a number of surface proteins, and is responsible for stimulating the inflammatory response in pneumococcal infections [9]. Cell wall polysaccharide (CWPS) is a uniquely identifying feature of all *S. pneumoniae* isolates. It was first described by Tillett and Francis in 1930 [17], but it took a further 50 years before the chemical structure of CWPS was fully elucidated. CWPS is comprised of glucose,

galactosamine, ribitol phosphate, phosphocholine and 2–acetamido–4–amino–2,4,6–trideoxy–galactose (AAT) [18]. The cell wall polysaccharide is responsible for the serological cross–reactivity between *S. pneumoniae* and other streptococci as it activates the alternative complement pathway in the early stages of inflammatory response [9, 19].

Pneumococci are divided into 93 different serotypes based on the expression of their capsular polysaccharide (PS) [20]. The Danish naming system has been used since the 1980s to classify the different pneumococcal serotypes [9, 10, 21, 22]. The capsular PS is the thickest layer that protects the inner components of the pneumococcus. While the CWPS is common to all serotypes, the structure of the capsular PS is unique to each serotype. In Pasteur's early observations of the pneumococcal cell, he recognised the capsule surrounding the cell when he wrote: "*Each of these little particles is surrounded at a certain focus with a sort of aureole which corresponds perhaps to a material substance*" [8]. The capsular PS was first isolated in 1917 by Dochez and Avery, in the urine of patients with pneumococcal pneumonia [23], but it was thought to be either a protein or of a protein nature due to the total nitrogen and nitrogen partition on the "active substance" [23]. It was isolated and identified as a carbohydrate in 1923 by Heidelberger and Avery [24].

Unlike peptidoglycan, the capsular PS does not produce an inflammatory response, instead it protects the bacteria from phagocytosis by acting as a shield from antibodies and by separating bound opsonins from their receptors on the phagocytes [9]. The capsular PS is the main virulence factor that protects the bacteria against the host's immune system [15, 25]. Encapsulated bacteria were found to be 100 000 times more virulent than non–encapsulated strains [15, 26]. Other factors contribute to the bacteria's virulence include the CWPS, enzymes such as autolysin, neuraminidase as well as the pneumolysin and pneumococcal surface proteins [15, 27].

1.3 Pneumococcal disease

The only natural reservoir of *S. pneumoniae* is the human nasopharynx and the bacteria is transmitted through respiratory droplets [28]. Both pathogen and host gain an advantage from nasopharyngeal colonisation. *S. pneumoniae* is able to exchange genetic material, with the host, and may gain properties enabling it to potentially become antibiotic resistant [29]. For the human host this colonisation promotes the release of the B–cells against the PS capsule.

In most cases the carrier is asymptomatic with disease being shown in only a small portion of the population [9]. The greatest of pneumococcal infections carriage rates are found in young children [30]. Studies have shown that in developed countries 40 – 60 % of young children are carriers compared to 12 % of older children, 6 – 10 % adolescents and only

3 – 4 % of adults are thought to be carriers [31, 32]. According to Gray *et al*., by the age of two, infants are colonised at least once by *Streptococcus pneumoniae.* Only one serotype is carried at a time and the first strain is always carried for the longest period of time [33]. Transmission is usually within high population areas, within families [30, 33, 34], in orphanages and day care centres [34-36] and closed communities [37].

From the nasopharynx, the bacteria may cause non–invasive and invasive pneumococcal infections; it may spread to the sinuses causing sinusitis, to the middle ear cavity causing otitis media or into the lungs causing pneumonia. In the worst cases, *S. pneumoniae* is known to cause systemic infections, with the detection of the bacteria in the bloodstream, including bacteraemia, endocarditis or meningitis all of which have considerable mortality rates [9, 38].

1.3.1 Non–invasive pneumococcal disease

Non–invasive pneumococcal infections occur outside the major organs and blood and are less serious than invasive diseases. Two of the main forms of non–invasive pneumococcal infections are middle ear infections and non–bacteremic pneumonia.

Non–bacteremic pneumonia is a less serious form of pneumonia, which, while displaying all of the characteristics of pneumonia including detection on the lungs by X–ray, is not found in the blood. Middle ear infections (otitis media – OM) are one of the most common infections in children and are typically caused by viral, bacterial or fungal pathogens with the most widely occurring bacterial pathogen being *S. pneumoniae* [39, 40]. Otitis media is an inflammation of the middle ear with an accumulation of fluid in the middle ear and swelling of the eardrum. The disease usually occurs in the first five years of life [41]. It has been reported that 60 % of children have experienced at least one episode of OM by the time they turn one year old [7].

1.3.2 Invasive pneumococcal disease

Invasive pneumococcal diseases (IPD) are of a more serious nature and include diseases in the blood or a major organ. In the US, in 1997, approximately 500 000 cases of pneumonia were reported with a fatality rate of 5 – 7 %, 50 000 episodes of bacteraemia (fatality rate = 20 %) and 3000 cases of bacterial meningitis with 30 % of the cases resulting in death were attributed to *S. pneumoniae* [42].

Bacterial meningitis is an infection of the membranes (meninges) covering the brain and spinal cord. *S. pneumoniae* is the leading cause of bacterial meningitis in adults and, since the introduction of the *Haemophilus influenzae* type b (Hib) conjugate vaccines, the main pathogen in infants [43]. The incidence of bacterial meningitis caused by *S. pneumoniae* in

the United States is between 13 – 19 % where it is estimated that 3000 to 6000 cases occur every year [7]. Pneumococcal meningitis has been found to be associated with higher rates of death and neurological conditions than meningitis caused by *Neisseria meningitidis* and Hib [44].

Bacteraemia is a bacterial infection of the blood and accounts for 70 % of IPD in children younger than 2 years of age [7]; in adults most cases of bacteraemia are cause by *S. pneumoniae* [45]. Bacteremic pneumonia is the inflammation of one or both lungs where *S. pneumoniae* is also found in the blood and accounts for 12 – 16 % of IPDs among children 2 years of age and younger [7]. It is estimated to be responsible for more than 50 % of all pediatric pneumonia [5].

Specific serotypes are responsible for certain types of disease; for instance, an Israeli study in 2011 found that the highest incidence of pneumonia was contracted from serotype 1, followed, in descending order, by 5, 22F, 7F, 14, 9V and 19A. Much lower incidence rates were found for serotypes 6A, 6B, 23A and 35B suggesting that the first seven serotypes have a higher disease potential in children less than five years of age [46].

Serogroups 3, 6, 19 and 23 are found to be the main serotypes isolated from middle ear fluid [1, 39, 47], serotypes 1 and 14 are mostly isolated in the blood and contribute mainly to bacteraemia, and serogroups 6, 10 and 23 were mostly found in the cerebrospinal fluid indicating that these serotypes are mainly responsible for bacterial meningitis [48-50].

1.4 Serogroup distribution of *Streptococcus pneumoniae* in Africa

In 2000, approximately 156 million new episodes of childhood clinical pneumonia occurred with 90 % of all cases occurring in sub–Saharan Africa and South Asia. The mortality rate of pneumonia is also largely concentrated in Africa and South Asia as illustrated in Figure 1.6 [3]. Of all these cases, 11 to 20 million of them (7 – 13 %) were severe enough to require hospitalisation [2]. About half the world's pneumonia and diarrhoea related deaths occur in just five mostly poor and populous countries: India, Nigeria, Democratic Republic of the Congo, Pakistan and Ethiopia (Table 1.1).

Table 1.1. Number of deaths in children under 5 years due to pneumonia in 2010 by country [3].

Rank	Country	Deaths among children under age 5 due to pneumonia and diarrhoea
1	India	609 000
2	Nigeria	241 000
3	Democratic Republic of the Congo	147 000
4	Pakistan	126 000
5	Ethiopia	96 000
	Total Worldwide	2 197 000

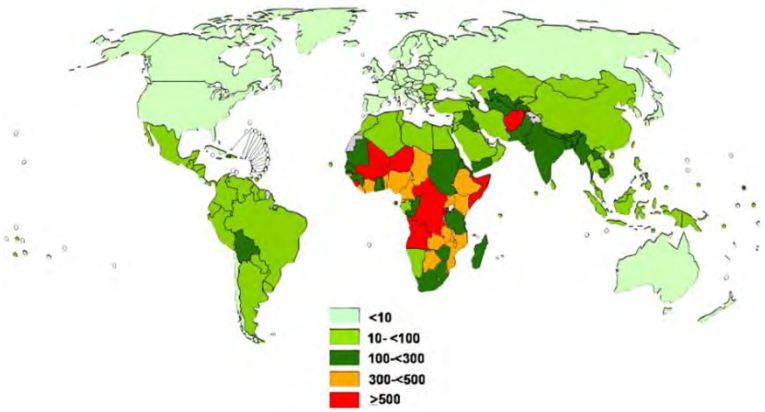

Figure 1.6. Mortality rate of children (deaths per 100 000) under 5 years of age due to *S. pneumoniae* [51].

Streptococcus pneumoniae causes approximately 75 % of all serious IPD infections in South African HIV positive children [52]. In 2000, approximately 10.8 % of the 870 000 deaths attributed to *Streptococcus pneumoniae* were from HIV positive children with 19.8 % of those deaths occurring in African children [51]. *S. pneumoniae* is the leading bacterial opportunistic infection in children who do not receive antiretroviral treatment (ART), and is up to 40 – fold greater in HIV positive children; this rises to 65 % in HIV infected children in Southern Africa where the prevalence of HIV in young children is less than 5 %. Children who receive ARTs have a 21–fold increase in IPD infection risks than those without HIV [53].

Figure 1.7 illustrates the serotype distribution of *Streptococcus pneumoniae* globally and in Africa. The main difference in the serotype distribution between developed and developing countries is the contribution of serotypes 1 and 5. In Africa, Asia and Latin America these two serotypes are responsible for the high incidents of invasive pneumococcal disease [54].

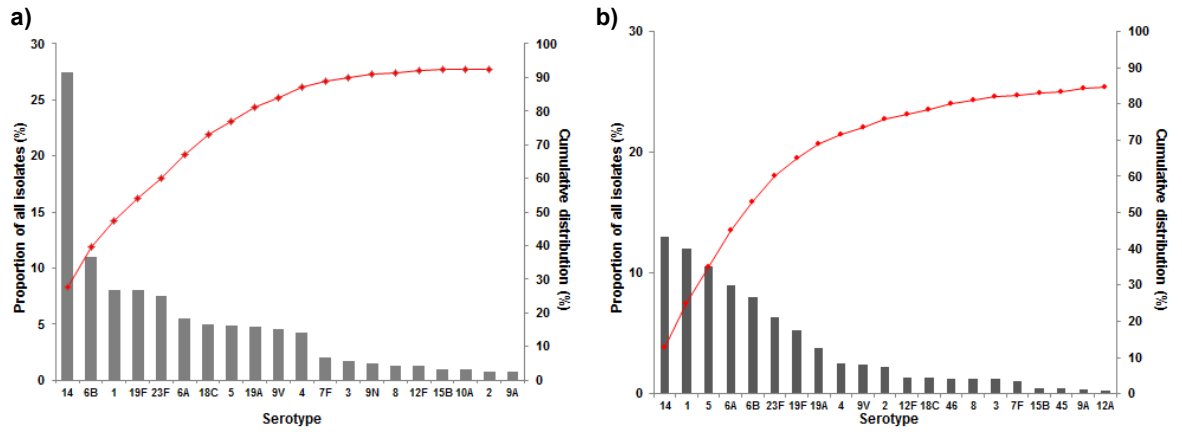

Figure 1.7. Serotype distribution a) globally and b) Africa [55].

Figure 1.8 illustrates the five most prevalent serogroups responsible for IPD in six African countries in young children. Serogroup Pn6 has the highest incidence rate in South Africa but is replaced by serogroup Pn1 in Egypt, Rwanda and Kenya, and Pn14 in Ethiopia and Gambia. In adults, this order changes and Pn1 is the dominant serotype in Rwanda, Kenya, and Egypt as well as in South Africa. In South Africa, in 2008, pneumonia caused 12.4 % of deaths in children under 15 years of age; this was the second most common cause of natural deaths in the country [56].

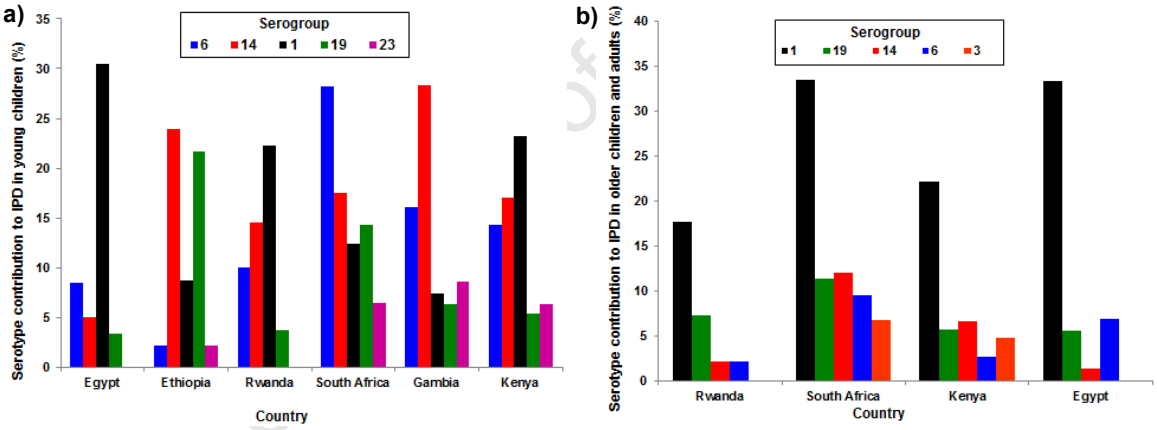

Figure 1.8. Five most prevalent serogroups responsible for invasive pneumococcal disease in a) young children, and b) adults in Africa [57].

Pn1 has been the dominant serotype in the meningitis belt over a number of years [58]. In one study, the serotype distribution of pneumococcal infections was examined in three countries situated in the African meningitis belt. The seasonal pattern of pneumococcal meningitis share some of the same conditions as those of the epidemic meningitis season and it was found that the highest incidence of cases were found during the dry season, during which respiratory infections and decreased host immunity occurs [58].

Table 1.2. Serogroup distribution by country in the African meningitis belt. Modified from Gessner *et al.* [58].

Serogroup	Burkina Faso	Senegal	Ghana
	Age 5+ yr.	Age 2+ yr.	Age 5+ yr.
1	18	90	51
3	–	8	2
5	–	8	–
6	–	13	1
12	2	6	–
14	2	2	1
19	2	4	–
Others	4	12	7
Total	28	143	62

The results (Table 1.2) showed that at least 60 % of all isolated cases in Burkina Faso, Senegal and Ghana were due to pneumococcal serotype 1. It was also noted that these incidents fell out of the usual age range for pneumococcal infections as they were recorded in children over the age of 2 in Senegal and over 5 years of age in both Burkina Faso and Ghana. These results suggest uniqueness in the epidemiology of Pn1 and are an indication that a Pn1 vaccine should be developed as a potential booster dose or monovalent vaccine to be administered in the later years of childhood.

1.5 Immune response to polysaccharide and conjugate vaccines

The ability to distinguish the body's own cells from foreign cells is the most important characteristic of the immune system. The immune system will launch an attack (immune response) when it encounters foreign cells or organisms (antigens).

There are many different types of cells that make up the immune system and which are responsible for the immune responses, three of which are described below.

- Phagocytes: These are large white cells that specialise in engulfing bacteria, viruses or any other foreign cells. There are three main types of phagocytes: granulocytes which are the first responders to the infection and specialise in large parasites. Macrophages are larger, longer lasting and can consume and destroy more foreign cells than granulocytes. Finally dendritic cells, while also responsible for destroying foreign cells, also activate the rest of the immune system. Both macrophages and dendritic cells reveal the antigens to T cells and stimulate the T cells during an immune response [6, 59, 60].
- T cells: The surface of T cells contain specialised antibody–like receptors that detect fragments of antigens on the surface of infected cells, instead of free–floating

antigens [60]. The molecules responsible for bringing these fragments to the surface are proteins called the major histocompatibility complex (MHC) molecules [61]. There are two main types of T cells: helper T (Th) cells and cytotoxic T lymphocytes (CTLs). The Th cells manage the body's immune response by interacting with other cells; some will coordinate phagocytes, some will stimulate B cells to produce antibodies and memory cells and others will activate the CTLs which directly attack the infected cells and are most useful in combating viruses.

- B cells: When a B cell is exposed to bacteria it becomes activated and will travel to either the lymph nodes or the spleen where it changes into either a memory or plasma cell [60, 62, 63]. Memory cells "remember" which antigens they were exposed to which will speed up the immune response when a secondary exposure occurs. When this second exposure occurs the memory cells will transform into plasma cells. Plasma cells express and release the antibodies of which there are five main types:
    - Immunoglobulin A (IgA) is concentrated in bodily fluids and guards the entrance to the body.
    - Immunoglobulin D (IgD) attaches to B cells and is important in instigating early B cell responses.
    - Immunoglobulin E (IgE) is responsible for the protection against parasitic infections and is responsible for allergy symptoms.
    - Immunoglobulin G (IgG) antibodies coat microbes which speeds up their uptake by other cells in the immune system. IgG also plays an important role in opsonophagocytosis and complement induced cytotoxicity by phagocytes [38].
    - Immunoglobulin M (IgM) are very effective at killing bacteria [59, 60, 64].

Vaccines rely on the memory B cell function as they expose the body to small amounts of antigen that will lead to the development of memory B cells that will survive until the next, potentially harmful exposure.

Antigens can elicit either thymus dependent (TD) or thymus independent (TI) responses. TD antigens interact with the MHC molecules on the surface on the antigen which will allow it to interact with T cells. The immune system's ability to react to a TD antigen is present from birth where the interaction with the T cells leads to an expression of a membrane protein (CD40) which activates the B cells into producing IgG and IgM antibodies and aid in the maturation of B cells into memory cells [65-67]. Molecules that generate TD responses are proteins or peptides [65].

TI responses do not stimulate the B cells into creating memory cells, however they do stimulate the production of large quantities of IgM and much less quantities of IgG [67]. TI antigens can react in two different ways with B cells; TI–1 antigens encourage the expansion and differentiation of B cells which induce an immune response in both adults and neonates [66] whilst TI–2 antigens do not possess this ability to induce a strong IgG response and therefore can only work in older children and adults [67, 68]. The different responses of the immune system to an antigen are important to know when developing an effective vaccine.

Polysaccharides are known as TI–2 antigens as they are hydrophilic molecules and they therefore cannot associate with the MHC proteins [69]. Figure 1.9 displays how PSs directly activate the B cells without the help of T cells, through an alternative pathway in the spleen [63]. The spleen however is not fully developed until the age of 1 – 2 years [62, 63] and so the production of capsular specific antibodies (IgG2 antibodies) is limited or even absent in young children [70, 71]. Memory cells are also absent with TI antigens and infections which reoccur cannot be dealt with in a timely manner [72].

As proteins are TD antigens, conjugating a PS to a protein carrier will transform the polysaccharide into a TD antigen as the protein will induce a T cell response which will lead to IgM–IgG antibody switching and initiate the maturation of B cells into memory cells [69, 73-75]. Table 1.3 compares polysaccharide and conjugate vaccines in terms of immune responses.

Table 1.3. Comparison of polysaccharide and conjugate vaccines [76].

Property	Polysaccharide vaccines	Conjugate vaccines
Immunogenicity (5 year old – adult)	High	High
Immunogenicity in young children	Poor	High
Response to booster	Poor	High
Avidity	Low	High
Bacterial activity	Low	High
Induction of memory	Some	Yes
Effect on colonisation	Some	Yes

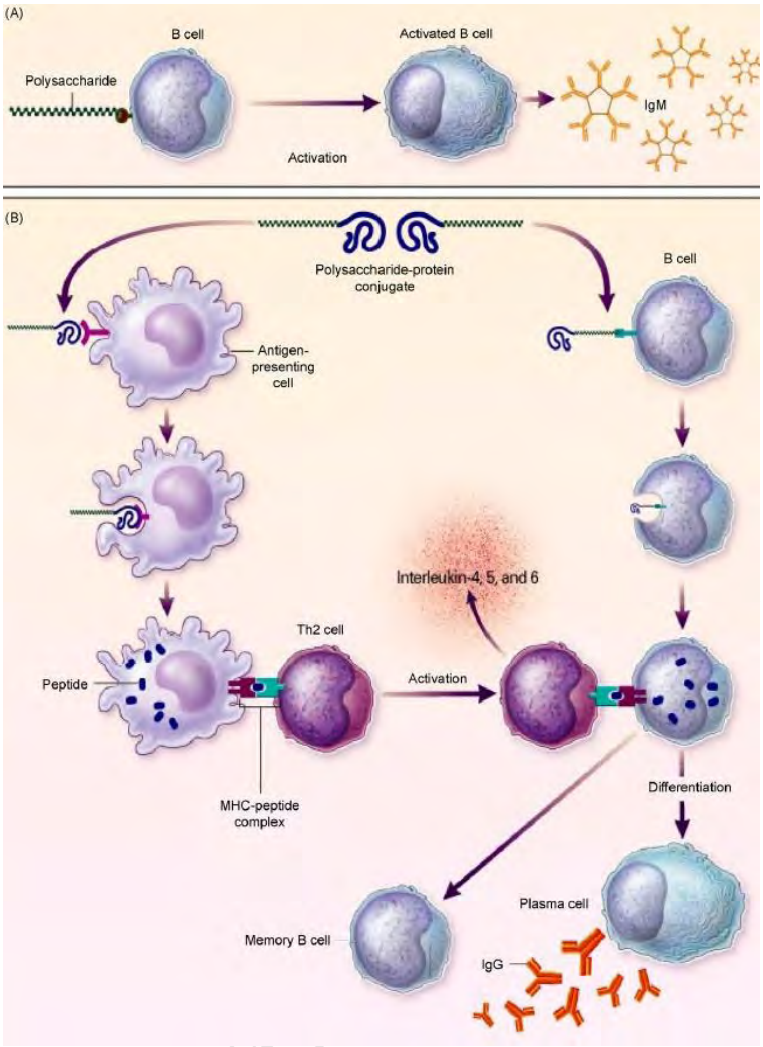

Figure 1.9. Immune responses induced by *Streptococcus pneumoniae*; A) polysaccharide vaccine and B) conjugate vaccine [38].

It was long thought that only peptide and protein antigens would elicit a T cell response. Recently it has shown that zwitterionic polysaccharides (ZPS) also have the ability to activate T cells in the absence of a protein carrier [74, 77, 78]. ZPS are polysaccharides that possess both positive (free amino groups) and negative (carboxylate or phosphate groups) charges. Some bacterial polysaccharide that are classified as zwitterionic polysaccharides include *Staphylococcus aureus* type 5 and type 8 polysaccharides, polysaccharide A (PSA) from *Bacteroides fragilis* and serotype 1 from *S. pneumoniae.* It was hypothesised that these polysaccharides interact with the MHC molecules. Studies of PSA showed that removing either the positive or negative charge eliminates the MHC binding and thus becomes a TI antigen [79-81].

Mertens *et al.* investigated the immune response of CD8+ T cells in mice when exposed to Pn1 PS. Pn1 PS does induce the production of T cells in the spleen and peritoneal cavity of mice and, as seen with PSA, removing one of the charged groups on the PS renders the production of T cells obsolete [82]. Trück *et al.* examined the memory B cell (MBC)

responses in adults following immunisation with the 23 valent pneumococcal polysaccharide vaccine as well as the 7–valent conjugate vaccine [83]. Figure 1.10 graphically displays the change in MBC after vaccination with the two vaccines specifically for Pn1 and Pn3 serotypes. Pn1 did not induce MBC, rather it lead to depletion of the pre–existing peripheral memory B cells. This lack of response has been shown to occur with other non–zwitterionic polysaccharides in the 23 valent polysaccharide vaccine [83]. It was also shown that the memory B cell responses were significantly different between the two different vaccine types for serotype 1 but not for serotype 3; this investigation determined that the Pn1 PS is not processed by the MHC pathway in humans as it was shown to do in mice and therefore cannot be considered a TD antigen.

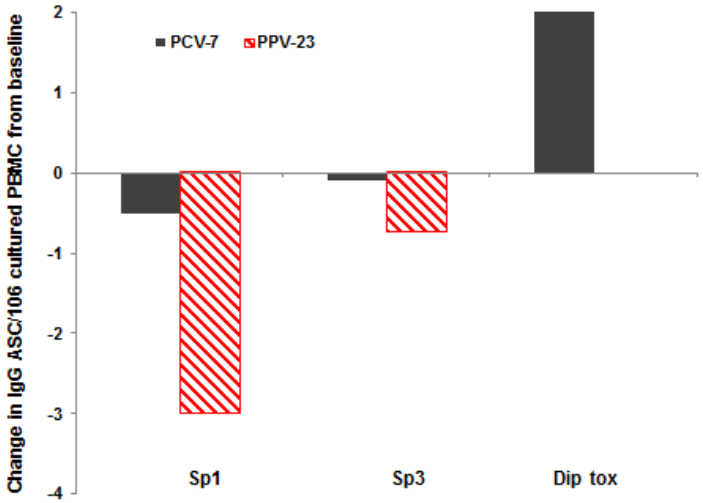

Figure 1.10. Change in memory B cell numbers pre**–** and post**–**vaccination. Participants received either one dose of PCV7 (black; n = 28) or a single dose of PPV23 (red; n = 28). Modified from Trück *et al.* [83].

1.6 Pneumococcal vaccines

1.6.1 Whole cell vaccines

The first recorded instance of a vaccine against *Streptococcus pneumoniae* was documented in 1911 in South Africa where workers in the diamond and gold mines experienced a very high incidence of pneumonia [84]. According to data released in 1907 at the Premier Diamond Mine, the rate of pneumonia occurrence was eight out of every thousand workers per month with two of the eight infected ending in death [85]. Sir Almoth Wright, known as the father of the typhoid vaccine, was brought in to investigate the best methods of protection against pneumonia. Sir Wright and his associates went on to inoculate 550 000 mine workers with a vaccine that consisted of dried, heat inactivated sputum from pneumonia patients and it was claimed that the incidence of pneumonia in mine workers was decreased by more than 50 % [10, 19, 86, 87].

Sir Wright's protégé, F. Spencer Lister, went on to show that pneumococcal pneumonia was not caused by a single serotype; a multitude of serotypes were capable of eliciting type–specific immunity in both animals and humans but it was necessary to inject a billion or more of the bacteria to elicit an immune response in man and up to 40 billion to produce an adverse effect [1, 88]. This was somewhat confirmed when Heidelberger *et al.* showed that 10 billion pneumococcal bacteria from serotypes 1 and 2 were needed to produce between 30 and 40 mg of capsular PS (amounts that are now used in the PS vaccine) [89].

Whole cell pneumococcal vaccines were again trialled during the First World War when the US military inoculated over 400 000 people. While some of the results suggested that these vaccinations were successful, many subjects showed negative reactions towards the vaccination and the trials were determined to be inconclusive [10, 19].

1.6.2 Pneumococcal polysaccharide vaccines

After the First World War, many investigations into the pneumococcus revealed the importance of the capsular PS and the resulting antibody response to it [10, 17, 19]. Tillet and Francis injected the polysaccharides of serotypes 1, 2 and 3 into humans and saw an immune response to one or more of the serotypes [90]. This was confirmed by Finland *et al.* a year later [91]. During the Second World War, clinical trials in the military demonstrated that pneumococcal pneumonia could be prevented by immunisation with specific capsular PSs. A tetravalent PS vaccine consisting of serotypes 1, 2, 5 and 7 was shown to be 86 % effective in preventing pneumonia from those four serotypes but it had no effect in prevention against other pneumococcal serotypes [10, 92]. Heidelberger *et al.* showed that six PSs in a single formulation was able to induce the same amount of antibodies as six polysaccharides injected separately [93]. The results of this trial prompted the release, in 1946, by Squibb and Sons, of two hexavalent vaccines, one specifically for adults and the other for children. However, these vaccines were released during the introduction of penicillin and other antibiotics that were shown to successfully treat pneumococcal and other bacterial infections and, due to bad sales, the vaccines were taken off the market in 1954 [9, 10, 19].

It took 10 years until Austrian and Gold showed that pneumonia still caused serious infections with a high mortality rate in spite of antimicrobial treatments [94]. Led by Austrian, multivalent PS vaccine formulations containing up to fourteen capsular PSs were developed, tested and found to be safe and immunogenic. Trials were again performed with mine workers in South Africa where a 13–valent PS formulation was found to be between 78.5 % and 82.3 % efficacious [9, 95, 96].

As a result of these trials, a 14–valent capsular PS vaccine was licensed in 1977 in the United States [9, 19, 97]. The capsular PSs included in this vaccine are shown in Table 1.4. The 14–valent vaccine included the 12 most common serotypes causing 70 – 80 % of disease in the United States, parts of Europe and South Africa. Serotype 2 was not among the common serotypes, especially in America, but was included due its prevalence in men predominantly from Malawi and Mozambique. Serotype 2 was also known to cause serious illness and was prevalent in Africa and parts of Europe [19, 98].

Table 1.4. Serotypes included in the licensed capsular polysaccharide vaccines.

Vaccine	Serotypes included	Date licensed
14 valent	1, 2, 3, 4, 6A, 7F, 8, 9N, 12F, 14, 18C, 19F and 25	1977
23 valent	1, 2, 3, 4, 5, 6B, 7F, 8, 9N, 9V, 10A, 11A, 12F, 14, 15B, 17F, 18C, 19A, 19F, 20, 22F, 23F and 33F	1983

With evidence increasing in support of microbial resistance and the discoveries of additional serotypes, the 14 valent vaccine was expanded to a 23–valent PS vaccine in 1983 [9, 98]. The 23 different serotypes provided coverage for 85 – 95 % of the serotypes found in Europe and the United States [37, 97-100] but less than 80 % in Asia [29, 101, 102]. The pneumococcal PS vaccine, much like other PS vaccines, has some major limitations in that it is weakly immunogenic; a decrease in the level of clinical protection was also noticed after a few years. A second dose, given after this decrease occurred, did not show a rise in antibody response [1]. As previously stated, the PS is a T–cell independent antigen and the immune system therefore needs mature B lymphocytes in order to elicit an immune response. As infants do not possess mature B lymphocytes, the PS vaccine is poorly immunogenic. The pneumococcal PS vaccine was also not as effective in the elderly, and in immunocompromised patients [9, 10, 29, 70, 102-106]. Whilst not proving to be very effective in the aforementioned groups, the vaccine was recommended for young children (under 2 years of age) who have an increased risk of pneumococcal disease, healthy adults over 65 years of age and for both young children and the elderly who live in homes, institutions or any other crowded living conditions. The vaccine is also not effective for those suffering from reoccurring middle ear infections, and certain types of cancer (blood, lymph and bone) [1, 9, 66, 87, 106, 107].

This poor immune response in infants to the pneumococcal PS vaccine led to the investigation of a second generation type of vaccine in which the PSs were covalently attached to different proteins.

1.6.3 Conjugate vaccines

Avery and Goebel were the first to show that attaching a polysaccharide to a protein increased the immunogenicity of the PS; they covalently attached the PS from serotype 3 to globulin from horse serum [108-112]. These conjugates were tested in rabbits and resulted in a type–specific immune response to the conjugate and not to either the polysaccharide or protein injected separately [1, 113]. Conjugation of a polysaccharide to a protein solved the major problem with PS vaccines in that they could induce an immunological memory and an immunological response in infants [107].

It took 50 years before the work performed by Avery and Goebel was used to create the first conjugate vaccine against Hib. The Hib conjugate vaccine was first developed by Schneerson *et al.* [114, 115] and led to a large reduction of the disease, where, of the 169 countries that introduced the conjugate vaccine into the infant immunisation schedule, 69 % of them describe coverage of above 80 % (Figure 1.11) [116].

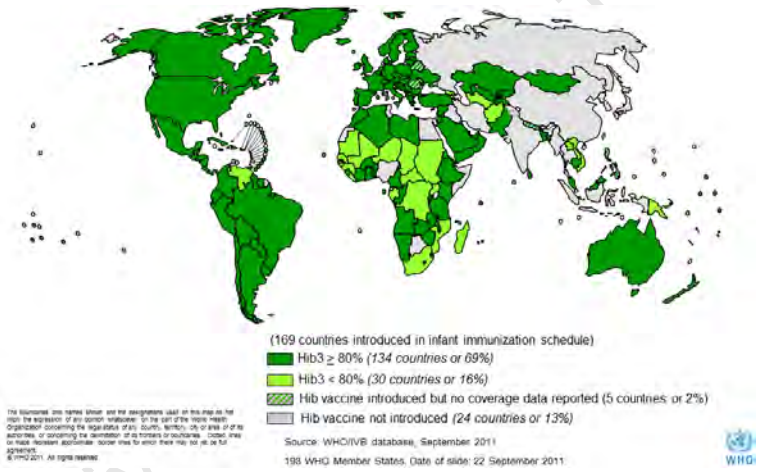

Figure 1.11. Coverage of Hib conjugate vaccine [116].

This success led to the investigation into other conjugate vaccines, most notably for the prevention of pneumococcal diseases. There is an added challenge to pneumococcal vaccines as there are a variety of different serotypes that cause illness amongst infants, so multivalent vaccines had to be developed where each serotype was separately conjugated to a protein and formulated together into a conjugate vaccine that could induce antibodies against each serotype [1, 10]. There are currently three licensed multivalent pneumococcal conjugate vaccines available. These are listed in Table 1.5 and are described in further detail below.

Table 1.5. Licensed pneumococcal conjugate vaccines [117].

Vaccine	Company	Serotypes included	Protein	Licensed date
Prevnar (PCV7)	Pfizer	4, 6B, 9V, 14, 18C, 19F, 23F	CRM_{197}	2000
Synflorix (PCV10)	GSK	1, 4, 5, 6B, 7F, 9V, 14, 18C, 19F, 23F	Protein D + DT + TT	2009
Prevnar 13 (PCV13)	Pfizer	1, 3, 4, 5, 6A, 6B, 7F, 9V, 14, 18C, 19A, 19F, 23F	CRM_{197}	2010

1.6.3.1 Prevnar7

The first commercially available pneumococcal conjugate vaccine (PCV) was Prevnar (PCV7). PCV7 was licensed by Pfizer (formally Wyeth) in 2000 in the United States, 2001 in the United Kingdom, as a three dose regimen given at 2, 4, and 6 months, followed by a booster dose at 12 to 15 months (a 3 + 1 schedule). The vaccine consisted of seven different serotypes conjugated to the cross–reactive material 197 (CRM_{197}) carrier protein, a non–toxic form of diphtheria toxoid (DT) that had already been successfully used in Hib as well as meningococcal group C (MenC) vaccines. The seven serotypes used in this vaccine were 4, 6B, 9V, 14, 18C, 19F and 23F which accounted for approximately 86 % of bacteraemia, 83 % of meningitis and 65 % of middle ear infections in children under 6 years of age in the United States [10, 118, 119]. An eighth serotype, Pn6A, was not included as it was thought that the cross reactivity within serogroup 6 meant that the capsular PS of one of them might protect against both serotypes and Pn6B was included instead of Pn6A due to the PS stability [1].

The conjugation chemistry involved in the production of this vaccine included periodate oxidation of the PS to form aldehydes, followed by reductive amination of the activated PS to the amines on the proteins with sodium cyanoborohydride, forming an imine which was reduced to form a stable amide linkage [120].

Figure 1.12 depicts how the incidence rates of IPDs dropped dramatically in the 5 years and under target group after the introduction of the vaccine in America and Australia. The efficacy of the vaccine in preventing vaccine–serotype–specific IPD in the United States as well as Europe was 97 %. The number of IPD cases in children below 5 years of age had fallen from an average of 17 240 cases per year before the introduction of conjugate vaccines to 4 454 cases in 2003 [2].

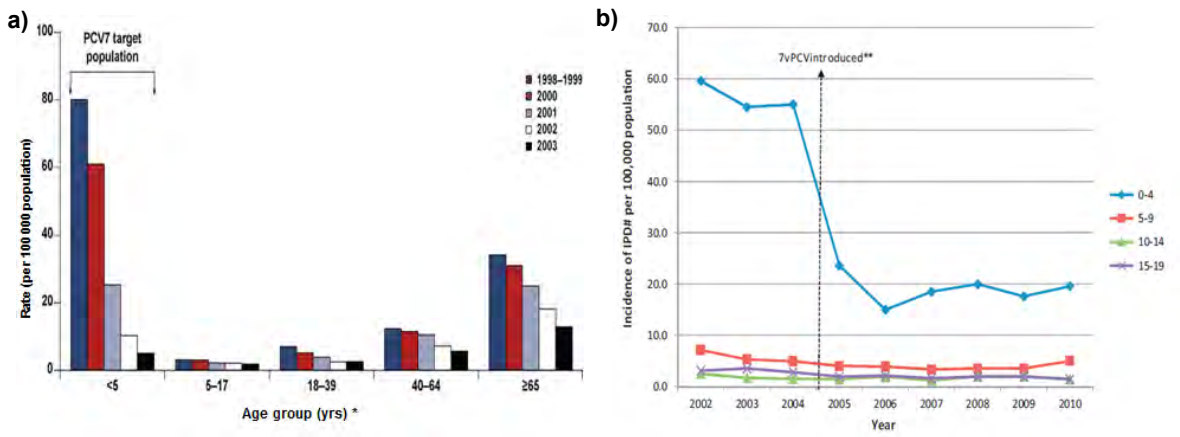

Figure 1.12. a) Rate of vaccine–type IPD in United States before and after introduction of PCV7, by age group and year [2]. *Difference between each age group in 2003 is statistically different to the age groups from 1998 – 1999. b) Incidence of IPD in Australian children (by age group) from 2002 – 2010; PCV7 was made available to all Australian children in 2005 [29].

An article by Whitney *et al.* in 2003 detailed the drop in invasive pneumococcal disease after the introduction of the 7–valent conjugate vaccine in 2000. The rate of disease dropped from an average of 24.3 cases per 100 000 people in 1998 – 1999 to 17.3 cases per 100 000 in 2001. The largest rate of decline of 69 % occurred in infants under two years of age [2, 121]. Further studies on the prevention of IPD [122, 123], OM [1, 122, 124] and pneumonia [125, 126] have also been reported. The reduction of IPD was documented in children with compromised immune systems such as sickle cell disease [127] and HIV [128] and the theory of herd immunity was described when a decrease in IPDs were shown in non–vaccinated populations (adults over 50 and infants that were too young to be immunised) after the roll out of the PCV7 vaccine in the United States. At the time the Centre for Disease Control (CDC) estimated over two – thirds of the reduction of IPD in the US was attributed to herd immunity [129].

Antibiotic resistance decreased with the introduction of the PCV7 vaccine. Antimicrobial resistance only became a problem in the targeted area in the 1990s when resistance to penicillin rose steadily (except for the slight drop in 1999) until the introduction of PCV7 at the end of 2000 (Figure 1.13) [130]. The data illustrated that the vaccine targeted the most common serotypes responsible for antibiotic resistance. Resistance to three different antibiotics were also determined before and after the introduction of PCV7 into the target population. Penicillin, erythromycin and tetracycline all showed decreases in antibiotic resistance after 2000 (Table 1.6) [130].

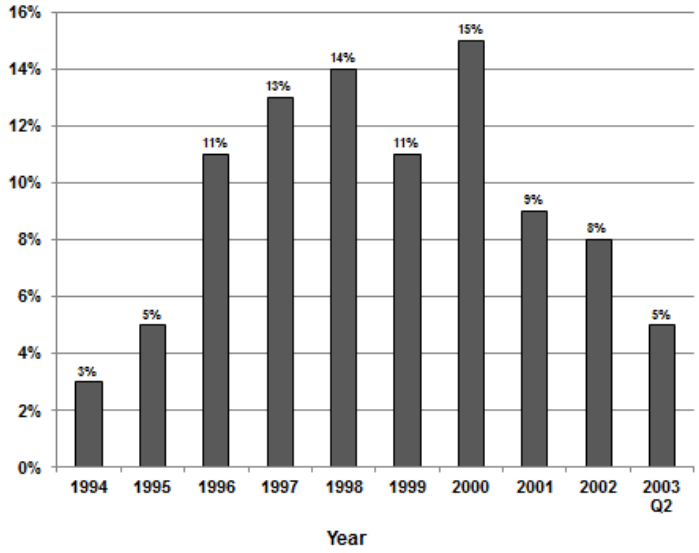

Figure 1.13. Reduction in penicillin resistance after the introduction of PCV7 in 2000 [130].

Table 1.6. Decrease in antibiotic resistance before and after the introduction of PCV7 [130].

Antibiotic	1998 – 1999	2001 – 2002
Penicillin	28.9 %	19.5 %
Erythromycin	29.5 %	15.0 %
Tetracycline	39.3 %	13.9 %

Whilst the incidence of carriage and IPDs decreased with the introduction of PCV7, serotypes that were not present in the vaccine became more prominent in contributing significantly to the incidence and carriage rates [38, 131-134]. The increase in these serotypes meant that the overall rate of IPD in young children in some countries had stabilised [131]. Singleton *et al*. found that the rate of IPD increased in Alaskan children after vaccination with PCV7 [132].

A study in the US looked at the change in serotype prevalence after the introduction of PCV7 [135]. While the annual number of cases decreased from 218 in 2000 to between 86 – 130 during 2002 – 2007 and the incidence of serotypes found in the vaccine decreased by 92 %, serotypes not included in the PCV7 vaccine increased by 18.4 % and serotypes related to those found in the vaccine (for example, serotypes from the same serogroup) increased by 207 %.

Serotype Pn19A was shown to be the cause of the largest increase in IPDs after vaccination. It was thought, that with Pn19F included in the conjugate vaccine, cross–protection for Pn19A would occur [136] but instead Pn19A went from being the ninth leading cause of IPD in the US, before the introduction of the vaccine, to the most prominent serotype in 2011, responsible for more than 40 % of IPD in children in the US, Europe and Asia [20, 137-142].

It was not just serotype replacement that was cause for the development of new conjugate vaccines; it was also the geographic spread of serotypes. While the serotypes found in PCV7 were estimated to cover over 80 % of IPDs in North America and Australia, it decreased to approximately 70 % in Western Europe and Africa and 50 % in South America and Asia (Figure 1.14).

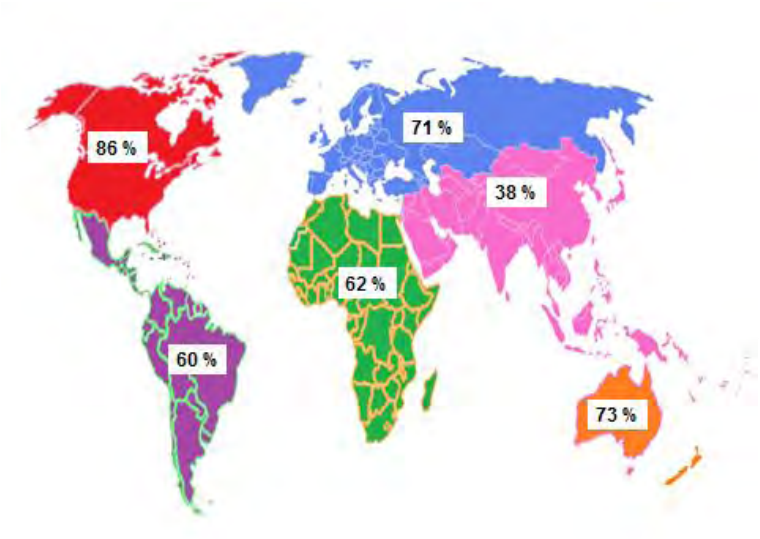

Figure 1.14. Serotype coverage of seven valent pneumococcal conjugate vaccine [48, 57]. Modified from PneumoAction [143].

This was due to the difference in serotype distribution in different countries. Most of the serotypes included in PCV7 were commonly found throughout the world but additional serotypes were found to be important in other regions.

1.6.3.2 Vaccine trials incorporating more serotypes

Due to the increase in non–vaccine serotype replacement, conjugate vaccines with additional serotypes underwent clinical trials; a 9–valent vaccine (Pfizer) and two 11–valent vaccines (GlaxoSmithKline (GSK) and Sanofi Pasteur). A summary of the serotypes and carrier proteins contained in these vaccines can be found in Table 1.7.

Table 1.7. Additional serotypes used in clinical trials for pneumococcal conjugate vaccines.

Vaccine	Additional serotypes*	Protein carriers	Clinical trial countries
PCV9	1, 5	CRM_{197}	South Africa and Gambia
PCV11PD	1, 3, 5, 7F	Protein D	Czech and Slovak Republics
PCV11DT	1, 3, 5, 7F	TT (1,4,5,7F,9V,19F,23F) DT (3,6B,14,18C)	Philippines

Serotype 1 is the second most common serotype in Africa and the fourth most common in South America and Asia [55]. It is known to cause the majority of complicated pneumonia and pleural empyema [144] and is responsible for up to 20 % of IPDs in developing countries, particularly among the African meningitis belt [54, 58, 145, 146] and Asia [147]. Serotype 1 is most widely found in children over 2 years of age and serotype 5 is most widespread in infants under 6 months [54, 148, 149]. Serotype 5 is the third most prevalent serotype in Africa and South America that causes IPD. Serotype 3 is commonly found in adults but after the introduction of PCV7, this serotype became more prominent in children [150]. Serotype 3 is associated with otitis media as well as IPDs especially in Latin America [20, 47, 151]. Serotype 7F was found to be the dominant serotype responsible for IPD with fatal outcomes in Germany [151].

The 9–valent vaccine demonstrated high efficacy levels in all of the clinical trials; in a trial of 40 000 infants in South Africa during 1998 to 2001, PCV9 was found to be 83 % effective in reducing IPD from the serotypes contained in the vaccine [152]. The study also took into account HIV–positive infants, whose risk of vaccine–preventable IPD is approximately 60 times higher than HIV–negative children. This 9–valent vaccine was found to be 65 % effective in combating IPD in these subjects. Whilst these values are lower than for HIV–negative subjects, the actual reduction in pneumonia would be 15 times greater than the HIV–negative children due to the higher risk of HIV–positive children [52, 121]. An added advantage of this vaccine was that it prevented 31 % of pneumonia associated with respiratory infections most common in South African hospitals [152]. The vaccine was also found to be 67 % effective against penicillin resistant IPD–causing pneumococcal strains and 56 % effective against trimethoprim–sulfamethoxazole resistant strains [153].

The Gambian trial of PCV9 was conducted from 2000 to 2004 and was used to investigate the efficacy against invasive pneumococcal disease. Children aged 6 – 51 weeks were given three doses of either PCV9 or a placebo. The vaccine was found to be 77 % effective against IPD caused by the nine serotypes included in the vaccine as well as 50 % effective against disease caused by all serotypes (measured by ELISA) [154, 155]. The 9–valent pneumococcal conjugate was shown not only to be effective against bacterial pneumonia but, in some instances, it provided protection against viral pneumonia [121]. Serotype 1, presented a problem in this study where cases of invasive diseases caused by Pn1 showed no reduction in vaccinated children compared to the placebo subjects [154, 155]. A trial in South Africa which looked at the 9–valent conjugate vaccine in HIV and non–HIV infected children also resulted in no levels of protection against serotype Pn1 [153]. Both of these outcomes were based on a small number of subjects and full conclusions about the efficacy of the Pn1 serotype could not be drawn.

The PCV11PD vaccine underwent clinical trials in the Czech and Slovak Republics to determine the vaccine's efficacy against OM in children between 2000 and 2002 [156, 157]. The vaccine was found to reduce middle ear infections caused by *S. pneumoniae* by 52.6 % and 35.3 % of infections caused by non–typeable *Haemophilus influenzae* (due to the protein carrier). Cross protection for non–vaccine serotypes was not identified. This vaccine did not go into production and instead a 10–valent vaccine conjugated to three different protein carriers was developed [20].

PCV11DT, from Sanofi Pasteur, underwent clinical trials in the Philippines during a time span of four years (2000 – 2004) [158, 159]. Young children were vaccinated with three doses of either the 11–valent vaccine or a saline placebo. The vaccine efficacy was investigated as well as safety and immunogenicity data. The vaccine provided a 22.9 % reduction of community acquired pneumonia in children less than two years of age. However there was no data to support the notion that the vaccine protected against clinical pneumonia [158]. The immunogenicity of this 11–valent vaccine co–administered with other vaccines was also determined. When PCV11DT was co–administered with a diphtheria–tetanus–pertussis, polio and Hib (polyribosyl–ribitol–phosphate conjugated to TT (PRP–TT)) vaccine, the response of the serotypes conjugated to tetanus toxoid (TT) was significantly reduced after both primary and booster vaccinations. This reduction did not occur in the four serotypes conjugated to DT and it was hypothesised that the tetanus protein had a suppressive effect on the pneumococcal conjugates [160].

Based on the immunogenicity and efficacy data of two PCV7 trials [123, 126] and the PCV9 South African trial [153], it was determined that licensure of any new pneumococcal vaccines should be based on immunologic non–inferiority, safety and use with co–administered vaccines in comparison to PCV7 [161, 162]. From these trials it was determined that the threshold antibody concentration to be used as a reference would be 0.35 µg/ml for ELISA assays and for ≥8 OPA results which correlates to the efficacy against IPD [163], thus a vaccine is proven to be effective and can be licensed if subjects reach an antibody titre of 0.35 µg/ml [20].

Following these trials, both GlaxoSmithKline and Pfizer released multivalent pneumococcal conjugate vaccines; Synflorix and Prevnar–13.

1.6.3.3 Synflorix

GlaxoSmithKline (GSK) marketed the 10–valent conjugate vaccine Synflorix (PHiD–CV/PCV10), in 2009, as a second generation conjugate vaccine that included the three serotypes 1, 5 and 7F in addition to the seven found in Prevnar. Synflorix also used three protein carriers, DT, TT and Protein D. Protein D was a new carrier protein, derived from

non–typeable *Haemophilus influenzae* and is produced from a recombinant *E. coli* strain [164].

Serotype 18C was conjugated to TT and serotype 19F to DT [165]. Protein D was used as the carrier protein for eight (serotypes 1, 4, 5, 6B, 7F, 9V, 14 and 23F) out of the ten serotypes, due to its potential to provide protection against acute otitis media caused by non–typeable *Haemophilus influenzae*. Due to the novelty of Protein D as a carrier protein it was thought to minimise the risk of interference (immune suppression due to epitope suppression and bystander interference) shown with proteins that were similar to an antigen included in some co–administered vaccines [156].

GSK produced a pneumococcal conjugate vaccine based on the conjugation method developed during their Hib studies. The conjugation procedure included a polysaccharide size reduction step by microfluidization followed by the activation of the PS with 1–cyano–4–dimethylamino–pyridium tetrafluoroborate (CDAP) before coupling the PSs to the three proteins [166].

Synflorix was originally formulated as an 11–valent vaccine as it included serotype 3 but this serotype was removed from the final licensed product as it was shown not to be effective against acute otitis media caused primarily by this serotype. An atypical immune response was shown for serotype 3 as antibody concentrations after a booster dose were below those generated after the first vaccine dose [157, 167].

A total of 14 clinical studies were used to provide support for the vaccine's 10 valent licensure with two studies from the 11–valent vaccine also made available to support the licensure [164]. A non–inferiority study was performed to compare PCV7 with Synflorix [168]. The test subjects were vaccinated with three doses of either Prevnar or Synflorix followed by a fourth booster dose 8 – 14 months following the last vaccination. OPA as well as serotype specific responses were monitored. It was found that PCV10 induced ELISA and OPA antibodies for all of the serotypes in the vaccine. The vaccine was also shown to be non–inferior to the seven serotypes in Prevnar in terms of the threshold responses for ELISA and OPA. However serotypes 6B and 23F in Synflorix showed lower ELISA levels than those of Prevnar (difference greater than 10 %) yet the OPA results backed up the non–inferiority claim for those two serotypes. The three additional serotypes, Pn1, Pn5 and Pn7F were also tested for antibody production. Subjects were first primed with the PCV7 vaccine and then given PCV10 as a booster dose. Approximately 85 % of subjects reached the ELISA threshold response for serotypes 1 and 5 and 95 % of subjects for Pn7F. The OPA results however were very low (Table 1.8) and it was not known whether these responses were of a sufficient value for PCV10 to provide protection against the serotypes 1 and 5 with just one

dose. With respect to Pn1, it has not been proven whether the conjugation strategy gives rise to a poor immune response or whether the protein carrier itself (Protein D) is not compatible with this specific serotype [10].

Table 1.8. Percentage of subjects reaching the threshold value for OPA for all serotypes in PCV10 after first priming with PCV7 followed by a booster dose of PCV10 [164].

Serotype	PCV7 primed + PCV10 booster
1	31.4
4	100
5	36.9
6B	94.9
7F	98.3
9V	100
14	100
18C	98.3
19F	98.3
23F	98.4

In accordance with the WHO requirements, a range of clinical studies of Synflorix were performed with co–administered vaccines. PCV10 was co–administered with *N. meningitidis* [169, 170], polio [171], whole–cell pertussis vaccines [117, 172], and measles, mumps, rubella and chickenpox vaccine [173] where both the safety and immunogenicity of the two vaccinations were maintained. PCV10 was also co–administered with the Hib vaccine in Korean infants and was found to be non–inferior to PCV7 [174]. Bermal *et al*. looked at the comparison of the co–administration of either PCV7 or PCV10 with the diphtheria–tetanus–whole cell pertussis based vaccines in Filipino and Polish children [171] and the ELISA results suggested that five of the seven serotypes reached the threshold percentages for non–inferiority (the exceptions being serotypes 6B and 23F in the Polish group) and that in both countries, PCV10 showed higher antibody titres against Pn18C and 19F than those in the PCV7 group. The majority (98.2 %) of infants vaccinated with PCV10 reached threshold titres against serotypes 1, 5 and 7F. The PCV10 vaccine increased the serotype coverage against IPD to 80 % or more in most regions (Figure 1.15) [48, 57].

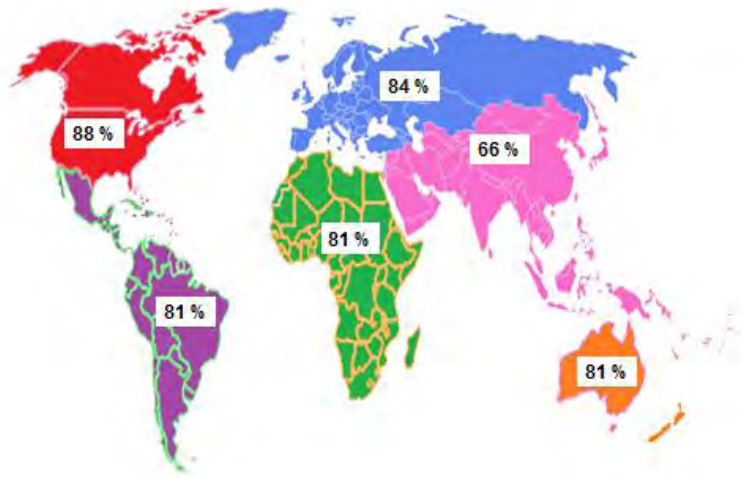

Figure 1.15. Predicted coverage of PCV10 [48, 57]. Modified from PneumoAction [143].

1.6.3.4 Prevnar13

By 2010, Pfizer had licensed their 13–valent vaccine that included serotypes 1, 3, 5, 6A, 7F and 19A in addition to those covered in PCV7 [175]. Initially it was thought that serotypes 6B and 19F would cross protect for serotypes of the same group but incidences of 6A and 19A were found to increase after PCV7 was licensed. These two serotypes are associated with high rates of antibiotic resistance and accounted for more cases in Europe and America of invasive disease than serotypes 1, 3, 5, and 7F combined (8.2 vs. 3.3 cases/100,000 children 2 years and under). Given the relative burden and importance of invasive pneumococcal disease due to serotypes 1, 3, 5, 6A, 7F, and 19A, adding these serotypes to the Prevnar formulation would increase coverage for invasive disease to >90 % in the US and Europe, and as high as 70 – 80 % in Asia and Latin America (Figure 1.16) [57].

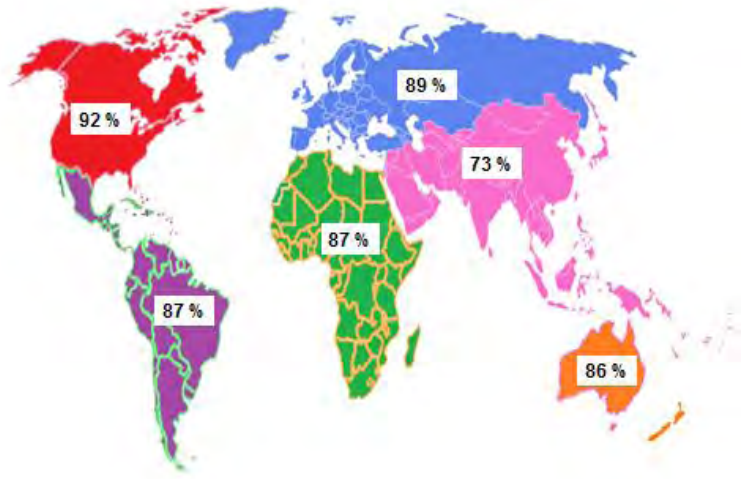

Figure 1.16. Predicted coverage of PCV13 [48, 57]. Modified from PneumoAction [143].

The method for conjugation used in PCV13 was based on the procedure followed for PCV7 and fourteen different clinical studies were used to support the licensure of this vaccine. Studies were performed to prove non–inferiority to PCV7 as well as the safety and immunogenicity and co–administration of the 13–valent conjugate vaccine.

The vaccine underwent adult clinical trials in the US, where a comparison was made between a single dose of either PCV13 or the 23–valent PS vaccine and antibody responses were measured before as well as one month after vaccination. The results showed that PCV13 was more immunogenic than the PS vaccine for most of the serotypes found in both vaccines [176]. A study of Japanese adults was undertaken and the same results were described with PCV13 being more immunogenic than the PS vaccine [177].

The German trial compared PCV13 vaccine to PCV7 in infants over four doses (Table 1.9). Whilst the antibody titres for all seven serotypes, found in both vaccines, were comparable, Pn6B results were lower in PCV13 with 77.5 % of infants reaching the threshold compared to 87.1 % of infants vaccinated with PCV7. The OPA results were slightly lower in all serotypes for PCV13 but all comparable to the 7–valent vaccine. The additional six serotypes elicited antibody and OPA responses considerably higher than the PCV7 vaccine [178].

Table 1.9. Comparison of the percentage of subjects reaching the threshold value for immunogenicity between PCV7 and PCV13 for serotypes not included in PCV7.

	German study [178]		**USA study [179]**	
Serotype	PCV7 (%)	PCV13(%)	PCV7 (%)	PCV13 (%)
1	1.4	96.1	12.0	98.9
3	6.3	98.2	43.8	97.8
5	31.6	93.0	5.2	98.9
6A	31.6	91.9	94.8	98.9
7F	4.0	98.6	80.4	100
19A	79.2	99.3	53.2	97.8

Non–inferiority was investigated in an additional US study where a three–dose schedule of PCV7 and PCV13 were compared one month after the last dose. Non–inferiority was confirmed for PCV13, although the threshold titres were slightly less than PCV7 for the seven common serotypes. The six additional serotypes, as expected, produced higher antibody titres in PCV13 when compared to the 7–valent vaccine. It was also shown that toddlers experienced higher immune responses than infants [179].

A Canadian study by Kellner *et al.* investigated the immunogenicity and tolerance of PCV13 co–administered with MMR, diphtheria–tetanus–acellular—pertussis–polio–Hib, hepatitis B, meningococcal C and varicella vaccines and compared to PCV7 in both infants and toddlers. Immune responses of the co–administered vaccines did not change when co–administered with the pneumococcal conjugate vaccines. One month after a three dose regime, more than 95 % of subjects had reached the threshold antibody level except for serotypes 23F (90 %), 5 (85 %) and 3 (80 %) and all but serotype 3 had reached 98 – 100 % efficacy levels [180, 181].

When PCV7 was introduced, there was some cross protection for serotype 6A (70 %) from serotype 6B (which was included in PCV7). PCV13 included both serotypes 6A and 6B and Cooper *et al.* investigated whether cross protection would transpire for serotype 6C [182]. The results suggested that 100 % of subjects reached the threshold of OPA responses for serotype 6A and 6B and 96 % of the subjects reached the OPA threshold for serotype 6C suggesting that PCV13 could provide cross protection serotype 6C.

Due to their recent market release, efficacy data on both the 10 and 13 valent vaccines is limited, and there are only a few investigations comparing the two vaccines. One investigation compared the coverage that the three PCVs had against IPDs in children less than 5 years of age as shown in Figure 1.17 [183]. A predicted increase from 48 % to 76 % and 79 % of coverage against IPDs in Africa had been achieved with PCV7, PCV10 and PCV13 respectively. This value is globally predicted to rise from 50 % with PCV7 to 75 % with the introduction of PCV10 and 77 % with PCV13. PCV13 would significantly expand coverage beyond that of Prevnar7, and provide coverage for 6A and 19A that is not dependent on the limitations of serotype cross–protection.

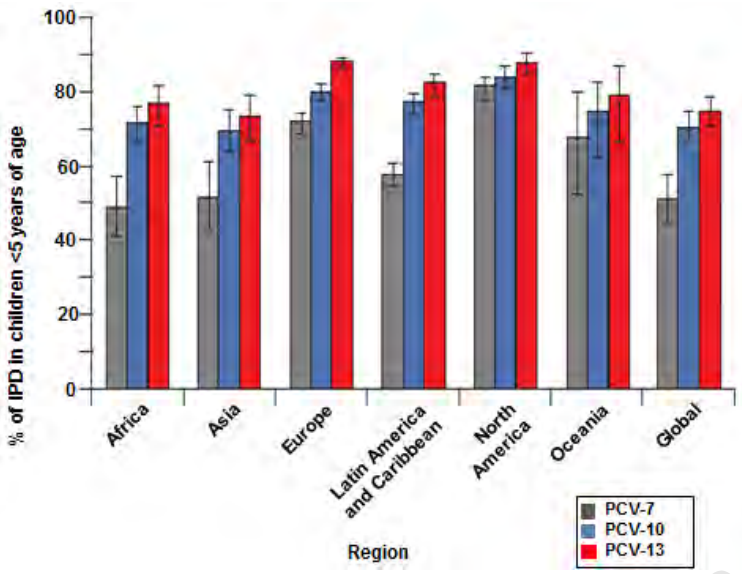

Figure 1.17. Proportion of IPDs in children under 5 years of age predicted to be due to serotypes included in the 7– 10– and 13 valent formulations [183].

1.6.4 Pneumococcal vaccines in development

Merck is currently developing a 15–valent pneumococcal conjugate vaccine containing the same serotypes covered in PCV13 with the addition of serotypes 22F and 33F. At the time of writing, the 15–valent conjugate vaccine had undergone preclinical evaluations in infant rhesus monkeys. These animals were chosen as they respond poorly to unconjugated pneumococcal PS [117, 184]. Infant rhesus monkeys were vaccinated three times with either PCV15 or PCV7 at 2 month intervals, and serotype–specific IgG antibodies were measured. The results indicate that antibody responses to PCV15 and PCV7 are comparable for the 7 common serotypes and that post–vaccination responses to PCV15 were >10–fold higher than baseline for the 8 additional serotypes [184].

The vaccine has also been tested in healthy human adults where IgG levels were again comparable to PCV7 with an increase in antibody levels amongst the eight additional serotypes of between 3– and 13– fold [185]. Limited information is available on the trials in toddlers, that had been previously immunised with PCV7 and received a dose of PCV15, although a conference abstract suggests that IgG concentrations and OPA levels increased after vaccination for all serotypes [186].

The increase in the number of serotypes in a conjugate vaccine increases the protection against pneumococcal diseases, but as with Prevnar, serotypes not included in the vaccine become more prevalent. In addition to this, the cost of producing a conjugate vaccine with more and more serotypes becomes very high, as does the complexity with conjugation chemistries, formulations and clinical trials [134, 187]. Therefore vaccines being investigated are composed of proteins and other components that are common across all pneumococcal

serotypes [10, 20]. A protein antigen that is expressed in all stages of pathogenesis of the disease, is found in all serotypes and is present on the cell surface would be the ideal protein for further investigation. Unfortunately, a single protein is not able to fulfil all the criteria and a protein vaccine would most likely contain a number of different pneumococcal proteins; Moffit and Malley found over 20 different pneumococcal proteins that would fulfil these criteria [129]. Moffit *et al.* investigated immunisation with killed cells of a non–encapsulated strain which would contain all the pneumococcal surface proteins without their protective capsular PS. One investigation determined that the non–encapsulated strain reduced nasopharyngeal colonisation by serotypes 6B and prevented cases of fatal aspiration pneumonia by serotypes 3 or 5 [188].

1.6.5 Pneumococcal serotype 1

Serotype 1 is responsible for up to 20 % of IPD in some developing countries and was the cause for several outbreaks in the African meningitis belt. It is ranked among the top three ranked serotypes in GAVI–eligible countries and is among the top six ranked serotypes among children under 5 years of age in regions with the highest pneumococcal disease burden (e.g. Africa, Asia and Latin America) [55]. Serotype 1 has the potential to cause epidemics and it was the cause of meningitis outbreaks in Burkina Faso and Northern Ghana [149, 189, 190].

The epidemiology of Pn1 disease shows that the infections occur in two different age ranges. The first age range occurs in children over two years of age which is in contrast to the age of 6 – 18 months, typical of IPD from most other serotype infections. Serotype 1 is rarely found in carriage studies as it is not found in the nasopharynx but is most commonly isolated in the blood, which shows an indication of its invasiveness.

The failures of Pn1 in the 9–valent trials may not be associated with the failure of the primary vaccine but could be due to a reoccurrence of the infection in the absence of a booster dose. This phenomenon has been documented in meningococcal serotype C conjugate vaccination without a booster dose [191].

Although there is limited data available regarding the immunogenicity of Pn1 conjugate vaccines, during the clinical trials for the two licenced pneumococcal conjugate vaccines the OPA results against serotype 1 were lower than most other serotypes and no data is available regarding a booster dose of Pn1 vaccine.

1.7 Aim and objectives

Serotype 1 is a pneumococcal serotype that is often found in young children and adults and is responsible for invasive outbreaks in rural, indigenous areas and is one of the most prevalent serotypes in Africa and other developing regions. With the introduction of multivalent conjugate vaccines, the frequency of Pn1 infections was expected to decrease; however, literature to date suggests that the conjugate vaccine against Pn1 is not as effective as against other serotypes. Due to the unique epidemiology of pneumococcal serotype 1, a different strategy to aid in epidemic control would be required.

The aim of this research project was to develop a process for the efficient purification of Pn1 polysaccharide and the preparation of an immunogenic conjugate with the overall goal of producing a monovalent serotype 1 vaccine that could either be used alone, as a booster dose or in combination with a meningococcal vaccine that would have great value in the African meningitis belt and among indigenous communities.

In order to achieve this aim, the specific objectives of this study were:

i. To develop an efficient process for the isolation and purification of Pn1 polysaccharide using a modified method of differential filtration with ethanol.
ii. To establish characterisation assays of the polysaccharide with respect to the WHO specifications including identity, composition, size analysis and purity (nucleic acids, proteins and CWPS).
iii. To perform detailed structural characterisation of the purified polysaccharide using a range of chromatographic and spectroscopic methods.
iv. To investigate size reduction by mechanical and chemical means to prepare Pn1 saccharide that would be amenable to conjugation chemistry and NMR characterisation.
v. To establish methods for the hydrazide–derivatization of carrier proteins BSA, TT, CRM_{197} and PLD.
vi. To investigate an alternate conjugation chemistry to that used commercially by utilising the Pn1 polysaccharide carboxyl groups and carbodiimide–based coupling to the derivatized protein carriers.
vii. To evaluate the immunogenicity of the prepared conjugates in mice using commercially available conjugate vaccines as comparators in order to identify the best conjugation methodology and carrier protein for further vaccine development.

CHAPTER 2. GENERAL METHODS

2.1 Fermentation of Pn1

Clinical isolates of *Streptococcus pneumoniae* serotype 1 were obtained from the National Institute of Communicable Diseases (NICD). A selection of these clinical isolates underwent clonal selection and the clonal isolate producing high levels of capsular polysaccharide and low levels of CWPS was chosen for PS production. A laboratory working seed was prepared from the chosen clonal isolate which was used to inoculate a volume of sterile growth medium which was incubated under the appropriate, pre–determined conditions. This starter culture (20 ml) was used, in turn, to inoculate a starter culture (200 ml) that was inoculated into a larger culture before a final inoculation into the fermentor [192]. This fermentation process is shown in the process flow in Figure 2.1. Small scale cultivations (2 – 5 L) were used to develop the media composition as well as certain process parameter optimisations. Process and feeding strategies were developed in a Wave Bioreactor, making use of a disposable cell culture system [193]. At the end of the fermentation process, the broth was inactivated with phenol, harvested and clarified by centrifugation before downstream processing (purification) was carried out.

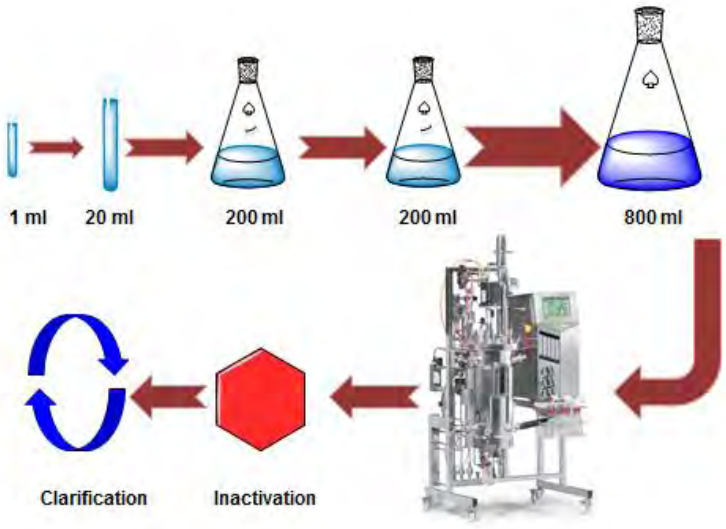

Figure 2.1. Outline of the process stages for the fermentation of a single fermentor batch of Pn1. Initially 1 ml of the laboratory working seed was used to inoculate a small amount of media (20 ml). This process was repeated in order to scale up the starter culture (800 ml). This was finally inoculated into several litres of medium (7 L in Wave bioreactor and between 15 – 30 L in fermentor). After fermentation, the broth was inactivated and clarified before purification can continue.

2.2 Purification of Pn1

Purification of Pn1 was based on the procedure described by Robert Liveyns *et al.* in 1989 where increasing ethanol concentrations was employed [194]. The general method of purification is described and deviations from this method will be further detailed in Chapter 4, Section 4.1.

A schematic representation of the purification process can be found in Figure 2.2. The inactivated fermentation broth was first clarified via centrifugation to a predetermined level. Following clarification, the supernatant was diafiltered (100 kDa membranes) against 25 mM sodium acetate (NaOAc), to remove all media components and other impurities, and concentrated down to approximately 6 L. The pH of this solution was adjusted to 7.8 with sodium hydroxide (3.5 M NaOH) and 18 g/L cetyltrimethylammonium bromide (CTAB) was added in sufficient quantities to precipitate out the polysaccharide. 93 g/L Celite was added to trap the newly formed PS–CTA^+ salt and this slurry was stirred for 5 minutes before being allowed to settle. Rate nephelometry was used to determine the amount of PS left in the supernatant after CTAB precipitation. The Celite slurry was loaded onto a Millipore VANTAGE™ Chromatography column (internal diameter: 127 mm, cross sectional area of 125 cm^2, with an adjustable bed height) and washed with an acetate buffer containing a small amount of CTAB (0.05 %) to trap any PS that may still remain in solution as well as to remove any excess cell debris and media that may remain. Increasing concentrations of ethanol (EtOH) were applied to the column, starting at 5 % and increasing up to 60 %, to elute off the PS. A flow rate of 60 – 80 ml/min was maintained throughout the elution process. Fractions of each ethanol wash were collected and monitored for aggregates at 550 nm and nucleic acids and proteins at 260 and 280 nm respectively. Polysaccharide elution was monitored using the uronic acid assay where the formation of a purple coloured complex was indicative of Pn1 elution. The fractions that tested positive for Pn1 were pooled together and solid sodium chloride (NaCl) added to produce a final concentration of 2 M NaCl. The PS was precipitated after a 1:1 volume of 96 % EtOH and the purified Pn1 was left at 0 – 4 °C overnight to allow for complete precipitation. The precipitated slurry was centrifuged for 10 min at 3500 rpm and the supernatant decanted. The wet pellet was dissolved in 125 ml water, diafiltered against seven volumes of 0.5 M NaCl buffer followed by seven volumes of water using a Labscale™ TFF system fitted with 2 x 100 kDa molecular weight cut off (MWCO) 50 cm^2 membranes fitted in parallel. The final purified PS was concentrated down and stored at – 20 °C.

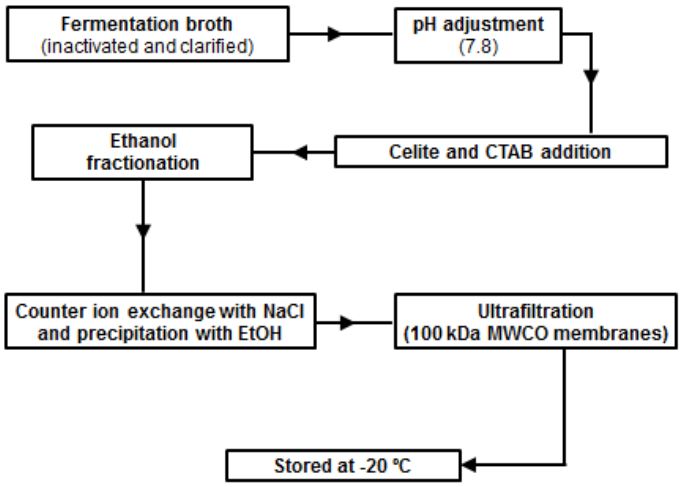

Figure 2.2. Process flow of the purification of Pn1 from the inactivated fermentation broth to final storage.

2.3 Colorimetric assays

Most carbohydrate and protein solutions in water are colourless. To determine their concentration in a solution, colorimetric assays have been developed. These colorimetric assays rely on a reaction between a reagent and the analyte in question. This reaction will produce a chromophore that can be measured at a specific wavelength. The concentration of the analyte in solution can be measured from the intensity of the colour using the Beer–Lambert law which relates the absorbance of the analyte to its concentration using Equation 2.1.

A cl Equation 2.1

Where A is a dimensionless number (often called absorption units), is the molar extinction coefficient which is structure, temperature and wavelength dependent, c is the concentration of the analyte in solution and l is the path length that the light must travel [195].

The ideal colorimetric reaction should be sensitive, selective and non–reversible. The resulting coloured product should be stable and should also be very different to the compound being examined. The main difficulty with colorimetric assays is their specificity. No single colorimetric assay is absolutely specific and many other compounds/molecules may interfere with the assay. These interfering compounds may react with the chromophore producing a coloured complex that will interfere with the absorbance of the compound tested. A control blank, whose absorbance is subtracted from the analyte absorbance, is used to compensate for this interference. A control blank contains all compounds found in tested solution except for the analyte being tested.

All incubations, other than those performed at room temperature, made use of a Stuart heating block that was able to reach temperatures of 200 °C. All absorbances measured in the colorimetric assays were determined using a Shimadzu UV–Vis 1700 Spectrophotometer with UV Probe 2.2.1 software.

2.3.1 Uronic acid assay

Saccharide concentrations for Pn1 were determined with the uronic acid colorimetric assay. The Dische carbazole protocol [196, 197] is a widely used method for the conversion of uronic acids into 5–formylfuronic acid by heating under strongly acidic conditions. The reaction of 5–formylfuronic acid with carbazole yields a pink coloured complex with an absorption maximum at 530 nm as shown in Figure 2.3.

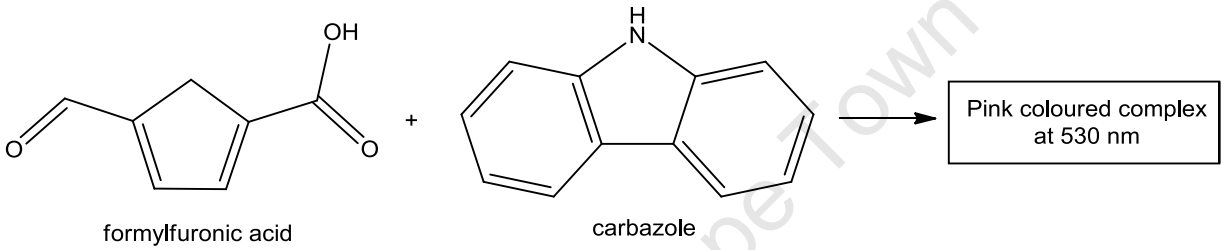

Figure 2.3. Schematic of the hydrolysed saccharide reaction with carbazole.

A modification of the Dische carbazole reaction for uronic acid in the presence of borate was developed and published in 1962 by Bitter and Muir [198]. The advantages of this modified procedure are:

- An approximate two fold increase in sensitivity.
- Maximum colour develops immediately.
- The colour is stable for at least 16 hrs.
- Improved reproducibility and reduction in interferences by chlorides and oxidants.

As Pn1 contains a galacturonic acid moiety in its repeating unit, the method was modified from the published method to use galacturonic acid as a standard instead of glucuronic acid. This standard was used to create a reference curve in the range of 0 – 50 µg/ml and water was used as a blank sample. The final volume of all of the solutions was 150 µl. All solutions were placed on ice and 900 µl of a 0.025 M solution of sodium tetraborate in concentrated sulfuric acid was added. Samples were incubated at 100 °C for 5 min to allow for hydrolysis to occur. After the samples were removed from the heat and cooled to room temperature, 30 µl of a 0.125 % solution of carbazole in ethanol was added and the samples were incubated for a further 15 min at 100 °C. The solutions were cooled to room temperature where the absorbances at 530 nm were recorded. A calculated correction factor of 1.5 was applied to all samples containing Pn1 to convert the amount of uronic acid in the

polysaccharide to the total amount of polysaccharide; this calculation is explained in Chapter 3, Section 3.3.1.2.

2.3.2 *O*–Acetyl Assay

The *O*–acetyl content of Pn1 was determined using the Hestrin method [199]. This is the preferred method for determining the concentration of *O*–acetyl groups present on a long–chain polysaccharide repeating unit. *O*–acetyl groups are released from the PS under alkaline conditions by hydroxylamine and converted to hydroxamic derivatives (Figure 2.4). These derivatives are complexed with ferric chloride to give a yellow complex that is detected using a spectrophotometer at 540 nm [200]. In order to account for interferences, a correction blank is also employed. In this case, the PS is reacted with hydroxylamine under acidic conditions. As hydroxamic derivatives are only formed under alkaline conditions, the generation of colour from the addition of ferric chloride will be indicative of interfering substances which will be corrected for.

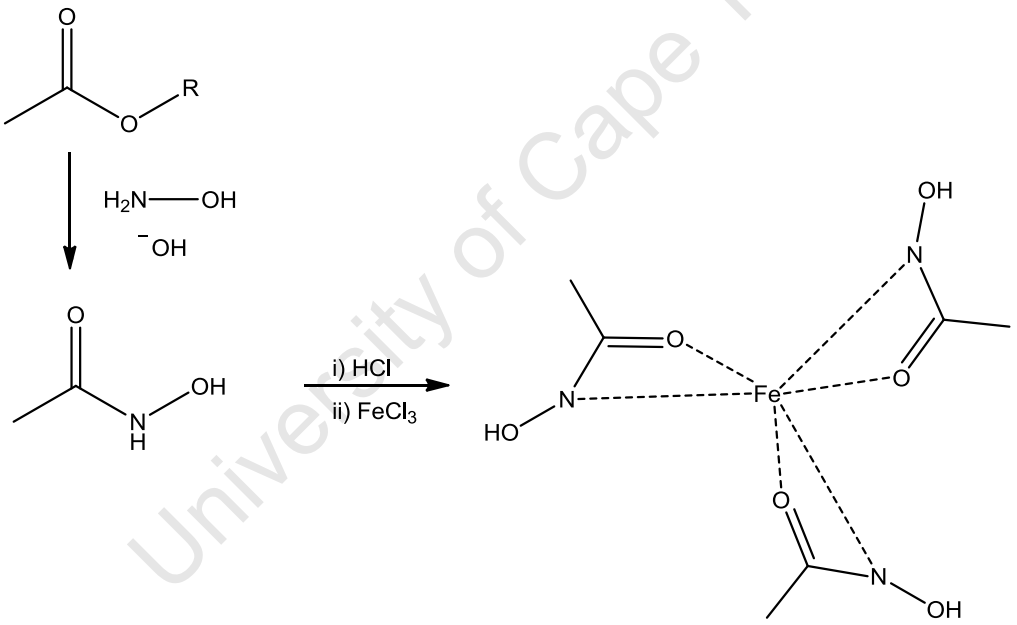

Figure 2.4. Schematic representation of the reaction of *O*–acetyl functional groups with hydroxylamine and the resultant reaction with ferric chloride.

Pn1 has both *O*–acetyl and *N*–acetyl groups on its repeating unit. *O*–acetyl groups are the more labile and are liberated in cold, dilute base, whereas *N*–acetyl groups require much stronger alkaline conditions for release. In order to calculate the mass percentage of *O*–acetylation on the PS, the concentration of the PS is determined and the percentage *O*–acetylation is calculated using Equation 2.2.

$$\text{Acetylation} \quad \frac{\text{concentration from acetyl assay}}{\text{concentration from uronic acid assay}} \quad 100 \qquad \text{Equation 2.2}$$

Acetylcholine chloride was used as the standard. One mole of acetylcholine chloride is equivalent to one mole of *O*–acetyl. A standard curve was created in the concentration range of 0 – 600 µg/ml and water was used as the blank sample. The final volumes of all samples were 500 µl. All samples and standards were tested in quadruplicate; two of each solution were labelled as reaction samples and the remaining two were used to correct for the interference (known as correction samples). The reaction standards and samples were treated as follows: 1.0 ml of 1 M hydroxylamine in 1.75 M NaOH was added to all solutions and left to react for 2 minutes where after 500 µl of a 4 M HCl solution was added and the solutions were shaken to ensure mixing. The correction solutions were treated slightly differently as first 500 µl of a 4 M HCl solution was added to all the solutions to make them acidic and hence block the formation of the hydroxamic derivatives. 1.0 ml of the 1 M hydroxylamine in 1.75 M NaOH solution was added to each correction solution. To both the reaction and correction solutions 500 µl of a 0.37 M ferric chloride ($FeCl_3$) in 0.1 M HCl solution was added with vigorous shaking. These solutions were left to react at room temperature for 20 minutes and vortexed to allow for the release of any bubbles that may have formed. The absorbance was read at 540 nm. The absorbance values for the correction tubes were subtracted from the reaction tubes to provide a final absorbance value corresponding to the amount of *O*–acetyl groups.

2.3.3 UV protein assay

This assay was specifically applied to the determination of protein concentration of TT and was performed by monitoring the UV absorbance at its maxima wavelength of 279 nm. Absorption by proteins in the UV spectrum, specifically at 260 – 280 nm, depends on the amount of tyrosine and tryptophan residues contained in the protein itself. Phenylalanine as well as disulfide bonds also absorb at 280 nm but to a small extent [201, 202]. The advantages of the UV absorption method are that it is both simple to perform and non–destructive to the sample. The protein concentration (in mg/ml) is calculated using Equation 2.3.

$$\text{Protein concentration} \quad \frac{A_2}{l} \quad w \qquad \text{Equation 2.3}$$

Where Mw is the molecular weight of the protein, A_{279} is the absorbance value at 279 nm, Ɛ is the extinction coefficient (in $M^{-1}cm^{-1}$) and l is the path length (1 cm). The extinction coefficient of TT is 185 210 $M^{-1}cm^{-1}$ [203] and its molecular weight is 150 kDa.

2.3.4 Bradford (Coomassie) protein assay

All protein concentrations, except for TT, were determined with the commercially available Bradford (Coomassie) assay kit [204]. This colorimetric method does not require the molar extinction coefficient of the protein to be known as it depends on the Coomassie Blue G250 dye binding to the protein. This binding, which can only occur in an acidic environment, results in a spectral shift from the red/brown colour of the dye absorbing at 465 nm to 610 nm producing a blue coloured complex. The difference between the two coloured solutions is greatest at 595 nm at which the absorbance is read. The binding of the protein to the dye is a result of hydrophobic interactions as well as van der Waals forces between the dye and certain basic amino acids (arginine, histidine and lysine). The number of these dye–amino acid linkages is approximately proportional to the total number of positive charges on the protein [205]. Low molecular weight proteins (under 3 kDa), free amino acids and peptides do not produce a colour with the Coomassie dye and hence are not interfering substances in this assay.

The reference curve was constructed with bovine serum albumin (BSA) in the concentration range of 25 – 2000 µg/ml. 30 µl of standard and prediluted sample were used, water was used as a blank sample. 1.5 ml of Coomassie reagent was added to each tube and mixed together. The solutions were left to react at room temperature for 10 minutes followed by the absorbance determination at 595 nm.

2.3.5 Trinitrobenzenesulfonic acid assay

In order to measure the amount of hydrazides coupled onto the carboxyls of the protein after protein derivatization, the trinitrobenzenesulfonic acid colorimetric assay was performed. This assay makes use of the 2,4,6–trinitrobenzene sulfonate (TNBS) reagent that was introduced as a colour reagent for amino acid analysis in 1960 by Satake [206]. TNBS is water soluble and does not react with ammonia or urea. TNBS reacts, under mild alkaline conditions, with amino groups via a Meisenheimer complex intermediate (Figure 2.5), to produce a coloured complex. The absorbance is measured at 550 nm as other amino groups will absorb at 340 and 420 nm [206].

This reaction distinguishes between hydrazine and hydrazides by the specific absorbance maxima of each complex. The TNBS–hydrazine complex has its absorbance maxima at 570 nm whereas hydrazides absorb most strongly at 550 nm. Amino acids do not interfere with this assay as the absorbance maxima for these complexes are approximately 420 nm [207].

The absorbance of the coloured complex is measured at 550 and 750 nm. During the calculations, the absorbance at 750 nm is subtracted from the 550 nm reading. This is to correct for the interference that light scattering has on the absorbance values [208].

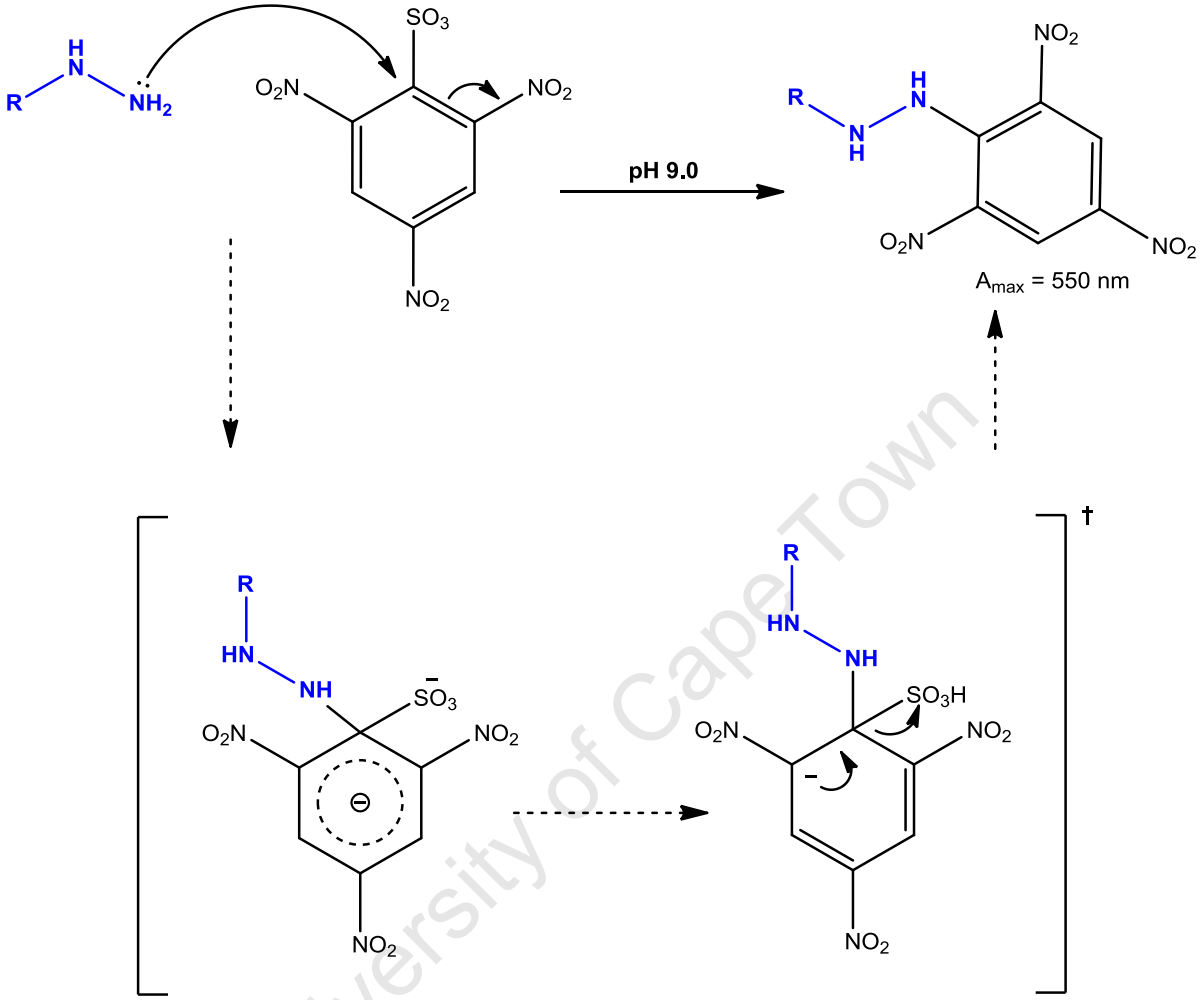

Figure 2.5. Schematic of reaction of hydrazide derivatized protein with TNBS, formation of a Meisenheimer complex intermediate and final complex formation.

Adipic acid dihydrazide (ADH) was used to construct the standard curve. As ADH contains a hydrazide grouping at each end of the molecule the molar concentration of hydrazides is double the molar concentration of ADH. The assay was performed in a 96 well microtitre plate. In the first two wells 100 µl of 2.5 mM ADH in water was added. The next two wells contained 100 µl of the sample to be tested and the last two wells used contained 50 µl of water. 50 µl of water was added to the remaining rows. 50 µl of each mixture from row 1 was transferred to the row 2 and mixed. This process was repeated for all rows in the well plate to create a dilution series. 100 µl of 0.1 N borate buffer (pH 9.0) was added to all the wells followed by 50 µl of a 0.1 % TNBS solution. The 96 well plate was covered and incubated at room temperature for 2 hours. The absorbance was read at 550 and 750 nm [209].

2.4 Immunological Assays

Biomolecular recognition is the ability of one biomolecule to interact with another specific type of biomolecule similar to a key fitting into a lock. The principle of biomolecular recognition is the basis for most immunological assays. In immunoassays the molecular recognition is between an antibody and an antigen which are the two fundamental molecules in the immune system. Both antibody (Ab) and antigen (Ag) cells contain recognition sites; if the recognition site of the antibody matches the recognition site of the antigen a Ab–Ag complex is formed. As the antibody will only react with a specific antigen, other antigens in the reaction mixture will remain unbound which creates high specificity in this form of analysis. In this way, no sample pre–treatment is needed [210]. Two different types of immunoassays were applied in this investigation, namely enzyme–linked immunosorbent assays (ELISA) and nephelometry.

2.4.1 ELISA

Enzymes are the most widely used labels in immunoassays. The enzyme label will act as a catalyst for the conversion of a colourless substance to a coloured product that can be detected at a particular wavelength. As the enzyme acts as a catalyst, only a small quantity is needed to convert a large number of substrate molecules, which would generate a large signal. ELISA can be classified into four main groups: direct, indirect, sandwich and competitive [211]. The competitive ELISA was used in these investigations.

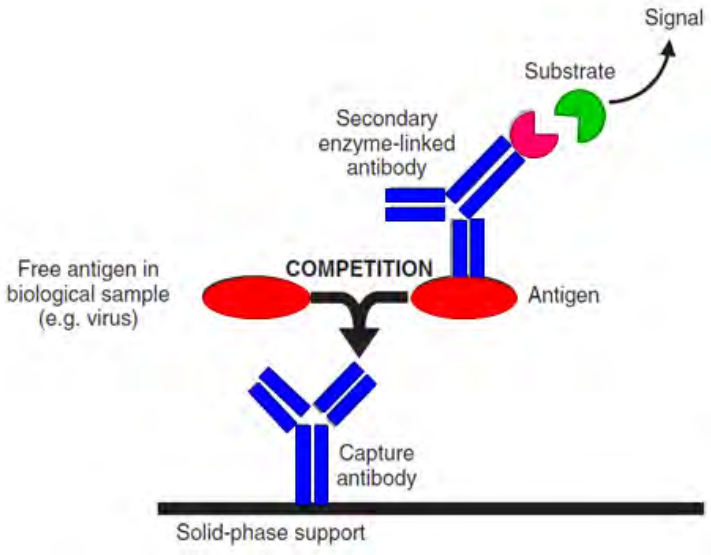

Figure 2.6. Pictorial representation of a competitive ELISA [212].

In competitive ELISA, as shown in Figure 2.6, the microplate is first coated with an antibody that is specific for the analyte being measured. The quantifiable analyte (antigen) is added to the plate along with an enzyme coated antigen which competes for the binding site of the antibody. After washing, to remove any unbound antigen, a colour reagent, that is specific to

the enzyme, is added and the absorbance measured. The intensity of the colour is proportional to the amount of enzyme added and is therefore inversely proportional to the amount of analyte present [212, 213].

100 µl of Pn1 PS immobilised antigen (1.5 µg/ml in PBS) was added to all wells of a 96 well plate (ELISA Plates F96 Maxisorp 96 well plates). The plate was covered and incubated overnight at 4 °C. Thereafter the plate was washed in a Biotek Platewasher with 0.03 % Tween 20 in PBS. 200 µl blocking solution (3 % BSA in PBS) was subsequently added and left to react for 1 hour at room temperature. The plate was washed with 0.03 % Tween 20 in PBS. One row acted as a negative control (water) and two rows acted as positive controls containing 50 µl of a 1.5 µg/ml Pn1 reference standard. 50 µl Ab/Ag diluent (0.3 % BSA in PBS) was added to the rows followed by 50 µl of sample that was diluted down throughout the sample rows. 50 µl of Type 1 antiserum working reagent (Statens Serum Institute (SSI), Cat No. SSI–AGGL–16744) was added to all wells and the plate was covered and incubated for one hour at room temperature. The plate was washed with 0.03 % Tween 20 in PBS and 100 µl goat antirabbit horse radish peroxidase (HRP) (Whitehead Scientific, Cat No. 474 1506) conjugate working reagent was added to all wells. The plate was again covered and incubated at room temperature for 45 min and washed a final time with 0.03 % Tween 20 in PBS. 100 µl of TMB Sureblue substrate (Whitehead Scientific, Cat No. 52–00.01) was added and left to react for 15 minutes followed by 50 µl of 0.5 M H_2SO_4 to stop the reaction. The absorbance of the plate was read at 450 nm on a Biotek plate reader.

2.4.2 Nephelometry

The principles of nephelometry rely on interactions between antibodies and antigens. A single antibody is specific for one particular antigen and when these two come into contact they bind to each other strongly and form a cluster (immune complex) that aggregates thereby increasing the turbidity of the sample [214].

When light is passed through the reaction solution, light is either scattered, absorbed or passes through the sample. Figure 2.7 shows schematically how a nephelometer works. The light source is set at a wavelength of 635 nm and is fixed at an angle of up to 90 degrees [215]. The laser beam passes through the sample into a light detector known as an Ulbricht sphere. If the sample contains particles the light is scattered and reflected inside the sphere and detected through a photodiode. In order to prevent the occurrence of stray light, the light source is accumulated into a narrow beam of high power density that results in a higher scattered intensity from the smaller particles. There is also a light trap situated at the bottom of the instrument that absorbs the portion of unscattered light (light not deflected by the

particles in the sample) [216]. The amount of light scattered is proportional to the concentration of antigen or antibody in the solution [215].

Nephelometry is used in numerous applications, automated drug solubility screening, quantification of proteins such as immunoglobulins in serum, monitoring polymerization reactions, monitoring effluent as well as monitoring changes in turbidity to test antimicrobial drugs [214-216].

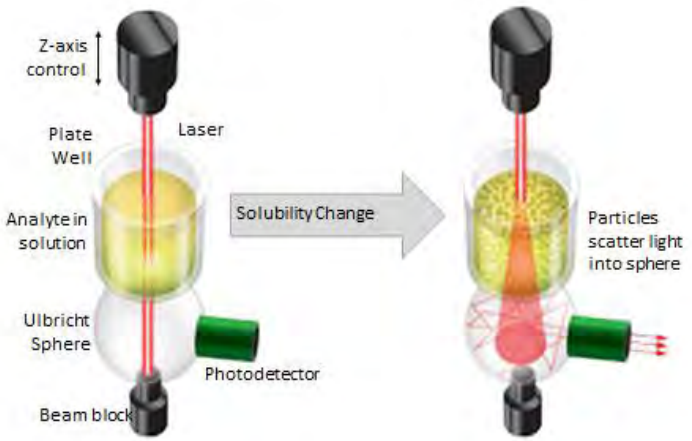

Figure 2.7. Schematic of the inner workings of a nephelometer [216].

Nephelometry can also be used to measure the change in intensity of the scattered light during the formation of the antibody–antigen complexes by measuring the kinetics of the binding reaction between the antigen and antibody [217]. Lee used nephelometry to determine both the PS and protein content in pneumococcal conjugate vaccines [218].

In this investigation, nephelometry was used during purification to determine the amount of PS left in the supernatant after CTAB precipitation. The procedure followed by the Immunochemistry group at The Biovac Institute is as follows: In a microplate, 10 µl of Pn1 working serum reagent (SSI, Cat No. 16744) was dispensed into all wells followed by 178 µl of 4 % polyethylene glycol (PEG) solution and mixed thoroughly. Pn1 standards and unknown samples are added and diluted down the rows. The plate was immediately analysed on the Nephelostar Galaxy nephelometer using software provided with the instrument.

2.5 Electrophoresis

Electrophoresis is the separation of macromolecules in an electric field. The capacity of an electric field to separate molecules carrying a charge is the foundation of electrophoresis. When an electrical field is applied between two electrodes, a charged molecule will be

attracted to the oppositely charged electrodes; i.e. a negatively charged compound will migrate towards the positive anode and the negative cathode will attract the positively charged molecules as shown in Figure 2.8 [210].

In biomolecule analysis the Lorentz force causes different molecules to move through the matrix under an electric field at different rates due to their net charges, masses and shapes [212]. The velocity of the molecule's movement increases with an increase in net charge and the electrical field strength, although friction acts as a counter measure and decreases a molecule's velocity. The frictional strength is primarily dependent on a molecule's mass and shape as well as the viscosity and porosity of the supporting matrix over which the electric field is applied [212, 219].

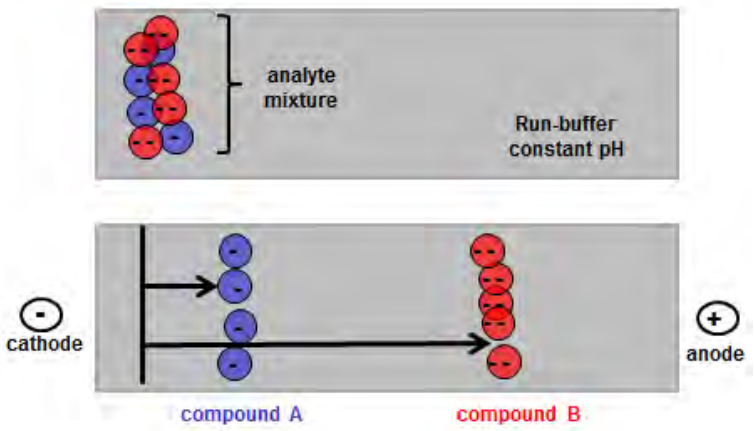

Figure 2.8. Schematic of electrophoresis [210].

2.5.1 SDS Page

One of the most common methods of separating proteins using electrophoresis is called sodium dodecyl sulfate polyacrylamide gel electrophoresis (SDS–PAGE). SDS–PAGE uses sodium dodecyl sulfate (SDS) to denature proteins and an electric field is applied across a polyacrylamide gel. The negative charges on the SDS destroy the complex structure of the proteins (denaturing them) and are attracted to the anode in the electric field. The protein will bind different amounts of the anionic detergent SDS depending on its relative molecular mass with SDS having a constant binding ratio of 1.4 g SDS to every gram of protein. Thus SDS–PAGE, with the inclusion of molecular markers can determine the relative size or difference in size of the proteins. The gels used for all SDS–PAGE experiments were Criterion XT 3 – 8 % Tris–acetate pre–cast gels based on a Tris–acetate buffer system (pH 7.0). These gels use discontinuous Tricine and acetate ion fronts that form moving boundaries that stack and separate the denatured proteins according to their relative molecular masses [212, 220].

This system used a pH neutral and stabilised solution of tris(2–carboxyethyl)phosphine as a reducing agent and a mixture of heat and SDS are used to denature the proteins. After the addition of the reducing agent and the SDS to the sample, it was heated at 95 °C for 5 min before being loaded onto the gel (Bio–Rad Criterion XT Tris–acetate 3–8 % resolving gel, Cat No. 345–9898). A XT Tricine Buffer kit (Bio–Rad, Cat No. 161–0797) was used for running buffer as well as the reducing agent. The gel was subjected to a constant electrical field of 150 V for 65 min with a starting current between 170 – 180 mA and a final current in the range of 85 – 95 mA [221]. Either of two different gel stains were used for detection: protein was detected using a Coomassie Blue R–250 stain and PS was detected using Schiff's stain (periodic acid) [221].

2.5.2 Western blot

The detection and identification of proteins is performed via a Western blot. Protein blotting is the transfer of proteins to a solid–phase membrane support. Once bound to membranes, these proteins can be used for biochemical or immunological analyses. The most commonly used protein blotting technique is known as Western blotting or immunoblotting. The two steps involved in Western blotting are the transferral of the proteins that have been separated via gel electrophoresis onto a membrane, followed by detection of the proteins by immunological methods. The membrane is composed of the hydrophobic polyvinylidene difluoride (PVDF) [221] that has a high protein binding capacity, target retention as well as a high resistance to cracking which makes it the preferred membrane for binding proteins. During the transfer the gel and membrane are sandwiched between filter paper and the two electrodes as shown in Figure 2.9 (all contained in a non–conductive cassette holder) and submerged under the conducting transfer buffer with an applied electric field [211, 222].

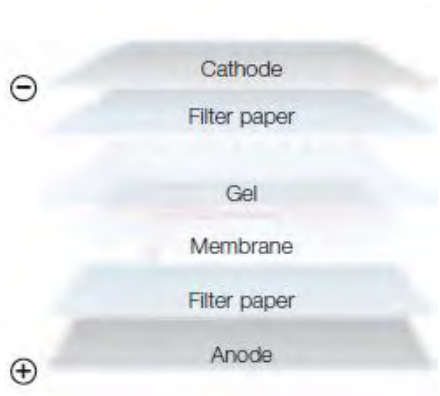

Figure 2.9. Schematic of the gel and membrane set–up for transferring proteins during Western blots [222].

The Western blot procedure was used, firstly, to separate protein components in samples obtained from downstream fermentation and secondly, to identify the proteins by use of an immunological detection system.

The membrane used was the Immun–Blot® PVDF membrane that was cut to approximately 13.5 x 9 cm. Due to the hydrophobic nature of PVDF, it was immersed in 100 % methanol for 2 minutes to pre–wet the membrane. The membrane was placed in cold transfer buffer (same buffer used to run the gels in SDS–PAGE (Section 2.5.1) for 10 minutes before the blotting sandwich was assembled as displayed in Figure 2.9. The sandwich was placed into the electrophoresis tank and run overnight at a maximum of 10 volts and 50 mA. The sandwich was disassembled and the membrane removed for detection. Detection was preceded by a blocking step in which the unoccupied binding site on the membrane were blocked to prevent any non–specific interactions. To do this the membrane was placed in Tris–buffered saline (TBS) for 10 min followed by 3 % bovine serum albumin (BSA) in TBS for 2 hours at 4 °C. The membrane was washed with Tween–20–TBS (TTBS) to remove any unreacted BSA. The membrane was incubated with a primary antibody (rabbit anti HIB (KPL, Cat. No. 4741506)) at room temperature for 2 hours and washed with TTBS to remove any unbound antibody. The membrane was incubated for a further hour at room temperature with a secondary antibody that was linked to horse radish peroxidase (HRP) (donkey anti rabbit HRP) (Jackson ImmunoReseach Laboratories, Cat. No. 711035152). Washing with TTBS followed by a wash with TBS (to remove traces of Tween) was performed and the membrane was incubated with Opti–4CN (Biorad, Cat. No. 170–8235) for 30 minutes at room temperature. Opti–4CN is an improved form of the colorimetric HRP substrate: 4–chloro–1–naphthol. A final wash was performed with deionised water before the membrane was dried between filter paper [223]. In the presence of HRP and peroxide, a water soluble blue product was generated that was precipitated onto the membrane where the enzyme was located, allowing visual detection of the target antigen sample [224, 225].

A molecular weight marker (PageRuler plus pre–stained protein ladder (10 – 250 kDa)) was employed for all western blot experiments. Western blots were also performed to ensure that the structural integrity of the protein after conjugation. In this case the procedure followed is as detailed above except that the antibody employed was rabbit anti–TT/DT or pneumolysoid (PLD) depending on the carrier protein and the secondary antibody used was Goat anti–rabbit IgG peroxidase (KPL, Cat no: 4741506) and the colorimetric substrate was 3,3',5,5'–tetramethylbenzidine (TMB) 1 component membrane peroxidase substrate (Sigma Aldrich, Cat. No. T8665).

2.6 Chromatographic methods

Chromatography is the most widely used method of separation in bioanalytical chemistry. There are numerous chromatographic methods available that make use of the different chemical and physical characteristics of molecules, namely their molecular size, ionic charge

and adsorption qualities. Whilst chromatographic methods can vary enormously, they all separate components through the use of a stationary phase and a mobile phase. The two principle forms of chromatography used in this investigation were liquid and gas chromatography. In both cases the liquid and gas in the different forms refer to the mobile phases.

The stationary phases in both methods are usually solid based in the form of a column. In general the sample containing the mixture of compounds to be separated is placed onto the stationary phase. The mobile phase is placed over the stationary phase and the compounds are separated based on their interactions with the stationary phase as shown in Figure 2.10.

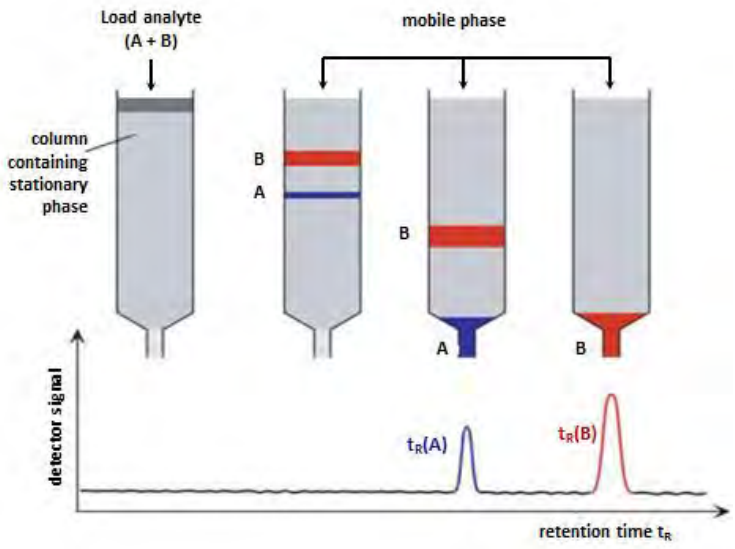

Figure 2.10. Principle of separation using chromatographic techniques [210].

In liquid chromatography these separated components are routinely detected by ultraviolet/visible (UV/Vis), refractive index (RI), fluorescence, conductivity and mass spectrometry (MS). In gas chromatography the compounds can be detected by numerous detectors including flame ionisation (FID), electron capture (ECD) or MS detectors [210].

2.6.1 Liquid Chromatography

Liquid chromatography began in the early 1900s, in what is now known as “classical column chromatography”, where a glass cylinder is packed with a fine powder and the sample is applied to the top of the column and a solvent is poured onto the column. As the solvent moves down the column, using gravity, the components of the sample move through the column at different speeds and become separated. Advances to this technique have resulted in a more sophisticated, automated technique known as high performance liquid chromatography (HPLC). In this technique, samples are placed in an autosampler for automatic injection onto the column. The solvent is continuously pumped through the column

at a high pressure and the separated compounds are analysed by a detector as they elute from the column. The retention, elution and hence the separation of compounds is achieved by changing the composition of the mobile phase or introducing strong solvents or additives [226]. There are four main properties by which the samples are separated and five main techniques of separation. These can be found in Table 2.1.

Table 2.1. Techniques used to separate compounds with liquid chromatography [227].

Property	Technique
Size	Gel filtration (SEC)
Charge	Ion exchange (IEX)
Hydrophobicity	Hydrophobic interaction (HIC)
Hydrophobicity	Reverse phase (RP)
Biorecognition (ligand specificity)	Affinity (AC)

The advantages of liquid chromatography over GC are numerous. Samples do not have to be volatile or heat stable so no derivatization is required. Sample preparation is therefore much less laborious and complex. The key prerequisite is that the sample must be able to dissolve in the mobile phase.

Two liquid chromatographic techniques were used in this study, namely: gel filtration chromatography and ion exchange chromatography.

2.6.1.1 Size exclusion chromatography

The simplest form of chromatographic techniques in bioanalytical analysis is size exclusion chromatography (also known as gel filtration or gel permeation chromatography). Size exclusion chromatography (SEC) is a very robust technique that separates molecules based on the differences in their relative size.

The compound solution is injected into a liquid solvent stream flowing through one or more columns packed with highly porous microparticles and the compound components are separated based on their size as shown in Figure 2.11 [227]. Each column has a characteristic exclusion limit which makes the column act as a molecular sieve. The molecules smaller or equal to the exclusion limit are retained as they are able to enter the pores and their progress is retarded compared to that of larger molecules. The molecules that do not enter the pores are eluted in the void volume as they pass through the column at the same speed as the mobile phase. Therefore, in size exclusion chromatography, molecules are eluted in order of decreasing size. Factors affecting the separation of molecules include: flow rate, stationary phase particle size, packing density of the stationary phase and the viscosity of the mobile phase.

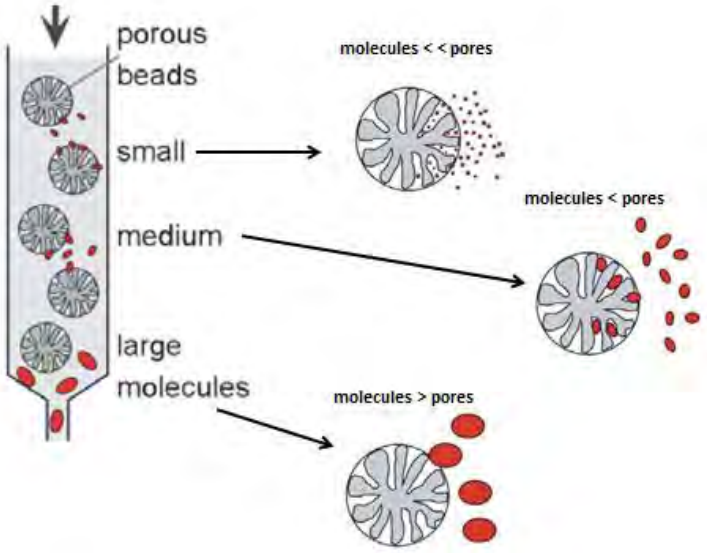

Figure 2.11. Schematic of compounds separated by size [227].

Detection of the compounds in the eluent is achieved using either an ultraviolet absorption (UV) or refractive index (RI) detector. The RI detector detects compounds based on the difference between the refractive index of the compound and the solvent whereas the UV detector identifies compounds based on their absorption of light at a specific wavelength.

Although this method is ideal for separating proteins, polysaccharides do not conform to standard elution principles as PSs are separated according to their apparent or hydrodynamic volume, which is not only dependent on the molecular weight but also by the molecular conformation in solution. Thus polysaccharides with an extended structure in solution may elute earlier than globular proteins of a higher molecular mass.

Chromatography of the samples was performed using an Agilent 1200 HPLC system, equipped with micro–vacuum degasser, quaternary gradient pump with degasser, auto–sampler, thermostatted column compartment, diode array detector (DAD), refractive index detector (set at 35 °C), fraction collector and Chemstation software. Separations were performed on one of two different column sets: either a Waters Ultrahydrogel guard column (code: WAT011565), Waters Ultrahydrogel 1000 column (code: WAT011530) and Waters Ultrahydrogel 500 column (code: WAT011535) columns mounted in series, in the order stated or Shodex guard column OHpak SB–G (code: F6709430), Shodex OHpak SB–805 HQ (code: F6429104) and SB–804 HQ (code: F6429103) columns mounted in series in the order stated.

The eluent for both sets of columns was 10 mM PBS buffer (pH 7.0) with an injection volume of 50 µl and a flow rate of 1 ml/min. The molecular weight was determined using a range of Pullulan standards shown in Figure 2.12. Molecular weights for the Pullulan standards were

given in the certificate of analysis received from the supplier. Table 2.2 details the elution time and corresponding molecular weights of the standards.

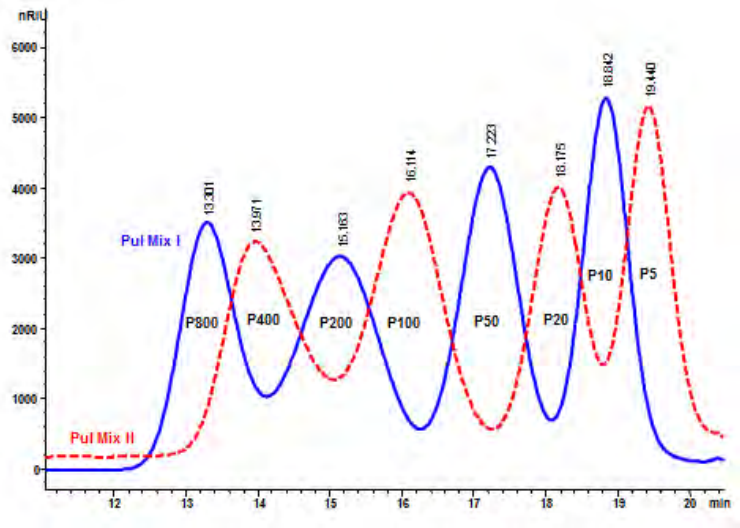

Figure 2.12. SEC–HPLC RID chromatograms of Pullulan standards on Shodex columns.

Table 2.2. Molecular weights and elution times of Pullulan standards for both sonication and microfluidization.

Standard	Mw (kDa)	Log (Mw)	Waters columns	Shodex columns
			Elution time (min)	Elution time (min)
P-800	788	2.897	15.126	13.168
P-400	404	2.606	16.040	13.924
P-200	212	2.326	17.077	15.113
P-100	112	2.049	18.068	16.121
P-50	47.3	1.675	19.172	17.239
P-20	22.8	1.358	20.169	18.202
P-10	11.8	1.072	20.806	18.871
P-11	5.9	0.771	21.433	19.476

2.6.1.2 Anion exchange chromatography

High Performance Anion Exchange Chromatography with Pulsed Amperometric Detection (HPAEC–PAD) is frequently used to separate and identify carbohydrates without derivatization. The technique is highly selective and sensitive. HPAEC–PAD relies on the notion that carbohydrates are weakly acidic and are partially ionised at high pH values (>12) and can thus be separated using anion exchange (neutral and cationic components will elute in the void volume) [228-230]. The column packing used in HPAEC is non–porous which minimises band broadening and is stable at high pH values and high pressures. There are various, specific column packings used for mono–, di– and poly– saccharides. The columns used in these investigations were the CarboPac PA1 and PA10, both of which are packed

with a polystyrene/divinylbenzene substrate onto which small icroBead™ quaternary amine functionalized latex is electrostatically attached as shown in Figure 2.13 [231].

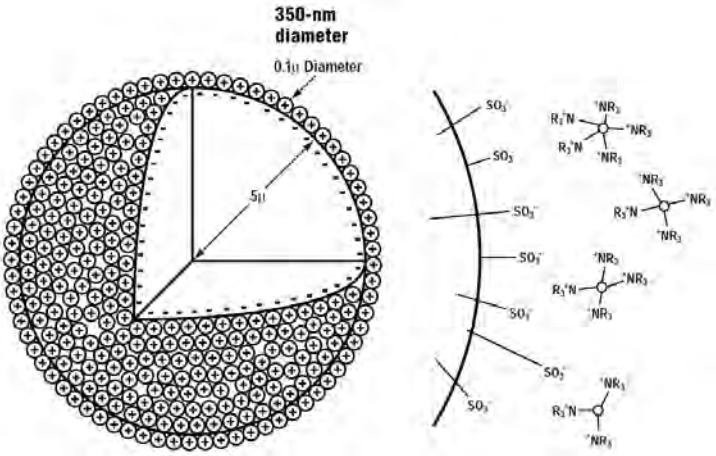

Figure 2.13. An anion exchange resin bead [231].

Along with the column, the mobile phase (eluent) composition is very important. The composition of the eluent affects the speed of separation as well as the selectivity and sensitivity of the detection. Sodium hydroxide is the eluent of choice but its concentration depends on the substances under investigation. For neutral polysaccharides (glucose, galactose) a low concentration (± 20 mM) of NaOH allows for a more likely interaction with the stationary phase and hence separation. However for sugar acids (Pn1) and oligosaccharides a higher concentration of NaOH is needed as these compounds interact strongly with the column. Acetate (or nitrate) is added to shorten run times. Acetate acts as a ”pusher” as it interacts with the anion exchange sites more strongly than hydroxide ions and will push out the charged compounds quicker [228, 231]. Acetate is also used in a gradient elution when there are mixtures of different size and different charged saccharides. As the eluent is a very important factor in the separation of saccharides, care must be taken to remove any contaminants such as carbonate. Carbonate contamination is very common as it is formed during the preparation of any alkaline solution through atmospheric carbon dioxide. Carbonate is a divalent ion at high pH values and can bind strongly to the anion exchange sites on the column which will not only interfere with the analysis of the saccharides but will drastically shorten the column lifespan [231-233].

The detection method used is pulsed amperometry (the detection of ions in a solution based on electric current or changes in electric current). The hydroxyl groups on the carbohydrates are oxidized on the surface of a gold electrode at a specific potential resulting in the loss of a proton. This proton loss creates a current flow that can be measured. This oxidation at the surface of the electrode blocks the electrode which must then undergo a rise in potential to remove the contaminants. The potential is lowered to renew the surface of the electrode.

This all takes place as a pulse sequence over less than a second which allows for data to be recorded at every second. This detection allows for high specificity as only functional groups at the specific potential can be oxidized [231, 234].

Chromatography of the samples was performed using a Dionex BioLC chromatography system with an thermostatted auto–sampler (set at 20 °C), thermostatted oven (set at 30 °C), gradient pump with degasser, electrochemical cell and borate trap (code: 047078) with Chromeleon software. Separations were performed on Dionex Carbopac PA1 analytical (code: 035391) and guard (code: 043096) columns. The separation method was previously described by Talaga *et al.* [235]. Solvent A was water, solvent B was a 100 mM NaOH solution and solvent C was a 100 mM NaOH containing 1 M sodium acetate solution. Gradients of the three solvents were used simultaneously to elute the carbohydrates by mixing the three eluents. This resulted in the following gradient of NaOH: 0 – 15 min, 18 mM; 15 – 18 min, 18 – 100 mM; 18 – 35 min, 100 mM; 35 – 55 min, 100 – 18 mM. The simultaneous gradient of sodium acetate was 0 – 18 min, 0 mM; 18 – 35 min, 0 – 300 mM; 35 – 55 min, 300 – 0 mM. An injection volume of 20 µl of the hydrolysed Pn1 polysaccharide was used and the flow rate was 0.4 ml/min. The following pulse potentials and durations were used: E1 = 0.1 V, t1 = 400 ms; E2 −2 V, t2 = 20 ms; E3 = 0.6 V, t3 = 10 ms; E4 = −0.1 V, t4 = 70 ms.

Pn1 PS was hydrolysed and derivatized for structural analysis on the HPAEC–PAD. The optimization of this method is detailed in Chapter 3, Section 3.4.3. Pn1 was first dried under vacuum at 45 °C (Thermo Speedvac Savant SPD131DDA Concentrator, 1.3 mbar, 3 hours). To this solid sample (between 0.1 – 0.5 mg) 1 ml 2 M trifluoroacetic acid (TFA) and 50 µg fucose were added. The solution was vortexed and irradiated by microwave (CEM Discover SP–D microwave) at 150 W and 121 °C for 60 seconds. Thereafter the samples were dried under vacuum at 45 °C and reconstituted in 500 µl water, filtered through 0.45 µm filters and into autosampler vials for HPAEC–PAD analysis.

This microwave procedure was compared to the conventional heating procedure where 1 ml 2 M TFA was added to a sample of Pn1 PS. Sample tubes were closed and placed in a preheated block for 2 hours at 121 °C. Samples were cooled to room temperature and transferred to Eppendorf™ tubes and dried under vacuum at 45 °C followed by reconstitution in 500 µl water, filtration through 0.45 µm filters before being placed into autosampler vials for HPAEC–PAD analysis.

2.6.2 Gas chromatography

The idea of gas chromatography (GC) was first suggested by Martin and Synge in 1941 [236] but it was only experimentally applied for analytical purposes in 1952 by James and Martin when modifications of the gas separation theory were applied to the separation of volatile fatty acids [237]. A simple GC consists of a carrier gas, an injector, a column and a detector. The mobile phase (carrier gas) in GC performs a different task to that used in LC. In GC the carrier gas is used only to transport the compounds through to the column. The retention time and separation of the compounds is based on their vapour pressure which is a temperature–dependant variable as well as the interaction between the compounds and the column (stationary phase). Hence the main adjustable variable is temperature so each component in the instrumentation is temperature controlled [226].

A schematic representation of the general layout of the gas chromatographic instrument is shown in Figure 2.14. When a sample is injected it is immediately vaporised in the injection port and taken up with the carrier gas through to the column where separation occurs. The column is situated in a temperature controlled oven and the temperature program starts at a relatively low temperature that normally separates the solvent from the sample. The compounds are separated through a heating program that is dependent on the nature of the compounds and the complexity of the samples. After separation the compounds leave the column and are recorded as a function of time. The most common detector used in GC analysis is a flame ionisation detector (FID). It is a simple yet highly sensitive detector where the carrier gas is mixed with hydrogen and combusted in air. Ions from the compounds are formed in this flame and collected in the form of a current that is proportional to the amount of sample injected [226]. The major development in GC was the introduction of open tubular capillary columns in 1957 by Golay [238-240], however this was improved upon in 1979 with the development of flexible silica material used in the tubing [240]. This tubing had major advantages over the traditional glass capillary columns in terms of flexibility and strength as well as inertness.

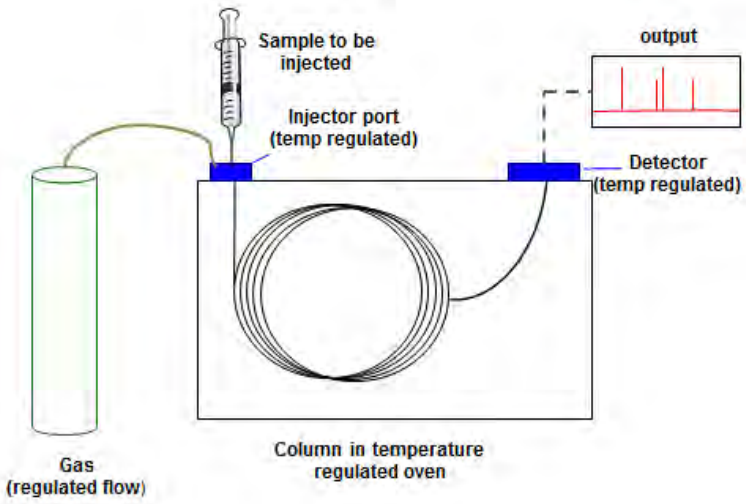

Figure 2.14. Schematic representation of an instrument used in gas chromatography.

Sugar monomers, released from the polysaccharides by hydrolysis must first be derivatized before analysis on the GC. There are two main hydrolysis/derivatization techniques used in polysaccharide analysis. The first produces alditol acetate derivatives. This method is preferred as it produces a single peak which corresponds to each monosaccharide derivative. This makes identification and quantification simple. The alditol acetate method is widely used for mixtures of neutral and amino– sugars, however carboxyl groups cannot be derivatized with this method and the alternate procedure is favoured [241]. The alternate hydrolysis procedure, methanolysis, followed by derivatization, produces a fingerprint of methyl glycoside derivatives for every monosaccharide component of the polysaccharide, as both furanose and pyranose ring forms of both α– and β– anomeric configurations are derivatized and detected. Due to the carboxyl groups on Pn1, this method was preferred, however due to the resistance of the GalA glycosidic linkages to hydrolysis; this method had to be optimised.

Pn1 PS was hydrolysed and derivatized for analysis on the GC. The optimisation of this method is detailed in Chapter 3, Section 3.4.4. Pn1 was first dried under vacuum at 45 °C (Thermo Speedvac Savant SPD131DDA Concentrator, 1.3 mbar, 3 hours). To this solid sample (between 0.1 – 0.5 mg) 20 µg *myo*–inositol (1 mg/ml solution in water) was added followed by 0.5 ml 3 N methanolic HCl (HCl/MeOH). Samples were irradiated with microwaves at 100 W and 121 °C for 60 seconds. Thereafter the samples were dried under nitrogen at 45 °C. 1 ml MeOH was added to each sample and dried an additional two times to remove any residual HCl. Finally 100 µl of silylating reagent (Hexamethyldisilazane/TMCS 2/1 (v/v), silylating mixture Fluka I according to Sweeley) was added to each sample and incubated at 80 °C for 20 min. Samples were evaporated under nitrogen at 45 °C and

reconstituted in 500 µl hexane. Samples were filtered through 0.45 µm filters and into autosampler vials for GC analysis.

The GC system used for separation of the hydrolysed polysaccharide was an Agilent 6820 gas chromatograph with a flame ionisation detector with a DB–5 column (30 m x 0.32 mm, 0.25 µm ID). Nitrogen was used as the carrier gas at a flow rate of 1 ml/min. The oven conditions followed the method by Kim *et al.* [242] which included an initial temperature of 50 °C for two minutes. The temperature was then raised at 30 °C/min to 150 °C followed by an increase of 3 °C/min to 220 °C and finally a raise in temperature of 30 °C/min to 300 °C where it was kept for 30 min. The inlet temperature was kept at 250 °C and the detector at 300 °C. An injection volume of 10 µl was used.

As a confirmatory method, GC–MS was used. The GC system used for the separation was an Agilent 7890A gas chromatograph with an electron–ionisation mass spectrometer. The column used was a DB–5MS column. The method used for the GC–MS was the same as for the GC–FID however the mass spectra were recorded on a JEOL GCmate II mass spectrometer and analysed using AMDIS_32 software.

This microwave procedure was compared to the conventional heating procedure where 1 ml 3 N HCl/MeOH and incubated at 121 °C for two hours. Samples were dried under nitrogen at 45 °C and washed twice with 1 ml MeOH to remove residual HCl. Samples were derivatized with the silylating agent as previously described.

2.7 Nuclear magnetic resonance spectroscopy

Nuclear magnetic resonance (NMR) is a spectroscopic method that is used to detect the reorientation of nuclear spin in an applied magnetic field [243]. The first nuclear magnetic resonance (NMR) signal was observed independently in 1945 by two physicists, Bloch and Purcell [244-246]. The physicists however were interested in the resonance aspect and did not investigate the structural analysis aspect; however chemists recognised this aspect and started to use NMR to investigate molecules. The most important advancement in NMR spectroscopy was the introduction of the superconducting magnet in the 1970s. This magnet provided a higher resolution to the analysis [247].

The technique involves monitoring the absorption of energy associated with the transition of nuclei between two magnetic energy levels. The nucleus behaves like a spinning magnet, this spinning nucleus generates a magnetic field and an associated magnetic moment which interacts with the applied magnetic field [243]. In order to record the NMR spectrum of a sample it must be placed in a homogenous magnetic field. The sample is spun to improve the magnetic field homogeneity and small magnetic fields are applied to the main field, in a

process known as shimming, in order to cancel out any errors in the static field. In order to keep the ratio of magnetic field strength to the transmitter frequency constant, thereby preventing the drifting of the signal, the instrument is "locked" onto a strong narrow signal, usually deuterium [247].

Analysis by NMR yields spectra of magnetic sensitive nuclei (e. g. ^{1}H, ^{13}C and ^{31}P) which depend on the structural environment of the nuclei and therefore provides a sensitive and non–destructive way of "looking" at the molecular structure of organic materials. The ^{1}H NMR spectrum requires the least amount of sample and forms the starting point for the analysis. The saccharides and derived products are investigated as deuterium–exchanged samples, hence each signal arises from a C–linked proton and the chemical shift value depends on its electronic environment. It can be regarded as a distribution of protons according to their electron density. 2D homonuclear correlation (COSY and TOCSY) experiments are used to trace the spin systems corresponding to each monosaccharide constituent. The most common solvent used in NMR experiments is deuterium oxide ($^{2}H_2O$ or D_2O) as deuterium has a different resonance frequency than that of a proton (^{1}H). D_2O is used as carbohydrates are highly hydrophilic compounds.

Samples analysed by NMR were lyophilized and exchanged twice with 99.9 % deuterium oxide and dissolved in 600 µl of the same D_2O, and introduced into a 5 mm NMR tube. NMR spectra were recorded on a Bruker *UltraShield*™ 400 MHz NMR machine at 303 K unless otherwise stated. All chemical shifts are reported in ppm. The ^{1}H NMR of Pn1 pneumococcal samples was referenced to the H3 of Cho–*P*–(*O*→ at 3.23 ppm and the ^{13}C referenced to 54.5 ppm of the C3 of CWPS; Cho–*P*–(*O*→ [248].

2.8 Conjugation of Pn1 to protein carrier

There are many steps involved in successfully conjugating a PS to a protein. Functional groups on the protein amenable for conjugation consist of amine and carboxyls groups. These groups can be directly linked to the PS or, in this case, the carboxyl groups on the protein are converted into hydrazides with the addition of the spacer linker, adipic acid dihydrazide (ADH). This renders the protein more reactive as well as providing better accessibility of the functional group to the PS. The PS is prepared for conjugation by first size reducing the polymer (by chemical or mechanical means) to reduce the viscosity of the PS as well as creating more terminal residues that may be used in certain conjugations. The Pn1 PS is "activated" by creating an active ester intermediate which converts the carboxyl groups in the polysaccharide into more reactive groups to allow for successful conjugation to the derivatized protein. Conjugation of the reactive polysaccharide and derivatized protein is then achieved with the addition of the two components into the same vessel. Factors such

as pH, temperature, reaction time, concentration and ratio of the reactants must be carefully monitored [10].

2.8.1 Protein derivatization

The general derivatization method used in this study is described below. Modifications to this method for the different proteins employed can be found in Chapter 5: Protein Derivatization. The protein was either dissolved in or dialysed against a 60 mM 2–(*N*–morpholino)ethanesulfonic acid (MES) buffer at pH 6.0 – 6.2. Solid ADH was added to the protein at room temperature in a ratio of 3.5 mg ADH / mg protein and the reaction mixture was stirred until all ADH dissolved. EDC, due to its very hydroscopic nature, was first dissolved in water to make up a 20 mM solution and this was added to the protein mixture at room temperature. A ratio of 0.15 mg EDC / mg protein was used. After mixing, the reaction was left unstirred at room temp for between 60 minutes and 16 hours depending on the protein and the desired level of derivatization required.

The reaction mixture was quenched by raising the pH to 10 with 1 M NaOH. The reaction mixture was diafiltered against a 30 mM NaCl/ 3 mM sodium carbonate (Na_2CO_3) buffer at pH 10.5 using a Labscale™ TFF system fitted with 3 x 50 K WCO 50 cm^2 membranes fitted in parallel. Diafiltration continued until the permeate was clear of hydrazide (excess ADH). To test the permeate for ADH, 2 drops of permeate was added to a mixture of 100 µl 0.1 % TNBS solution and 100 µl 0.1 M sodium borate, pH 9.0 followed by room temperature incubation for 5 min. An orange colour indicates the presence of ADH. SEC–HPLC was used to track the derivatization of the proteins.

2.8.2 Polysaccharide size reduction

2.8.2.1 Sonication

For the sonication investigations the polysaccharide was first solubilised in water, placed in a 50 ml beaker and cooled in an ice bath. The sample was exposed to a pre–set energy power output for a pre–determined time. The sonication cycle consisted of a 59s pulse with 15s break intervals. The total energy input was read from the sonicator display. Samples were passed through 0.45 um filters to remove any trace metal shed by the sonicator probe before analysis on SEC–HPLC. Sonication was performed on a VibraCell model VCX 750 ultrasonic processor at the University of Stellenbosch.

2.8.2.2 Microfluidization

For microfluidization; polysaccharide samples of Pn6B and 14 were first dissolved in water at concentrations of 20 mg/ml. Samples were diluted to either 10 mg/ml (Pn6B and 14) or 5 mg/ml (Pn1) due to the viscous nature of the polysaccharides. The samples were passed

through a Microfluidics M–110PS microfluidizer processor at a variable pressure for a predetermined amount of passes.

In preparation for the conjugations used in the animal studies: 0.583 g of Pn1 was subjected to size reduction via microfluidization. 3.5 L of Pn1 Batch 019 (concentration: 166.7 µg/ml) was concentrated down to 125 ml using 2 x 30 kDa MWCO membranes on the Labscale TFF system. The concentrated sample was passed through a Microfluidics M–110PS microfluidizer processor four times at a pressure of 22 000 psi.

2.8.3 HOBt mediated EDC conjugation

The final HOBt mediated conjugation method applied to Pn1 and derivatized protein is detailed below. The optimisation of this method and its application to other protein carriers can be found in Chapter 6, Section 6.3. The conjugation reaction was performed on a 100 mg Pn1 scale with an initial polysaccharide–protein mass ratio of 2:1.

To the microfluidized Pn1, sufficient NaCl was added to give a Pn1 solution in 0.2 M NaCl. The derivatized protein was added to the polysaccharide solution at a ratio of 1 mg protein for every 2 mg polysaccharide. The pH of the mixture was monitored and adjusted to approximately 7.0 if needed. In a separate bottle EDC (2:1 w/w Pn1) and HOBt (1:1 molar ratio with EDC) were dissolved in a 1:1 solution of 10 mM MES/0.2 M NaCl, (pH 7.2) and dimethylsulfoxide (DMSO). The pH was checked and raised to approximately 6.50 with 1 M NaOH if necessary. The EDC/HOBt solution was added slowly to the PS–protein solution and checked for signs of precipitation. The pH of the solution was adjusted to 6.80 with 0.1 M NaOH and left overnight at room temperature. The reaction mixture was dialysed extensively (3 x 2 L exchanges over a period of 2 days) in Slide–A–Lyzer cassettes of 10 kDa MWCO against 10 mM PBS (pH 7.2).

2.8.4 Triazine mediated conjugation

This optimised triazine conjugation method resulted in a conjugate that was used in the animal studies. It was performed on a 100 mg polysaccharide scale and three different derivatized protein carriers (CRM_{197}, TT and PLD) were used.

To the microfluidized Pn1, sufficient NaCl was added to give a Pn1 solution in 0.2 M NaCl. The polysaccharide solution was cooled on ice to between 0 – 4 °C with stirring. The activating species of 2–chloro–4,6–dimethoxy–1,3,5–triazine (CDMT) and N–methyl–morpholine (NMM) was first formed in DMSO and added with continuous stirring to the cooled Pn1 PS. After a further 5 min at 0 – 4 °C the PS solution was placed at room temperature and allowed to react for one hour where after the pH was measured to be between the range of 7.50 – 8.00. The derivatized protein was added to the polysaccharide

solution at a ratio of 1 mg protein for every 2 mg polysaccharide and the mixture was left to react at room temperature for 20 hours. The conjugate solution underwent extensive dialysis (3 x 2 L exchanges over a period of 2 days) in Slide–A–Lyzer cassettes; 10 kDa MWCO against 10 mM MES/0.2 M NaCl (pH 7.2).

2.8.5 Conjugate purification

In order to produce a conjugate vaccine for use in animal or human models – unreacted reagents and reactants, unwanted by–products as well as any other impurities must be removed. Whilst dialysis and diafiltration can remove a large amount of the smaller molecules, the unconjugated polysaccharide and protein often remain. Chromatographic methods such as size exclusion and hydrophobic interaction chromatography are widely used to remove protein and polysaccharide.

2.8.5.1 Gel filtration liquid chromatography

For purification of the conjugates, Sephacryl S500 HR packing was briefly investigated as a comparison to other purification technologies.

Sephacryl media consists of cross–linked allyl dextran with N,N'–methylene bisacrylamide to form a hydrophilic matrix that provides high chemical stability and tolerance for high flow rates. The porosity of the packing is determined by the dextran component and the S500 HR media was chosen as the packing material for these investigations as it has a fractionation range (Mr) of $1x10^4$ – $1x10^8$. The S500 column was attached to an ÄKTA–FPLC system equipped with a pump as well as a UV and conductivity detector. The running conditions, unless otherwise stated, can be found in Table 2.3.

Table 2.3. Running conditions of the S500 HR packing material.

	S500 HR column (XK16/40)
Packing volume	125 cm^2
Bed height	40 cm
Load volume	4 ml
Protein sample concentration	2.1 mg/ml
Mobile phase	0.2 M NaCl
Flow rate	0.9 ml/min
Volume of fractions collected	100 ml
Detector used	UV

2.8.5.2 Hydrophobic interaction chromatography

Most proteins have hydrophobic areas or patches on their surface, depending on the number of amino acids with hydrophobic functional groups (such as alanine, isoleucine, leucine,

methionine, phenylalanine, tryptophan, tyrosine and valine). To avoid contact with water, many of these residues are folded inside the protein's structure but a few of them remain on the surface. As with ammonium sulfate precipitation, when the protein is released from the salt, it will interact with another hydrophobic medium. If this hydrophobic medium is found on a chromatographic resin the protein (and conjugate) is able to be separated from the unconjugated saccharide or any other components as the protein will interact with the column. The mechanism for this interaction could be due to surface tension, van der Waals forces, entropic considerations as well as the charge masking effect of small ions [249, 250]. When the salt concentration is decreased, the protein will be released from the column and elute.

0.5 mg of sample was loaded onto a GE Healthcare HiTrap Phenyl HP (5ml) column and 25 ml 1 M ammonium sulfate solution was used to bind the conjugate to the column and elute off the free saccharide. This mobile phase was changed to 0.05 M sodium phosphate (pH 7.0) for 25 ml to elute off the conjugate. The flow rate was kept constant at 0.4 ml/min throughout the elution. The column was washed with 25 ml 1 M ammonium sulfate before the next sample was loaded. The elution of the compounds was monitored at 280 nm.

2.8.5.3 Ammonium sulfate precipitation

Most proteins are water soluble and their solubility is a function of the ionic strength and pH of the solution. At low concentrations, the presence of salt stabilises the various charged groups on the protein molecule, thus attracting the protein into the solution and enhancing its solubility. At high salt concentrations the maximum solubility of the protein can be reached and beyond this specific concentration, the water molecules become more and more attracted to the salt than to the protein due to the higher charge of the salt. This competition for hydration leads the proteins to start interacting with each other thus resulting in aggregation and eventually precipitation of the protein. The precipitation can be collected by centrifugation and the protein pellet is re–dissolved in a low salt buffer. The commonly used salt for this purpose is ammonium sulfate, due to its relative cost effectiveness and high solubility even at lower temperatures.

Ammonium sulfate ($(NH_4)_2SO_4$) is a salt that is widely used to precipitate proteins. It has been determined that polyvalent anions are more effective at salting out than monovalent anions and that the best combination for salting out a protein would be to use a polyvalent anion with a monovalent cation [251]. Both anions and cations have been arranged in the "Hofmeister series" which defines their ability to salt out proteins and other macromolecules. In terms of sulfate and ammonium ions, they are on the kosmotrope ends of the anion and

cation series; kosmotropes are known as “water structure makers” which have stabilising, salting out effects on proteins [251-254].

A saturated ammonium sulfate solution was prepared by dissolving 550 g ammonium sulfate ($(NH_4)_2SO_4$) in 1000 ml water and cool at 2 – 8 °C. Two volumes of saturated ammonium sulfate was added to the conjugate sample, mixed and left overnight at 2 – 8 °C. The solution was centrifuged to pellet out the conjugate and the supernatant was removed. The procedure was repeated and the final pellet was re–dissolved in 10 mM phosphate buffered saline (PBS) (pH 7.2).

2.8.5.4 Deoxycholate precipitation

The deoxycholate precipitation method for separating conjugated and unconjugated saccharide was first developed as a means of quantifying the amount of unconjugated saccharide in Hib conjugates, as the PRP–TT conjugate did not bind to hydrophobic interaction (HIC) columns. The method takes advantage of the PRP–TT conjugates ability to bind to deoxycholic acid (DOC) and precipitate out in acidic conditions leaving the unconjugated saccharide in the supernatant. The unconjugated saccharide is quantified using the appropriate assay and express as a percentage of the total PS in the conjugate [255, 256].

1 ml of appropriately diluted sample was used; a PS concentration of 50 – 100 µg/ml was preferred, the pH of the diluent must not fall out of the range of 6.7 – 7.2. 100 µl freshly prepared 1 % w/v DOC (pH 6.8) was added, with mixing to each tube. The samples were incubated at 2 – 8 °C for 30 min. 1 M HCl (50 µl) was added and precipitation was immediately visible. The samples were centrifuged for 30 min to pellet out the DOC–conjugate. The supernatant was assayed for PS using the colorimetric test for uronic acid. Care must be taken to remove any remaining traces of ammonium sulfate when used in conjugate purification as the ammonium sulfate will interfere in the colorimetric assays.

2.8.6 Formulation

In order to produce the conjugate in a form suitable for animal studies, the conjugates had to be formulated onto an aluminium–based adjuvant. The general formulation protocol is described below and further explanation of this in relation to specific conjugates can be found in Chapter 6, Section 6.4.

In order to minimise bio burden in the conjugates, all formulations were performed under a laminar flow hood that was tested before and during use for any bacterial contamination. In all but one formulation, the final volume used was 1000 ml. Over a period of 90 minutes, 0.067 M $AlCl_3$ was slowly added to 0.25 M Na_3PO_4 solution.

$$\text{flow rate}\left(\frac{\text{ml}}{\text{min}}\right) \quad \frac{\text{addition volume}}{\text{time added}} \qquad \text{Equation 2.4}$$

The pH was left to stabilise over a period of 160 min after which 0.2 M succinic acid was slowly added (flow rate calculated as per Equation 2.4). A further volume of 0.25 M Na_3PO_4 was added using the same flow rate as before to raise the pH. After the pH had stabilised, 2 % Tween–80 and 2 M NaCl were added. The appropriate amount of antigen (conjugate) was added to give a final PS concentration of 2 µg/ml and the formulation was made up to the final volume with WFI grade water. Finally, the formulation was left to stir for a further 120 min at room temperature to allow the pH to fully stabilise and allow for maximum antigen absorption before storage at 4 °C.

CHAPTER 3. STRUCTURAL CHARACTERISATION OF Pn1 PS

3.1 Introduction

In order to analyse the composition and determine the repeating unit of the polysaccharide specific information is needed:

- The identity, relative amounts and sequence of the monosaccharides in the repeating unit.
- The anomeric configuration of the glycosidic linkages, as well as the position on each residue of the linkage.
- Whether the sugar is a furanose or pyranose ring form.
- Any functional group modifications, positions of groups such as acetylation, phosphate groups, sulfate groups and any other modifications [257].

The molecular weight distribution of the PS should also be established. The purity and hence the chemical composition of a PS must first be determined in order to be used for further production or manufacturing purposes. As saccharides cannot be detected by absorption due to the absence of a chromophore, colorimetric assays in which a chromophore is generated are used to estimate the presence of certain specific sugars such as uronic acid, hexosamines and methylpentoses as well as certain functional groups. For the manufacture of vaccines, the WHO have established recommended values for specific sugars, functional groups and contaminants of each bacterial serotype [162, 258, 259].

To determine the identity and relative proportions of monosaccharides in the PS, a more comprehensive analysis is needed. This can be achieved by hydrolysing the PS into its monosaccharide components which can then be analysed using chromatographic methods such as HPLC [260, 261], GC [242, 262-266] and HPAEC [228, 229, 231, 234, 267, 268] . The glycosidic linkage position and size of the ring structures can be identified by cleavage reduction or methylation analysis [269-273]. The anomeric configuration used to be confirmed by the oxidation with chromium trioxide [274-277] but has been replaced by modern techniques such as NMR [278-285].

3.2 The structure of Pn1 polysaccharide

While Neufeld and Handel, in 1910, were the first to identify the first two (serotypes 1 and 2) of the 90–odd serotypes of *S. pneumoniae,* it was Heidelberger, Avery and Goebel who investigated the composition of the capsular PS of serotype 1 [286-288]. In the early studies of Pn1 PS in 1925, Heidelberger *et al.* found that the polysaccharide was not very soluble in its isoelectric form and could only be fully dissolved in an acidic or alkaline solution. They also discovered that it contained 5 % nitrogen, had an optical rotation of + 300° and an

isoelectric point of approximately 4; however, in 1948, Alberty and Heidelberger, confirmed the isoelectric point of Pn1 to be 2.8 [289]. The polysaccharide was hydrolysed into reducing sugars with a mineral acid but at the time, the identity of the sugars could not be determined. The formation of reducing sugars was detected when the PS was treated with nitrous acid and half of the 5 % nitrogen was released. This suggested that the nitrogen must be an integral part of the polysaccharide. No sulfur or phosphorus was detected. The polysaccharide tested positive for glucuronic acid but yielded mucic acid on oxidation which suggested that it contained galacturonic and not glucuronic acid. Both acidic and basic properties were shown for this PS, which was, at the time, different to the other two PSs studied (serotype 2 and 3) [286].

Avery and Goebel reported the first evidence of the presence and immunogenicity of the *O*–acetyl functional group on Pn1 PS [287]. The authors were able to detect antibodies for the acetylated polysaccharide in type 1 antipneumococcal horse serum; the de–*O*–acetylated PS did not elicit antibodies.

Further investigations into the composition of Pn1 were performed by Smith *et al.* who hydrolysed the polysaccharide with H_2SO_4 [290]. Galacturonic acid (GalA) and glucosamine (GlcN) were detected as well as the presence of a methylpentose and a hexose that behaves in a similar fashion to galactose. The PS contained 60 % uronic acid, 8 % amino sugar and 4 % total nitrogen was also reported. This hexosamine could not account for the entirety of the nitrogen and it was suggested that other nitrogenous material may be part of the polysaccharide structure. Guy *et al*. purified and modified the Pn1 PS in order to determine the repeating unit [291]. Through nitrous acid deamination, it was determined that the polysaccharide contains disaccharides of galacturonosyl–galactosamine and galacturonosyl–glucosamine. Residues of 2–amino–2–deoxyhexosylglucose were also identified. The partial structure of the polysaccharide was determined to be galacturonosyl–(1→3)–glucosaminyl–(1→3)–galacturonic acid.

At the time the polysaccharide structure was known to consist of galacturonic acid (major constituent) and a hexosamine. The polysaccharide contained *O*–acetyl groups that were important in terms of its immunology and was amphoteric and contained nitrogen as a constituent in addition to that of the hexosamine.

It was only in 1980, that Lindberg *et al*. provided the structure of the hexosamine [292]. The sugar was not isolated and identified but was rather determined as products of deamination (similar to those performed by Guy *et al.*). The optical rotation of the purified polysaccharide was found to be in agreement with previous studies and was indicative of a D–configuration for all three sugars in the repeating unit. NMR studies showed the presence of an *N*–acetyl

peak (at 2.06 ppm), the presence of methyl protons at 1.29 ppm which was thought to belong to a 6–deoxyhexosyl residue. The presence of an *O*–acetyl group was confirmed with a peak at 2.20 ppm and the three signals in the anomeric region were suggestive of three saccharides in the repeating unit. As galacturonic acid accounted for 60 % of the makeup of the polysaccharide, two of the sugars in the repeating unit were thought to be galacturonic acid. When the polysaccharide was *N*–acetylated the *N*–acetyl peak doubled in size which suggested that the third sugar could have been a diaminotrideoxy–sugar where only one of the amino groups was acetylated. In order to confirm the structure of the amino sugar, the polysaccharide was deaminated with nitrous acid followed by acid hydrolysis and detected as 2–amino–2,6–dideoxyglucose in its alditol acetate form by GLC–MS. When borohydride reduction preceded the acid hydrolysis, peaks indicative of 2–amino–2,4,6–trideoxyhexoses were detected by the mass fragmentation pattern. The authors concluded that in order for the results in the deamination reaction to have occurred, the starting sugar must have been 2–acetamido–4–amino–2,4,6–trideoxygalactopyranose (AAT) [292]. The linkage sites of the two galacturonic acid residues were determined to be through O4 and O3 and the AAT sugar was determined to be linked through O3. The repeating unit is shown in Figure 3.1 with a non–stoichiometric amount of *O*–acetyl groups whose location was not determined.

It took another 20 years before the position of *O*–acetyl group was determined by Stroop *et al*. through the use of NMR spectroscopy [293]. The authors determined that the group is situated on the GalA residue (residue B in Figure 3.1) as the PS was able to survive through periodate treatment, and therefore must be on either the C2 or C3 position of the 4–substituted GalA residue.

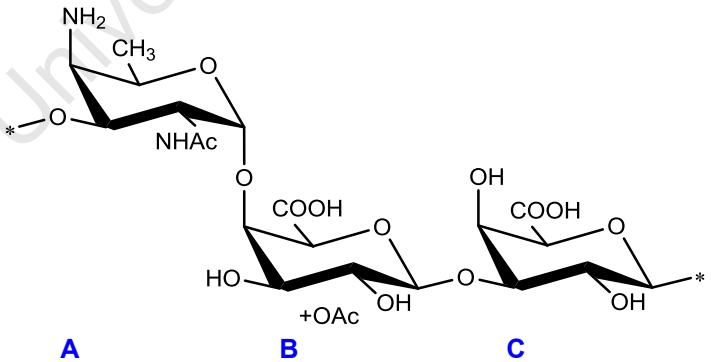

[3)-α-D-AAT*p*-(1→4)-α-D-Gal*p*A-(1→3)-α-D-Gal*p*A-(1→]$_n$ + (OAc)

Figure 3.1. Structure of Pn1 polysaccharide consisting of A – 2**–**acetamido**–**4**–**amino**–**2,4,6**–**trideoxy**–** galactose, B – galacturonic acid with *O***–**acetylation and C – galacturonic acid.

3.3 Colorimetric assays

Of the colorimetric, analytical tests required by the European Pharmacopoeia [294], only two were used to identify Pn1 namely: uronic acid and *O*–acetylation.

Colorimetric assays were assessed in terms of their linearity and working range, the precision of the assay, the assay's accuracy and its specificity.

- **Linearity:** An assay's linearity evaluates the procedure's ability to obtain a response that is directly proportional to the concentration or amount of analyte in the given sample, and within a given range. In determining linearity, a minimum of five concentrations was recommended [295, 296]. Samples were prepared in triplicate and the mean absorbance was plotted against the concentration of the analyte in question. This plot was used to determine linearity and subsequently a regression line was calculated. Also determined were the y–intercept, the correlation coefficient and slope of the regression line. The linear range of the assay was determined from the 2nd order polynomial plot [295, 296].
- **Assay precision:** The precision of an assay is determined by how close the agreement (degree of scatter) is of a number of samples. The precision of an assay depends on firstly, the repeatability of the assay and the intermediate precision. The repeatability (intra–assay precision) is the variation experienced by a single analyst on a particular instrument. The repeatability is measure by analysing multiple (in this case 10) replicates of the same sample. The relative standard deviation is calculated for all samples and reported. Intermediate precision is reported as the analysis of the same assay by either a different analyst or instrument or on a different day. The reproducibility of an assay is calculated with the results of the assay performed by different laboratories. This was not performed for the colorimetric assays in question [295-297].
- **Assay accuracy:** Accuracy is regarded as the closeness of a measured value to the true or accepted value. It provides an indication of any systematic error or bias in the method. Accuracy is determined by the measurement of the recovery of the sample in question by direct comparison with the true value. In this case a sample of known concentration at the lower, middle and upper level of the linearity curve was assessed. The percentage recovery of the sample must conform to the acceptable limits of 90 – 110 % [296, 297].

- **Limit of Detection (LOD):** The limit of detection is considered to be the lowest amount of sample that can be detected (not quantified). The detection limit was calculated by determining the minimum level at which the sample can be detected. It is usually calculated by comparing the absorbances of the lower concentration of samples to that of the blank (signal to noise ratio). A ratio of 2:1 is considered an acceptable value for the detection limit [295, 297].
- **Limit of Quantitation (LOQ):** The quantitation limit is the lowest amount of sample that can be determined with suitable precision and accuracy. The LOQ was calculated in a similar fashion to the detection limit, by comparing the signal to noise ratio. However in this case, an acceptable value for the limit of quantification was taken as ratio of 10:1 [295, 297].
- **Specificity:** Assay specificity is the ability to assess whether the other substances in the sample may interfere with the assay detection. In determining specificity, a number of different substances normally found with the analyte in question, such as buffers, reagents, proteins etc., are analysed to determine if interferences do occur. Assay specificity was evaluated by investigating for matrix interferences caused by buffers, reagents etc. [295-297].

3.3.1 Uronic acid assay

The first instance of the use of carbazole to quantify uronic acid saccharides was reported by Dische in 1946 when uronic acid was quantified by its hydrolysis with concentrated H_2SO_4 for 20 minutes in a boiling water bath, followed by the addition of a 0.1 % alcoholic solution of carbazole. This colour reaction reached its maximum intensity after 2 hours [196]. In 1949 Dische modified this procedure by decreasing the concentration of sulfuric acid used as well as the temperature and length of incubation [197]. In this way a difference between uronic acids (i.e. glucuronic vs. galacturonic acid) could be determined. In 1958, Bowness determined that 5–formylfuroic acid was responsible for the colour formation with carbazole. Another compound formed during hydrolysis: 2,5–diformylfuran also reacts with carbazole although this reaction gives rise to different absorption spectra (550 nm) under the same conditions and does not interfere with the absorption at 530 nm [298].

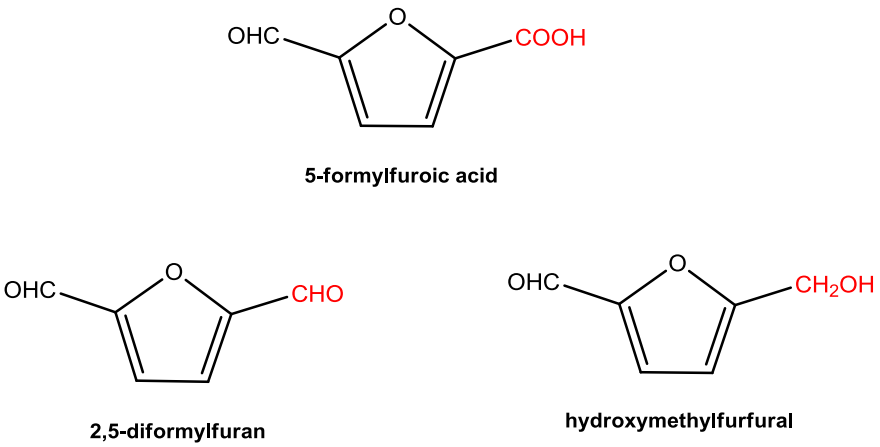

Figure 3.2. Structures of 5–formylfuroic acid, the major colour contributor to the uronic acid–carbazole colorimetric assay as well as 2,5–diformylfuran and hydroxymethylfurfural (HMF).

In 2007, Li *et al.* confirmed Bowness' findings when it was demonstrated that 5–formylfuroic acid was the major contributor to the coloured complex with carbazole, however, it was also shown that another derivative of carbohydrates – hydroxymethylfurfural (HMF) – absorbed in the 530 nm spectrum when complexed with carbazole as shown in Figure 3.2 [299], this however is not a hydrolysis product of uronic acid and should not interfere in the analysis of Pn1.

Bitter and Muir, 1962, published a modified method of the Dische carbazole reaction where borate was added to the concentrated sulfuric acid to increase the intensity of the colour change allowing for an increase in sensitivity to a concentration as low as 4 µg/ml [198].

3.3.1.1 Assay optimisation

According to the European Pharmacopeia, glucuronic acid (GlcA) is used as the reference standard to produce the standard curve [294]. However, in the development of the colorimetric assay it was determined that glucuronic acid produces a more intensely coloured complex than galacturonic acid (GalA) which is the major component of Pn1 [197, 198]. This result indicated that GalA would result in a far more accurate calculation of the uronic acid concentration than GlcA. Therefore both uronic acid monosaccharides were subjected to the colorimetric assay and the absorbances compared. Figure 3.3 shows the difference in absorbance between GlcA and GalA. Both standards gave a linear response over the concentration range (0 – 50 µg/ml) with a correlation coefficient (R^2) for the regression for Glc = 0.9996 and 0.9983 for GalA, however the GlcA standards produced on average a 71 % greater absorbance than those of the GalA standards. This proved the hypothesis that GalA gives a more accurate representation of the uronic acid concentration in Pn1 PS.

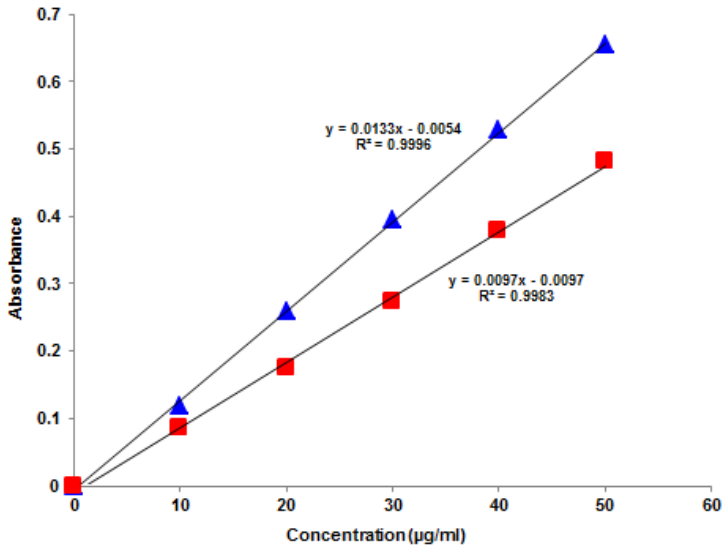

Figure 3.3. Comparison between glucuronic acid (blue) and galacturonic acid (red) for use as a standard in the uronic acid colorimetric assay.

3.3.1.2 Correction factor

As Pn1 is not solely constructed of GalA residues, a correction factor needed to be determined. The correction factor would account for the difference in the total mass of the polysaccharide not accounted for by the assay itself. Pn1 comprises of three sugars, two of which are galacturonic acid moieties and one modified amino sugar, and thus the theoretical uronic acid composition was determined by Equation 3.1.

$$\text{composition} = \frac{\sum W \text{ component}}{\sum W \text{ repeating unit}} \times 100 \qquad \text{Equation 3.1}$$

Hence, the percentage composition of uronic acid residues in Pn1 is equal to [(240.14+198.10)/660.92] × 100 = 66.3 %. (Molecular weight of Pn1 repeating unit = 660.92 taking into account two sodium counter–ions for the carboxyl groups and chloride counter–ion for the amino grouping). The WHO state that Pn1 polysaccharide should theoretically consist of 55.17 % uronic acid [162, 300], with the European Pharmacopoeia suggesting a typical specification of above 45 % [294]. The value of 66.3 % far exceeds the recommended minimum value and corresponds to a purity of 68 %. To correct for the amino residue not accounted for by the uronic acid assay (total composition is 100 %), a correction factor is required. The correction factor for this assay was assessed by dissolving 5 mg pure Pn1 PS in 100 ml water (50 µg/ml) and performing a further two–fold serial dilution (from 50 µg/ml to 6.25 µg/ml) of these solutions. The polysaccharide concentration was determined by the uronic acid assay. The data generated suggested that the uronic acid contribution to the total polysaccharide is 66.8 % (average uronic acid concentration for an accurately prepared 50 µg/ml solution of Pn1 is 33.425 µg/ml). Hence, the correction factor for the assay was experimentally calculated using Equation 3.2 and determined to be 1.50.

$$\text{Theoretical correction factor} \quad \frac{100}{\text{c omposition accounted for by uronic acid assay}} \qquad \text{Equation 3.2}$$

This corresponded well with the theoretical uronic acid composition. Applying this calculated correction factor, the average Pn1 concentration was 50.32 with a standard deviation of 0.68 (compared to the originally prepared concentration of 50 µg/ml) (Table 3.1). The calculated percentage relative standard deviation (RSD) for samples was all within specification limits of ≤ 2 % at 1.36 %.

Table 3.1. Values for determination of the correction factor for Pn1 polysaccharide.

Dilution	Average Absorbance (530 nm)	Calculated uronic acid concentration (µg/ml)	Calculated Pn1 concentration (µg/ml)
1	0.415	33.02	49.53
2	0.208	33.44	50.16
4	0.104	34.12	51.18
8	0.049	33.60	50.40

3.3.1.3 Assay validation

Linearity shows that the method can produce results that are directly proportional to the concentration of the analyte in samples within a given range. The linearity of the assay was assessed by preparing and analysing a number of standards including 0, 10, 20, 30, 40, 50, 100, 200, 500 and 1000 µg/ml, in triplicate, and plotting the mean absorbance against concentration (µg/ml).

The results were shown to be linear across the tested range of 0 – 50 µg/ml using D–galacturonic acid as standard (Figure 3.4). The slope and intercept of regression line obtained were 0.0123 and –0.0011 respectively with correlation coefficient (R^2) = 0.9954.

Non–linearity was evaluated for the assay and found to be at concentrations greater than 100 µg/ml. The slope and intercept of the regression line obtained were 0.0032 and 0.5325 respectively with correlation coefficient (R^2) 0.8435. It's important to note that although linearity for this assay continues at concentrations greater than 50 µg/ml and up to 200 µg/ml, standards 100 µg/ml and 200 µg/ml were excluded from the standard curve because the respective OD's are above 1.000. Thus, 0 – 50 µg/ml was the working concentration range for the D–galacturonic acid standards.

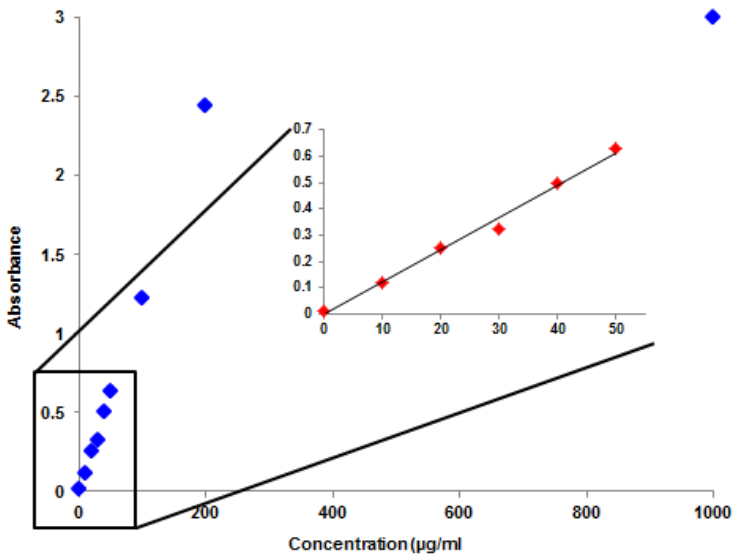

Figure 3.4. Graph of absorbance vs. concentration of GalA to determine linearity and working range of the uronic acid colorimetric assay.

The precision experiments were carried out using a standard Pn1 saccharide concentration of 50 µg/ml. Ten replicates of this standard were assessed resulting in an average concentration of 50.02 µg/ml and a standard deviation of 0.412. The relative standard deviation was calculated to be 0.82 %, well under the specification of ≤ 2 %.

The accuracy of the assay was assessed by analysing a sample of known concentration at the lower, middle and upper level of the linearity curve. The percentage recovery was calculated as shown in Equation 3.3 and found to be within acceptable limits of 90 – 110 % as shown in Table 3.2.

$$\text{ec}\quad\text{overy}\quad\frac{\text{Calculated concentration}}{\text{Actual concentration}}\quad 100 \qquad \text{Equation 3.3}$$

Table 3.2. Calculation of percentage recoveries to determine the accuracy of the uronic acid assay using different concentrations of Pn1 polysaccharide.

Theoretical concentration (µg/ml)	Experimental concentration (µg/ml)	Percentage recovery (%)
12.5	11.29	90
25	23.86	95
50	50.83	102
100	103.15	103

The limit of detection of this assay was determined to be less than 5 µg/ml and LOQ of this assay was calculated to be 10 µg/ml. Finally the specificity of the uronic acid colorimetric assay was evaluated by analysing for matrix interferences including buffers, reagents and water (Table 3.3). To this end, a reference standard was prepared by diluting 75 µl of a 50 µg/ml Pn1 PS solution with 75 µl of purified water to yield a final sample volume of 150 µl (1:2 dilution; 25 µg/ml final concentration). Testing samples were prepared with 75 µl of the

interfering substance (analyte) and 75 µl of a 25 µg/ml Pn1 PS standard solution. The acceptance criterion was that no optical difference should be observed between the reference sample and the testing samples.

Table 3.3. Analysis of potential interfering species in the uronic acid assay.

Blank/Analyte	Optical difference	Blank/Analyte	Optical difference
Pn1 PS	N/A	5 % EtOH in 0.05 M NaOAc	N
0.2 M NaCl	N	10 % EtOH in 0.05 M NaOAc	N
10 mM PBS	N	15 % EtOH in 0.05 M NaOAc	N
10 % CTAB	N	30 % EtOH in 0.05 M NaOAc	N
Saturated ammonium sulfate	Y	60 % EtOH in 0.05 M NaOAc	N

Saturated ammonium sulfate was the only reagent found to interfere in the uronic acid assay. Therefore, if saturated ammonium sulfate is used during any processing, it would have to be completely removed in order to ensure no interference when assaying for uronic acid content.

3.3.2 *O*–Acetyl assay

The Hestrin protocol is the preferred method for determining the concentration of *O*–acetyl groups present on a long–chain polysaccharide repeating unit [199, 301]. *O*–acetyl groups are released from the polysaccharide under alkaline conditions by hydroxylamine and converted to hydroxamic derivatives. These derivatives are reacted with ferric chloride to give a yellow complex that is detected using a spectrophotometer at 540 nm. In order to account for interferences, a correction blank is also employed. In this case, the polysaccharide is reacted with hydroxylamine under acidic conditions. As hydroxamic derivatives are only formed under alkaline conditions, the generation of colour from the addition of ferric chloride will be indicative of interfering substances which can be corrected for.

3.3.2.1 Assay optimisation

When first performing the colorimetric assay, absorbance values for the same sample changed over a short period of time. Upon further examination bubbles were visible in the solution. This was later determined to be due to the nitrous oxide gas released as hydroxylamine has the ability to reduce ferric ions into ferrous ions according to Equation 3.4. The ferrous ions do not however complex with hydroxamic acids [200, 302].

$$2NH_2OH + 4Fe^{+3} \rightarrow 4Fe^{+2} + N_2O + 4H^{+} + H_2O \qquad \text{Equation 3.4}$$

Dissipation of the gas bubbles by means of shaking seemed to work over a short period of time but bubbles would continue to form. The time between the addition of ferric chloride to

the hydroxamic acid derivatives and the absorbance reading was investigated. Samples were mixed thoroughly after ferric chloride addition and allowed to stand for a maximum of 60 min. Absorbance readings were taken at 0, 10, 20, 30 and 60 minutes and are plotted in Figure 3.5. It was determined that all bubbles had dissipated after 10 minutes but absorbance values only stabilised after a period of 20 minutes. This lag time between addition and absorption reading was taken into account for all further testing.

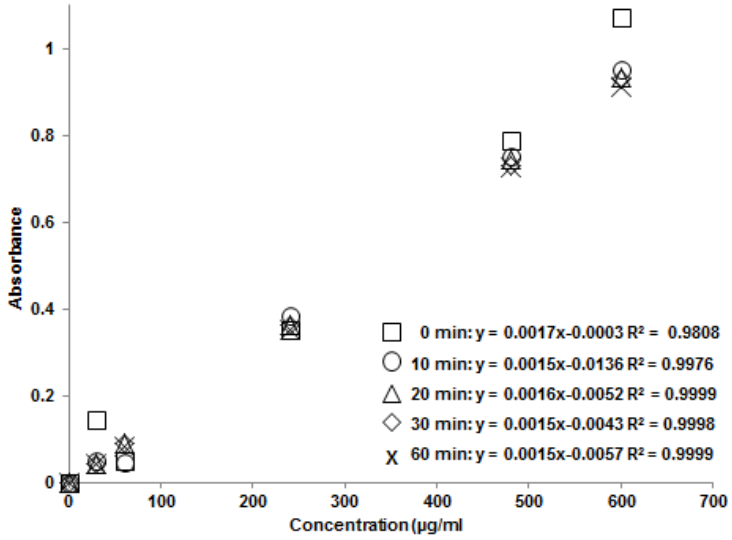

Figure 3.5. Comparison of reaction time after the addition of the ferric chloride colour reagent.

3.3.2.2 Assay validation

There is no specific correction factor for the *O*–acetyl assay as the WHO specification is based on dry weight [162]; rather, the percentage *O*–acetylation on the polysaccharide is calculated. For this determination, the concentration of the polysaccharide in the solution must be confirmed using an appropriate colorimetric assay (For serotype 1 the uronic acid assay is employed) and the percentage *O*–acetylation determined using Equation 3.5.

$$\text{acetylation} \quad \frac{\text{concentration of acetyl groups}}{\text{concentration of the polysaccharide}} \quad 100 \qquad \text{Equation 3.5}$$

In order to determine the linearity of the assay, standards containing a range of concentrations from 0 – 6000 µg/ml of acetylcholine were prepared in triplicate as per the method reported and the resultant mean absorbance against concentration of the standard were plotted. The results were shown to be linear across the test range of 0 – 500 µg/ml using acetylcholine as the standard as shown in Figure 3.6 The slope and intercept of the regression line obtained were found to be 0.0009 and –0.0024 respectively with a correlation coefficient (R^2) value of 0.9998. Non–linearity was observed for concentrations greater than 1000 µg/ml. The slope and intercept of the graph with these absorbances included change to 0.0005 and 0.1215 respectively with the correlation coefficient decreasing to 0. 3 82. It's

important to note that although linearity for this assay continues at concentrations greater than 600 µg/ml and up to 1000 µg/ml (R^2 = 0.9998) and even to 3000 µg/ml (R^2 = 0.9981), standards 1000 µg/ml and above have been excluded from the standard curve because the respective OD's are close to 1.00. Thus, 0 – 600 µg/ml is the working concentration range for the acetylcholine standards.

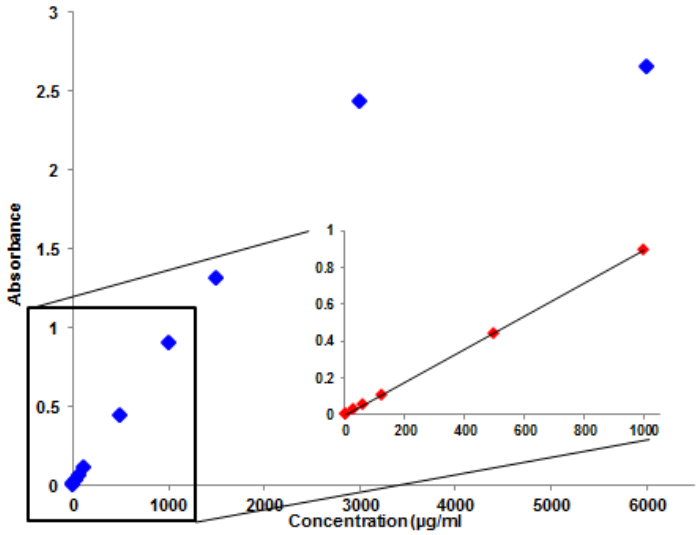

Figure 3.6. Graph of absorbance vs. concentration of acetylcholine to determine linearity and working range of the *O*–acetyl colorimetric assay.

The concentration working range of the acetylcholine standard was determined from the linearity testing, where after (i) assay precision; (ii) assay accuracy; and (iii) assay specificity was performed. The precision experiments were carried out using a 1 mg/ml Pn1 PS solution. The *O*–acetylation pattern of this standard was determined to be 23.74 %. Ten replicates of the 1 mg/ml Pn1 PS standard were analysed and returned an average *O*–acetylation percentage of 23.73 % with a standard deviation of 0.446. The range of these samples (calculated as ± twice the standard deviation) was determined to be within 22.84 – 24.62 % and the relative standard deviation was calculated at 1.88 % that was within the acceptable specification limits of ≤ 2 %.

The accuracy of the assay was assessed by analysing a sample of known concentration at the lower, middle and upper level of the linearity curve. The percentage recovery was calculated as shown in Equation 3.6 and found to be within acceptable limits of 90 – 110 % as shown in

Table 3.4.

$$\text{ec overy} \quad \frac{\text{Calculated concentration}}{\text{Actual concentration}} \quad 100 \qquad \text{Equation 3.6}$$

Table 3.4. Accuracy results used in the *O*–acetyl assay.

Dilution	*O*–acetylation groups on Pn1 (%)	Percentage recovery (%)
1	22.15	93
1.67	22.77	96
2.5	22.06	93
5	22.91	97

By calculating the ratio between the blanks and the samples the detection limit of this assay was determined to be 4 µg/ml and the limit of quantification was calculated at 15 µg/ml.

The specificity of the test method was evaluated by analysing for matrix interferences including buffers, reagents and water. To this end, a reference standard was prepared by diluting 250 µl of a 1 mg/ml (polysaccharide) standard with 250 µl of purified water to yield a final sample volume of 500 µl (1:2 dilution; 500 µg/ml final Pn1 concentration). Testing samples were prepared with 250 µl of the interfering substance (analyte) and 250 µL of the 1 mg/ml (polysaccharide) standard. The acceptance criterion is that no optical difference should be observed between the reference sample and the testing samples (Table 3.5).

Table 3.5. Substances tested in determining assay specificity.

Blank/Analyte	Optical difference	Blank/Analyte	Optical difference
Pn1 PS	N/A	5 % EtOH in 0.05 M NaOAc	N
0.2 M NaCl	N	60 % EtOH in 0.05 M NaOAc	Y
0.05 M sodium phosphate	N	0.1 M MES	Y
10 % CTAB	N	Saturated Ammonium sulfate	Y

It should be noted that a high percentage of ethanol, saturated ammonium sulfate and MES buffer were found to interfere in the *O*–acetyl assay. Therefore, if any of these reagents are used during the process, they would have to be completely removed in order to ensure no interference when assaying for *O*–acetylation content.

3.3.3 Summary of colorimetric methods

Two colorimetric assays were optimised from the European Pharmacopoeia methods to enable the accurate quantification of Pn1 polysaccharide. The colorimetric assays were validated in terms of linearity, precision, accuracy, LOD, LOQ and specificity. The standard used in the uronic acid assay was changed to galacturonic acid, as it provided a better correlation to Pn1 PS than glucuronic acid. A correction factor to enable the accurate quantification of Pn1 PS was calculated to be 1.5 for the uronic acid assay. No correction factor was needed for the O–acetyl assay, and it was determined that in order to achieve

stable absorbance readings, the complexed solution had to be vigorously mixed and left to stand for 20 minutes for complete dissipation of any bubbles.

3.4 Polysaccharide hydrolysis

While colorimetric assays give an indication of the identification and quantitation of certain functional groups (uronic acids, methylpentoses, *O*–acetyl groups) they cannot accurately determine the identity and quantity of the total number of monosaccharides in the repeating unit without the use of a correction factor. For this, more sensitive and specific detection methods are needed. The conventional method of identifying and quantifying polysaccharides is first to hydrolyse the material and then separate and quantify the constituent monosaccharides on a chromatographic column.

There are many different methods to hydrolyse a polysaccharide into its monosaccharide components. Both chemical and enzymatic approaches are commonly used for a variety of polysaccharides. Enzymatic methods make use of the specificity of enzymes to target their substrates present in complex mixtures. There are two main types of enzymes which promote the hydrolysis of polysaccharides: endohydrases which will hydrolyse the internal glycosidic linkages, and exohydrases which will hydrolyse terminal glycosidic linkages [303]. Enzymatic methods are fast, very sensitive and highly specific [304].

The most common chemical approach for polysaccharides is acid hydrolysis. The rate of hydrolysis of polysaccharides is dependent on many different factors including ring structure, anomeric configuration, type of glycosidic linkage, chain length and the type of monosaccharide residues contained in the polysaccharide [303]. Many different acids have been investigated for use in the hydrolysis of polysaccharides, including sulfuric acid (H_2SO_4) [305, 306], hydrochloric acid (HCl) [306, 307], hydrofluoric acid (HF) [308] and trifluoroacetic acid (TFA) [306, 309]. TFA has many advantages over the aforementioned acids. Reaction times are shorter with TFA and, due to its volatility, there is no need for neutralisation as TFA can be removed by evaporation [310, 311].

The acid hydrolysis reaction can follow one of two different mechanisms. Both the ring oxygen as well as the glycosidic oxygen can be protonated. If the glycosidic oxygen is protonated, Figure 3.7, the glycosidic linkage is cleaved and a carbocation is formed on the anomeric carbon. This carbocation can react with water to give a mixture of both α and β anomers of the original ring form. If the ring oxygen is protonated, a ring conversion can occur yielding a mixture of α,β–pyranose and α,β–furanose ring forms [312]. However, different polysaccharides behave differently during hydrolysis due to their monosaccharide composition: on the Pn1 PS repeating unit the uronic acid and 2–acetamido saccharides will not be fully hydrolysed.

The carboxylic acid functional group on the uronic acid has an electron–withdrawing, inductive effect on the sugar. This group creates an electron deficient C1, slowing down hydrolysis reaction mechanism which produces a hydrolysis resistant sugar. The acetamido group will be deacetylated and then protonated in the acidic medium, this provides the functional group with a stronger electron withdrawing inductive effect than the carboxylic acid functional group.

As with other deoxy–sugars, the 2–acetamido–4–amino–2,4,6–trideoxygalactopyranose residue of Pn1 was found to be very sensitive to acid hydrolysis and completely degraded during analysis [313].

In 1992, Yu Ip *et al*. investigated acid hydrolysis of the pneumococcal serotypes 6B, 14, 18C and 23F with hydrofluoric acid (HF) followed by trifluoroacetic acid (TFA) and TFA on its own and separated and identified on HPAEC–PAD [308]. The hydrolysis with HF and TFA was found to be optimal in hydrolysing the pneumococcal serotypes that contained a phosphodiester bond (6B, 18C and 23F). For Pn14, optimal hydrolysis conditions were determined to be a 16 hour reaction at 98 °C with 2 N TFA.

Methanolysis is an alternate method of cleaving glycosidic bonds and produces *O*–methyl glycosides. Methanolysis is less destructive than acid hydrolysis for neutral monosaccharides, acetamido–sugars, uronic acids and sialic acids as methyl glycosides are more stable than the open chain or reducing sugars formed by hydrolysis with acid [304, 312, 314].

While the reaction mechanism (Figure 3.8) is similar to the acid hydrolysis procedure, the methanol is a much stronger nucleophile than water. Protonation of the glycosidic oxygen is followed by the glycosidic cleavage and formation of the anomeric carbocation; the reaction with methanol results in a mixture of α– and β–anomers of a 1–*O*–methylated saccharide. The protonation of the ring oxygen may also occur which would result in the observed formation of mixtures of α and β anomers of both pyranose and furanose ring forms [312, 315].

Carboxyl groups can be converted into methyl esters and *N*–acyl groups are cleaved during methanolysis [312, 314]. The AAT sugar in the Pn1 PS is destroyed during the methanolysis procedure and hence a re–*N*–acetylation step is not needed. The resultant products can be directly analysed by HPAEC or derivatized and analysed on GC.

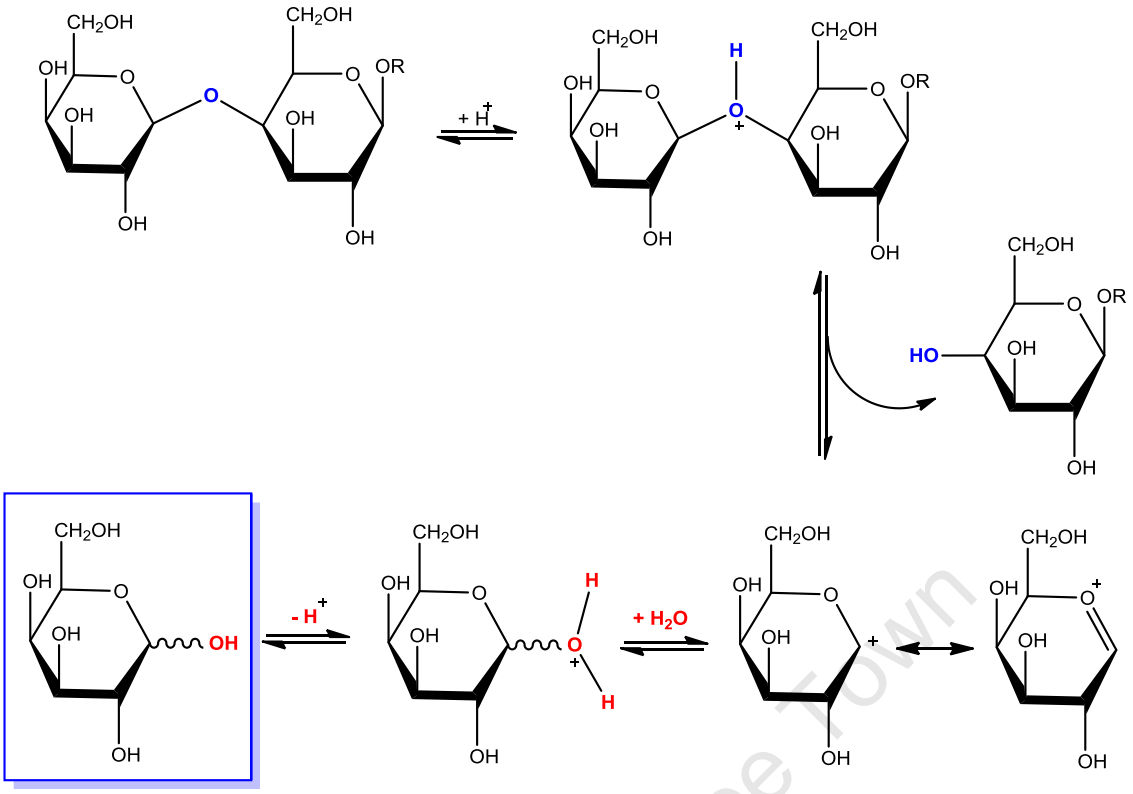

Figure 3.7. Simplified reaction mechanism of the acid catalysed hydrolysis of a model (β–1,4) – galactan [312].

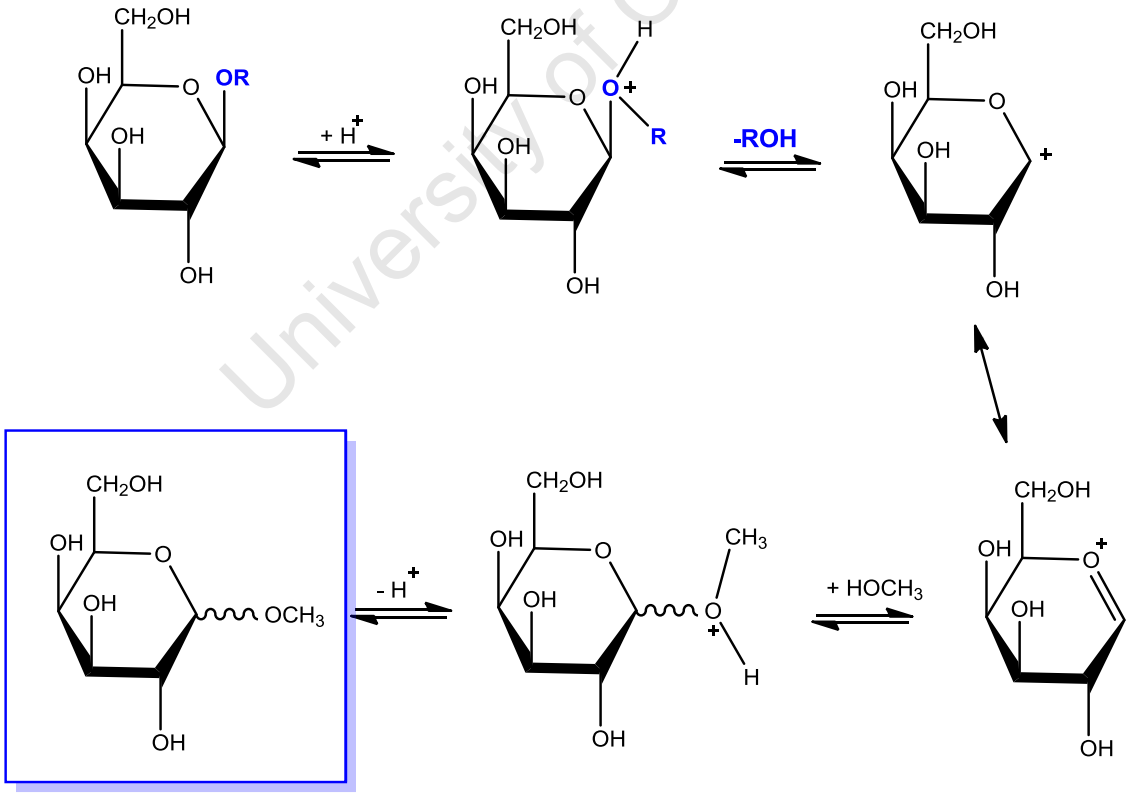

Figure 3.8. Simplified reaction mechanism of the cleavage of a glycosidic linkage (model (β–1,4) – galactan) using the methanolysis procedure [312].

Sweeley and Walker, in 1964, used methanolysis and GC to analyse a number of different glycolipids and gangliosides and determined that a 0.5 N methanolic HCl (HCl/MeOH) at 75 – 80 °C for 24 hours was sufficient enough to form the methyl glycosides of hexoses, neuraminic acid and hexosamines [316]. It was Sweeley and Walker that determined in order to detect hexosamines, a re–*N*–acetylation step would need to be included in the procedure before derivatization. Chambers and Clamp, determined the stability of monosaccharides in HCl/MeOH and found them to be unstable in 4 M and 6 M HCl/MeOH at 100 °C [307]. The methanolysis of glycopeptides and oligosaccharides was found to be complete within 3 hours at 85 °C. Bleton *et al.* studied the characterisation of neutral sugars and uronic acids with Sweeley's methanolysis in 1 6 and determined their mass spectral fragments [263]. The methanolysis of hyaluronic acid [317], agarose [318], and pectins [319, 320] amongst other polysaccharides have also been studied.

Kim *et al.* investigated a GC method to quantify *Streptococcus pneumoniae* polysaccharides, activated polysaccharides and polysaccharide–protein conjugates (Table 3.6) [242]. The 13 serotypes found in Prevnar–13 were subjected to methanolysis followed by re–*N*–acetylation and trimethylsilylation. Peaks were confirmed by comparing the retention times against monosaccharide standards as well as mass spectral analysis. Pn1 PS could not be fully hydrolysed due to the acid resistant glycosidic bonds which was first reported by Talaga *et al.* in 2002 [235]. Kim hypothesised that the extra peaks in the hydrolysed Pn1 chromatogram shown in Figure 3.9 were due to disaccharides and trisaccharides that could not be hydrolysed (based on retention time comparison with model di– and tri–saccharides). The presence of these saccharide units was always reproducible and were used in conjugation with the GalA monosaccharide residues, to quantify the saccharide and compared well (102 %) with the colorimetric method.

Table 3.6. Summary of hydrolysis and methanolysis work performed on pneumococcal serotype 1 polysaccharides.

Author	Serotype		Reagents	Temperature (°C)	Time (min)
Talaga *et al*. [235]	1, 3, 4, 5, 6B, 7F, 9V, 14, 18C, 19F, 23F	a)	2 N HCl/MeOH	80	24 hr.
			+ 2 M TFA	121	120
		b)	2 M TFA	121	120
		c)	48 % HF	65	120
			+ 2 M TFA	121	120
Kim *et al.* [242]	1, 3, 4, 5, 6A, 6B, 7F, 9V, 14, 18C, 19A, 19F, 23F		3 N HCl/MeOH	121	120
			MeOH, py, Ac_2O	RT	30
			TMS	80	20

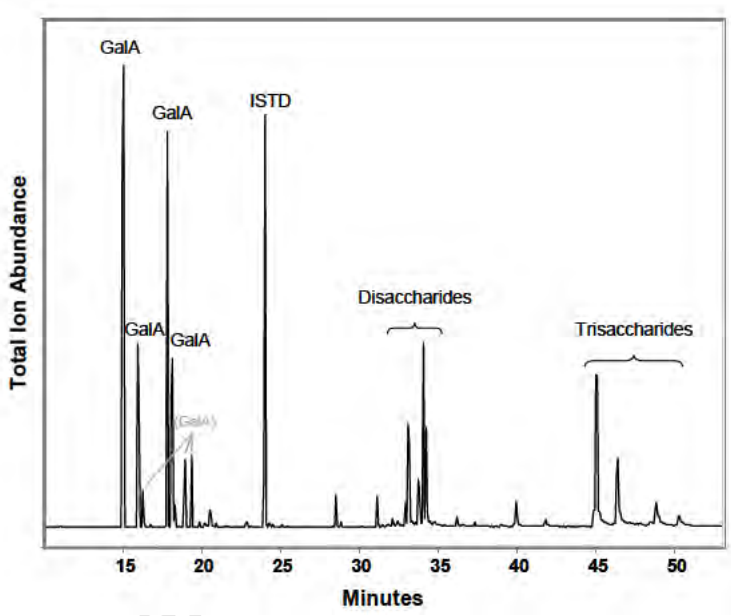

Figure 3.9. GC chromatogram of hydrolysed Pn1 from Kim *et al.* [242].

The combination of methanolysis followed by hydrolysis with TFA has been successfully applied by both De Ruiter *et al*. and Talaga *et al.* [235, 311]. De Ruiter *et al.* investigated the hydrolysis of various polysaccharides from fungi, plants and animals that contained uronic acid residues [311]. Comparisons of methanolysis followed by TFA hydrolysis with H_2SO_4 and TFA acid hydrolysis were made using HPAEC analysis. The method used a 16 hr. methanolysis at 80 °C followed by hydrolysis conditions of 2 M TFA, at 121 °C for 1 hour. In this way the polysaccharide was converted into methyl glycosides through the methanolysis and subsequently into the monosaccharide residues after hydrolysis. This resulted in the complete hydrolysis of most of the polysaccharides when compared to acid hydrolysis alone as shown in Figure 3.10 with respect to citrus pectin. Only monosaccharides could be detected from this method compared to the presence of oligomers in the TFA hydrolysed sample.

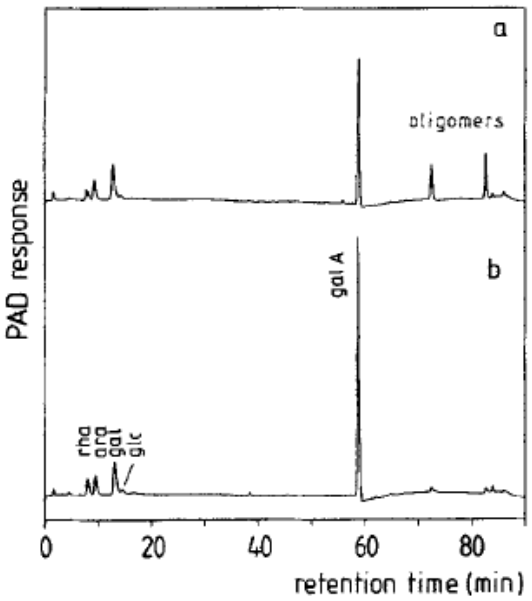

Figure 3.10. Chromatograms of citrus pectin after a) TFA hydrolysis and b) methanolysis followed by TFA hydrolysis [311].

Talaga *et al.* [235] applied a combination technique of acid hydrolysis and methanolysis to eleven pneumococcal serotypes and cell wall polysaccharide using three different methods; TFA hydrolysis, methanolysis followed by TFA hydrolysis and HF followed by TFA hydrolysis (Table 3.6). The hydrolysed samples were separated and identified by HPAEC–PAD. It was determined that the best results were achieved with the TFA hydrolysis for most of the polysaccharides. Serotypes 3, 5 and 9V which contained glucuronic acid (GlcA) were best hydrolysed with methanolysis followed by TFA hydrolysis. Pn1, however, proved difficult to fully hydrolyse as the AAT sugar is known to be destroyed during acid hydrolysis [292, 321] and the linked GalA disaccharide residue that remains after the AAT sugar had been destroyed was very resistant to acid hydrolysis. Although the methanolysis/hydrolysis method produced a superior hydrolysis of Pn1 PS, Figure 3.11, it was not suitable to be used as a quantitative method for Pn1 due to the low recovery of GalA.

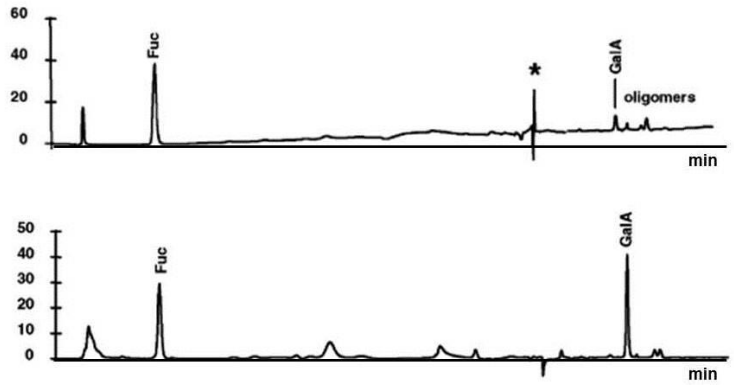

Figure 3.11. HPAEC**–**PAD chromatograms of hydrolysis of Pn1 PS by a) TFA hydrolysis and b) methanolysis and TFA hydrolysis. Fucose (Fuc) was used as the internal standard [235].

The advantage of methanolysis and TFA hydrolysis over other hydrolysis methods is that both reactants can be removed by evaporation and thus both reactions can be performed in the same reaction vessel, eliminating major losses and improving the reproducibility of the reactions.

3.4.1 Microwaves

Due to the resistance of Pn1 PS to conventional hydrolysis, an alternate strategy was sought. Microwaves and microwave heating were investigated as the techniques have been applied to many different chemistry–related fields [322-331]: from protein and peptide analysis [332-335] to glycosylations [336, 337], methylation [338] and esterifications [339]. Microwaves have also been used to derivatize compounds for GC analysis [340]. Much work has recently been performed on the extractions and hydrolysis of compounds [341-350] as well as degradation studies on hyaluronic acid [351-353].

Microwave energy comprises of electromagnetic waves in the range 300 MHz to 300 GHz that corresponds to wavelengths of 1 cm to 1 m and is found between infrared and radio frequencies. They consist of oscillating magnetic and electric fields at right angles to each other (Figure 3.12). The fluctuation of the electric field causes liquids to heat when exposed to microwave energy. Liquid can be heated by two different mechanisms; polar molecules align their dipole moments to the changing electric field which cause them to rotate back and forth as well as colliding with the nearest molecules generating heat. The other mechanism is based on ions in solution that migrate to the oppositely charged side of the electric field. The consequence of this movement is collisions between the ions and other molecules in solution which again, generates heat. These two mechanisms contribute simultaneously to the rate of heating [332, 335, 354].

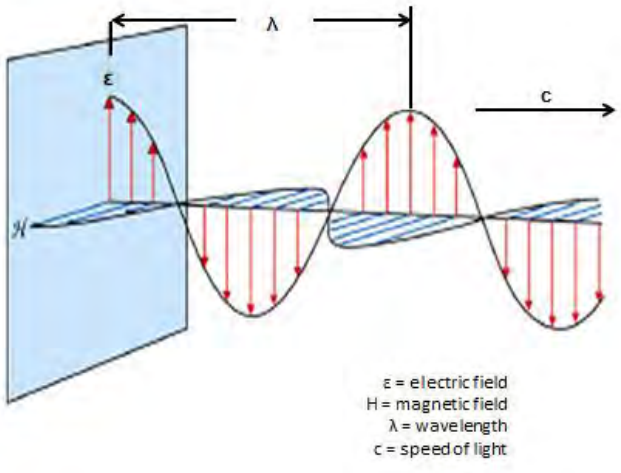

Figure 3.12. Schematic representation of a microwave [354].

The use of microwaves in chemical synthesis became popular after published articles by Giguere and Gedye in 1986 [322, 355]. The authors identified that microwave heating results in faster reaction times of a few minutes, compared to the hours of traditional thermal heating. The difference between conventional thermal heating and microwave heating is the way in which the heat is transferred to the sample. In conventional heating the thermal energy must first heat the heating mantel which in turn heats the outer surface of the container. The hot outer surface of the container transfers the heat onto the reaction mixture. The heat transfer is very slow and inefficient, and can result in some parts of the reaction mixture heating up before the ideal temperature is reached. When the heat source is switched off, the heat is still being transferred from the reaction container to the reaction mixture.

The energy that comes with microwave heating, on the other hand by–passes the heating mantel and container as most mantels and containers are permeable to microwaves. The energy interacts directly with the reaction mixture. This allows for the heat to be transferred quicker and more evenly than thermal heating. Due to the by–passing of the reaction vessel, when the heat source is switched off, the reaction does not continue to heat and therefore reduces the risk of overheating. Figure 3.13 shows the difference between conventional and microwave heating.

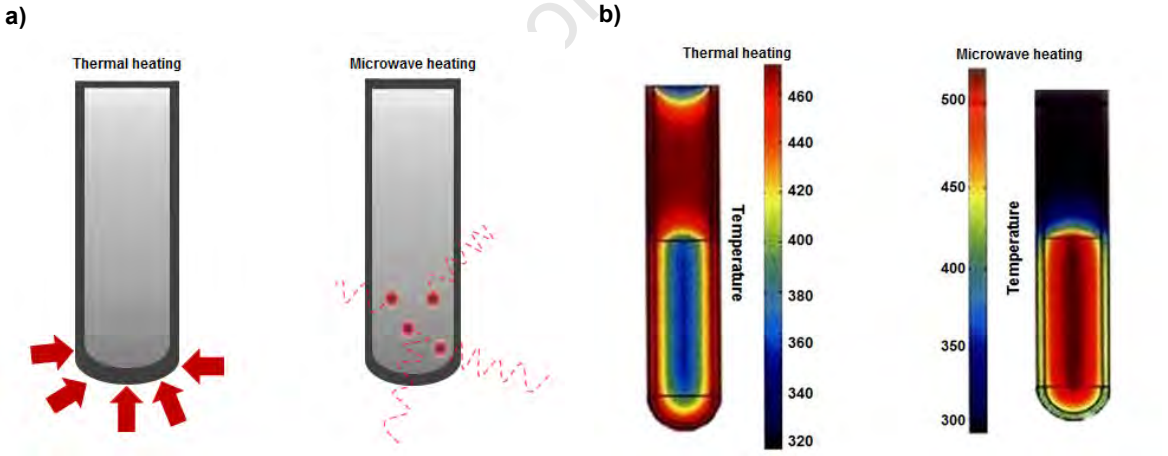

Figure 3.13. a) Conventional thermal heating compared to microwave heating [354] and b) inverted temperature gradient in conventional heating and microwave heating [323].

The use of microwaves in the hydrolysis of carbohydrates has been gaining popularity. The hydrolysis of starch was one of the first carbohydrates investigated and Yu *et al.* found that the microwave hydrolysis of starch in dilute acid was complete within 5 min instead of 60 min by conventional heating. The effects of salt on the acid hydrolysis of oligomers and glucose was also investigated and it was found that the addition of some inorganic salts could further decrease the hydrolysis time of starch [344, 356].

Plant seed gums, consisting of galactomannans have also been the subject of microwave assisted acid hydrolysis. Hydrolysis was shown to be complete within two minutes using a very dilute (0.00625 N) sulfuric acid solution compared to the conventional acid hydrolysis of over 40 hours with either 2 N H_2SO_4 or 4 hr. with 1 M TFA solution [343]. This demonstrated the superiority of microwaves when compared to thermal conventional heating and resulted in the use of milder reaction conditions and reactants, higher yields, enhanced selectivity, faster reactions and purer products [325, 327, 342, 346].

Pn1 PS has not been the subject of microwave assisted hydrolysis investigations. As the monosaccharide components of Pn1 render it acid resistant it was thought that stronger conditions would be able to fully hydrolyse the sample. The two known methods of analysis of Pn1, namely TFA hydrolysis and methanolysis were investigated with microwave heating and analysed on both HPAEC and GC. Optimisations of reaction time, temperature, acid concentrations and power were investigated and the resultant method was compared to the classical heating methods.

3.4.2 Chromatographic methods

The two most widely used chromatographic methods in the structural identification and characterisation of polysaccharides are high performance anion exchange chromatography (HPAEC) and gas chromatography (GC). HPAEC makes use of the weakly acidic nature of monosaccharides to separate them at high pH using a strong anion exchange stationary phase [231]. GC is a much more sensitive method of analysis and is less susceptible to interferences from salts and proteins [303], however saccharides do need to be derivatized in order to be volatile enough to be used in this method.

3.4.2.1 HPAEC–PAD

There have been many different high performance liquid chromatographic systems used to analyse hydrolysed saccharides. However, it was only after the quaternary ammonium resin anion–exchange columns, with pulsed amperometric detection, were developed that the method was able to be applied to all carbohydrates [210, 212, 303, 314].

Carbohydrates are weakly acidic, at high pH these carbohydrates are partially ionised and can be separated with a strong anion exchange stationary phase (Table 3.7). In most cases, the sequence of elution is based on the pKa value of the monosaccharide, due to the acidic nature of uronic acids these residues are retained on the column the longest and need the help of acetate to enable its elution.

The detection of these separated saccharide residues is based on the electric current generated by their oxidation on a gold electrode [231]. The oxidation on the surface of the electrode slowly covers the electrode, decreasing its sensitivity. The electrode is therefore continuously regenerated by raising the potential on the surface so as to oxidise the gold. This in turn causes desorption of the carbohydrate oxidised products, and once this is accomplished the electrode potential is the lowered to reduce the surface back to gold [231, 233, 314].

Table 3.7. Dissociation constants of common carbohydrates (in water at 25 °C) [231].

Sugar	pKa
Fructose	12.03
Mannose	12.08
Xylose	12.15
Glucose	12.28
Galactose	12.39
Galacturonic acid	3.51

The advantage of HPAEC–PAD over GC is that no derivatization is needed prior to injection and samples can be in aqueous solutions. The analysis run time is also shorter compared to GC. While the instrument itself is expensive, eluents such as sodium hydroxide and sodium acetate are relatively inexpensive.

3.4.2.2 GC–FID

Gas chromatography has been used in sugar analysis for many years due to its superior resolution and robustness. GC analysis requires very small amounts of sample and is a very sensitive technique, although the sample preparation is time consuming as samples need to be made volatile enough through derivatization [304, 315]. There are two main derivatization procedures; in the first a single derivative is produced from each saccharide (e.g. alditol acetates), the second procedure produces several derivatives (e.g. methyl glycosides) depending on the anomeric configuration of the saccharide [303]. The alditol acetate derivatives produce a simple chromatogram that is easy to quantify. Having a number of peaks is advantageous as the methyl glycoside peaks always form in the same ratios; this pattern is therefore reproducible and can be used as a 'fingerprint' for a specific compound [303].

Sample loss due to derivatization must be taken into account and the use of an internal standard allows for this as the loss of sample and the loss of internal standard will be of the same proportion so the ratio of sample to internal standard will remain the same. Internal standards are also used to account for the difficulty to inject a reproducible proportion of the

sample onto the column [314]. Internal standards should be a compound similar to the analyte being investigated but should not normally be present in the sample and it should elute at a completely different time from the saccharide of interest. In these investigations, *myo*–inositol was used.

The simplest detector used in carbohydrate GC analysis is a flame ionisation detector. The mobile phase delivers the separated components to the flame whose ionisation changes as the molecules pass through it, producing an electrical current. This detection method can be used for all carbohydrates however identification is based on the comparison of standards that are run separately. Another detector that is used in saccharide analysis is the mass spectral detector. This detector measures the mass to charge (m/z) ratio of the compound and is reproduced as a mass fragmentation pattern which is unique to each compound. Thus a comparison of the mass fragmentation patterns of the sample to a library of standards will help identify the saccharide without the need to run a separate standard.

3.4.3 TFA hydrolysis of Pn1

The microwave assisted acid hydrolysis technique has been compared to its conventionally heated hydrolysis in many investigations. A comparison of the TFA hydrolysis of bacterial cell carbohydrates using conventional and microwave heating was undertaken in 2008 by Zhao and Monteiro [346]. The 4 M TFA hydrolysis took 5 hours at 105 °C in a heating block (conventional) but only 5 min at 120 °C with the assistance of microwave heating. The qualitative results, in Figure 3.14, show that the peak area percentage of each monosaccharide obtained via conventional and microwave heating are comparable.

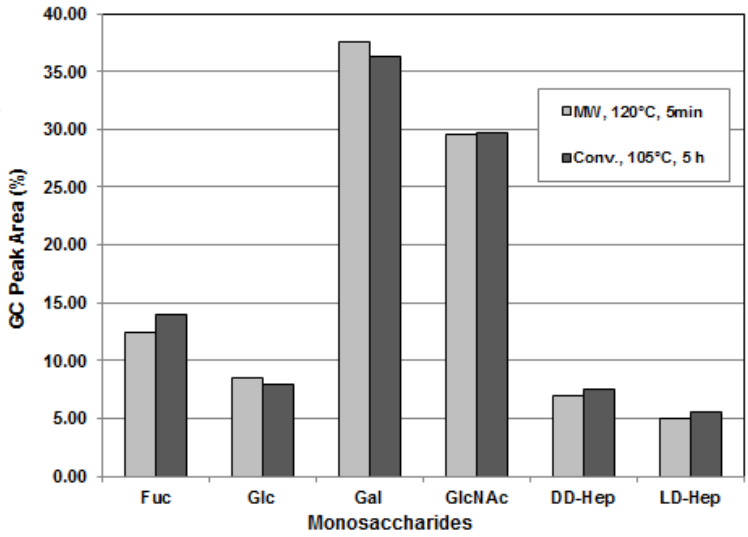

Figure 3.14. Comparison of the data of TFA hydrolysis by conventional and microwave heating [346].

As HPAEC–PAD was the analysis method of choice in literature for TFA hydrolysis, it was used to investigate the best conditions for hydrolysis of Pn1 polysaccharide with microwaves. Figure 3.15 illustrates the typical chromatograms resulting from the TFA microwave hydrolysis of Pn1 on the HPAEC–PAD where the internal standard fucose eluted at approximately 2.8 min and the peak corresponding to the GalA monosaccharide eluted at 31 min. A peak, at approximately 10 min, was hypothesised to be due to the degradation of the AAT sugar and was detected in all hydrolysed Pn1 samples. Literature suggests that the response factor of GalA is a fraction of the response factor of fucose [235] and hence recoveries were determined relative to the fucose peak area.

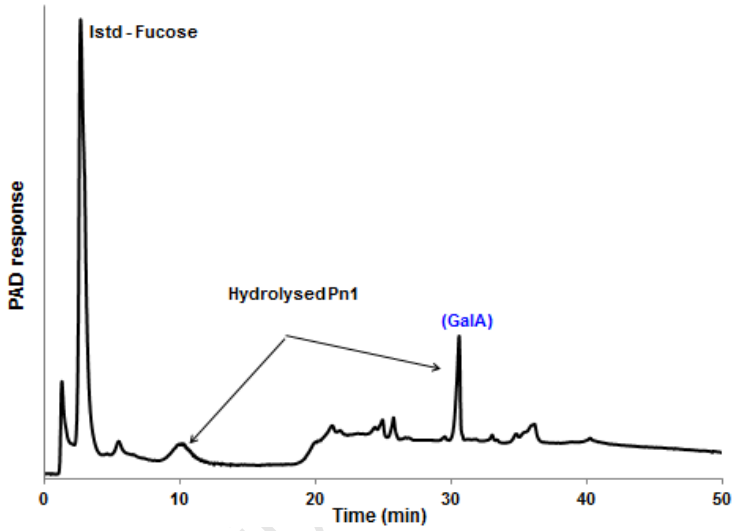

Figure 3.15. Representative chromatogram of hydrolysed Pn1 PS using HPAEC–PAD (microwave conditions: 2 M TFA, 150 W, 1 min).

The concentration of TFA (2 M vs. 5 M), reaction times (1, 2, 5 min) and power output (100, 150 W) of the microwave were determined on a 2 mg polysaccharide scale (Table 3.8). The temperature of the reaction is maintained automatically by the instrument and rises to a set point except when the pressure maximum is reached which causes a halt in the increase of temperature until the pressure is decreased to within the prescribed limits. This meant that the temperature of the reaction had to be monitored at all times but throughout the investigations, the temperature did not increase above 123 °C.

As the same amount of polysaccharide was used for all microwave variations, a comparison between the internal standard and the resultant GalA peak areas were used to determine the optimised parameters. From the comparison, it was determined that 2 M TFA gave a better recovery of 46 % than the 5 M concentration (7 %). It was thought that the lower recovery of GalA was due to the destruction of the saccharide before hydrolysis could be achieved. This effect was confirmed when the results of the different hydrolysis times were compared. The highest recovery was found in the one minute hydrolysis and the recovery then decreased

and extra peaks detected as the reaction time increased which again suggested the destruction of the polysaccharide. A concentration of 2 M TFA, a reaction time of one minute and 2 mg Pn1 PS were subjected to different power outputs of 100 or 150 W. Lower recoveries of GalA occurred in the lower power setting. The 150 W samples did not show complete recovery of GalA and a higher microwave power was attempted but due to the volatility of the TFA, the reaction tube reached its maximum pressure and the sample could not be analysed.

Table 3.8. Comparison of variables investigated for optimised microwave conditions.

TFA conc. (M)	Reaction time (min)	Power setting (W)	HPAEC–PAD peak area (%) of GalA
5	1	100	7
2	1	100	46
2	1	150	55
2	2	150	42
2	5	150	18

It was determined from the above investigations that the optimised hydrolysis method aided by microwave heating was 150 W power output, 2 M TFA and a reaction time of one minute. This was compared to the hydrolysis method which made use of conventional heating of 2 M TFA at 121 °C for 2 hours. The highest temperature reached during microwave analysis was 123 °C.

Figure 3.16 shows the superiority of the microwave method compared to the conventional heating method; a much smaller peak corresponding to GalA was found in the conventional method along with many extra peaks. This was either due to incomplete hydrolysis (peaks after the GalA at 29 min) or degradation of the saccharide residues found before the GalA elution. The GalA peak of the microwaved sample appeared much larger in the chromatogram as did the peak at 10 min which was hypothesised to be due to the degraded AAT sugar. The recovery of GalA using the microwave method was much higher at 76 % compared to the 8 % achieved with conventional heating (Table 3.9). This shows the superiority of the microwave method both in terms of recovery as well as reaction times.

Table 3.9. Comparison of variables between microwave and conventional heating.

Source of heat	TFA (M)	Temperature (°C)	Reaction time (min)	GalA peak area (%)
Heating block	2	121	120	8
Microwave	2	123	1	76

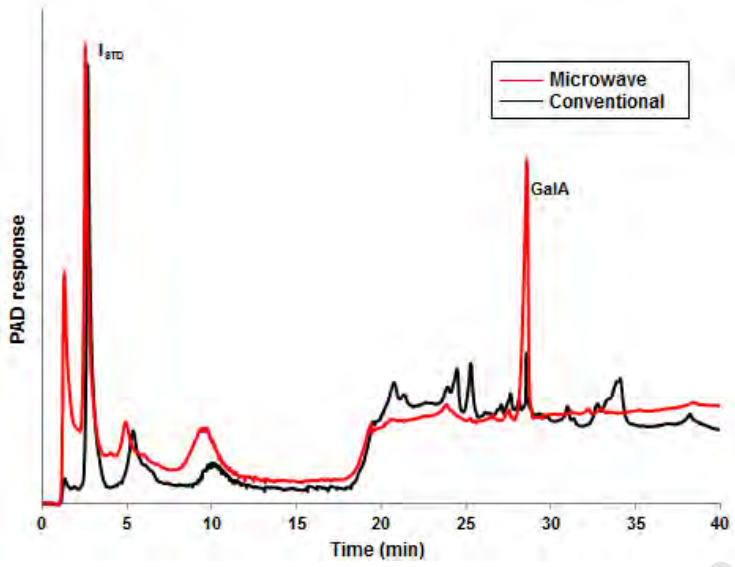

Figure 3.16. Chromatograms of hydrolysed Pn1 using conventional (black) and microwave (red) heating analysed on HPAEC–PAD. Microwave conditions: 2 M TFA, 150 W, 1 min. Conventional conditions: 2 M TFA, 120 min, 121 °C.

3.4.4 Methanolysis of Pn1 PS

There have been few reported investigations into the microwave assisted methanolysis of polysaccharides. Nakanishi *et al*. cleaved phenylbenzylsaccharides in 15 minutes using a household microwave instead of the overnight procedure that is usually employed [357]. In 2004, Itonori *et al.* found that the methanolysis of carbohydrates from glycosphingolipids was complete in under two minutes [325, 358]. Microwave assisted methanolysis has also been used for fatty acids with complete esterification achieved in one minute compared to the traditional heating times of 6 – 8 hr. [359]. Two diterpene molecules extracted from green coffee oil underwent methanolysis by microwave and conventional means. A 99 % recovery of the diterpenes was achieved after 3 min at 100 °C compared to only a 26 % recovery after 2 hours of conventional heating [360]. This demonstrates not only that microwave assisted methanolysis speeds up reaction times but that it results in higher recoveries when compared to traditional methods.

In this investigation, GC–FID was used to determine the optimal microwave conditions including: acid concentration, reaction temperature, reaction time and power values. Figure 3.17 displays the typical chromatogram of the trimethylsilyl– (TMS) derivatives of microwave–hydrolysed Pn1 PS, (the reaction to produce volatile derivatives is detailed in Figure 3.18).

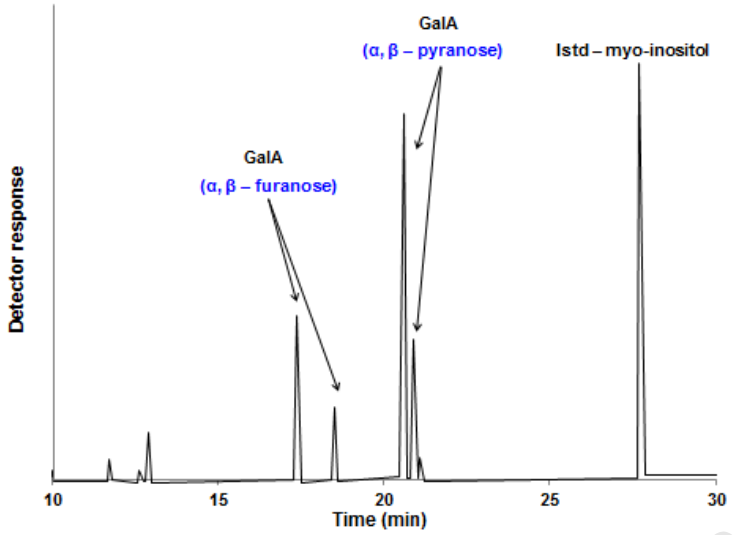

Figure 3.17. Representative chromatogram of hydrolysed Pn1 PS using GC–FID (microwave conditions: 3 N HCl/MeOH, 100 W, 121 °C, 1 minute).

The internal standard (*myo*–inositol) eluted at 27 min, and four peaks were detected for the GalA portion of Pn1. The peaks corresponded to the α and β conformations of the furanose (17.4 and 18.5 min) and pyranose (20.8 and 21.2 min) methyl glycosidic ring forms of GalA; the order of which was β–furanose, α–furanose, α–pyranose, β–pyranose [361]. These peaks were confirmed with GC–MS (Figure 3.19). In determining the optimised microwave conditions and the comparisons with the conventional methods, the recoveries of GalA were determined as a percentage of the total area of peaks in the chromatogram relative to the internal standard.

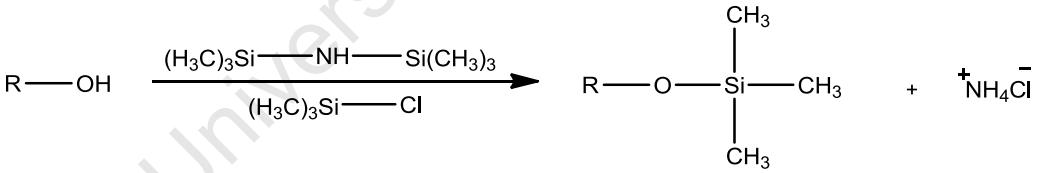

Figure 3.18. Derivatization procedure producing volatile derivatives for GC–FID analysis.

The fragmentation patterns of the furanose and pyranose ring forms are very similar; both contain fragments of 73, 133, 147, 159, 217 and 234 m/z. The difference in the patterns, which is used to identify the furanose and pyranose ring forms is the 204 m/z fragment: in the pyranose ring form this fragment is the base peak and the ratio of 204:217 is greater than 1. In the furanose fragmentation pattern the 217 fragment is the base peak and the 204 fragment peak is present only in trace amounts and the ratio of 204:21 is <<<1 [312, 362]. The fragments at 73, 89, 103 are all known TMS derivatives [312, 362].

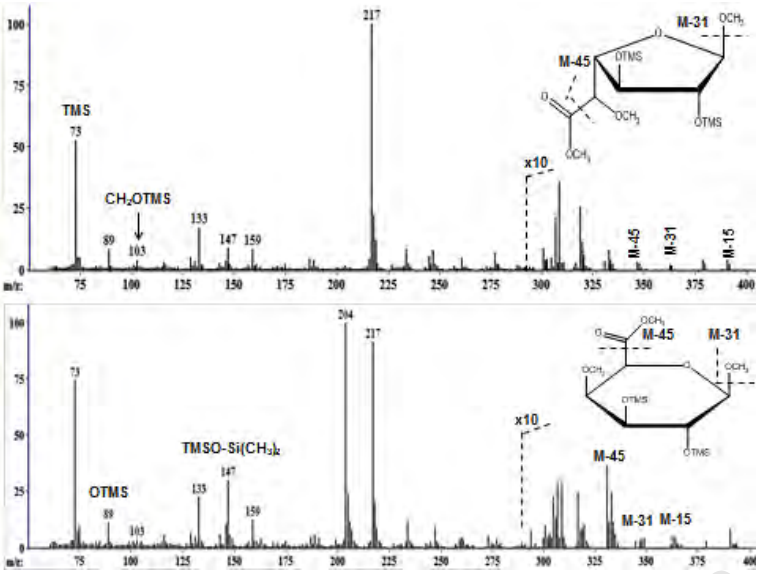

Figure 3.19. Mass spectral data for a) furanose (17.4 and 18.5 min) and b) pyranose ring forms (20.8 and 21.2 min) of GalA from GC–MS.

Two different power outputs: 100 W and 150 W were compared however, due to the high volatility of methanolic HCl, 150 W was too powerful which led to the upper pressure limit of the reaction vessel and microwave instrument being reached and the instrument terminated the reaction. The preferred concentration (2 N vs. 3 N) of methanolic HCl was determined when the 3 N HCl/MeOH produced the better results (1.8 fold increase in recovery) compared to the 2 N HCl/MeOH sample which revealed evidence of incomplete hydrolysis as the presence of disaccharides at 34 – 36 min (Figure 3.20) was identified, this has been described by Kim *et al*. when conventional thermal heating was applied [242].

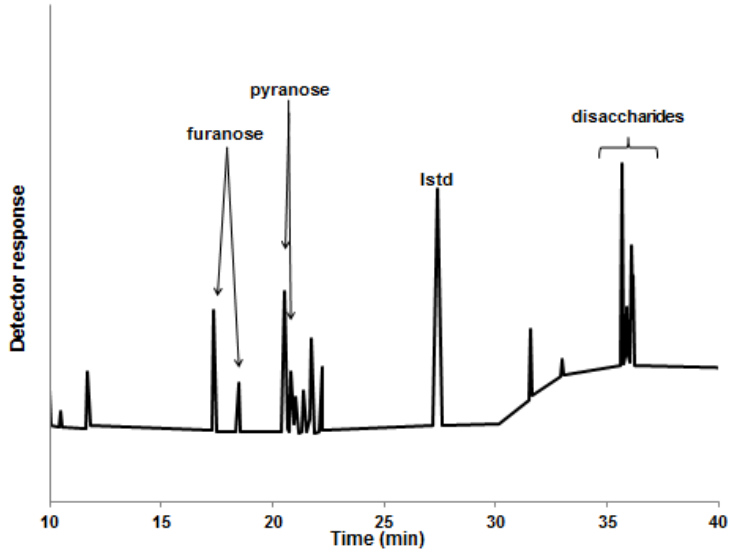

Figure 3.20. GC–FID chromatogram of Pn1 polysaccharide after microwave methanolysis (2 N HCl/MeOH, 121 °C, 100 W, 1 minute).

The reaction variables and resulting peak areas are collected in Table 3.10. The percentage of GalA as a total of the GC peak area was determined to be 21 % in the case of 2 N HCl/MeOH but increased to 60 % for 3 N HCl/MeOH. The percentage of peak area dominated by the disaccharides was 41 % in 2 N HCl/MeOH. This suggested that the stronger acid would be best suited to the hydrolysis of Pn1 PS. With a power output of 100 W, the temperature reached a maximum of 121 °C, therefore two different temperatures were examined, 100 °C and 121 °C. The higher temperature again produced a better recovery of GalA. As most investigations into microwave assisted methanolysis suggested a maximum recovery of the components after 2 minutes, the optimal reaction time was also studied. In the case of Pn1 PS, the best recovery was determined after a one minute reaction (60 %) with only 38 % of GalA recovered after a two minute reaction.

Table 3.10. Reaction variables tested in the optimisation of microwave assisted methanolysis of Pn1 PS.

Conc. HCl/MeOH (N)	Temp (°C)	Reaction time (min)	Power (W)	% GalA (% GC peak area)
2	121	1	100	21
3	121	1	100	60
3	100	1	100	18
3	121	2	100	30
3	121	1	150	–

The optimal conditions for microwave assisted methanolysis were found to be a 3 N concentration of methanolic HCl with a reaction time of one minute, reaction temperature at 121 °C and a power output of 100 W. These optimised conditions were compared to the conventional methanolysis method and reaction conditions are detailed in

Table 3.11. The reaction time for the conventional method was 2 hours compared to the much faster one minute reaction using microwaves. An increase in recovery was also found in the microwave sample, no peaks corresponding to disaccharides were detected and the chromatogram was relatively clean (Figure 3.21). Peaks were detected before 10 minutes but were superimposable to the conventional method; a number of these peaks were identified as plasticisers by their mass fragmentation patterns (not shown). The mass fragmentation of a few peaks suggested that they were of some carbohydrate origin and were hypothesised to be due to the degradation of the AAT sugar. The conventional method produced a chromatogram with peaks eluting in the region of 36 min which corresponded to disaccharides and a recovery of 26 % of GalA compared to the 61 % recovery from the microwave method was calculated.

Table 3.11. Comparison of conventional and microwave assisted methanolysis of Pn1 PS.

Source of Heat	Conc. HCl/MeOH (N)	Temp (°C)	Reaction time (min)	% GalA
Heating block	3	121	120	26
Microwave	3	121	1	61

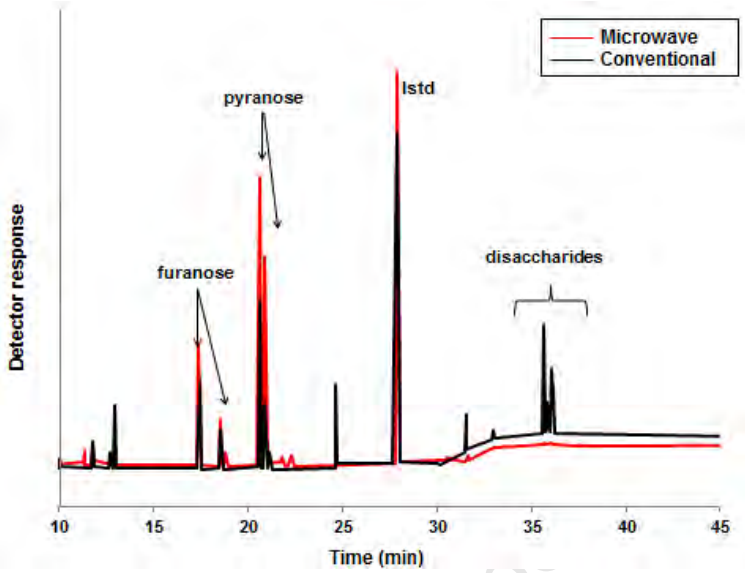

Figure 3.21. Chromatograms of Pn1 after methanolysis using conventional (black) and microwave (red) heating analysed on GC–FID. Microwave conditions: 3 N HCl/MeOH, 100 W, 1 min, 121 °C. Conventional heating: 3 N HCl/MeOH, 120 min, 121 °C.

3.4.5 Combination of methanolysis and TFA hydrolysis

The Talaga *et al*. investigation [235] investigated the alternate method of hydrolysis during which methyl glycosides were created, followed by the use of TFA to hydrolyse the remaining glycosidic linkages. Although this did not lead to a quantifiable method for Pn1 in the literature, it did produce the best results and a comparative investigation was undertaken between the conventional and microwave assisted combination hydrolysis using both HPAEC–PAD and GC–FID analysis.

3.4.5.1 HPAEC–PAD

The reaction details were taken from the optimised methods in the GC analysis section and details of the reactions are given in Table 3.12. The order of methanolysis and acid hydrolysis was also investigated; whether the acid resistant glycosidic bond should be broken first with methanolysis followed by acid hydrolysis into the monosaccharide components or acid hydrolysis should first be performed and methanolysis should follow as a gentler method to break any remaining glycosidic linkages.

Table 3.12. Reaction conditions for comparison of a combination of methanolysis and hydrolysis using microwave and conventional heating.

	Microwave		Conventional	
	Methanolysis	TFA hydrolysis	Methanolysis	TFA hydrolysis
Concentration of reagents	3 N	2 M	3 N	2 M
Reaction time (min)	1	1	120	120
Reaction temperature (°C)	121	121	121	121
Power (W)	100	150	–	–

The HPAEC–PAD comparison was made of the two methods as depicted in Figure 3.22. The first noticeable difference was determined with the appearance of extra peaks at 2.8 and 3.4 min in the sample that underwent methanolysis first. These peaks were hypothesised to be due to the degradation of the AAT sugar as it has been shown that amino sugars are more sensitive to acid hydrolysis conditions after methanolysis [235].

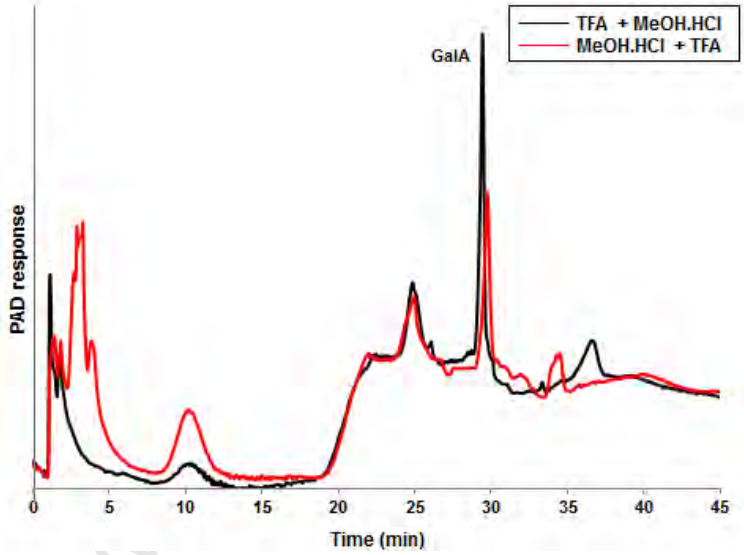

Figure 3.22. HPAEC–PAD chromatograms comparing the order of methanolysis and acid hydrolysis of Pn1.

Low recoveries were determined in both methods when compared to just TFA hydrolysis. Additional degradation products were also detected for these two methods. As microwave assisted TFA hydrolysis on its own was able to achieve a 76 % recovery on HPAEC–PAD, it was theorised that the additional step is not needed and causes destruction of the saccharides. These samples were repeated three times and compared to the conventional combination methods of both methanolysis followed by acid hydrolysis and the hydrolysis followed by methanolysis. The relative peak areas when compared to the internal standard show the two heating methods to be comparable for both combinations with the conventional heating producing an average of 15 % recovery of GalA which is in accordance with the values determined by Talaga *et al*. The microwave heating gave slightly higher recoveries

but these were not significant (Table 3.13). In this case, the advantage of the microwave method is purely one of reaction time.

Table 3.13. Comparison of relative peak areas of GalA after methanolysis and TFA hydrolysis.

Source of Heat	MEOH–TFA	TFA–MEOH
Heating block	12	17
Microwave	19	23

3.4.5.2 GC–FID

Whilst the combination literature methods were analysed on HPAEC–PAD, a derivatization step was added and the samples were analysed on GC–FID. Since the methanolysis with GC analysis had been optimised, the TFA hydrolysis was investigated. As before, reaction time, reaction temperature and microwave power were investigated, details of which can be found in Table 3.14. The concentration of TFA was kept constant at 2 M throughout the investigations. Reaction times of 20, 30 and 60 were compared with recoveries of GalA, based on peak area, increasing with increasing reaction time with a one minute reaction producing the highest recovery at 61 %. Power output levels were tested with 150 W showing an increase in recovery compared to that at 100 W. Finally, three different reaction temperatures were examined with the conventional temperature of 121 °C producing the highest GalA peak area of 65 % of the total peak area of the chromatogram, the higher temperatures led to the degradation of the GalA peaks as described in the literature [235, 242]. From the data, the optimised conditions were found to be a 2 M TFA solution, at a temperature of 121 °C, a reaction time of one minute and a power output of 150 W.

Table 3.14. Comparison of variables for the optimisation of TFA conditions in combination with methanolysis.

Conc. TFA (M)	Temp (°C)	Reaction time (sec)	Power	% GalA (peak area)
2	121	20	150	38
2	121	30	150	44
2	121	60	150	61
2	121	60	150	65
2	130	60	150	60
2	150	60	150	51
2	121	60	150	69
2	121	60	100	27

This method was compared to the combination method described by Talaga *et al*. in which conventional thermal heating was used. Whilst the concentration of the reagents, the temperature and the order in which the methanolysis and hydrolysis were performed remained the same when using conventional or microwave heating, the reaction time was

much faster with microwave heating only requiring one minute for the methanolysis and one minute for the TFA hydrolysis compared to two hours each for the conventional heating. The chromatogram (Figure 3.23) details much larger peaks for the microwaved sample in comparison to the conventionally heated sample. The relative peak area of the GalA peaks for the microwave sample was determined to be 64 % whereas the conventionally heated sample was only 17 %. Extra peaks were detected in the conventionally heated sample, which indicated that the product had degraded. Both the methanolysis procedure and the combination procedure performed better in the microwave heated sample than the conventionally heated samples in terms of reaction times and recoveries of GalA.

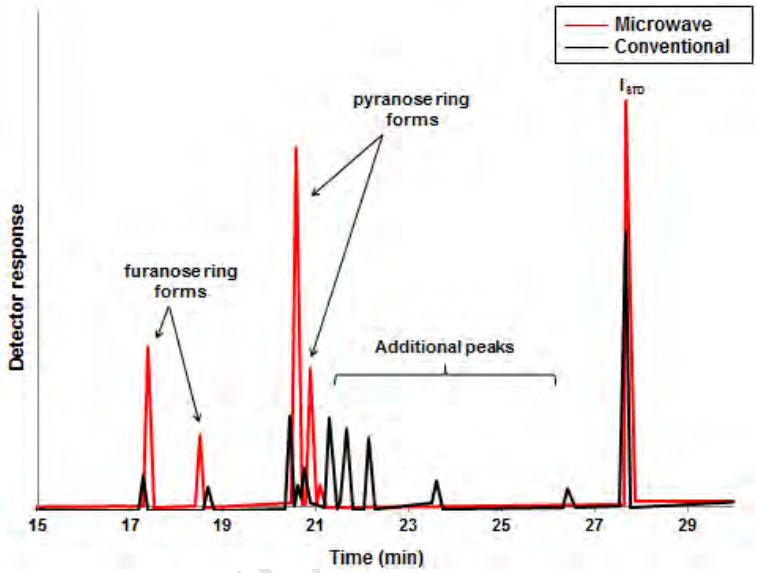

Figure 3.23. Comparison of conventional (black) and microwave assisted (red) hydrolysis of Pn1 polysaccharide.

3.4.6 Summary

The hydrolysis of Pn1 by conventional methods proved difficult due to the inductive effects of the carboxylic acid functional group. Alternate means of hydrolysis utilising microwave assisted heating were investigated with both methanolysis and acid hydrolysis yielding a greater recovery of GalA than the conventional hydrolysis. For HPAEC–PAD hydrolysis, the optimal hydrolysis method involved microwaving the Pn1 polysaccharide in 2 M TFA for one minute at 121 °C using 150 W power which produced a recovery of 76 % compared to only 8 % with conventional thermal heating. Microwave–assisted methanolysis proved to be successful for GC–FID analysis with an increase in recovery from 26 % to 61 %. The optimum method to produce methyl glycosides consisted of 3 N MeOH/HCl microwaved at 121 °C for 60 seconds, compared to 2 hours for conventional heating (with all other conditions kept constant). A combination of methanolysis and TFA hydrolysis was also investigated and was found to be successful with GC–FID analysis with a highest recovery of 69 % achieved.

3.5 Nuclear magnetic resonance spectroscopy

Nuclear magnetic resonance (NMR) is a technique widely used in analysing the structure of a polysaccharide including: the identity of the monosaccharides in the repeating units, their relative amount and their connectivities. In NMR analysis, the nuclear spin levels of an atom are split by a strong magnetic field and by inducing transitions between different energy levels a signal is formed and recorded. The nucleus of an atom behaves like a magnet when exposed to magnetic fields and has an inherent angular momentum which is also known as spin. Every elementary particle (electrons, protons etc.) has an associated spin quantum number that is either an integer or half integer for example, protons have a quantum number of one and electrons have a quantum number of ½. NMR spectroscopy can only be performed on nuclei if the total spin is not equal to 0. Table 3.15 lists the most common elements used in NMR spectroscopy.

Table 3.15. List of abundance of most common elements used in NMR spectroscopy.

Isotope	Spin number	Abundance (%)
^{1}H	½	99.9
^{13}C	½	1.1
^{15}N	½	0.37
^{31}P	½	100

As organic molecules are mainly composed of carbon and hydrogen they are the two most common forms of NMR spectroscopy and since hydrogen is more abundant than ^{13}C, it is by far the most common element monitored with NMR.

Each proton in a molecule is affected by the chemical environment that surrounds it. Any change in the chemical environment can change the degree of shielding on the proton and hence its chemical shift. The electronegativity of a neighbouring group will reduce the electron density of the proton and the nucleus is therefore deshielded and can be found further downfield. The methyl protons on an acetate functional group can be shifted as much as 1 ppm due to the neighbouring oxygen or nitrogen atom.

In this way ^{1}H NMR can be used to elucidate the number of different environments that protons exist in. If, however, two or more protons are in the exact same chemical environment they have the same chemical shift, but the intensity of the peak will integrate for more than one proton. The chemical shift of the proton reflects its molecular structure and can be used in the clarification of a compound's structure [195].

The proton NMR spectra of polysaccharides can often be complex with overlapping peaks especially in the ring proton region (3.5 – 4.5 ppm). Some characteristic signals can be identified; the most important of these are the anomeric protons (H1). Anomeric protons are usually found with a chemical shift of 4.4 – 5.5 ppm depending on their configuration (Table 3.16). The number of signals in this anomeric region is indicative of the number of saccharides contained in the polysaccharide repeating unit. Other distinctive signals include the methyl protons of acetyl (*O*– and *N*–) functional groups (2.2 – 2.0 ppm) and the H6 proton of 6–deoxysugars (1.15 – 1.35 ppm).

Table 3.16. Proton chemical shifts and coupling patterns of commonly found resonances in the NMR spectra of polysaccharides [363].

	Chemical Shift range (ppm)	**Coupling pattern**
H1 of α sugars	5.5 – 5.0	d, 3 – 5 Hz
H1 of β sugars	5.0 – 4.4	d, 8 Hz
H1 of α–*manno* sugars	5.5 – 4.9	d, <2 Hz
H1 of β–*manno* sugars	5.0 – 4.6	d, <2 Hz
ManNAc H2	4.7 – 4.3	d, 3 – 5 Hz
α–*manno* H2	4.4 – 3.9	d, 4 Hz
α–GalA H5	5.0 – 4.6	d, ~1 Hz
N–acetylamino sugar methyl	2.15 – 2.00	s
H6 of 6–deoxysugars	1.35 – 1.15	d, 6 Hz

The anomeric signals can be determined in the ^{13}C NMR spectra with signals appearing between 90 – 110 ppm. ^{13}C NMR has the added advantage of being able to distinguish between methyl (CH_3), methylene (CH_2) and methine (CH) carbon groupings through the Distortionless Enhancement by Polarization Transfer (DEPT) experiment. Three different DEPT spectra are needed in order to fully differentiate between the different carbon multiplicities: DEPT–45, DEPT–90 and DEPT–135 (where the number is indicative of the flip angle of the proton pulse). In a DEPT–45 experiment all three carbon groups are shown. In the DEPT–90 signal only CH groups are visible and in the DEPT–135 experiment the CH_2 groups are shown in a different phase to the CH_3 and CH groups and therefore appear as negative peaks on the spectrum. Since methine groups are found in a different part of the spectra, using just the DEPT–135 experiment may allow for the identification of the three carbon multiplicities. Other distinguished signals can be identified in the carbon spectra, these are tabulated in Table 3.17.

Table 3.17. Common chemical shifts in the ^{13}C NMR spectra of polysaccharides [363].

	Chemical shift, ppm
Uronic acid C6	170 – 180
N–acetylaminosugar carbonyl carbon	170 – 180
Furanose sugar C1 (α,β)	101 – 111
Pyranose sugar C1 α	91 – 101
β	95 – 105
Unsubstituted furanose ring carbons	70 – 85
Unsubstituted pyranose ring carbons	65 – 75
Glycosylated hydroxymethyl groups	65 – 68
Unsubstituted hydroxymethyl groups	61 – 64
C–N in amino sugars	48 – 55
N–acetyl methyl carbons	23 – 25
6–deoxyhexoses C6	15 – 19

As ring protons in carbohydrates are often broad and overlap in the ^{1}H NMR ring region and not distinguishable. Two dimensional NMR methods are used to identify these protons. The simplest of these 2D methods is ^{1}H–^{1}H correlated spectroscopy (COSY). COSY is used to identify neighbouring protons, however cross peaks are only seen with correlations due to geminal and vicinal coupling only.

Protons in a single spin system can be assigned using ^{1}H–^{1}H Total Correlation Spectroscopy or TOCSY experiments [195]. Correlations can be made over five or six bonds in the same ring system as long the J couplings are large enough. Small or zero J couplings and the presence of heteronuclear atoms such as oxygen or nitrogen can disrupt this correlation.

The Heteronuclear Single–Quantum Correlation (HSQC) spectrum is the heteronuclear equivalent of the COSY spectrum and consists of a plot of the 1D proton spectrum along one axis and the 1D carbon spectrum of the molecule along the other axis and hence linkages between protons and carbons can be determined [195]. This method is particularly useful if the proton spectrum of the molecule is very crowded and not well resolved. Correlating the carbon spectrum to the proton spectrum will also identify if or when two protons are attached to the same carbon.

Heteronuclear Multiple Bond Correlations (HMBC) connects carbons and protons that are separated by two or three bonds and is thus considered a long–range correlation. For carbohydrates this is important as it allows for glycosidic linkages to be identified by comparing the chemical shifts of the carbons in the polysaccharide to that of the monosaccharide standard a difference is revealed. Glycosylation causes a large downfield shift in the α–carbons, in the range of 6 – 8 ppm and a much smaller upfield shift of between

1 – 2 ppm in the β–carbons [363]. Using this technique allows for the determination of both the attachment position on the sugar residues as well as the position of the sugar in the repeating unit as correlations can be seen from one saccharide to its neighbour through the glycosidic linkage.

While many polysaccharides contain only protons, carbons and oxygens, many will also contain nitrogen (as amino or *N*–acetylated sugars) and phosphorus (phosphate group). These can be determined by recording either the ^{15}N or ^{31}P NMR and using 2D methods (e.g. HSQC or HMBC) to correlate the linkages to the protons.

3.5.1 Cell wall polysaccharide contaminant

The presence of phosphocholine in cell wall polysaccharide was determined in 1968 by Brundish and Baddily and confirmed by Watson and Baddily in 1974 [364]. Structurally wise it was thought to contain a single phosphocholine group on the repeating unit. Kulakowska *et al.* determined that there were two phosphocholines on the CWPS of a non–encapsulated *S. pneumoniae* strain [365] and in 1999 Karlsson *et al.* investigated the cell wall polysaccharide of one non encapsulated and three encapsulated (serotypes 18B, 32A and 32F) strains of *S. pneumoniae* with proton, carbon and phosphorus NMR [366]. It was found that the non–encapsulated strain and serotype 18B contained CWPS with only one phosphocholine residue but both serotypes 32A and 32F were found to have two phosphocholine residues on their CWPS. Therefore the amount of phosphocholine found on CWPS seemed to be strain and serotype dependant. In 1980 Jennings *et al.* investigated the CWPS of Pn1 and found only one phosphocholine present, this was confirmed with proton and carbon NMR spectra [18] however Vialle *et al.* showed with ^{31}P NMR that the CWPS of Pn1 contained two phosphocholine residues (Figure 3.24) [248].

As Pn1 PS does not contain any phosphate groupings, the ^{31}P spectrum should represent the CWPS and simply by counting the number of peaks found in this spectrum, the number of phosphocholine residues can be determined [248]. Three peaks were identified in the ^{31}P spectrum (Figure 3.25) that corresponded to the one ribitol phosphate (1.3 ppm) on the CWPS, the other two peaks at –0.3 and –0.8 ppm confirmed the presence of two phosphocholine residues. This was confirmed with ^{1}H–^{31}P HMBC NMR experiment (not shown).

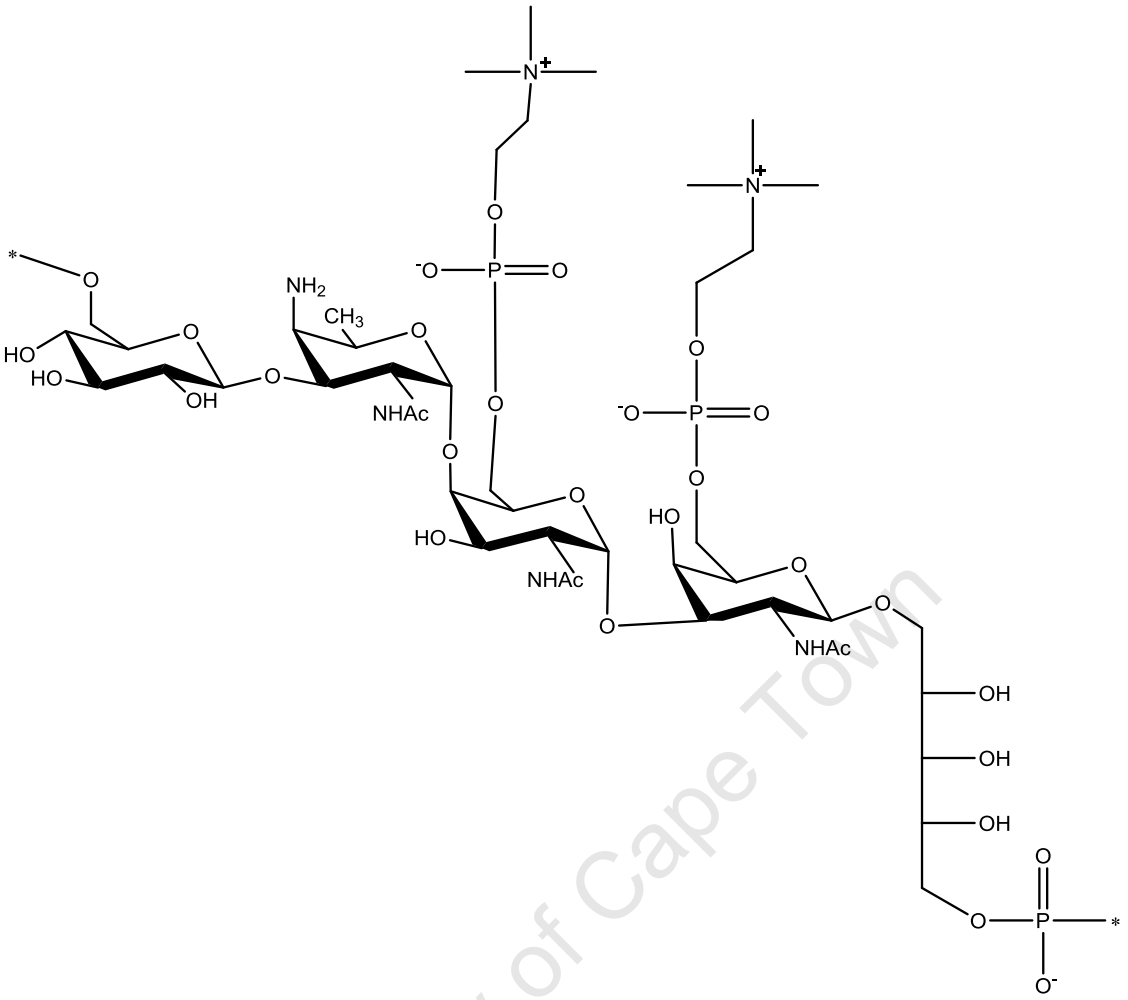

Figure 3.24. Structure of pneumococcal cell wall polysaccharide (CWPS), containing two phosphocholine groups as found for Pn1.

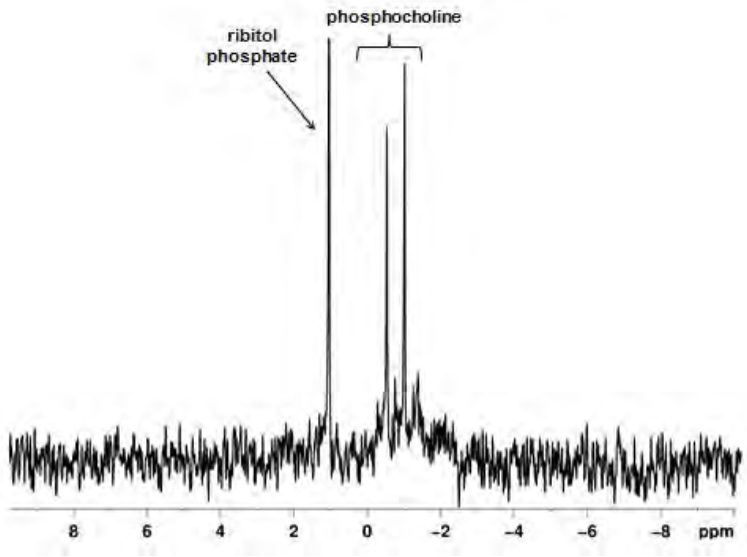

Figure 3.25. ^{31}P NMR spectrum of Pn1 polysaccharide detailing the peaks from the phosphocholine group on the CWPS molecule.

As cell wall polysaccharide is considered to be a contaminant it must be quantified. This was calculated from the proton NMR spectra. The methyl peak of the phosphocholine residue at 3.23 ppm was integrated and compared to the methyl group of the AAT sugar at 1.30 ppm and the *N*–acetyl peak of the AAT sugar at 2.05 ppm. As there are two phosphocholine residues on the CWPS found in Pn1 this peak integrated for 18 protons. As CWPS also contains signals which overlap with the H6 methyl signal *N*–acetyl signal of the AAT sugar these must be corrected for before a calculation can be performed. The corrected methyl and *N*–acetyl peaks integrate for three protons each. Taking this into account the mol percent CWPS was determined using the following equation:

$$\text{CW PS} \quad \frac{I_{PCho}/18}{I_{NAc}/3} \times 100 \qquad \text{Equation 3.7}$$

Where I_{PCho} is the peak integration of the phosphocholine peak and I_{NAc} is the integration of the *N*–acetyl peak. The same equation can be applied when using the methyl peak of the amino sugar by substituting the integration of the methyl peak for the *N*–acetyl peak. An alternate method of comparison to calculate the percentage of CWPS contamination would be to use the anomeric signal for the unacetylated GalA residue. However due to the viscosity of the sample and the resultant broad spectral peaks, this cannot be achieved. The WHO has not released guidelines for the amount of CWPS contamination allowed in a purified batch of polysaccharide however Marburg *et al*. suggested a value of less than 3 % (w/w) [217, 367]. Whilst this was the initial limit suggested, all purified polysaccharides described were found to contain more than 3 % CWPS contamination and this was only decreased to below 3 % after hydrolysis was performed.

3.5.2 Extent of *O*–acetylation

The effect on immunogenicity of Pn1 PS by removing the *O*–acetyl functional group was shown in the very first studies of the polysaccharide, before the full structural characterisation of Pn1 was known [286, 288, 368, 369]. Due to the importance of the *O*–acetyl group, the WHO determined specifications for the levels of *O*–acetylation on the polysaccharide. Already discussed is the colorimetric assay based on the Hestrin method [199], however NMR is also able to quantify the levels of *O*–acetylation. The advantage of using NMR to determine *O*–acetylation is that it can be used to determine the position(s) of the *O*–acetylation.

The introduction of an *O*–acetyl group in any position on the saccharide will result in a large downfield shift on the α–proton in the ^{1}H spectra but only small shifts in the ^{13}C NMR spectra [363]. The proton which is linked to the acetylated carbon is shifted to such a degree that it

appears in the anomeric proton region and with the help of HSQC can be easily recognised and identified.

Jansson *et al* performed an in–depth investigation into the shifts in the ^{13}C NMR spectra in 1987 [370]. The authors determined that the deshielding of the substituted carbon (α–carbon) is between 0.7 – 3.5 ppm when an *O*–acetyl group is added in any position. The carbon next to the substituted carbon (the β carbons) experience a shift upfield of 1.2 – 2.8 ppm with shift effects becoming smaller the further away the carbon is situated. D–Galactopyranosyl derivatives show a greater shift in their ring protons due to the acetylation, than D–glucopyranosyl derivatives [370].

As Pn1 PS is often *O*–acetylated on two different positions (C2 and/or C3 of GalA (residue B)) two peaks are identified in the ^{1}H NMR spectrum. These two peaks were integrated and compared to the integration of the peak at 2.05 ppm corresponding to the *N*–acetyl peak and the ratio of the two (Equation 3.8) determined the percentage of *O*–acetylation of the polysaccharide.

$$\text{acetylation} \quad \frac{I_{OAc}}{I_{NAc}} \times 100 \qquad \text{Equation 3.8}$$

3.5.3 NMR structural analysis of Pn1 polysaccharide

The structural analysis of Pn1 polysaccharide by NMR has been performed by Stroop *et al.* in 2002 [293]. The authors had difficulty assigning spectral peaks for the native polysaccharide due to the wide, poorly resolved lines – and thus removed the *O*–acetyl group resulting in the sharpening of the signals which allowed for assignment of the ^{1}H and ^{13}C spectra. In order to assign the native polysaccharide it was degraded by periodate oxidation followed by treatment with base which lead to an oligosaccharide fragment of three repeating trisaccharide units. This treatment allowed for the location of the O–acetyl groups to be identified on the 2– and 3– position of the 4–linked galacturonic acid residue (residue B) of the polysaccharide.

In this investigation, the structure of the polysaccharide produced by *Streptococcus pneumoniae* serotype 1 was investigated using both 1D and 2D NMR spectroscopic techniques.

As reported by Stroop *et al.*, the 1D proton spectra of native polysaccharide (Figure 3.26) produced very broad, overlapping peaks which made identification of the anomeric and ring regions impossible. Only the peaks with unique chemical shifts could be identified by inspection. These were the phosphocholine peak at 3.23 ppm of the CWPS contaminant, which was used as a reference for all other assignments. The *N*–acetyl peak of the AAT sugar was assigned at 2.05 ppm. Two peaks corresponding to the methyl peak (1.30 ppm)

of the AAT sugar and two peaks equivalent to the *O*–acetyl peak of the GalA sugar (2.20 ppm) were also identified.

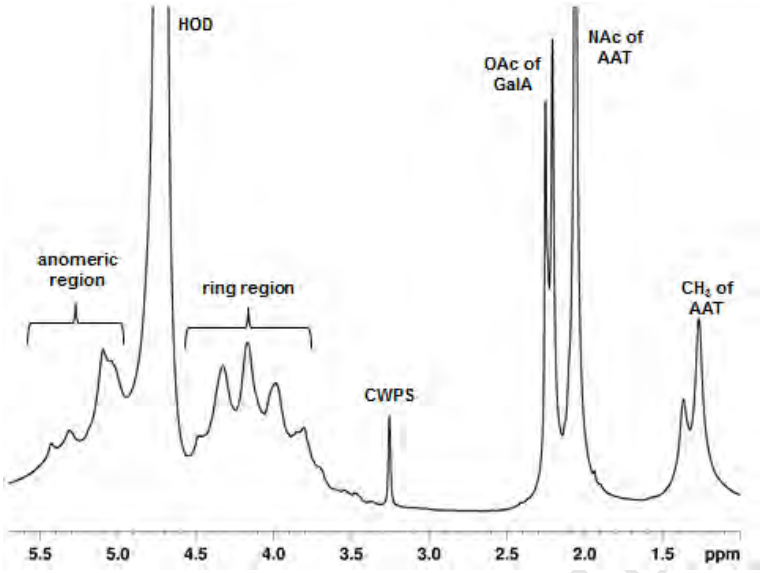

Figure 3.26. 1D ^{1}H NMR spectrum of Pn1 polysaccharide.

Due to this complexity of the *O*–acetylation pattern on the polysaccharide, other peak assignments were not possible; therefore a de–*O*–acetylated Pn1 PS was first used to fully identify the structural backbone of the polysaccharide.

3.5.3.1 De–O–acetylated Pn1 polysaccharide

Removing the *O*–acetyl group on the GalA sugar residue provided NMR spectra with much narrower peaks and enabled further peak identifications (Figure 3.27a). Identification of the signals in the NMR spectra was made by comparison to the related saccharide monomer. Three peaks were identified in the anomeric region that corresponded to H1 of α–AAT and two α–GalA sugars at 5.00 (A), 5.08 (C) and 5.22 (B) ppm respectively. Further assignments for the AAT sugar could be made for signals at 2.05, 3.67 and 4.74 ppm analogous to the NAc group and H4 and H5 respectively. The absence of the *O*–acetyl grouping resulted in a single peak for the methyl group of the AAT sugar (1.27 ppm) which suggests that the *O*–acetyl group of the GalA moiety has an influence on the methyl environment. Cell wall polysaccharide contamination was confirmed with the peak at 3.23 ppm in the ^{1}H and 55 ppm in the ^{13}C spectra, corresponding to the methyl peak of the phosphocholine residue.

The ^{13}C NMR spectrum (Figure 3.28), whilst complex, did show the presence of the trisaccharide repeating unit with signals at 100.0, 97.9 and 100.1 ppm corresponding to C1 of AAT, and the two GalA residues respectively. Characteristic signals at 16.6 ppm (NAc) and 23.3 ppm (C6) of the AAT sugar were also observed. There are two amino resonances

that are more upfield than the rest of the ring resonances which correspond to amino groups linked in the C2 and C4 position of AAT sugar.

These assignments were confirmed by 2D $^{1}H–^{1}H$ (TOCSY) (Figure 3.29) and $^{1}H–^{13}C$ (HSQC) (Figure 3.30) correlation experiments and allowed for the full elucidation of the AAT and two GalA spin systems. The methyl to H5 coupling of the AAT sugar is clearly visible in the 2D TOCSY spectrum. From the expanded spectrum, the correlations of the de–*O*–acetylated sugar could be identified from the anomeric protons of each sugar residue to the H2, H3 and H4. Additional cross peaks are labelled. The glycosylation linkages were identified by their change in chemical shift from the monomeric standards and confirmed the linkages as 3–linked AAT (residue A), 4–linked GalA (residue B) and 3–linked GalA (residue C). The complete assignments of the NMR signals are collected in Table 3.18 and were in close agreement with the literature assignments by Stroop *et al*. Unlabelled signals in the TOCSY spectrum correlating to near 4.6 ppm were attributed to the β–GalNAc and β–Glc spin systems of the CWPS. Other signals corresponding to CWPS were identified in the HSQC where the H1/C1 and H2/C2 of the phosphocholine (Cho–*P*–(O→) group were assigned at 4.33/59.9 ppm and 3.68/66.5 ppm respectively.

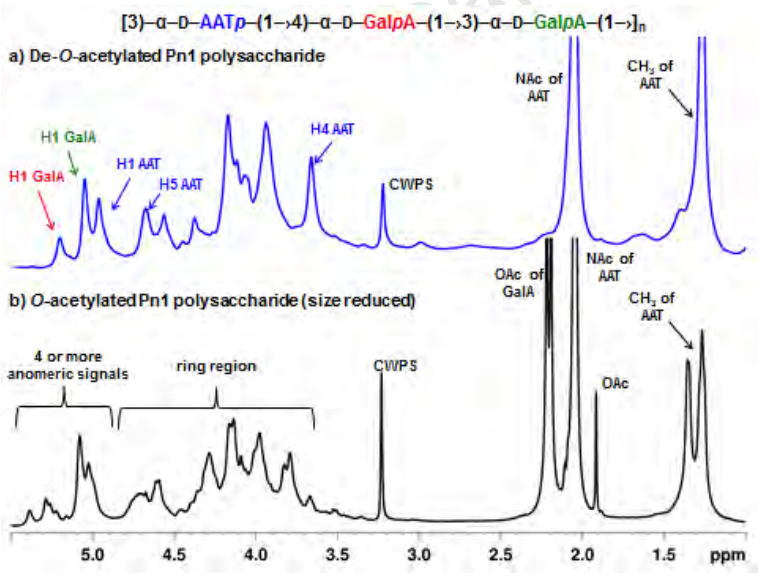

Figure 3.27. 1D ^{1}H pre–sat NMR spectra of a) de–*O*–acetylated and b) *O*–acetylated Pn1 polysaccharide.

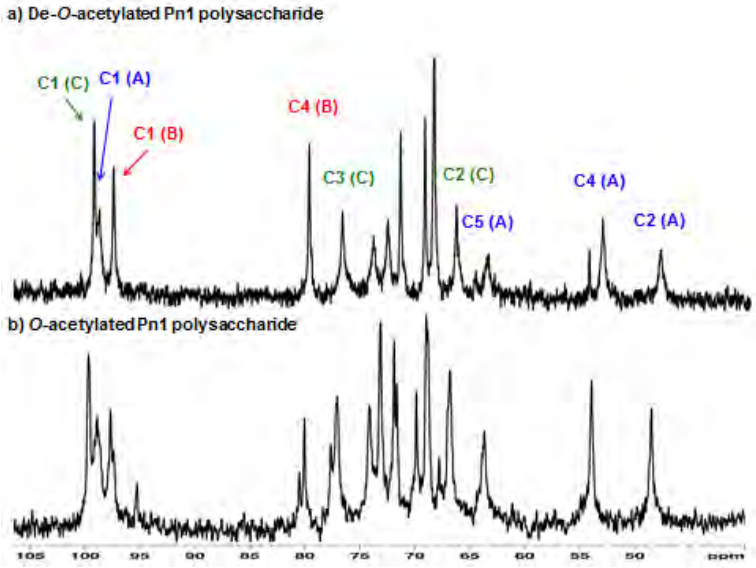

Figure 3.28. 1D ^{13}C NMR spectra of a) de–*O*–acetylated and b) *O*–acetylated Pn1 polysaccharide.

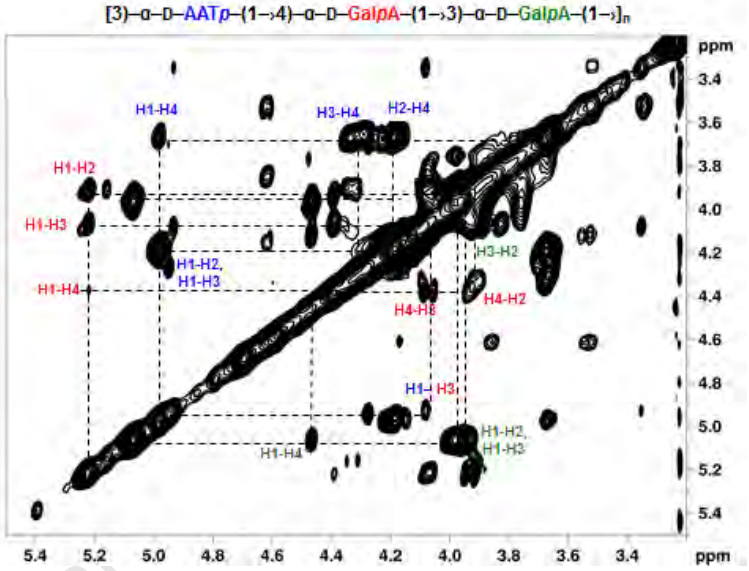

Figure 3.29. Expanded ^{1}H–^{1}H TOCSY spectrum of de–*O*–acetylated Pn1 polysaccharide.

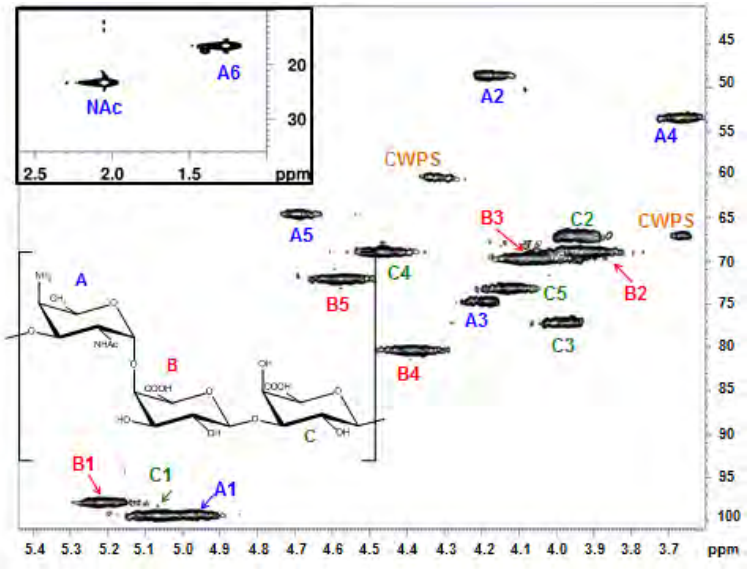

Figure 3.30. Expanded $^{1}H–^{13}C$ HSQC spectrum of de–*O*–acetylated Pn1 polysaccharide.

Table 3.18. Proton and carbon assignments for de*O*Ac of Pn1 polysaccharide, (Underlined figures represent glycosylation shifts). Chemical shifts are reported in ppm.

Residue	H1	H2	H3	H4	H5	H6	NAc
	C1	C2	C3	C4	C5	C6	
3)–α–D–AAT–(1→ (A)	5.00	4.16	4.28	3.67	4.74	1.27	2.05
	100.0	48.6	74.2	53.5	63.8	16.4	23.3
4)–α–D–GalA–(1→ (B)	5.22	3.92	4.06	4.40	4.58		
	97.9	68.8	69.7	80.4	71.9		
3)–α–D–GalA–(1→ (C)	5.08	3.98	4.01	4.47	4.13		
	100.1	66.7	76.9	68.9	73.3		

3.5.3.2 O–acetylated Pn1 polysaccharide

The native polysaccharide was size reduced, which resulted in narrower, and better resolved peaks in the 1D ^{1}H NMR spectra (Figure 3.27). The sharpness in resolution of the peaks was most prominent in the anomeric region where four or more anomeric peaks could be detected. The additional peaks in the anomeric region corresponded to new H1 signals due to the acetylation patterns. Signals, corresponding to the proton attached to the carbon at which acetylation took place, have shifted to the anomeric region due to the deshielding of the proton by the *O*–acetyl group. Further differences were observed due to the *O*–acetylation on (B) GalA. Signals at 2.19 and 2.23 ppm corresponded to the *O*–acetyl group. Literature suggests that this *O*–acetylation can occur on either the C2 or C3 position [293]. This would then give rise to two different peaks for H1 of the residue. The other noticeable signal is an additional peak at 1.35 ppm which is assigned to H6 of the AAT residue due to it being in a different chemical environment when the repeating unit is acetylated. Due to the acetylation, the ^{13}C was more complex and no further assignments could be made by inspection and hence 2D spectroscopic techniques were needed.

1D TOCSY experiments, using along mixing times, enabled the identification of all the protons belonging to an isolated spin system. This procedure was applied to certain peaks to determine the spin system connectivities and proved to be useful in identifying the *O*–acetylation linkages on either C2 or C3 of GalA (structure B), as well as identifying the twinning phenomenon experienced by the methyl group of the AAT sugar due to the *O*–acetylation pattern. The spin system associated with the methyl peak of AAT, with a shift of 1.35 ppm, showed a strong correlation to H5 of AAT sugar (Figure 3.31). Negative peaks in the 1D TOCSY spectrums were assigned to dipolar coupling. It was therefore theorised that the *O*–acetyl peak at 2.23 ppm was acetylated to the C3 position. The anomeric signals of the AAT sugar and the GalA residue (structures A and C) were also subjected to 1D TOCSY. The anomeric signal from the AAT sugar correlated to H2, H3, and H4 of the AAT sugar. A small correlation to the *N*–acetyl protons as well as to certain protons on the GalA residues was identified. The anomeric signal from the C3 *O*–acetylated GalA residue showed correlations to H3 and H4 of GalA residue C and H2, H4 of the C3 acetylated GalA residue (Figure 3.32).

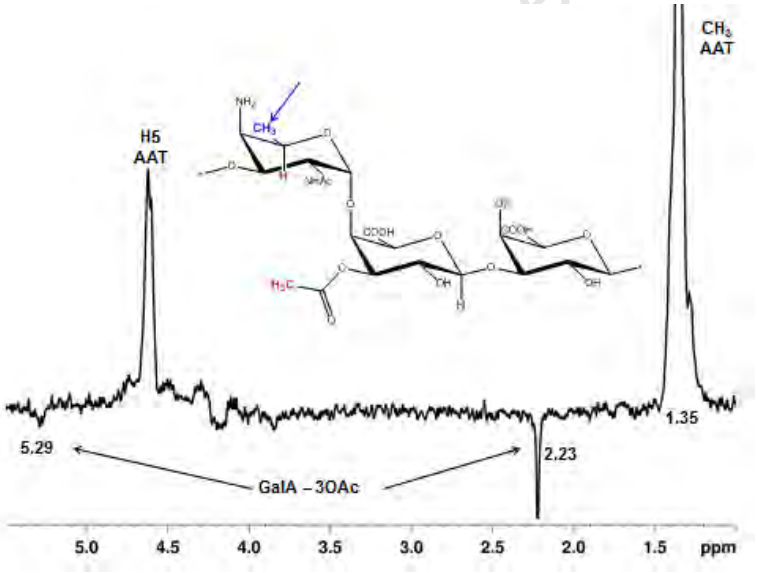

Figure 3.31. 1D TOCSY spectrum of Pn1 PS from methyl protons on AAT residue showing correlation to acetylation position C3 (B) GalA.

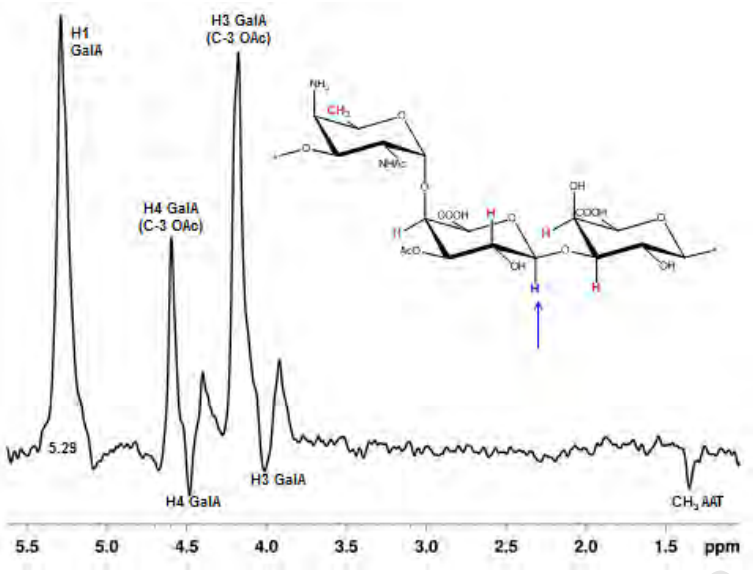

Figure 3.32. 1D TOCSY spectrum of Pn1 PS from anomeric proton on (B) GalA acetylated at position C3.

2D TOCSY of the acetylated Pn1 PS showed similar cross peak correlations to the de–*O*–acetylated Pn1 (Figure 3.33). The (C) GalA residue can be traced from the anomeric proton at 5.08 ppm through to the H2, H3 and H4 residues. The polysaccharide is a mixture of de–*O*–acetylated and *O*–acetylated at position C2 and C3 of the (B) GalA residue, and complicates not just this residue but also that of the AAT sugar. From the anomeric signal the AAT sugar can be traced to H2, H3 and H4, however cross correlations also occurred from two different H4 through to H5 as well as H2 and H3. It is theorised that the acetylation on the (B) GalA residue influences the peaks in the AAT sugar spin system. The (B) GalA residue with no acetate, acetate on C2 and on C3 brings up three unique spin systems, some of which could be correlated in the TOCSY spectrum.

The acetylated HSQC was more complicated due to the three different acetylation patterns on the (B) GalA residue; however assignments made from the de–*O*–acetylated PS aided in the full spectral elucidation (Figure 3.34). As with glycosylation linkages, the position of *O*–acetylation could be determined from the change in chemical shift when compared to the monomeric related saccharide. The acetylation on either the C2 or C3 of the residue caused a shift upfield in the spectrum with peaks at 5.04 and 71.7 ppm corresponding to the C2 acetylated residue and 5.27 and 73.1 ppm corresponding to the C3 acetylated residue. For the acetylation on C2, the shift for the α–carbon (C2) was calculated to be a shift downfield of 2. ppm and shifts of the β–carbons (C1 and C3) were upfield shifts of 2.8 and 0.7 ppm respectively. For the C3 acetylated GalA residue; a shift of C3 was determined to be 3.4 ppm and for the β–carbons (C2 and C4) shifts upfield of 1.6 and 2.6 ppm were measured. Full spectral assignments for the polysaccharide acetylated on both positions are collected in Table 3.19 and Table 3.20. The assignments made in this study are similar to those

described by Stroop *et al.* however some differences were identified. The shifts for some atoms in the AAT sugar change with the addition of the acetylation, apart from the methyl group, other shifts have not been described in literature. C5 shifts from 4.74 ppm in the de–*O*–acetylated polysaccharide to 4.62 ppm in the acetylated spectra. C4 and C3 of the AAT sugar also showed a shift in the *O*–acetylated spectra from 4.28 and 4.67 ppm to 4.19 and 3.80 ppm respectively. The GalA on which the *O*–acetylation is found (residue B) showed a number of different chemical shifts than those seen in the de–*O*–acetylated spectra as well as the literature. The main changes in chemical shift observed in the *O*–acetylated HSQC spectrum were due to the points of attachment of the *O*–acetate groups. Literature identified these points as 4.99/70.4 ppm and 5.23/77.8 ppm, although this investigation showed similar chemical shifts for the acetylation on C2 of 5.04/71.7 ppm, different shifts of 5.27/73.1 ppm were determined for acetylation on C3. The proton chemical shift was found at 5.27 ppm compared to 5.23 ppm of the literature value, whereas a greater difference was noted for the carbon chemical shift values: 73.1 ppm compared to 77.8 ppm identified by Stroop *et al.* [293]. The change in chemical shift between the acetylated and non–acetylated carbon corresponds to 3.4 ppm for the present study and 8.3 ppm for the study by Stroop *et al.* The shift difference should be in the range of 0.7 – 3.5 ppm [370]; the large shift of 8.3 ppm is indicative of a glycosylation linkage rather than *O*–acetylation and hence may have been incorrectly assigned.

Literature has not reported any other chemical shifts on residue B due to the acetylation however this investigation determined a number of shifts relating to the acetylation patterns as presented in Table 3.19 and Table 3.20. The anomeric signals for the acetylated polysaccharide shifted and were identified at 5.38/95.1 ppm for the PS with C2 acetylation and 5.29/97.5 ppm for the PS with C3 acetylation. The protons and carbons on either side of the acetylation point were also affected and experienced shifts. Residue C (GalA) was not affected by the *O*–acetylation.

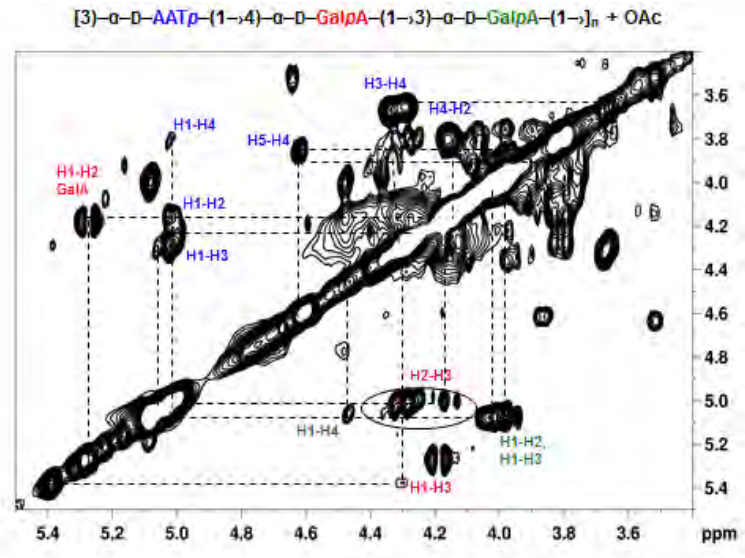

Figure 3.33. Expanded ^{1}H–^{1}H TOCSY spectrum of *O*–acetylated Pn1 polysaccharide.

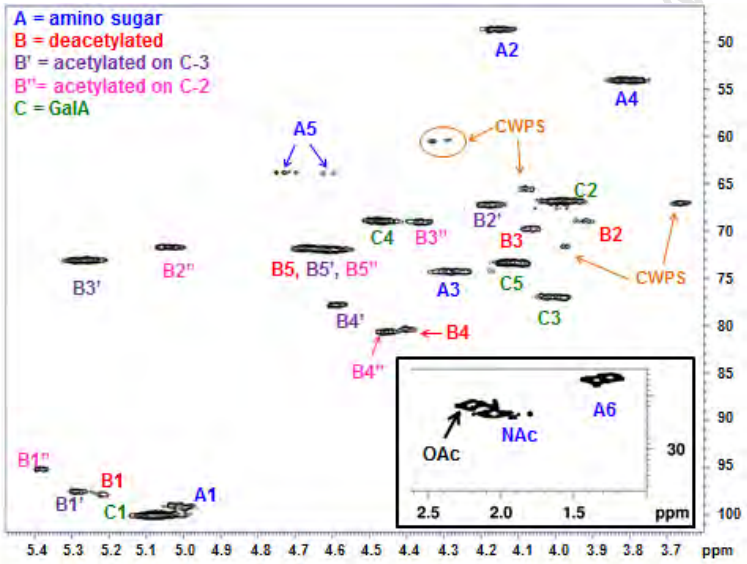

Figure 3.34. Expanded ^{1}H–^{13}C HSQC spectrum of *O*–acetylated size reduced Pn1 polysaccharide.

Table 3.19. Proton and carbon assignments for Pn1 polysaccharide acetylated on C2 GalA (B). (Underlined figures represent glycosylation shifts; the bold figures represent points of *O*–acetylation). Chemical shifts are reported in ppm.

Residue	H1	H2	H3	H4	H5	H6	NAc	OAc
	C1	C2	C3	C4	C5	C6		
3)-α-D-AAT-(1→	5.02	4.16	4.19	3.80	4.62	1.35	2.05	
(A)	99.3	48.6	74.6	54.0	63.9	16.8	23.3	
4)-α-D-GalA(2OAc)-(1→	5.38	**5.04**	4.36	4.45	4.58			2.19
(B)	95.1	**71.7**	69.0	60.7	71.9			21.3
3)-α-D-GalA-(1→	5.08	3.98	4.01	4.47	4.13			
(C)	100.1	66.7	76.9	68.9	73.3			

Table 3.20. Proton and carbon assignments for Pn1 polysaccharide acetylated on C3 GalA (B). (Underlined figures represent glycosylation shifts; the bold figures represent points of *O*–acetylation). Chemical shifts are reported in ppm.

Residue	H1	H2	H3	H4	H5	H6	NAc	OAc
	C1	C2	C3	C4	C5	C6		
3)-α-D-AAT-(1→	5.02	4.16	4.19	3.80	4.62	1.27	2.05	
(A)	99.3	48.6	74.6	54.0	63.9	16.4	23.3	
4)-α-D-GalA(3OAc)-(1→	5.29	4.17	**5.27**	4.59	4.67			2.23
(B)	97.5	67.2	**73.1**	77.8	71.8			21.6
3)-α-D-GalA-(1→	5.08	3.98	4.01	4.47	4.13			
(C)	100.1	66.7	76.9	68.9	73.3			

3.5.4 Summary

Both 1D and 2D NMR techniques were employed to fully assign the proton and carbon spectra for the Pn1 polysaccharide. The native polysaccharide displays a poorly resolved spectrum with wide, overlapping peaks that made identification of any signals, apart from methyl and acetyl groups, very difficult. The possibility of two different points of O–acetylation could be determined from this spectrum. De–*O*–acetylation of the polysaccharide produced a proton spectrum that allowed for the further identification of the anomeric protons as well as some protons on the AAT sugar. From the carbon spectrum, the anomeric signals were assigned by inspection but it was the 2D methods that allowed for full identification of the signals. The assignments from the de–O–acetylated PS were then used to assign signals for the fully acetylated spectrum. By size reducing the native polysaccharide, the proton and carbon 1D spectra became clearer however no extra assignments could be made. The advantage of size reducing the polysaccharide became apparent in the 1D TOCSY and 2 D methods where spectra was obtained that allowed for correlations and identifications to be assigned. The 1D TOCSY experiments allowed for the identification of the points of O–acetylation and definitely showed that the polysaccharide was a mixture of de–O–acetylated and O–acetylated (on either C2 or C3, residue B) GalA. For the first time in

the investigation, the HSQC of the now size reduced polysaccharide displayed crosspeaks that could be identified. Shifts seen at 5.04/71.7 ppm and 5.27/73.1 ppm were indicative of the O–acetylation points on C2 and C3 of the GalA residue B. The two signals corresponding to the methyl group of the AAT sugar on the de–O–acetylated and acetylated polysaccharide were also identified. By comparison with the monosaccharide standards and the literature on the Pn1 PS, the peaks relating to each different acetylated polysaccharide could be assigned and the full structural elucidation of Pn1 polysaccharide was achieved.

CHAPTER 4. PURIFICATION OF PN1 POLYSACCHARIDE

4.1 Purification methodology

Pneumococcal bacteria have a polysaccharide capsule surrounding each cell. This capsular polysaccharide is known to be a major virulence factor as it prevents antibodies from attaching to the cell and therefore blocks the immune system's phagocytic response [13, 14]. The major component of the pneumococcal polysaccharide vaccine is the capsular polysaccharide whereas the pneumococcal conjugate vaccine contains the capsular polysaccharide conjugated to a protein. In order to utilise the capsular polysaccharide in a conjugate, it must be separated from the killed bacteria and cell debris and other contaminants such as proteins, nucleic acids and cell wall polysaccharide [371-373]. This is achieved through a purification process which must take into account the physical and chemical properties of the polysaccharide, and those of all the impurities. A sufficiently pure product is usually only achieved in a multi–step purification process. In the case of both the seven and thirteen valent Prevnar conjugate vaccines, the purification process for the polysaccharides contains 16 different steps including multiple different chromatographic systems and numerous membrane separations to obtain the pure polysaccharide [374].

The purification procedure for pneumococcal serotype 1 polysaccharide used in this investigation makes use of a quaternary ammonium detergent (CTAB) to precipitate negatively charged polymers. This is useful as most bacterial polysaccharides are anionic (exceptions include pneumococcal serotypes Pn14 which is neutral and Pn1 which is zwitterionic), however, the structure of Pn1 has an unusual repeating motif. Each repeating unit has a minimum of one positive and one negative charge leading to the common three dimensional configuration characterised by a right–handed helix with negatively charged grooves, the positive charges being on the outer surface of the lateral boundaries [82]. Polysaccharides exhibiting this motif are referred to as zwitterionic capsular polysaccharides shown below in Figure 4.1. If it is assumed that one carboxyl and one amino moiety occupy the zwitterionic nature of Pn1, then there is a second carboxyl group available for the precipitation with CTAB.

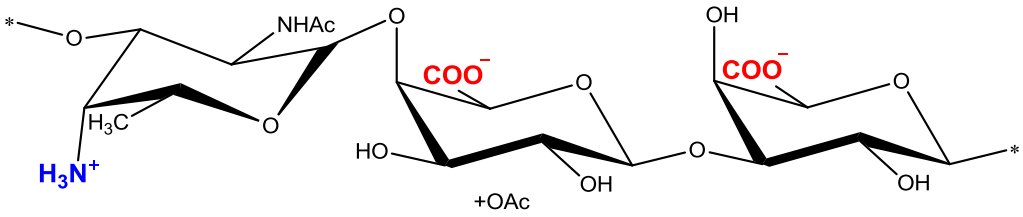

Figure 4.1. Zwitterion capsular polysaccharide structural motif of Pn 1 with the negatively charged carboxyl groups shown in red and the positively charged amino sugar shown in blue.

Once a precipitate has formed, Celite is added to the CTA^+ precipitated polysaccharide solution in order to trap the insoluble polysaccharide. The solution is stirred at high speed to ensure complete mixing and trapping of the polysaccharide. Once the Celite slurry containing the trapped Pn1 PS in its CTA^+ salt form has settled, the excess supernatant is removed and the Celite slurry is packed onto a chromatography column, in this case the illipore VANTAGE™ Chromatography column.

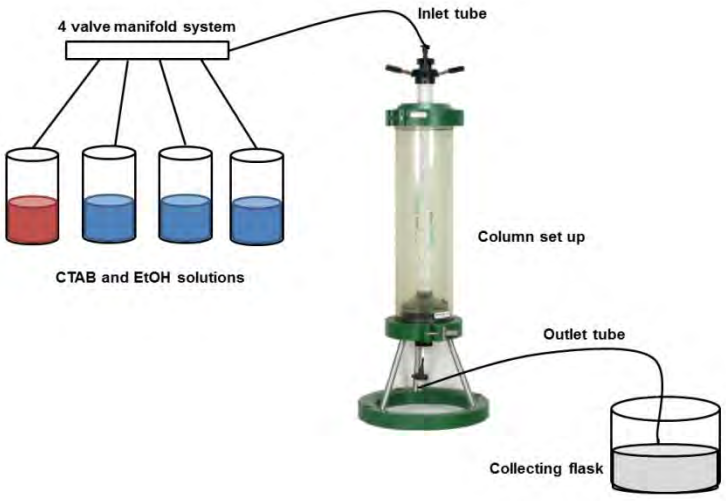

Figure 4.2. Schematic (not to scale) of the purification set–up including elution buffers, column and collection flask.

The apparatus and arrangement for the purification is detailed in Figure 4.2. After the column has been loaded, the elution buffers are connected via a 4–way manifold and sequentially passed onto and through the column. The following buffers are used to elute the polysaccharide and fractions of elution collected:

- 0.05 % CTAB in 0.05 M NaOAc (pH 6.0): This is the first buffered solution and it is introduced to wash media components from the Celite cake whilst still maintaining a low level of CTAB to ensure that the polysaccharide remains in its insoluble CTA^+ salt form.
- 5 % Ethanol (EtOH) in 0.05 M NaOAc (pH 6.0): As certain media components are only slightly soluble in aqueous solutions, a low concentration of ethanol was introduced to remove these components.

- 10 % EtOH in 0.05 M NaOAc (pH 6.0): Small quantities of nucleic acids and proteins are removed in this step.
- 15 % – 30 % EtOH in 0.05 M NaOAc (pH 6.0): Increasing EtOH concentrations are used to elute the polysaccharide. As Pn1 PS is very viscous, once it starts to elute, the pressure on the column increases and the flow rate decreases. The polysaccharide elutes as a viscous, opaque solution and elution is terminated when the flow rate increases and the pressure decreases.

The fractions collected are tested for the presence of Pn1 PS with the uronic acid colorimetric assay. A sample containing Pn1 polysaccharide changes from colourless to purple to indicate the presence of Pn1 PS. The positive fractions are pooled together.

Solid NaCl is added to these pooled fractions in order to precipitate the polysaccharide. Sodium chloride is used to change the counter ion of the Pn1 PS from CTA^+ to sodium, the polysaccharide is then insoluble in ethanol and will precipitate in an alcoholic solution. While a final concentration of 2 M NaCl is sufficient to allow for full counter ion exchange, the EtOH concentration of the solution must be maintained at a concentration of approximately 60 % in order to achieve complete precipitation. This is achieved with the addition of 96 % ethanol to the point where precipitation occurs. An equivalent volume of ethanol to the volume of the pooled fractions is sufficient for precipitation to occur.

The precipitated polysaccharide is collected by centrifugation and re–dissolved in a minimum volume of water. In order to remove any excess ethanol and CTA^+, the polysaccharide is diafiltered against seven volumes of 0.5 M NaCl followed by seven volumes of water using two 100 kDa MWCO membranes in parallel. The diafiltration set–up is shown in Figure 4.3.

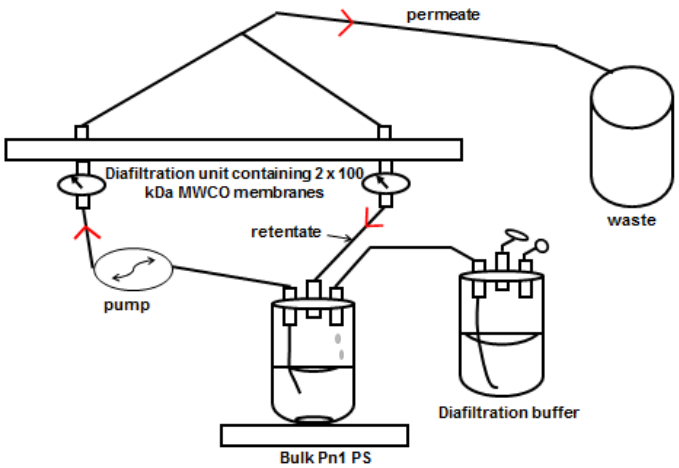

Figure 4.3. Diafiltration set–up for the final step in the purification of Pn1 polysaccharide.

Each batch of purified polysaccharide must be fully characterised with validated test methods to determine the identity, purity and molecular size of the polysaccharide. Whilst there are numerous analytical methods available, they only provide complementary information and thus a combination of methods must be applied to achieve a more complete description of the polysaccharide. There are combinations of colorimetric tests that characterise the polysaccharide in terms of total nitrogen, phosphorus, hexosamine, methylpentose, uronic acid and *O*–acetyl groups. NMR is also used to identify and characterise the polysaccharide as well as to check for any impurities [10, 375].

The analytical tests used to characterise the purified Pn1 PS are summarised below and the WHO – accepted criteria is reported in Table 4.1:

- **Polysaccharide identity and composition** – These tests include colorimetric assays and NMR that provide information on the identity and purity of the polysaccharide as well as any impurities, such as CWPS, that may be present. For the identity and composition to be confirmed the WHO have defined specifications for each serotype and colorimetric test. For Pn1 the theoretical value for the uronic acid colorimetric assay is 55.17 % and the *O*–acetyl assay should give a theoretical value of 5.47 % [162]. The CWPS impurity is best determined through NMR as described in Chapter 3, Section 3.5.1 and while there is no recommended limit on contamination, it must be kept to as low as possible.
- **Protein impurity** – The protein content is determined using the Bradford Coomassie assay for Pn1 with bovine serum albumin used as a reference. According to the WHO, protein contamination should not be greater than 3 % by dry weight [14, 162].
- **Nucleic Acid impurity** – Each batch of polysaccharide should contain, by the WHO recommendations, a nucleic acid contamination of not more than 2 %. This is calculated from the measurement of the absorbance of the polysaccharide solution at 260 nm [162, 375].
- **Molecular size distribution** – This is used as a test of manufacturing between each batch of Pn1 PS purified. While the WHO does not set a limit on the distribution, as it is a strain and serotype dependant characteristic, it does suggest the use of size exclusion chromatography with a refractive index detector [162, 375].

Table 4.1. Defined criteria to determine Pn1 polysaccharide identity and purity. All values are based on mass percentage calculations.

	Uronic acid	***O*–acetyl**	**Protein**	**Nucleic acid**
Accepted criteria (%)	55.17	5.47	3	2

The general method for the purification of Pn1 PS is described in Chapter 2. To establish and optimise the process, the general method was applied to small scale cultivations to determine whether this purification process could be applied to Pn1. This process was optimised by investigations into the following areas:

- The inactivation of the fermentation process was explored to determine whether phenol or DOC inactivation gave the best recoveries of high quality, high purity polysaccharide.
- The optimal pH of the clarified fermentation broth was determined resulting in the maximum precipitation of the polysaccharide after the addition of CTAB.
- The concentration of ethanol required to elute the pure polysaccharide from the Celite filtration compound packed into a chromatography column.

Fermentation of Pn1 was performed 19 times; 14 of which were carried out in the fermentor and 5 in the WAVE bioreactor. Batch and fed–batch methodologies were evaluated and all batches were clarified and proceeded through to the purification downstream process.

4.1.1 Purification optimisation

4.1.1.1 Establishment of process parameters

Three small scale cultivations of Pn1 were used to determine the optimum pH needed to achieve maximum CTA^+ precipitation. All three batches were cultivated over 4 hours before inactivation with phenol. The initial pH was measured and the polysaccharide content was determined by ELISA. Differences in the cultivation such as optical density as well as the length of time used for inactivation account for the differences in polysaccharide content as the optimisation of the cultivation process occurred simultaneously. The pH of each batch was adjusted to 8.0, 7.8 and 5.5 in order to determine which pH would allow for maximum polysaccharide precipitation. Table 4.2 details the data for the three batches.

The fermentation broth was clarified by centrifugation to remove any dead cells and particulates in the broth. A final concentration of 18 g/L CTAB for each batch was used to precipitate out all of the polysaccharide in solution. A sample was taken before as well as 5 min after the CTAB was added and rate nephelometry was used to shown that only trace amounts of Pn1 PS were left in the supernatant after CTAB addition (Figure 4.4).

Table 4.2. Initial values for three cultivations of Pn1 to determine the optimum pH for CTAB precipitation.

Batch	Initial polysaccharide content (mg)	Initial pH	Adjusted pH
1	595	7.65	8.0
2	234	7.13	5.5
3	340	7.15	7.8

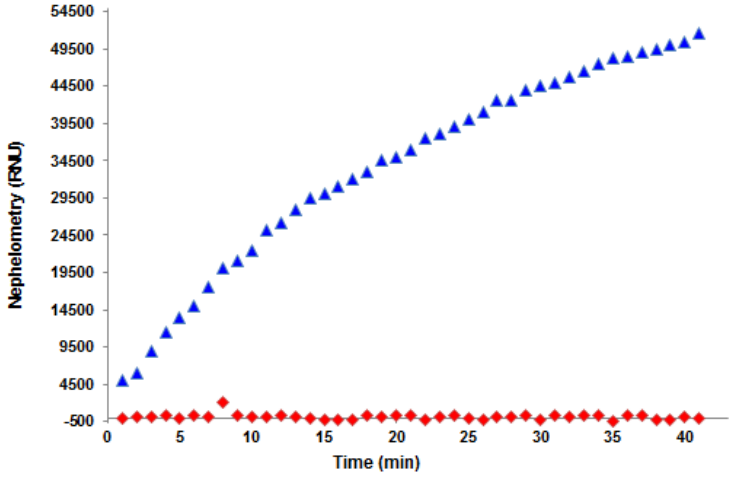

Figure 4.4. Rate nephelometry for the determination of PS concentration in the fermentation broth (blue) and the supernatant after CTAB precipitation (red).

Celite was added to achieve a final concentration of 93 g/L. This 'slurry' was packed onto a column and washed with 0.05 % CTAB in 0.05 M NaOAc to elute all the remaining media components from the fermentation. Increasing concentrations of ethanol were passed through the column to elute out the polysaccharide. As it was not known when the polysaccharide would precipitate out, the first batch was eluted with only two different concentrations of ethanol (20 % and 30 %), but a more thorough examination of the optimal concentration to elute the polysaccharide was performed for batches 2 and 3. Fractions were collected and tested with the uronic acid assay for the presence of polysaccharide. The results of this assay, (Table 4.3), revealed that the polysaccharide eluted in ethanol concentrations of between 10 % and 30 % for all three batches.

Fractions that tested positive for uronic acid were pooled together and sodium chloride was added in its solid form to obtain a final concentration of 2 M NaCl. NaCl precipitates the polysaccharide as a counter ion exchange takes place with the CTAB forming the sodium salt of the polysaccharide. This sodium form of polysaccharide is insoluble in ethanol and therefore precipitates out. This however, did not occur so an equivalent volume of 96 % EtOH was added to reduce the polarity sufficiently to enable precipitation.

Table 4.3. Results from the uronic acid assay in determination of the elution profile of Pn1 with increasing concentrations of EtOH.

Batch	Polysaccharide elution* (Y/N)						
	0.05 % CTAB	5 % EtOH	10 % EtOH	15 % EtOH	20 % EtOH	30 % EtOH	60 % EtOH
1	N	n/a	n/a	n/a	Y	Y	n/a
2	N	N	Y	Y	Y	N	N
3	N	N	N	Y	Y	Y	N

*Uronic acid assay used to test for polysaccharide elution. Purple colour change suggests Pn1 elution.

The precipitated polysaccharide was pelleted out by centrifugation, dissolved in 250 ml water and diafiltered against seven volumes of 0.5 M NaCl followed by seven volumes of water using a Labscale™ TFF system fitted with 2 x 100 K WCO 50 cm^2 membranes fitted in parallel. This purified Pn1 PS was analysed on the SEC–HPLC (Figure 4.5) as well as with a range of analytical assays to determine the amount of polysaccharide purified as well as the percentage *O*–acetylation (Table 4.4).

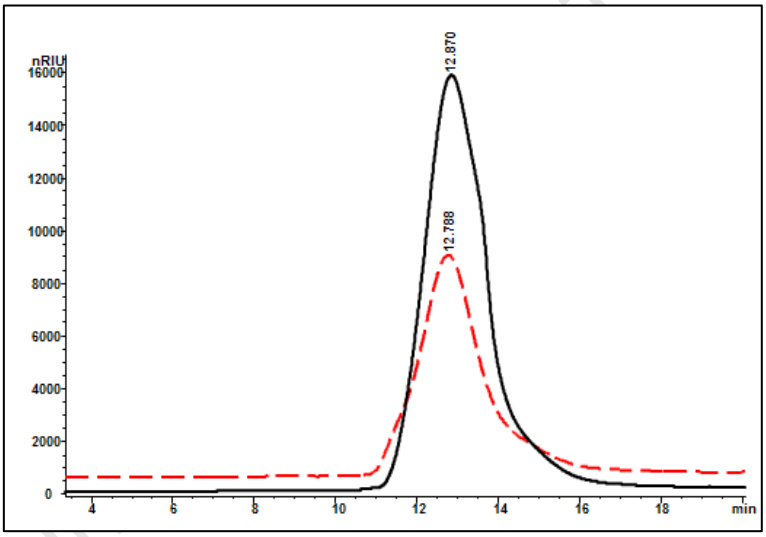

Figure 4.5. SEC–HPLC RID chromatogram of a representative purified Pn1 polysaccharide (red, dashed). The profile of a reference Pn1 PS is shown (black, solid) for comparison.

Table 4.4. Analytical results to determine identity and purity of the polysaccharide.

Analytical calculations	Batch 1	Batch 2	Batch 3	Acceptance criteria
PS Content (UA assay) (mg)*	133	62	64	–
O–acetylation (colorimetric assay) (mass %)	5.16	19.33	31.13	>5.47
Nucleic acid (%)	Not performed	0.65	0.69	<2
Protein (%)	Not performed	4.34	3.45	<3
% Recovery	22	27	19	

*Based on dry weight

The recoveries of the three batches (22 %, 27 % and 19 % for batches 1, 2 and 3 respectively) were within the range seen in previous polysaccharide purifications, with the

lower pH range providing the higher recovery value. However, with Pn1 PS, the *O*–acetylation value is important. The first batch was only analysed for uronic acid and *O*–acetyl percent and the results revealed only a small amount of *O*–acetylation. This could have been due to the adjusted pH of 8.0 which could cause de–*O*–acetylation. The other two batches were subjected to a full colorimetric assessment. The results confirm that Pn1 PS can be purified at both pH values (7.8 and 5.5). Cell wall polysaccharide and *O*–acetylation patterns were not determined with NMR for the three batches. A purification pH of 7.8 was determined to be the optimal pH for purification for allowing the CTA^+ polysaccharide salt to form and precipitate out of solution. The ethanol fractionation range was determined to be between 10 – 30 % with low nucleic acid contamination; however, the levels of protein contamination were high and above the suggested range.

4.1.1.2 Inactivation strategies

Streptococcus pneumoniae is a Biological safety level (BSL) 2 pathogen and represents a particular hazard to health through infection by the respiratory route [162]. The bacteria is fermented under BSL2 conditions but must be killed before it can proceed to purification in an ungraded room, therefore the inactivation of *Streptococcus pneumoniae* is an important linkage between the upstream (fermentation) and downstream (purification). This inactivation step should be able to inactivate the bacterial cells and to aid in the release of the capsular polysaccharide into the fermentation media with minimum cell lysis, without affecting the composition and structure of the polysaccharide.

Two different inactivation strategies were investigated where both phenol and sodium deoxycholate were compared as methods of inactivation. These two different strategies have been used to inactivate *S. pneumoniae* for the production of the two licensed conjugate vaccines [164, 376]. The DOC process has been shown to reduce protein contamination yet still preserves the integrity of the polysaccharide. DOC also facilitates the release of autolysin which is known to be responsible for cleaving the CWPS from the capsular polysaccharide [10, 13, 371].

Both cultivations were 4 hours long and reached the same optical density. Table 4.5 details the initial conditions of each batch. The fermentation broth was clarified by centrifugation and the pH of both batches was adjusted to 7.8 with 3.5 M NaOH.

Table 4.5. Initial conditions for two cultivations of Pn1 to determine the optimum inactivation strategy.

Batch	Inactivation method	Initial PS content (mg)	Initial pH
1	1 % Phenol	187	7.3
2	0.12 % DOC	197	5.3

CTAB was added to each batch and rate nephelometry was used to determine if all the polysaccharide had precipitated. All of the polysaccharide had precipitated out when the final concentration of CTAB in the solution was at 18 g/L when phenol was used as the method of inactivation (Figure 4.6), this was not the result seen with DOC inactivation. The rate nephelometry showed that no polysaccharide had precipitated out of solution when 18 g/L CTAB was added. The amount of CTAB in solution was raised to 30 % and then 50 % however the rate nephelometry showed that the polysaccharide concentration increased when increasing amounts of CTAB were added. It was hypothesised that the sodium deoxycholate was interfering with the assay, by the co–precipitation between the CTA^+ and DOC salts.

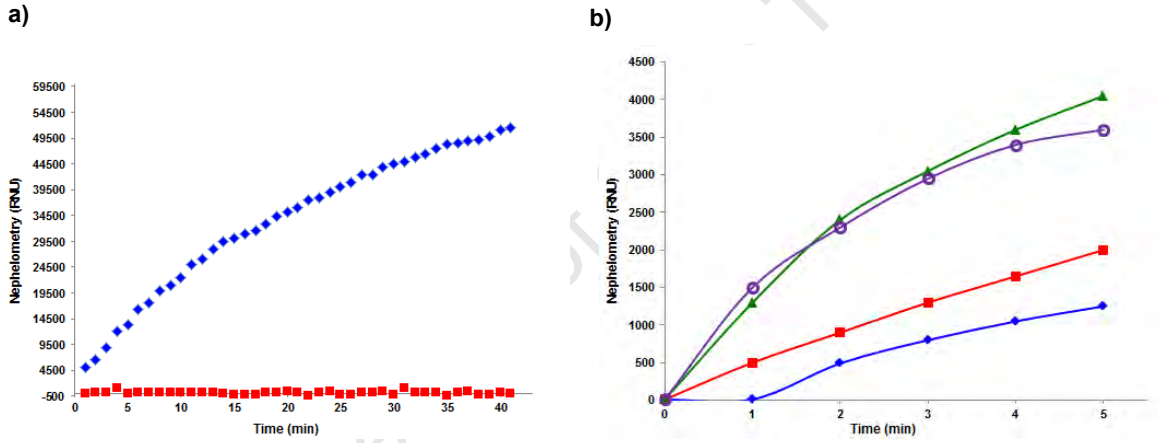

Figure 4.6. CTAB precipitation monitored by rate nephelometry of a) the phenol inactivated batch – comparison between fermentation broth (blue) and the supernatant after CTAB addition (red) and b) the DOC inactivated batch – comparison between fermentation broth (blue) and the supernatant after CTAB addition of 18 g/L (red), 30 % (green) and 50 % (purple).

Whilst the nephelometry result of the DOC inactivation was noted, purification of both batches continued. Celite was added and the polysaccharide was eluted with increasing concentrations of ethanol. The ethanol elution pattern for the phenol inactivation was similar to previous batches with elution taking place in 5 % – 30 % EtOH fractions. The uronic acid colorimetric assay was used to determine where the polysaccharide eluted (as shown in Table 4.6). For the phenol inactivated batch, the fractions that tested positive for PS were pooled together and solid NaCl added to precipitate out the polysaccharide. As before, the precipitation process was aided by the addition of the equivalent volume of 96 % EtOH, before centrifugation and diafiltration were performed to obtain the purified polysaccharide.

Table 4.6. Polysaccharide elution patterns with increasing concentrations of ethanol.

Batch	Polysaccharide elution* (Y/N)						
	0.05 % CTAB	5 % EtOH	10 % EtOH	15 % EtOH	20 % EtOH	30 % EtOH	60 % EtOH
1	N	Y	Y	Y	Y	Y	N
2	N	N	N	N	N	N	N

*Uronic acid assay used to test for polysaccharide elution. Purple colour change suggests Pn1 elution.

No polysaccharide was found in any of the fractions collected from the DOC–inactivated batch. After this result, further literature investigations were performed and a publication on the optimisation of conditions for the PS production of Pn23F was found which suggested that in order to obtain polysaccharide from DOC inactivated cultivations, the fermentation broth was diafiltered and concentrated by tangential filtration to remove the excess sodium deoxycholate [373]. The supernatant that was left after CTAB/Celite precipitation was diafiltered against 1.5 volumes 0.2 M NaCl followed by 1.5 volumes of 5 M NaCl using a Labscale™ TFF system fitted with 2 x 50 K WCO 50 cm^2 membranes in parallel. 18 g/L CTAB was added to precipitate out the polysaccharide. Precipitation did not occur and was hypothesised to be due to the high levels of sodium in the solution, which prevented a counter ion exchange with the CTA^+. An alcohol precipitation was attempted where 96 % EtOH was added to the solution until precipitation was seen. The precipitate was extracted by centrifugation, re–dissolved in water and diafiltered as performed in previous batches. The analytical results for both batches are tabulated in Table 4.7.

Table 4.7. Analytical results of purified Pn1 after undergoing phenol or DOC inactivation.

Analytical calculations	Batch 3 Phenol	Batch 4 DOC	Acceptance criteria
PS Content (UA assay) (mg)*	128.3	83.2	–
O–acetylation			
Colorimetric assay (mass %)	23.8	32.7	>5.47
NMR (mol %)	87.7	–	–
Impurities			
Nucleic acid (%)	0.646	–	<2
Protein (%)	5.3	–	<3
CWPS (mol %)**	1.5*	–	–
CWPS (mass %)**	3.0*	–	–
% Recovery	69	42	–

*Based on dry weight
**Average of calculations with CH_3 and NHAc groups of amino sugar as reference.

The phenol inactivated batch gave a high recovery of 69 % compared to 42 % recovery of the DOC inactivated batch. Due to the potential loss of polysaccharide trapped in Celite, the DOC result may not be a true reflection of the purification process. The analytical results for the phenol inactivated batch confirmed the identity of the purified Pn1 PS which resulted in

an *O*–acetylation level of 24 % by colorimetric assay and approximately 88 % as determined by NMR. The CWPS contamination was determined to be 3.0 % (w/w) which is the limit suggested by Merck for their purified polysaccharide [217]. Protein contamination was found to be 5.3 % which is above the specified limit of 3 %. It was hypothesised that this was due to the inclusion of early eluted fractions with low polysaccharide concentrations but high protein concentrations.

The proton NMR spectrum of the purified polysaccharide is shown in Figure 4.7. The purified polysaccharide was compared to a reference sample to confirm the identity of the polysaccharide. The CWPS contamination was confirmed with a peak at 3.23 ppm corresponding to the methyl groups on the phosphocholine residue [366]. All other peaks compared well with the reference spectrum.

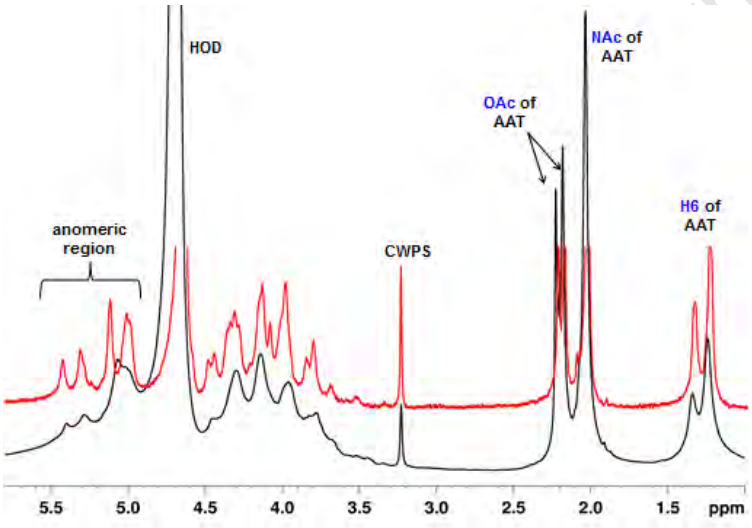

Figure 4.7. ^{1}H NMR spectrum of purified Pn1 PS (black) with phenol inactivation. A reference Pn1 PS spectrum is shown for comparison (red).

As the initial purification of the DOC inactivated batch did not prove successful, four batches were fermented with two inactivated using phenol and two with DOC. These four batches were used as a comparison for the optimal inactivation strategy. Preliminary data for the four batches before purification was performed are compiled in Table 4.8.

All batches were clarified by centrifugation before CTAB precipitation. After clarification the pH of the phenol inactivated batches were adjusted to 7.8 using 3.5 M NaOH before CTAB was added. The DOC inactivated batches were first diafiltered against 7 volumes of 25 mM NaOAc using a 100 kDa MWCO Pellicon 2 membrane.

CTAB and Celite precipitation, column loading and fractionation using ethanol was performed with the uronic acid assay used to determine PS elution as shown in Table 4.9. Purification continued as previously described.

Table 4.8. Initial conditions for two cultivations of Pn1 to determine the optimum inactivation strategy.

Batch	Inactivation strategy	Volume (L)	Initial PS content (mg)	Initial PS concentration (mg/L)	Initial pH
5	1 % phenol	6	924	154	6.44
6	1 % phenol	4	720	180	6.84
7	0.12 % DOC	2	310	155	5.31
8	0.12 % DOC	4	608	152	5.30

Table 4.9. Polysaccharide elution patterns with increasing concentrations of ethanol.

Batch	Polysaccharide elution (Y/N)						
	0.05 % CTAB	5 % EtOH	10 % EtOH	15 % EtOH	20 % EtOH	30 % EtOH	60 % EtOH
5	N	N	Y	Y	Y	Y	N
6	N	N	Y	Y	Y	Y	N
7	N	N	Y	Y	Y	N	N
8	N	N	Y	Y	Y	N	N

*Uronic acid assay used to test for polysaccharide elution. Purple colour change suggests Pn1 elution.

For the phenol batches, elution of the polysaccharide took place between 10 – 30 % EtOH and elution in the DOC batches was completed within the ethanol concentration range of 10 – 20 %. The purified polysaccharides were diafiltered using 100 kDa MWCO regenerated cellulose membranes with 7 volumes of 0.5 M NaCl followed by 7 volumes of water. Full analysis to determine the purity of the polysaccharide was performed (Table 4.10).

The phenol batches produced an average of 463 mg Pn1 PS compared to the 221 mg from the DOC batches, however the fermentation volumes were different in each case and thus, simply comparing polysaccharide amounts do not give a clear indication of superiority. The average recovery for the phenol batches was calculated at 56 % compared to 46 % for the DOC inactivated batches. It must be noted that as the fermentation volume increased so did the PS content which was expected, but the recovery also increased with increasing volumes: the recovery from the 2L batch was only 40 % whereas 59 % of the PS in the 6 L fermentation batch was recovered. This is a known occurrence as the same amount lost in the 6 L and 2 L batches would have a different impact on the recoveries for the two batches with the smaller batch impacted the most and hence revealed a lower recovery.

Table 4.10. Analytical results of purified Pn1 after undergoing phenol or DOC inactivation.

Analytical calculations	Batch 5 Phenol	Batch 6 Phenol	Batch 7 DOC	Batch 8 DOC	Acceptance criteria
Initial fermentation volume (L)	6	4	2	4	–
UA content (%)	71.6	70.1	78.8	67.8	> 55.17
PS Content (UA assay) (mg)*	548.2	378.1	126.2	315.5	–
O–acetylation					
Colorimetric assay (mass %)	23.6	23.4	22.4	23.7	> 5.47
NMR (mol %)	90	75	89	70	–
Impurities					
Nucleic acid (%)	0.69	0.53	1.22	0.61	<2
Protein (%)	5.15	0.94	13.7	0.97	<3
CWPS (mol %)**	2.0	2.7	2.6	2.5	–
CWPS (mass %)**	4.0	5.4	5.2	5.0	–
% recovery	59	53	40	52	–

*Based on dry weight.
**Average of calculations with CH_3 and amino groups of amino sugar as reference.

The analytical results show that the levels of *O*–acetylation were approximately 23 % for both inactivations according to the colorimetric assay. Nucleic acid and protein contamination were all within the acceptable limits. CWPS contamination was determined to be within the range of 4 – 5.5 % (w/w). The NMR of each batch confirms the identity of the purified polysaccharide as being pneumococcal serotype 1 as shown in Figure 4.8 and Figure 4.9. It was interesting to note that both batches of Pn1 PS that were inactivated with DOC show *O*–acetylation mainly on C2 of the middle GalA residue (75 %) whereas the batches inactivated with phenol show a more evenly spread *O*–acetylation pattern between C2 (60 %) and C3 (40 %). This was theorised to be due to the fermentation pH, an increase in the pH brings about a migration of the *O*–acetyl group from C2 to C3 of the GalA residue. This also suggested that the bacteria may acetylate at only one position (C2) and not at both as previously suggested [293]. The mechanism for the *O*–acetyl migration is intramolecular via an ortho–ester intermediate as depicted in Figure 4.10 [164].

Small traces of acetate buffer were identified in the phenol inactivated batches but apart from CWPS, no other contaminants were found in the NMR analysis. The chromatograms from the SEC–HPLC data of each purified batch show that the molecular weight range of the batches were approximately 1000 kDa compared to Pullulan standards (Figure 4.11).

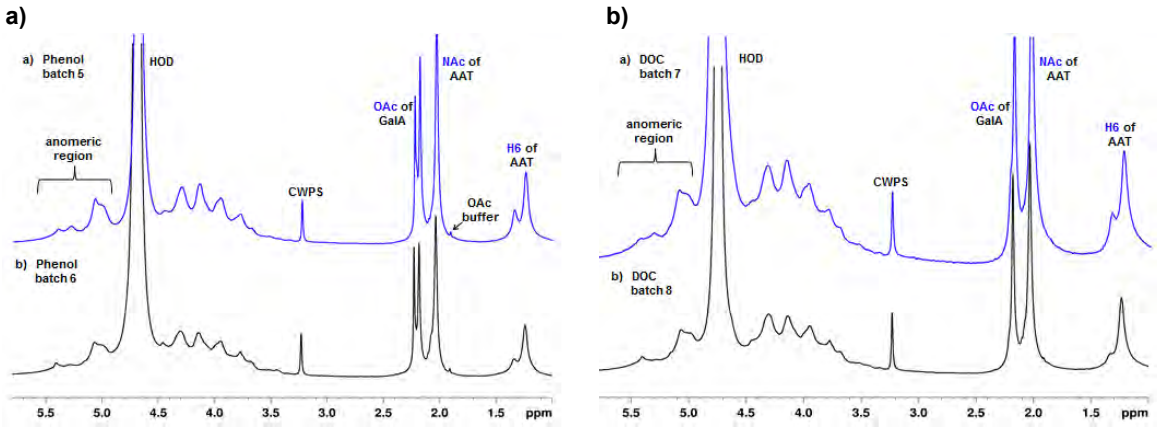

Figure 4.8. ^{1}H NMR overlays of batches inactivated with a) phenol and b) DOC.

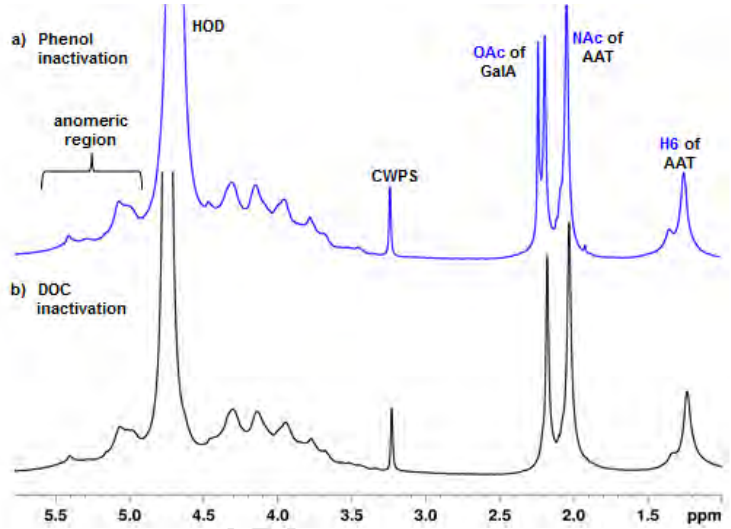

Figure 4.9. ^{1}H NMR overlays of batches inactivated with phenol (blue, top) and DOC (black, bottom).

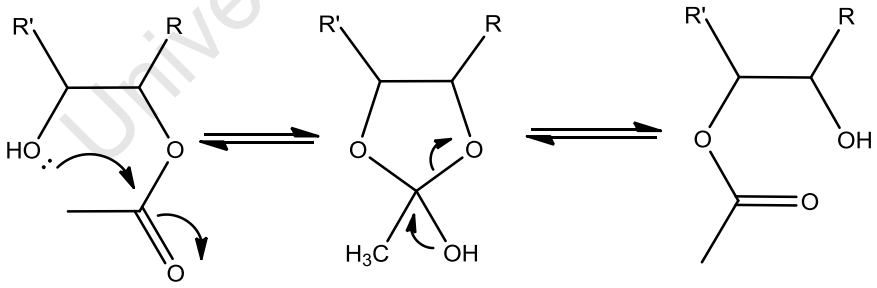

Figure 4.10. Migration of O–acetyl group from C2 to C3 on GalA residue in Pn1 PS.

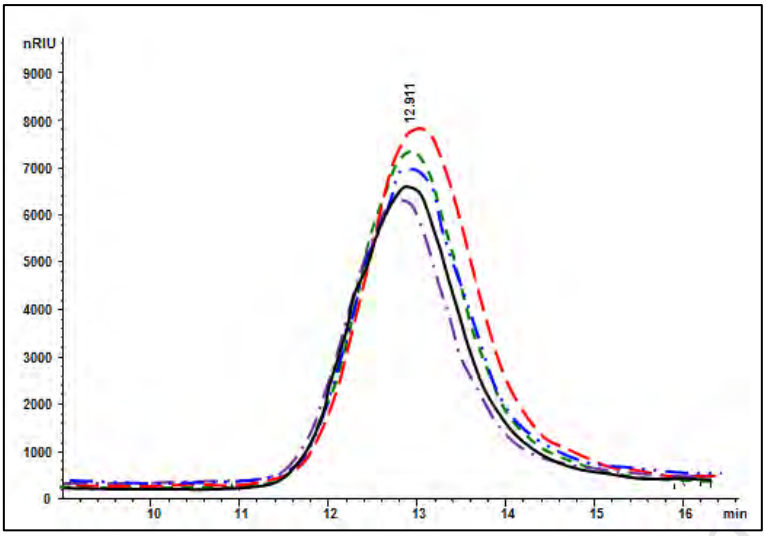

Figure 4.11. Size comparison of four batches of either DOC (red and green) or phenol (blue and purple) inactivation. A known Pn1 PS (black) is shown for reference.

From the last four batches the results confirm the phenol inactivation to be superior to DOC in polysaccharide yield and *O*–acetyl content. The phenol inactivated batches were purified to a greater extent in terms of protein, nucleic acid and CWPS contaminants. It is important to note that the protein contamination was reduced significantly by not collecting the 10 % EtOH fractions (which is high in nucleic acid contaminants). The PS produced from both phenol batches were within WHO specification for protein, nucleic acid and CWPS. Thus, phenol was chosen as the preferred inactivation method for future fermentation and purification batches.

4.1.2 Large scale fermentation batches

With an inactivation strategy and purification process parameters established following the small scale cultivations; the next step was to scale up the fermentation volume. The purification volumes were 6 L, 15 L or 30 L: the 15 and 30 L batches were fermented in a fermentor and the 6 L batches were fermented using disposable technology, namely a Wave Bioreactor. The results of all these purifications can be found in the Appendix. Three batches are explained in some detail; Pn1–007 was fermented using disposable bag technology, Pn1–019 is included as a representative sample and the Pn1–018 provided a unique outcome. Before purification commenced, initial PS content was determined (Table 4.11).

Table 4.11. Initial conditions for three cultivations of Pn1 using disposable technology and traditional fermentation methods.

Batch No:	Pn1–007	Pn1–018	Pn1–019
Fermentation mode	Wave	Fermentor	Fermentor
Fermentation volume (L)	6	15	15
Method of inactivation	phenol	phenol	phenol
Initial pH	7.91	7.05	7.09
Initial PS content (g)	2.40	9.04	5.12
Initial PS concentration (mg/L)	400	602	341

As with previous batches, the fermentation broth was first clarified to remove any cell debris and insoluble media components. Following clarification the pH of the solution was adjusted to 7.8 followed by CTAB/Celite addition. Again, rate nephelometry was used to confirm that the polysaccharide had precipitated in the CTA^+ salt form. The purification continued with the ethanol elution of the polysaccharide from the Celite column. During the purification investigation, it was decided to reduce the number of EtOH concentrations to three; the 5 % EtOH which elutes out the nucleic acids and proteins, the 15 % and 30 % which elutes off the polysaccharide and 60 % EtOH was added as a final wash to remove any remaining polysaccharide trapped in the Celite. Table 4.12 details the fractions that tested positive in the uronic acid assay for the presence of polysaccharide and Figure 4.12 shows graphically the percentages of polysaccharide and CWPS eluted in each ethanol fraction. Nucleic acid, protein and aggregate percentages are also shown for each fraction. The positive fractions were pooled; NaCl and EtOH added to promote precipitation, and subsequent centrifugation and diafiltration were carried out. Full analysis of each batch was performed and detailed in Table 4.13.

Table 4.12. Polysaccharide elution patterns with increasing concentrations of ethanol.

Batch	Polysaccharide elution				
	0.05 % CTAB	5 % EtOH	15 % EtOH	30 % EtOH	60 % EtOH
Pn1-007	N	N	Y	Y	N
Pn1-018	N	N	Y	Y	Y
Pn1-019	N	N	Y	Y	N

*Uronic acid assay used to test for polysaccharide. Purple colour change suggests Pn1 elution.

The Pn1–018 purified batch produced the highest levels of Pn1 polysaccharide out of all the fermented and purified batches in this study; however the recovery from batch Pn1–007 was much higher at 69 % compared to approximately 51 % for Pn1–019 and only 43 % for Pn1–018. The *O*–acetylation assays gave an unusual result for Pn1–018 which was that no *O*–acetylation was present on the polysaccharide after purification. The results from the

colorimetric assay were confirmed by NMR analysis (Figure 4.13), however it was not known why this would have occurred as fermentation proceeded as per previous batches and no contamination was seen. The NMR gave an acetylation level of 67 % for both Pn1–007 and Pn1–019. The pattern of *O*–acetylation between the two batches was different with Batch Pn1–019 showing a position ratio between C2 and C3 of 65:35 where Pn1–007 gave a position ratio of 49:51 C2:C3. The difference in position of *O*–acetylation was hypothesised to be due to the pH of the inactivated fermentation broth. From the NMR it was concluded that the bacteria acetylates at the C2 position of the GalA residue and an increase in pH causes a migration to the C3 position, the extent of migration depends on the pH of the fermentation batch, the temperature and the time since fermentation to analysis.

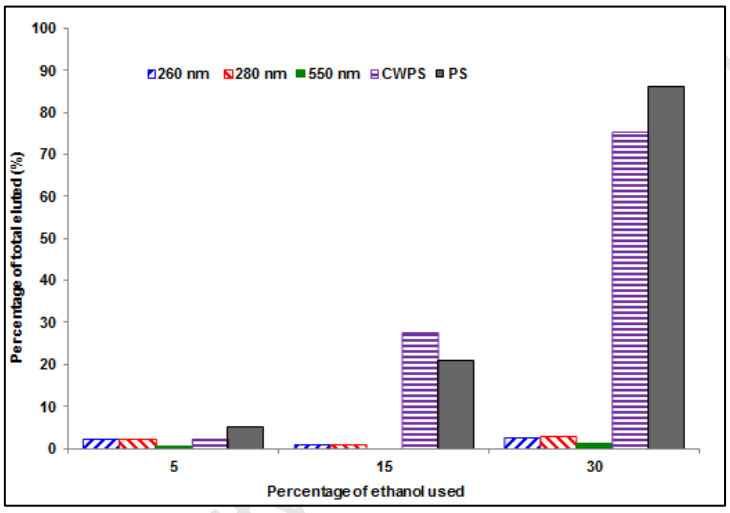

Figure 4.12. Total amounts of nucleic acid, protein, aggregates, CWPS and PS during EtOH fractions on a representative purification.

The nucleic acid contamination in Pn1–007 was not significant but was found to be approximately 1 % in Pn1–018 and Pn1–019, which was still within acceptable limits. The protein contamination of Pn–018 was higher than acceptable limit at 3.1 % whilst the other two batches were within specification. This high value for Pn1–018 could be attributed to the inclusion of the 60 % ethanol fraction in the pool. This fraction tested positive for a large amount of polysaccharide and hence was included in the pooled fractions but since each fraction was not tested for protein, it was possible that this fraction may have been contaminated with a large amount of protein.

Table 4.13. Analytical results of three purified Pn1 polysaccharide batches.

Analytical calculations	Pn1-007	Pn1-018	Pn1-019	Acceptance criteria
UA content (%)	66.6	70.2	74.1	> 55.17
PS Content (UA assay) (g)*	2.3	7.6	4.0	–
O–acetylation				
Colorimetric assay (mass %)	23.7	0	23	>5.47
NMR (mol %)	67	0	67	–
Impurities				
Nucleic acid (%)	0.004	1.2	1.1	<2
Protein (%)	0.6	3.1	1.7	<3
CWPS (mol %)**	2.2	1.2	1.9	–
CWPS (mass %)**	4.4	2.4	3.8	–
% recovery	69	43	51	–

*Based on dry weight
**Average of calculations with CH_3 and NHAc groups of amino sugar as reference.

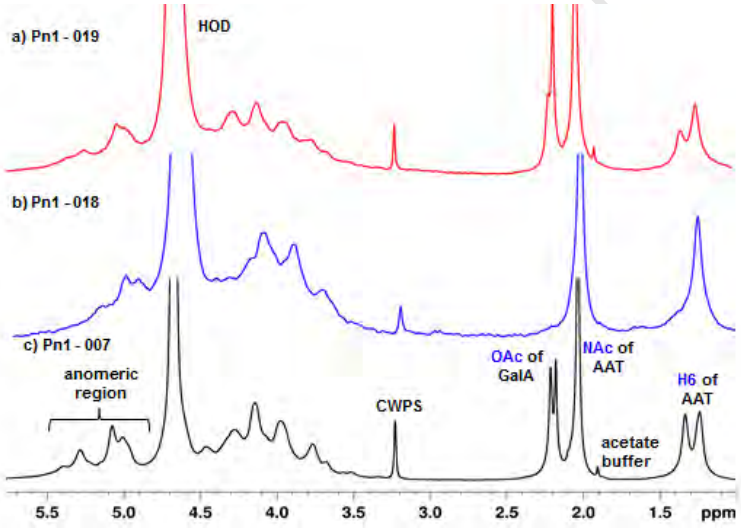

Figure 4.13. ^{1}H NMR overlays of three batches of purified Pn1 polysaccharide, a) Pn1–019 and b) Pn1–018 and c) Pn1–007.

4.1.3 Summary

A strategy for the purification of Pn1 was successfully implemented. The inactivation strategy developed was based on a patent by Liveyns *et al.* and it was determined that phenol inactivation provided the optimum amount of polysaccharide when compared to DOC inactivation. The inactivated fermentation broth was transferred to downstream processing after clarification. The CTAB/Celite “slurry” was generated and packed into a column and washed with a low concentration of CTAB to remove excess media components before the polysaccharide was eluted with increasing concentrations of ethanol. Polysaccharide fractions eluted with low ethanol concentrations were not included as the levels of protein and nucleic acid were too high. Counter ion exchange with NaCl was followed by

precipitation with 96 % ethanol before final separation by centrifugation and diafiltration to obtain the purified Pn1 PS. Figure 4.14 details the final process flow for the purification of Pn1 along with all analytical tests performed throughout the process. This polysaccharide conformed to all specifications determined by the World Health Organisation in terms of identity, structural integrity and purity. The polysaccharide was deemed sufficiently pure to be further conjugated to a carrier protein in the preparation of a conjugate vaccine for animal testing.

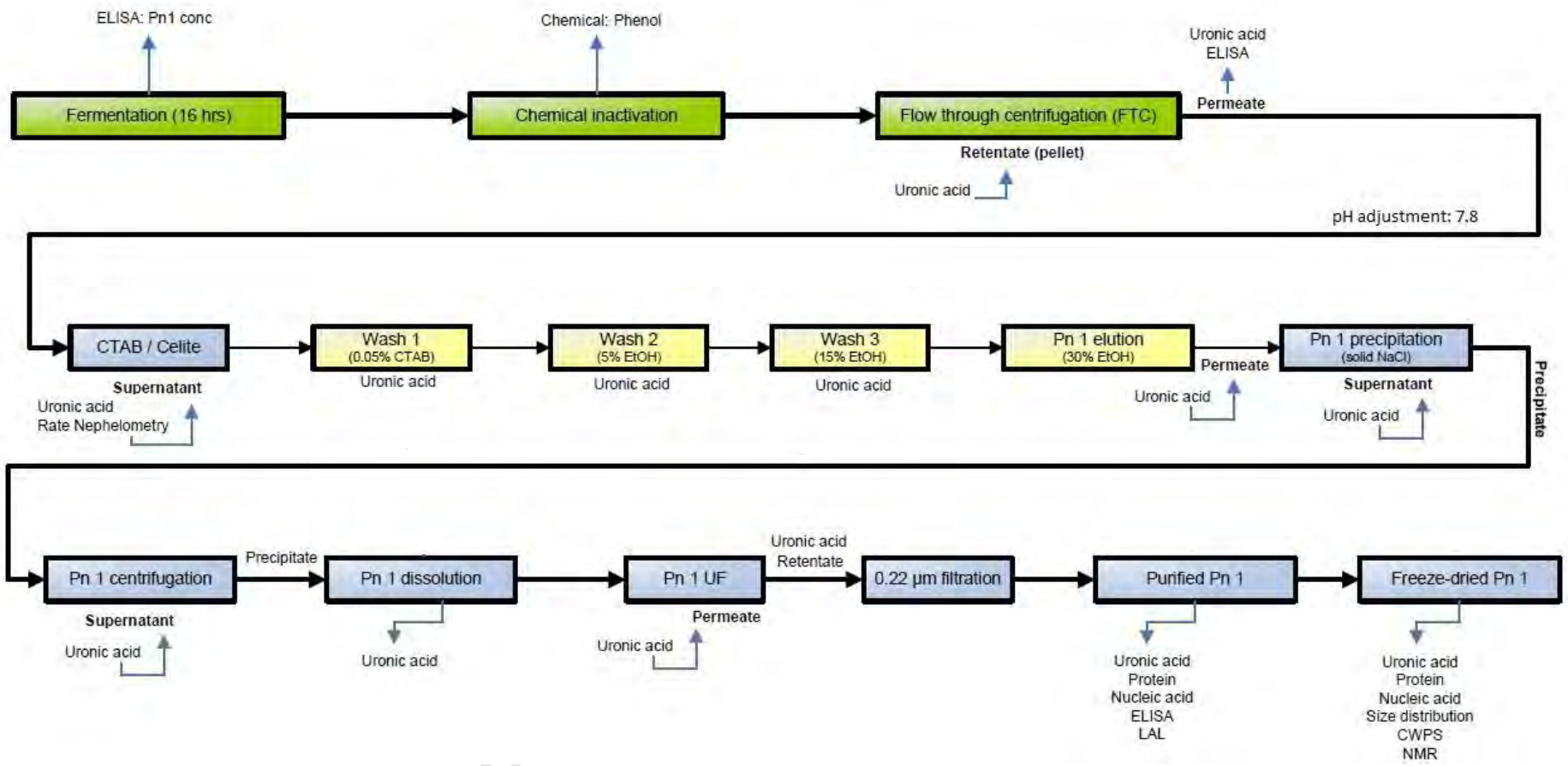

Figure 4.14. Final process flow for the purification of Pn1 polysaccharide including diafiltration steps as well as all analytical assays performed.

4.2 Polysaccharide size reduction

There are two different molecular weight distributions for polysaccharides that are used in commercially available vaccines:

1. Full sized or size–reduced bacterial polysaccharides that are randomly activated at various sites along the chain with or without a linker. A cross linked, lattice–like structure is formed when the polysaccharide is coupled to a protein [107, 164, 377]. These conjugates have a very high molecular mass, and are difficult to characterise on a molecular level.
2. Shorter polysaccharide fragments (oligosaccharides) that are either attached to the protein at one singular point that generally corresponds to their terminal or cross–linked to the protein [107, 378-380].

There is evidence that shows that the shorter chain fragments of polysaccharides are able to elicit a greater T cell–dependent antibody response than the longer chain PS; they optimise T cell help by bringing antigen specific B cells and helper T cells into a more favourable physical relationship for cell–cell interactions [381]. Conjugates that contain saccharides as small as a disaccharide have been shown to elicit antibodies to some bacterial polysaccharides or the corresponding bacteria itself [380]. However, the size of the saccharide must be sufficiently large to be effective in raising antibody immunity by expressing the complete epitope of the native antigen [10, 107, 380, 381].

The relationship between immunogenicity and polymer chain length has been shown for a variety of polysaccharides in both animal and human studies [382-385]. The studies have provided direct evidence that a reduction in the polysaccharide size below a certain minimum can result in a reduced immunogenicity. These studies [383, 384] formed the historical basis for the introduction of molecular size specifications that would provide confidence that the potency of pneumococcal polysaccharides used in vaccine formulations remains, however these were based on polysaccharide vaccines and not conjugate vaccines [385].

Anderson *et al.* carried out detailed studies of the effects of oligosaccharide chain length on the immunogenicity of PRP for Hib conjugate vaccines [380, 381]. The investigations compared conjugates containing saccharides with 8 and 20 ribose–ribitol phosphate repeating units. The conjugate containing the 20 repeating units was found to prime infants for a secondary response better than the 8 repeating unit conjugate. However, a later study of conjugates with 4–, 6– and 12– repeating unit conjugates showed no difference in animal antibody response [381].

Despite the opposing thoughts with respect to immunogenicity and chain length, an advantage of size reduction is a reduction in the viscosity of the polysaccharide in solution. Due to the number of hydroxyls and other functional groups in the polysaccharide, inter– and intra–molecular forces, including hydrogen bonding and van der Waals forces, are present which gives the polysaccharide a very high apparent hydrodynamic size. By interrupting these forces, the viscosity of the polysaccharide in solution decreases, making the solution easier to work with and allowing a more efficient conjugation.

Table 4.14 best describes the variability of polysaccharide size and size reduction methods of some licensed conjugate vaccines. Synthetic (Quimi–Hib), full length (ActHIB) and size reduced (HibTITER) PRP has been used in conjugate vaccines against Hib. Both chemical and mechanical means of size reduction have been applied to different serotypes in pneumococcal conjugate vaccines with GlaxoSmithKline making use of microfluidization as described in this chapter. The conditions used in the GSK process are a maximum of 50 passes through a M110S Microfluidics machine for a period of two minutes at a maximum pressure of 12 328 psi [386].

Table 4.14. Currently licensed vaccines using various polysaccharide sizes.

Serotype	Conjugate Vaccine	Method of polysaccharide size reduction	Manufacturer
Hib conjugates			
B	HibTITER®	Periodate oxidation	Pfizer
B	ActHIB®	Native PS used	Sanofi Pasteur
B	Quimi–Hib®	Synthetically produced	Heber Biotech
Meningococcal conjugates			
A	MenAfriVac®	Periodate oxidation	Serum Institute of India Limited (SIIL)
C	NeisVac–C®	Periodate oxidation	GlaxoSmithKline
Tetravalent	Menveo®	Acid hydrolysis	Novartis
Pneumococcal vaccines			
7 valent	Prevnar®	Acid hydrolysis and periodate oxidation	Pfizer
10 valent	Synflorix®	Microfluidization	GlaxoSmithKline
13 valent	Prevnar13®	Acid hydrolysis and periodate oxidation	Pfizer

The traditional methods of size reduction are:

1. Acid and base catalysed hydrolysis where either an acid or base is added to the sample to be hydrolysed and the sample is heated to a desired temperature over a period of time.

2. Chemical manipulation of a reactive group on the polysaccharide that leads to fragmentation, e.g. oxidation of the diols on the ribitol chain of PRP to form aldehydes and resulting in fragmentation of the polysaccharide.

The use of chemical size reduction has distinct disadvantages, including:

- Many of the pneumococcal polysaccharides are unstable at extreme pHs. For example Pn1 contains a very labile *O*–acetyl grouping that will be removed at a basic pH (above 8.0).
- The ability to obtain and control the size of the polysaccharide is very difficult using traditional methods and even if the desired size is achieved it is very difficult to reproduce.
- As they are chemically selective, these methods may break susceptible bonds and leave the more resistant bonds intact.
- It is specific to certain groups of saccharide and not generally applicable to all polysaccharides.
- Side reactions may occur.

Alternatives to the use of chemicals are sonication and microfluidization. Although these methodologies require specialised instrumentation, they have the advantage of yielding suitable fragmentation that: (i) is reproducible, (ii) requires minimal post fragmentation work–up (iii) is relatively quick to perform and; (iv) does not require additional chemicals or reagents.

4.2.1 Mechanical size reduction

Two different types of mechanical size reduction were investigated in this study, namely sonication and microfluidization.

Sonication is a process by which an electrical signal is converted into a mechanical vibration. This vibration, in the case of polysaccharides, causes the glycosidic bonds between the different saccharides to break. The essential component of a sonicator is the generator: it creates an ultrasonic electrical signal that powers a transducer which, in turn, changes the electrical signal to a mechanical vibration using piezoelectric crystals. This mechanical vibration is amplified to the required power output before transferring it to the probe which vibrates through the solution when placed in the sample. The amplitude or power output (that controls the rate of vibration) and the time a sample is sonicated can be controlled depending on the sample requirements [387].

Sonication works by creating an effect known as cavitation that occurs as a result of liquids not moving as fast as the movement of the probe, so the vibrations create a series of microscopic bubbles in the solution, pockets (cavities) of space wedged between the

molecules form and collapse again under the weight of the solution, sending out tiny shockwaves into the surrounding substance. Thousands of these bubbles forming and collapsing constantly create powerful waves of vibration that cycle into the solution and break the polymeric chains [387].

One consequence of high power output focused in the tip of a probe is that sonication can generate substantial and rapid heat. A burst of a sonicator probe for just a few (1 – 2) seconds can cause water to boil. Consequently, when heat labile samples are processed, the samples must be kept cold and the sonication must be performed in short bursts interspersed with cooling periods. A further consequence of the high power output is that the tip itself disintegrates posing a contamination issue. Although particles can be removed by introducing a filtration step post–sonication, this potential contamination issue renders the method not suitable for manufacturing processes. An alternative method for size reduction, namely microfluidization, allows for the control and reproducibility of the sonication without the contamination.

Microfluidization involves the use of an interaction chamber containing fixed geometry micro– channels and a pump. The pump in the instrument amplifies hydraulic pressure to the selected level which, in turn, imparts this pressure to the sample. The pressure is controllable in the range of 2 500 to 30 000 psi that the pump delivers at a constant rate to the sample. As the pump travels through its pressure stroke it drives the sample through the interaction chamber. The sample travels at a very high velocity through the micro–channels that are designed to create high shearing and impact forces that disrupt (break) any non–branching glycosidic bonds in the polysaccharide. As the pump completes its pressure stroke it reverses direction and draws through the next volume of sample. At the end of the intake stroke it again reverses direction, drives the sample into the interaction chamber and the process is repeated. This allows for the processing of large volumes of sample in a repeatable procedure. The sample can be recirculated through the chamber if the desired size is not achieved from the first pass [388].

In order to investigate the application of microfluidization the M–110PS model was acquired that permits a minimum sample volume of 25 ml. By utilising the specifically designed fixed geometry diamond interaction chamber technology, and a ceramic (Zirconia) plunger, the M–110PS is capable of processing a wide variety of applications such as particle size–reduction and cell disruptions including the most difficult yeast and plant cells in as few as 1 – 2 passes. The process is repeatable and scalable to pilot and/or production volumes. The microfluidizer has a pressure operating range of 0 – 30 000 psi and the return coil has to be cooled to between 2 – 6 °C to avoid the sample heating up.

Two different methods; namely sonication and microfluidization, were investigated in order to initiate and develop a simple and general fragmentation strategy that could be applied to a wide variety of polysaccharides, irrespective of their chemical structure.

4.2.2 Sonication

During the investigation into the sonication technique, Pn1 polysaccharide was in limited supply and a model compound was sought. Hyaluronic acid (HA) (Figure 4.15) is composed of a disaccharide repeating unit of glucuronic acid and *N*–acetylglucosamine, which is structurally similar to the galacturonic acid and the AAT amino saccharide of Pn1 and was thus chosen as a model compound for the initial sonication investigations.

The main objective of the experiments described below was to determine if the degree of depolymerisation could be consistently controlled by changing time or power variables, without altering the structure of the polysaccharide. The targeted molecular size range post sonication was 50 – 100 kDa for all polysaccharides.

a) Hyaluronic acid

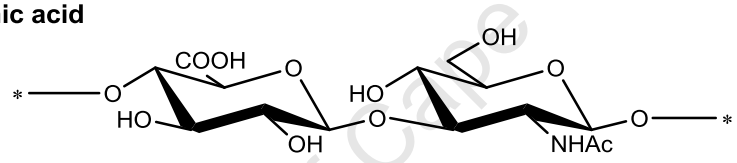

b) *Streptococcus pneumoniae* serotype 1

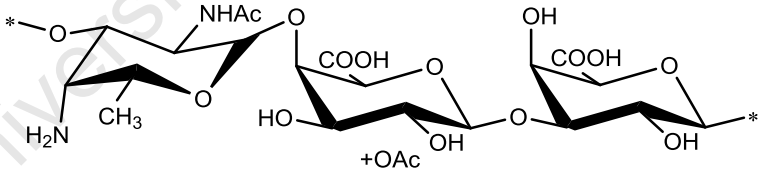

Figure 4.15. Structures of a) HA and b) Pn1.

10 ml of an HA solution in water (at 5.00 mg/ml concentration) was placed in a 50 ml beaker and cooled in an ice bath before the sample was subjected to sonication with varying power outputs as described in Table 4.15.

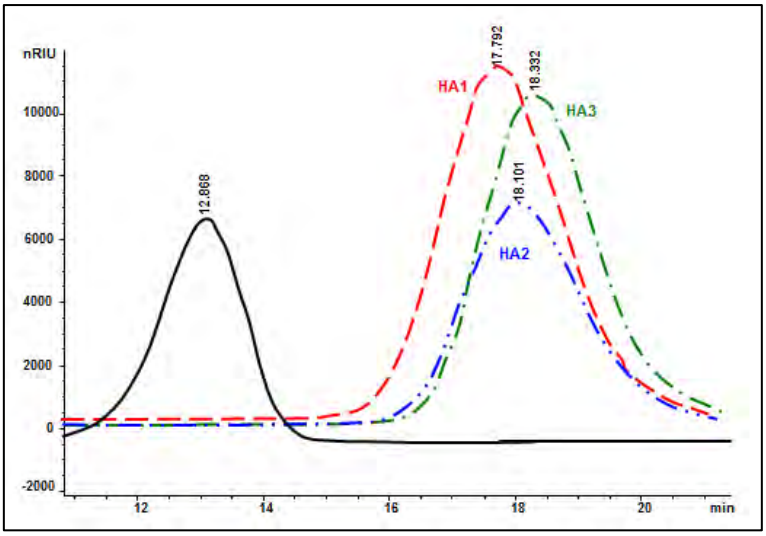

Figure 4.16. SEC–HPLC RID chromatograms of hyaluronic acid samples. Comparison of full size (black) HA with 85 kDa HA1 (red), 67 kDa HA2 (blue) and 56 kDa HA3 (green).

Table 4.15. Summary of sonication conditions and the resultant size distribution of HA.

Sample	Time (min)	Power output (kJ)	Retention time (min)	Size (kDa)	Size reduction
HA	0	0	12.868	3360	–
HA1	30	71.64	17.792	85	39.5 fold
HA2	60	37.77	18.101	67	50 fold
HA3	45	104.58	18.332	56	60 fold

The HA samples were significantly reduced in size with the molecular size decreasing from 3000 kDa to 50 – 100 kDa, a 40 – 60 fold size reduction when the higher power outputs were applied. Higher power outputs were required due to the larger size of the native polysaccharide (Figure 4.16). Both HPAEC and NMR analysis were performed on sample HA2 to investigate if the integrity of the sample had been maintained after sonication and that no epimerization occurred.

The resulting HPAEC–PAD chromatograms (Figure 4.17) before and after sonication both display a peak eluting at 16 min, corresponding to *N*–acetylglucosamine. With this chromatographic method the glucuronic acid moiety was not seen. A peak that eluted at 9.0 min was due to the presence of glycerol; this was expected due to the filtering of the sample to remove any traces of metal shavings. As the GlcA peak was not observed NMR was needed to confirm that the structural integrity of the polysaccharide remained in place.

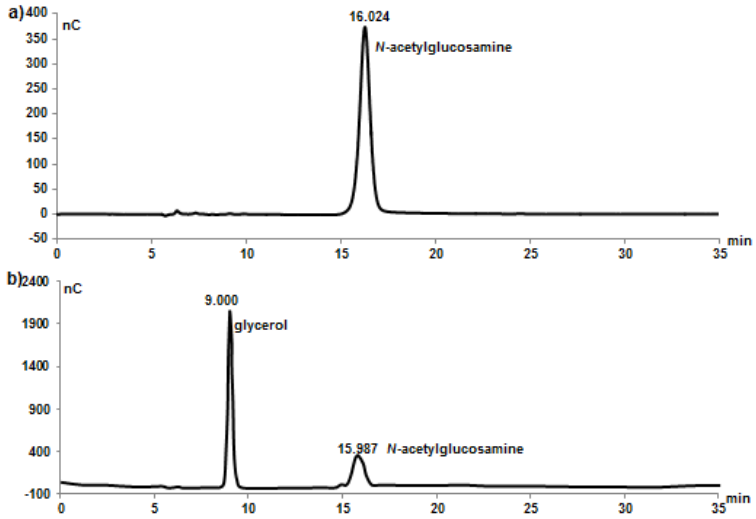

Figure 4.17. HPAEC analysis of HA a) full length and b) HA2: sonicated – 67 kDa.

Figure 4.18 details the proton (^{1}H) and carbon NMR spectra respectively of the sonicated sample (HA2). The fully characterised 2D proton–carbon correlation (HSQC) spectrum is displayed in Figure 4.19. The anomeric signals of both *N*–acetyl glucosamine and glucuronic acid in the ^{1}H NMR were found with chemical shifts of 4.56 and 4.46 ppm respectively. The methyl peak at 2.02 ppm corresponded to the acetate peak of *N*–acetyl glucosamine. Peaks due to the presence of glycerol were seen in the proton spectrum (insert in Figure 4.18) and confirmed in the ^{13}C spectrum. All peaks identified in both the ^{1}H and ^{13}C spectra confirmed that no epimerization had taken place during sonication.

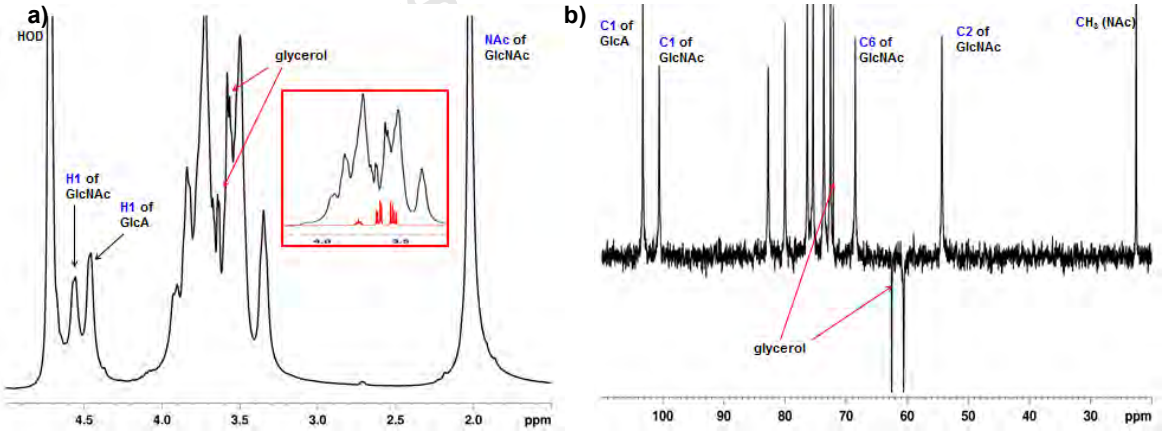

Figure 4.18. ^{1}H and ^{13}C NMR spectra of sonicated HA. The insert in the ^{1}H NMR is of a glycerol overlay confirm the presence of the impurity.

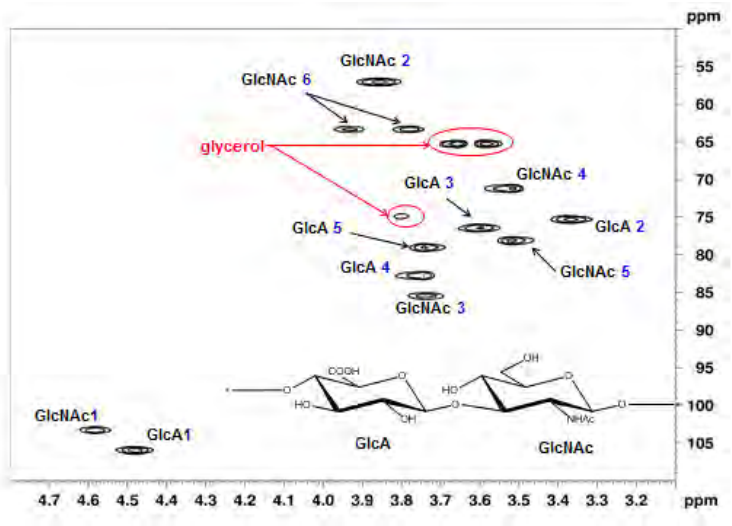

Figure 4.19. Expanded proton–carbon correlation spectrum (HSQC) of sonicated HA.

The 2D HSQC spectrum (Figure 4.19) further confirmed the identity of the hyaluronic acid with all peaks from the proton and carbon spectra correlated and identified. No epimerization had taken place as the peaks identifying both glucuronic acid and *N*–acetyl glucosamine were confirmed.

With the knowledge that the structural integrity of the polysaccharide is maintained after sonication, attention turned to the size reduction of Pn1 PS by means of sonication. Pneumococcal polysaccharide serotype 1 was made available from two sources:

1. Chengdu Institute of Biological Products (CDIBP).
2. Pn1 fermented and purified at The Biovac Institute, (Biovac).

20 ml of Pn1 from both sources were separately solubilised in water (at 5 mg/ml concentration), placed in a 50 ml beaker and cooled with an ice bath. Pn1 was subjected to various power outputs for between 30 and 60 min. The data generated from the analysis of the polysaccharide is presented in Table 4.16 and the SEC–HPLC chromatograms are displayed in Figure 4.20.

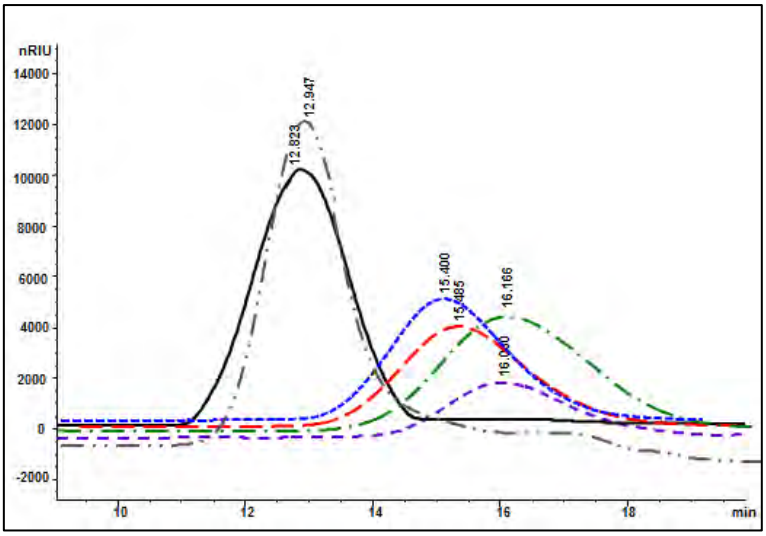

Figure 4.20. SEC–HPLC RID chromatograms of full length (grey) and sonicated (purple) Pn1 Biovac batch sample, as well as the chromatograms of CDIBP full length (black), CDIBP–1 (blue), CDIBP–2 (red) and CDIBP–3 (green) samples.

Table 4.16. Summary of sonication conditions and the resultant size distribution of Pn1 from CDIBP as well as a sample from TBI.

Source	Sample	Time (min)	Power (kJ)	Retention time (min)	Size (kDa)	Size reduction
CDIBP	Pn1	0	0	12.823	1188	–
	1	45	68.22	15.400	178	6.7 fold
	2	60	77.74	15.485	169	7.0 fold
	3	60	98.24	16.166	110	10.8 fold
Biovac	Pn1	0	0	12.947	1061	–
	1	30	54.32	16.060	118	9.0 fold

A reduction in size was achieved with all samples of Pn1 that underwent sonication. A small power output of 54.32 kJ produced a size reduction to 118 kDa from 1061 kDa (9 fold reduction) for the Biovac sample, whereas a CDIBP sample was subjected to a 68.22 kJ power output yet a size reduction from 1188 kDa to only 178 kDa (7 fold reduction) was achieved. While the reduction in size of the two different samples are similar (7 vs. 9 fold reduction) differences between the levels of size reduction could be explained in two ways. Firstly, due to the shedding of the metal tip on the sonicator, the size reductions of the samples will never be completely reproducible, the same power and time could be used for different samples, and the outcome will not be exactly the same. Secondly, the purity of the samples should be taken into account when comparing size reduction. It was thought that the Pn1 from CDIBP contained more contaminants (protein and nucleic acid) than that purified at Biovac. Therefore, more energy may have been used to break up the contaminants than the actual polysaccharide.

Proton NMR spectra were recorded for the native (full sized) and sonicated (size reduced) Pn1 from both CDIBP and Biovac. The CDIBP sample contained an extra peak at 1.91 ppm corresponding to the methyl group of free acetate from trace amounts of acetate buffer. It was observed that the NMR spectrum for both samples (Figure 4.21) were sharper post sonication, especially in the ring proton and anomeric region. The observed broad lines in the parent NMR spectrum were due to the lack of molecular motion. Increasing either the temperature, or in this case, reducing the size of the polysaccharide resulted in an increase in the molecular motion and therefore a better resolved spectrum with sharper peaks.

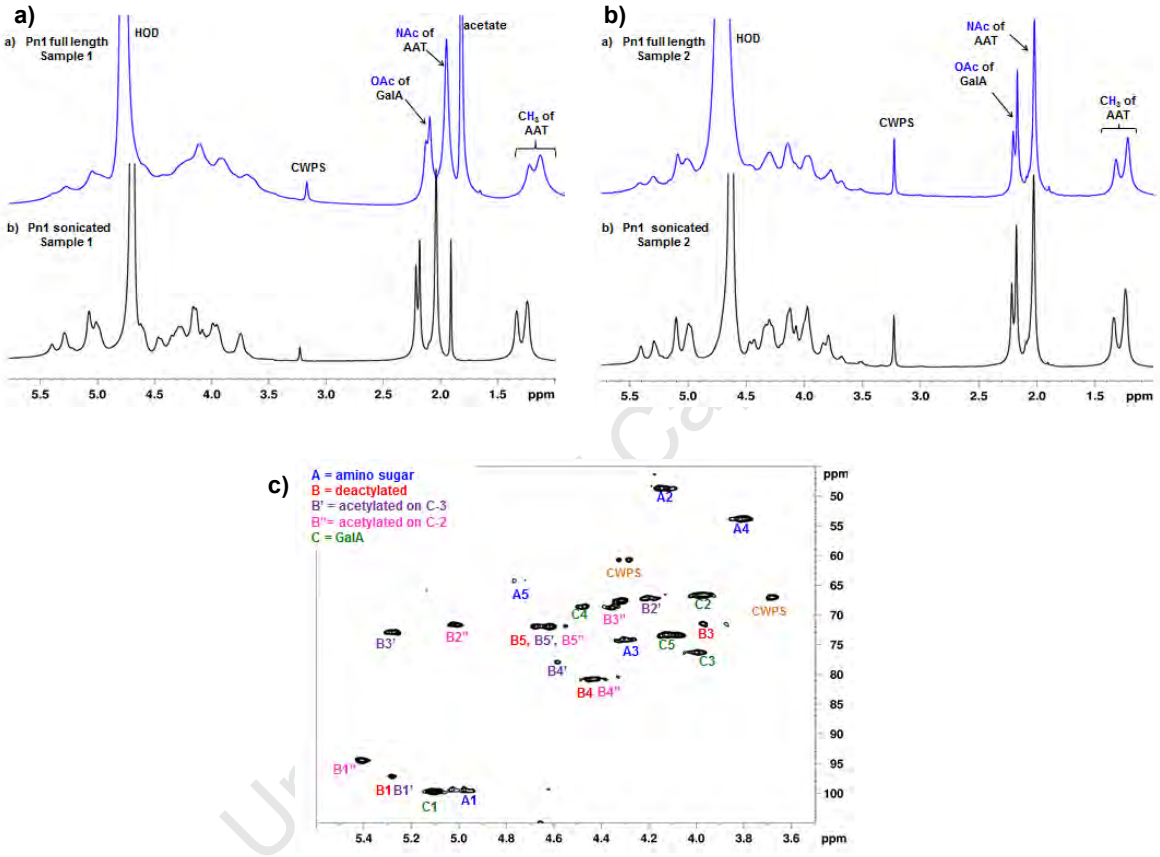

Figure 4.21. ^{1}H NMR analysis from (a) CDIBP and (b) Biovac detailing the full sized and sonicated Pn1 polysaccharide. (c) ^{1}H–^{13}C HSQC of sonicated Pn1 polysaccharide (CDIBP sample).

The anomeric region revealed four proton signals post sonication corresponding to the acetylation at two different positions. The sharper signals were possibly due to the disruption of the intramolecular forces (hydrogen bonding) in the polysaccharide. The most labile bond on Pn1 is the *O*–acetyl bond on the GalA residue. It is thought that the *O*–acetyl functional group is important for the polysaccharide's immunogenicity and therefore needs to remain attached to the polysaccharide. No loss of the *O*–acetyl peak was observed after size reduction as the *O*–acetyl peak can still be seen at 2.20 ppm. The *N*–acetyl peak of the amino saccharide was identified at 2.05 ppm and was seen before and after size reduction. The peak at 3.23 ppm corresponded to the cell wall polysaccharide (CWPS) which was

present in small quantities in all samples. The methyl peak of the amino saccharide at 1.29 ppm along with the *O*– and *N*– acetyl peaks confirmed that the conformation Pn1 remained intact after sonication. The HSQC spectrum was used to fully characterise the polysaccharide (Figure 4.21c).

4.2.3 Microfluidization

The microfluidizer technology was investigated with the pneumococcal polysaccharides Pn1, Pn6B and Pn14. The primary aim of this investigation was to achieve a reduction in polysaccharide size to the smallest size possible without affecting the integrity of the polysaccharide or its polydispersity. Pn14 polysaccharide was used to further evaluate 1) the conservation of area under the peaks before and post microfluidization and 2) the polydispersity of the polysaccharide peaks in the chromatograms to quantitate the heterogeneity of molecular size. Molecular weights under 200 kDa for Pn6B and Pn14 and under 400 kDa for Pn1 were the size targets decided upon at the beginning of the investigation.

4.2.3.1 Pn6B

To investigate the reduction in size that the microfluidizer can induce on a molecule, 25 ml of Pn6B, solubilised in water (at 10 mg/ml concentration), was loaded into the sample reservoir. The polysaccharide was exposed to 15 000 psi for an increasing number of passes, 2, 4, 6 and 8, through the chamber. After the desired number of passes a sample was taken and analysed on SEC–HPLC, with the remainder of the solution returned to the glass reservoir for more passes.

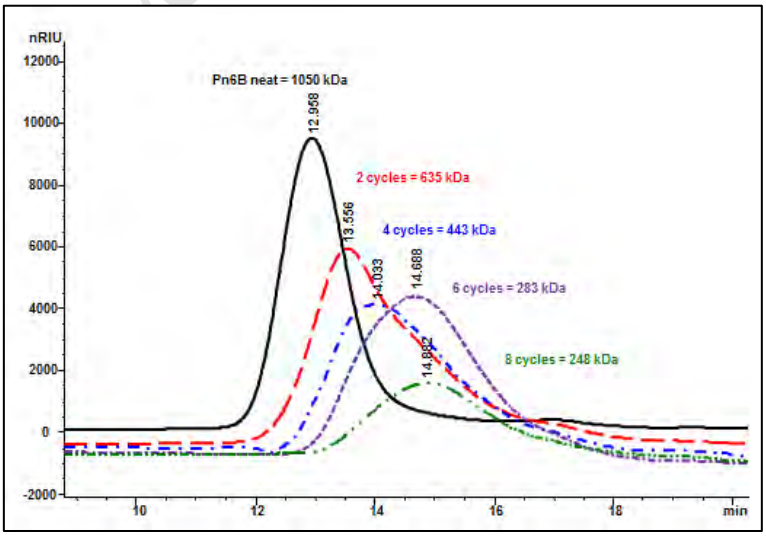

Figure 4.22. SEC–HPLC RID chromatograms of Pn6B full length (black) and after microfluidization at 15 000 psi and 2 cycles (red), 4 cycles (green), 6 cycles (blue) and 8 cycles (purple).

Table 4.17. Summary of the resultant size distribution of Pn6B whilst increasing the number of passes through the microfluidization chamber.

Number of Passes	Retention time (min)	Molecular weight (kDa)	Size reduction
0	12.958	1050	–
2	13.556	635	1.7
4	14.033	443	2.4
6	14.684	283	3.7
8	14.862	248	4.2

The results in Table 4.17 and Figure 4.22 illustrate the effect on size reduction that the increasing number of passes at a specific pressure had on the polysaccharide. The polydispersity of the PS increased with the amount of times the polysaccharide was subjected to microfluidization. The decrease in molecular weight was most noticeable during the first pass, with additional passes having less and less impact on the apparent molecular weight and it was hypothesised that the pressure exerted on the sample would have greater size reducing power than the number of times the sample is exposed to microfluidization. The Pn6B sample was exposed to 22 000 psi for 3 and 4 passes, and the size of the PS reduced from 1050 kDa to 206 kDa and 196 kDa after 3 or 4 passes respectively. A summary of the results for Pn6B is shown in Table 4.18.

Table 4.18. Summary of the microfluidization variables and the resultant size distribution of Pn6B.

Initial molecular weight (kDa)	Pressure (psi)	Number of passes	Final molecular weight (kDa)	Size reduction
1050	15 000	2	635	1.7
		4	443	2.4
		6	283	3.7
		8	248	4.2
	22 000	3	206	5.1
		4	196	5.4

The sample subjected to a pressure of 22 000 psi and 4 passes through the instrument was found to be in the required size range. This sample was subjected to full proton, carbon, phosphorus and 2D HSQC analysis for structural confirmation. The structure of Pn6B polysaccharide is shown in Figure 4.23.

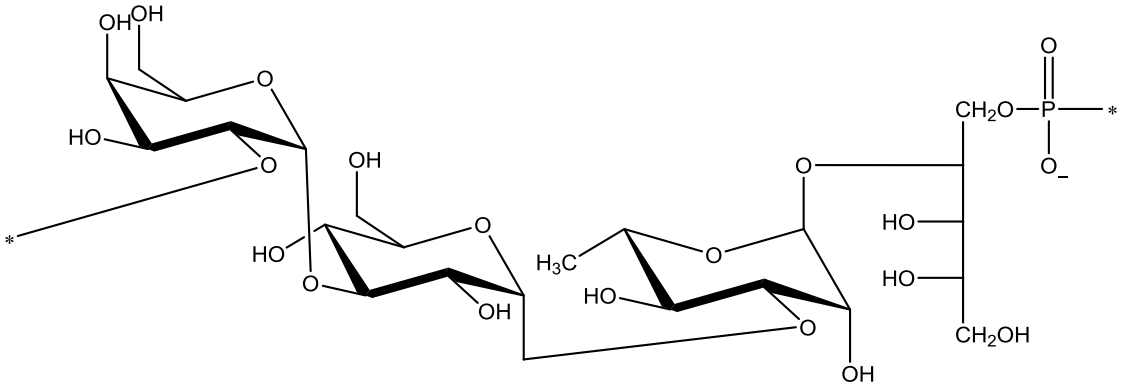

Figure 4.23. Structure of serotype Pn6B.

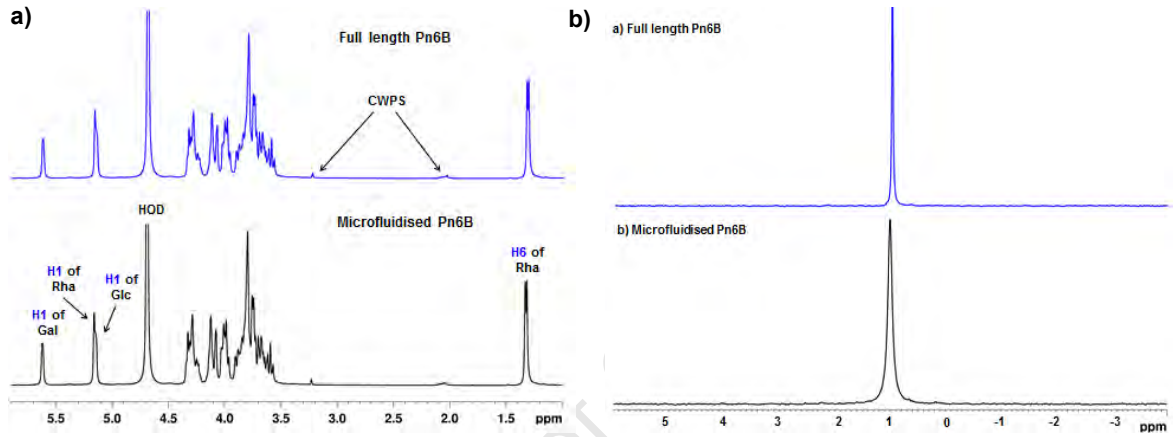

Figure 4.24. ^{1}H and ^{31}P spectra of full length (blue) and microfluidized (black) Pn6B polysaccharide.

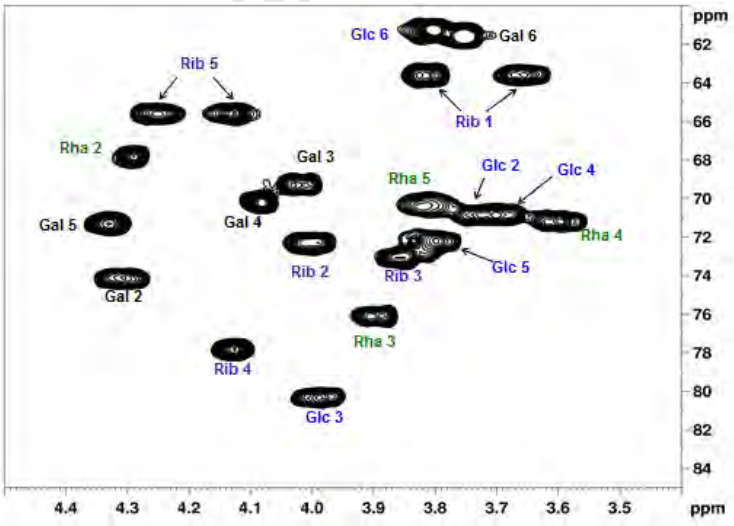

Figure 4.25. Expansion of ^{1}H–^{13}C HSQC spectrum of microfluidized Pn6B.

The Pn6B microfluidized sample was less viscous than the native polysaccharide and yielded well–resolved spectra containing the same proton, carbon and phosphorus resonances as the parent polysaccharide which was indicative that microfluidization had no impact of the structural integrity of the Pn6B saccharide. The three alpha anomeric protons

from galactose (Gal), rhamnose (Rha) and glucose (Glc) were detected at 5.67, 5.16 and 5.15 ppm respectively (Figure 4.24). One signal for a methyl group at 1.32 ppm corresponded to C6 of Rha. The ^{31}P spectra confirmed that the ribitol phosphate structure was retained after size reduction with a single peak at 1.09 ppm [389]. The 2D HSQC (Figure 4.25) again confirmed that structural integrity was maintained after size reduction.

4.2.3.2 Pn14

Pneumococcal serotype 14 was subjected to the same conditions as described for Pn6B. The sample was solubilised in water at a concentration of 10 mg/ml and exposed to 2, 4 and 6 passes through the microfluidizer at 10 000 psi. After each set number of passes, a sample was taken and analysed on SEC–HPLC. The pressure employed for the Pn14 polysaccharide was slightly lower than that used for Pn6B (10 000 instead of 15 000psi) due to the relative initial size of the polysaccharide. During the Pn6B investigations it was seen that the polydispersity of the polysaccharide increased significantly after 8 passes so the maximum number of passes that Pn6B was subjected to was 6 passes. The results of these investigations can be seen in Figure 4.26. Elution times and corresponding molecular weights can be found in Table 4.19.

Table 4.19. Changes in Pn14 molecular weight as the number of passes through the microfluidizer is increased, the pressure remained constant at 10 000 psi.

Number of Passes	Retention time (min)	Molecular weight (kDa)	Size reduction
0	13.128	904	–
2	13.549	639	1.4 fold
4	13.843	509	1.8 fold
6	14.509	290	3.1 fold

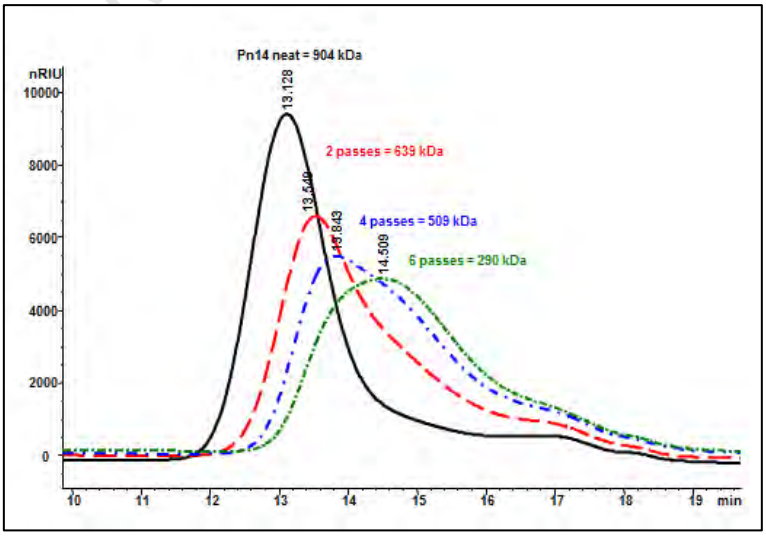

Figure 4.26. SEC_HPLC RID chromatograms of Pn14 full length (black) and after microfluidization at 10 000 psi with 2 cycles (red), 4 cycles (blue) and 6 cycles (green).

As with Pn6B, the results demonstrated the effects of an increasing number of cycles at a constant pressure to which the polysaccharide was subjected. The molecular weight decreased from 904 kDa before size reduction to 290 kDa after 6 passes at 10 000 psi. Table 4.19 details the increase in elution time and hence the decrease in size dependant on the number of passes through the system. Molecular polydispersity was seen to increase with increasing number of passes which was in agreement with the findings of the Pn6B study. The results in Figure 4.26 also illustrated that the area under the curve remained constant and there was no apparent loss in molecular mass irrespective of the number of passes the sample was exposed to. This was expected using the microfluidizer processor as the interaction chamber has a very small void volume and the system loop is also of low volume, thus losses should be low.

As with Pn6B, the molecular weight of the polysaccharide was not reduced to within the desired range. By increasing the amount of times that the solution is passed through the machine, it is the polydispersity, and not the size, of the polysaccharide that changes. Thus a change in the pressure applied throughout the microfluidizer was increased to determine whether it would elicit a decrease in the polysaccharide size. The pressure was increased to 16 000 and to 22 000 psi, and the sample was subjected to 3 and 4 passes through the instrument. The reduction in molecular weight of this sample is shown below in Table 4.20.

Table 4.20. Summary of the changes in variables and the resultant change in molecular weight for Pn14.

Initial molecular weight (kDa)	Pressure (psi)	Number of passes	Final molecular weight (kDa)	Size reduction
904 kDa	10000	2	639	1.4 fold
		4	509	1.8 fold
		6	290	3.1 fold
	16 000	3	271	3.3 fold
		4	238	3.8 fold
893 kDa	22 000	3	192	4.7 fold
		4	173	5.2 fold

With a pressure of 16 000 psi, a size reduction to under 200 kDa was not achieved. The increase in pressure to 22 000 psi was able to reduce the size of Pn14 to 192 after 3 passes and 173 kDa after 4 passes.

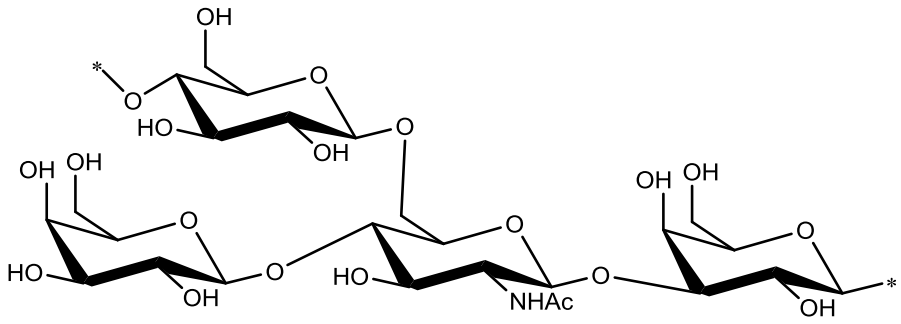

Figure 4.27. Structure of Pn14.

The structure of Pn14 is depicted in Figure 4.27. The Pn14 microfluidized samples were less viscous than the native polysaccharides and yielded well–resolved NMR spectra, Figure 4.28, containing the same proton and carbon resonances as the parent (full length) polysaccharide, indicating that microfluidization had no impact of the structure of Pn14 saccharide. Less CWPS and no peak corresponding to the acetate buffer could be detected in the microfluidized spectrum as ultrafiltration was performed after microfluidization. A single peak at 2.05 ppm in the proton spectrum was identified as the *N*–acetyl peak from the *N*–acetylglucosamine (GlcNAc) saccharide residue. It was presumed that the 4 peaks would be seen in the anomeric region of the NMR spectrum due to the four saccharide residues found in Pn14. This, however, was not the case as only three clear signals could be seen. These three peaks at 4.75, 4.50 and 4.40 were identified as the anomeric protons of GlcNAc, a mixture of one Gal and the Glc residue and the remaining Gal residue respectively. Confirmation of the four saccharides was determined with the HSQC spectra recorded in Figure 4.29.

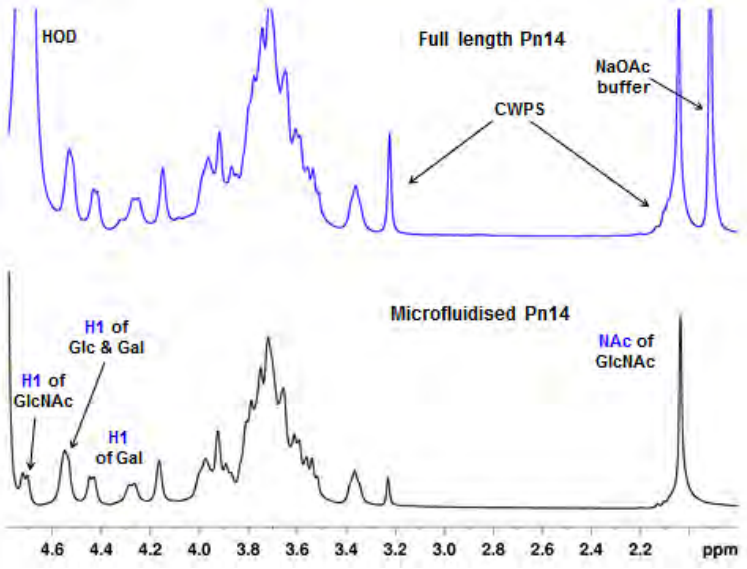

Figure 4.28. ^{1}H NMR analysis of Pn14 a) full length and b) microfluidized.

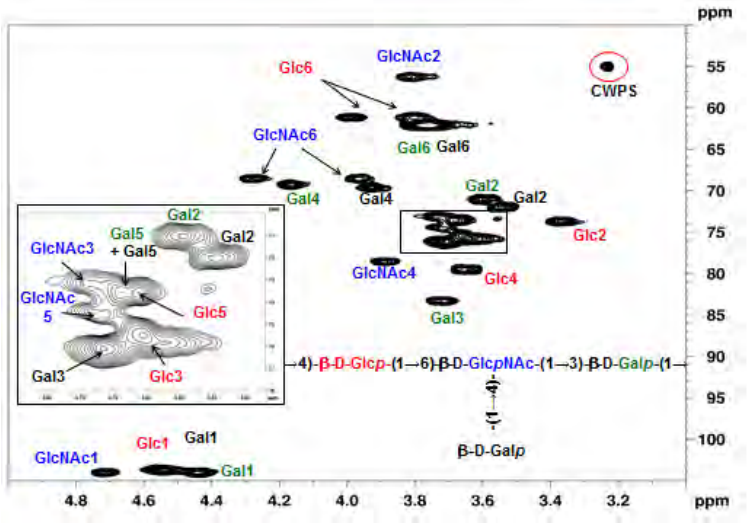

Figure 4.29. Expanded $^{1}H–^{13}C$ HSQC analysis of Pn14.

4.2.3.3 Pn1

Pn1 PS, that was fermented and purified at The Biovac Institute was solubilised in water at a concentration of 5 mg/ml and loaded into the microfluidizer reservoir. Following the experience gained from Pn6B and Pn14 investigations, Pn1 was exposed to a high pressure of 20 000 psi for a maximum of 4 passes. Samples were taken after 3 and 4 passes and analysed on SEC–HPLC.

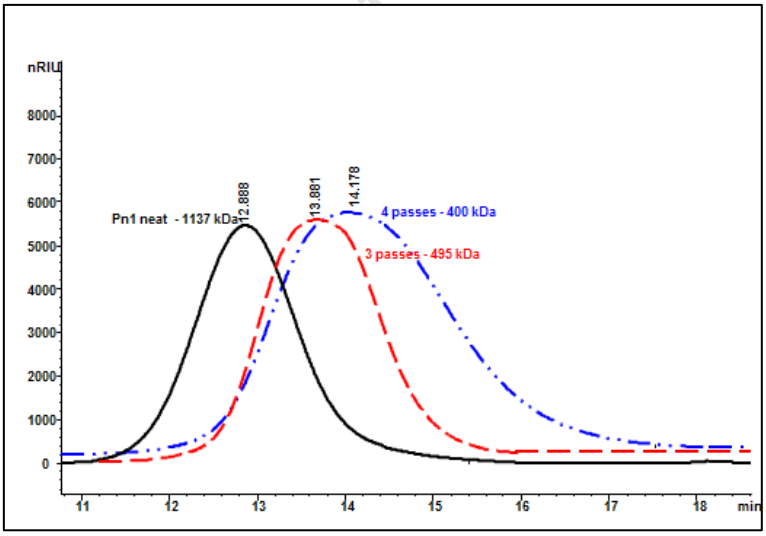

Figure 4.30. SEC–HPLC RID chromatograms of Pn1 microfluidization (20 000 psi) of three (red) and four (blue) passes. A Pn1 (full size) chromatogram is shown (black) for reference.

As seen in both Figure 4.30 and Table 4.21, a 2.8 fold decrease in molecular weight from 1137 kDa to 400 kDa occurred after 4 passes at 20 000 psi. The size reduction after 4 passes was within the required molecular weight of 400 kDa.

Table 4.21: Microfluidization variables resulting in molecular weight changes in Pn1.

Initial molecular weight (kDa)	Pressure (psi)	Number of passes	Retention time (min)	Final molecular weight (kDa)	Size reduction
		0	12.888	1137	–
1137	20 000	3	13.881	495	2.3 fold
		4	14.178	400	2.8 fold

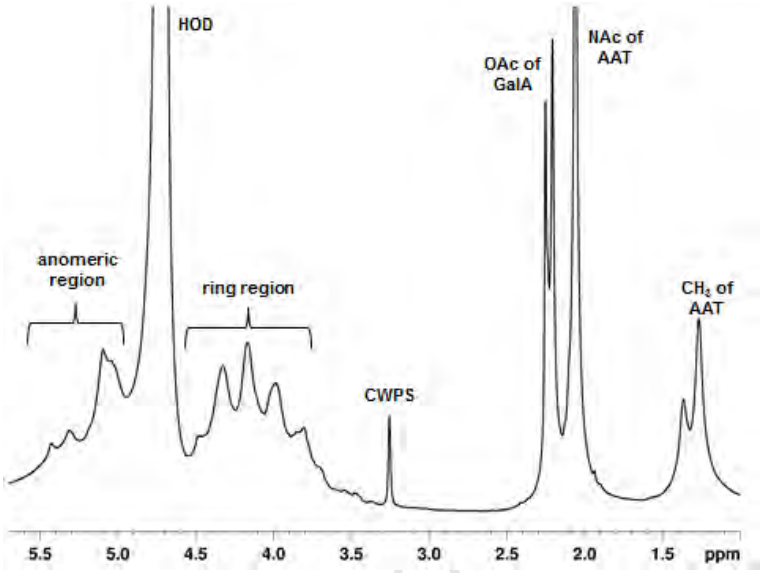

Figure 4.31. ^{1}H NMR spectrum of microfluidized Pn1.

The proton NMR spectrum was recorded for the microfluidized Pn1 (Figure 4.31) and a comparison was made with a reference Pn1 PS (a full set of spectra can be found in Chapter 3, Section 3.5). The *O*–acetyl signals at 2.2 ppm were present, as well as the *N*–acetyl peak at 2.05 ppm. Three anomeric signals corresponding to the H1 of the ATT (amino) saccharide as well as the two GalA residues could be seen at approximately 5.0 ppm. As with the previous samples, a peak at 3.23 ppm corresponded to the CWPS. The methyl peak of the amino saccharide at 1.3 ppm along with the *O*– and *N*– acetyl peaks confirm that Pn1 had not changed in any way after sonication. HSQC (not shown) confirmed the structural identity of the polysaccharide.

4.2.4 Consistency

Pn1 was used to determine consistency of the microfluidization process. Three different batch samples of Pn1 were exposed to 22 000 psi for four cycles. The results are summarised in Table 4.22.

Table 4.22: Results for 3 batches of Pn1 before and after microfluidization at 22 000 psi for 4 cycles.

Pn1 batch	Before Microfluidization		After Microfluidization		
	Retention time (min)	Molecular size (kDa)	Retention time (min)	Molecular size (kDa)	Size reduction
1	12.723	1305	14.497	320	4.1 fold
2	12.888	1120	14.339	357	3.1 fold
3	12.847	1162	14.260	377	3.1 fold

From the table it can be seen that microfluidization can produce consistent size reduction from 1100 – 1305 kDa to achieve sizes of between 320 and 380 kDa using the same microfluidization conditions.

4.2.5 Summary

Size reduction using sonication was achieved for two polysaccharides. The experiments with HA demonstrated that the degree of depolymerisation could be controlled by sonication conditions such as time or power output. For HA, a decrease a 40 – 60 fold reduction was achieved with a power output of over 100 kJ. This proof of concept was applied to Pn1 to yield a decrease in size of 6.7 – 10.8 fold.

Size reduction using microfluidization was achieved for three different pneumococcal polysaccharides. Investigations with Pn6B and Pn14 showed that an increase in pressure, rather than an increase in the number of passes through the microfluidizer, produced an increase in the size reduction. For Pn1 to achieve a reduction in size as specified, it was determined that 22 000 psi was required. Pn1 PS from three different batches (and hence three different molecular weights) was subjected to the same conditions in order to determine consistency. A size reduction to less than 400 kDa was achieved. A comparison of the reduction in size between the two techniques is detailed for Pn1 in Table 4.23.

Table 4.23. Comparison of size reduction between sonication and microfluidization for pneumococcal serotypes 6B and 1.

Polysaccharide	Sonication	Microfluidization
Pn1	6.7 – 10.8 fold	2.3 – 2.8 fold

A simple and general fragmentation method was developed using mechanical means that has been applied to a variety of polysaccharides irrespective of their chemical structure. Size reduction using methods such as sonication and microfluidization, described above, have been shown to be successful in creating polysaccharide fragments for conjugation. The polysaccharides were analysed by chromatographic and spectroscopic means to determine that the structural integrity was maintained. No epimerization was seen in any of the samples. Table 4.24 compares the two techniques.

Table 4.24. Comparison of sonication and microfluidization.

	Sonication	Microfluidization
Polysaccharide recovery	√	√
Scalability	X	√
Polydispersity	√	X
Degree of size reduction	√	X
Preservation of integrity	√	√
Control	X	√
GMP	X	√
Time	X	√

*a tick is indicative of a superiority, a cross indicates an inferiority

Polysaccharide recovery as well as the integrity of the samples is maintained with both techniques. The advantages of the sonicator are that the polydispersity of the sample is maintained throughout size reduction and much smaller sizes are achievable. Due to the shedding of metal particles on the sonicator probe, the sonication results are not repeatable and it is therefore not able to be used in a good manufacturing practice (GMP) environment. The control and consistency of the microfluidizer as well the scalability and use in a GMP process makes the microfluidizer the preferred method.

CHAPTER 5. PROTEIN DERIVATIZATION FOR CONJUGATION

A carrier protein is a protein used for coupling with saccharides or peptides that are not sufficiently large or complex on their own to induce an immune response and produce antibodies [120]. Ideally, a carrier protein induces a strong helper effect to a conjugated B cell epitope without inducing an antibody response against itself. Many proteins can be used as carriers and are chosen based on safety, immunogenicity, solubility, and availability of useful functional groups through which conjugation with the desired molecule can be achieved [120, 175, 390].

There are many suitable proteins available that can function as carrier proteins. The earliest and most widely used group of proteins are the bacterial toxoids which are toxins that have been altered either by chemical or genetic means to be non–toxic. Proteins can be isolated from natural sources, or produced by recombinant or synthetic means. Inactivating a toxic protein, which could be as simple as substituting one amino acid in the sequence for another or chemically inactivating the toxin with formaldehyde or heat, provides a non–toxic protein that retains its interactive binding capacity and effectiveness [391-395]. Examples of chemically inactivated bacterial toxins include; diphtheria toxoid (DT), tetanus toxoid (TT), and the genetically inactivated cross–reactive material CRM_{197}. Bacterial outer membrane proteins such as outer membrane complex C (OMPC) (derived from *Neisseria meningitidis* b) and pneumococcal adhesion protein (PsaA) can also be used. In general the albumin protein class, consisting of ovalbumin, human serum albumin (HSA), bovine serum albumin (BSA), could be used as protein carriers although issues with autoimmune responses have resulted in this class of proteins only being used in laboratory testing. Carrier proteins need to be non–toxic, non–reactogenic and should be available in large amounts at high purity [390, 396-398].

5.1 Background to derivatization strategies

Whilst the concept of attaching saccharides to proteins was first developed in 1929 by Avery and Goebel [109, 110] whereby *p*–aminophenol β–glucoside and *p*–aminophenol β–galactoside were synthesised and conjugated to serum albumin, it took until 1980 before Schneerson *et al*. [114] made use of this technology to prepare Hib conjugates by first derivatizing four different proteins, BSA, HSA, hemocyanin and DT with a 6 carbon spacer adipic acid dihydrazide (ADH) in the presence of 1–[3–(dimethylamino)propyl]–3–ethyl carbodiimide hydrochloride (EDC) (Table 5.1) and subsequently chemically linking the derivatized proteins to the PRP capsular polysaccharide. The polysaccharide was also activated as most saccharides do not have the necessary functional groups (aldehydes,

carboxyl groups) to form direct, covalent linkages with the amino groups of the proteins. While the conjugation was successful, the conjugate showed solubility problems, and hence this method was modified in 1986, so that the polysaccharides (Hib and pneumococcal serotype 6A) were first activated with the addition of cyanate groups on the hydroxyls of the saccharide followed by conjugation to TT (not derivatized) with the addition of ADH in the presence of EDC [115]. This modification (using non derivatized TT and activating *in situ* with the activated polysaccharide) improved the conjugation efficiency and the stability of the product. Derivatization of the carboxyls on the carrier protein to hydrazides is needed for a number of reasons. Firstly, the hydrazide groups have a lower pKa (pKa = 4 – 5) than the lysine amino groups (pKa = 10.5) [390, 399] which makes the protein more reactive at the neutral/mildly acidic conditions used in conjugations, this pH is also required to prevent the protein from aggregating and cross reacting with other protein molecules. Secondly, toxoiding a protein blocks the amino groups; the toxoids would therefore contain a limited number of lysine groups available for conjugation [390].

Table 5.1. List of reaction conditions for derivatization of protein.

Author	Protein	ADH	EDC	pH	Reaction time (hr.)	Temp.	Dialysis
Schneerson *et al.*[114]	BSA, HSA, DT	3.45 (w/w)	0.1, 0.3, 0.6 (w/w)	4.7	3	RT	0.2 M NaCl,
Lee, Frasch [390]	TT	0.42 M*	20 mM	6.5	4	RT	NaCl/Na_2CO_3 (pH 10.5)

*Hydrazine could also be used at the same concentration as ADH.

Lee and Frasch, in 2005, modified the derivatization procedure to use with the tetanus toxoid protein by adjusting the concentration of the reagents, the pH as well as the dialysis conditions [390].

The novelty of the Schneerson *et al.* publication, modified by Lee and Frasch in 2005 is based on derivatization of the carboxylic groups on acidic amino acids of toxoid protein carriers ADH (or hydrazine) in the presence of EDC to form hydrazide–derivatized proteins (Figure 5.1) with the reaction conditions compiled in Table 5.1 [114, 390]. This approach to derivatizing proteins relies on the carbodiimide molecule reacting with the carboxyl group of the aspartic and glutamic acids on the protein. The electron deficient carbon atom in EDC is attacked by the carboxylate and a highly reactive *O*–acylisourea is formed, which reacts with nucleophiles, such as the hydrazine functional grouping on ADH or hydrazine itself, to form a hydrazone bond. If no nucleophile is present, the carbodiimide will rearrange to form a stable *N*–acylurea. The reaction is performed in aqueous solutions at room temperature, which is especially important for manipulations with biological molecules. An acidic environment is needed to catalyse the reaction, presumably through the protonation of the carbodiimide

nitrogen. In this acidic environment, coupling to hydrazide is advantageous over primary amines due to the low pKa of hydrazides in comparison to other primary amines.

In the patent by Lee and Frasch, after derivatization, the reaction is quenched with sodium hydroxide to hydrolyse any unreacted EDC or its stable by–product, *N*–acylurea [400]. EDC–catalysed proteins have a propensity to polymerize or precipitate: this is due to the change of the protein's isoelectric point (pI) after derivatization. Proteins carry positive, negative and zero net electrical charges depending on the pH of the surrounding environment. The net charge of a protein is the sum of all its positive and negative charges which are determined by the acidic and basic side chains of the amino acids of the protein. If the protein contains more acidic than basic groups the isoelectric point of the protein is found at a low pH value, hence the protein is classified as acidic. A basic protein will thus contain more basic groups and will therefore have a higher pI. Most pIs of proteins are found in the pH range of 4 – 7. By derivatizing the carboxyl groups on the protein with hydrazide groups, the pI and hence the solubility of the protein will change.

This aggregation and subsequent precipitation of the protein is largely due to its pH environment. Through controlling the pH by buffer exchanging the solution after derivatization, the derivatized protein will remain soluble and stable until needed for conjugation [400]. The derivatized protein is diafiltered against a sodium carbonate/sodium chloride (Na_2CO_3/NaCl) buffer at pH 10.7 using a 50 KDa MWCO membrane; the high pH keeps the protein (in this case, TT) soluble and stable for conjugation. The diafiltration step also removes residual hydrazine/hydrazide, EDC break–down products and salts which would all affect the pH of the solution.

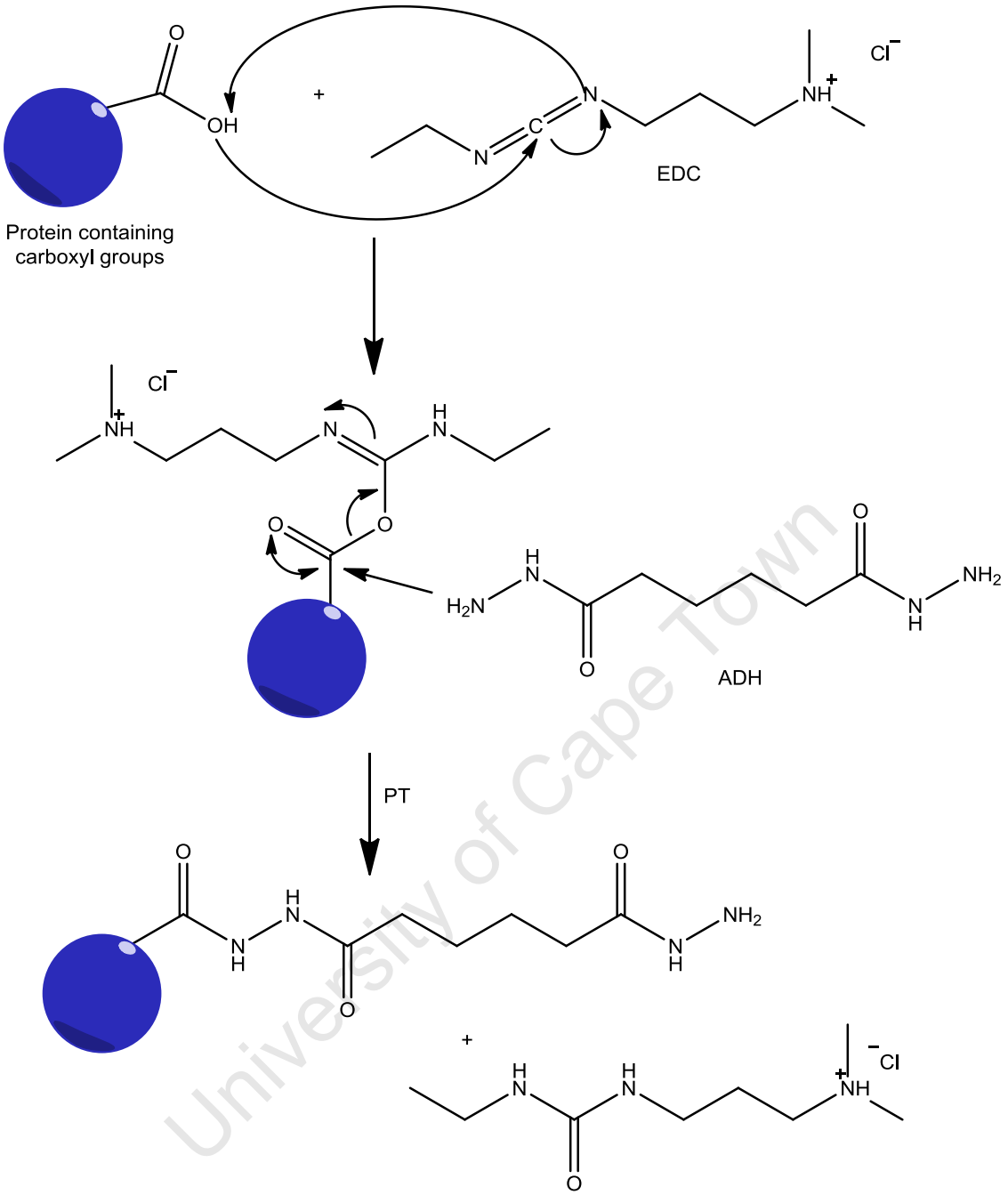

Figure 5.1. Schematic representing the mechanism of protein derivatization.

Table 5.2. Licensed conjugate vaccines that make use of DT, TT, OMPC or CRM_{197} as protein carriers [175, 375, 386, 390, 401-405].

Serotype	Licensed Name	Date licensed	WHO prequalified [406]	Protein	Manufacturer
Haemophilus influenzae type b					
	ProHIBIT®	1987	–	DT	Sanofi Pasteur
	HibTITER®	1988	–	CRM_{197}	Pfizer
	PedvaxHIB®	1989	2003	OMPC	Merck
	Vaxem–Hib®	1990	1997	CRM_{197}	Novartis
	ActHIB®	1993	1998	TT	Sanofi Pasteur
	Quimi–Hib®	2003 (Cuba)	2010	TT	Heber Biotech
	Sii HibPro®	2007 (India)	2008	TT	Serum Institute of India Ltd
Combination Hib and meningococcal					
C	Menitorix®	2009	–	TT	GlaxoSmithKline
C, Y	MenHibrix®	2012	–	TT (Hib)	GlaxoSmithKline
Meningococcal					
C	Meningitec®	1999 (UK)	–	CRM_{197}	Pfizer
C	NeisVac–C®	2000 (UK)	–	TT	Baxter International*
C	Menjugate®	2000 (UK)	–	CRM_{197}	Novartis
A	MenAfriVac®	2009 (India)	2010	TT	Serum Institute of India Ltd
A, C, W–135, Y	Menactra®	2005	–	DT	Sanofi
A, C, W–135, Y	Menveo®	2010 (FDA)	–	CRM_{197}	Novartis
A, C, W–135, Y	Nimenrix®	2012 (EU)	–	TT	GlaxoSmithKline
Pneumococcal					
4, 6B, 9V, 14, 18C, 19F, 23F	Prevnar®	2000 (FDA)	–	CRM_{197}	Pfizer
1,4,5,6B,7F,9V,14,18C,19F, 23F	Synflorix®	2009	2010	Protein D, TT–18C, DT–19F	GlaxoSmithKline
1, 3, 4, 5, 6 (A&B) 7F, 9V, 14, 18C, 19(A&F), 23F	Prevnar13®	2010 (FDA)	2010	CRM_{197}	Pfizer

*Used under licensed for distribution by GlaxoSmithKline.

5.2 Protein carriers in conjugate vaccines

Of all the protein carriers mentioned, only five; TT, DT, CRM_{197}, OMPC and Protein D have been licensed for use in vaccines (Table 5.2) [407, 408]. Pneumococcal, meningococcal and Hib licensed conjugate vaccines all make use of protein carriers either in their native or derivatized form.

5.2.1 Hib vaccines

A summary of the four licensed Hib conjugate vaccines is given in Table 5.3 and are explained in the subsequent sections.

Table 5.3. Characteristics of the four Hib conjugate vaccines. Modified from Eskola [409].

	PRP-DT	**PRP-TT**	**PRP-CRM_{197}**	**PRP-OMPC**
Carbohydrate length	sized	Full sized	Oligosaccharide	Full sized
Carbohydrate dose (µg)	25	10	10	15
Protein	DT	TT	CRM_{197}	OMPC
Protein dose (µg)	18	24	25	250
Conjugation chemistry	ADH/EDC	ADH/EDC	reductive amination	bigeneric space

5.2.1.1 Native protein carriers

The first conjugate vaccine was licensed in 1987 by Sanofi Pasteur to protect against *Haemophilus influenzae* type b (ProHIBIT) and employed DT as the carrier protein [390, 409]. This was followed in 1 88 by Pfizer's (then Wyeth) conjugate HibTITE which employed CRM_{197} as the carrier protein. HibTITER used the reductive amination conjugation method to couple the polysaccharide of Hib directly to the CRM_{197} protein. Sanofi Pasteur released another Hib conjugate vaccine onto the market in 1993 where they changed the protein carrier from DT to TT in ActHIB. This conjugate vaccine employed the modified Robbins conjugation chemistry where the ADH spacer was first added to the polysaccharide followed by conjugation with the underivatized TT in the presence of EDC. This vaccine improved the conjugation efficiency as well as the product stability compared to the Hib–DT conjugate [390, 409].

5.2.1.2 Derivatized protein carriers

Merck licensed their Hib conjugate vaccine, Pedvax, in 1989 where OMPC was used as the carrier. Both the polysaccharide and the protein were derivatized separately before conjugating the two via a bigeneric spacer, i.e. a spacer molecule that is made from parts of the derivatized protein and polysaccharide (Figure 5.2). The protein was derivatized with a thioether (*N*–acetylhomocysteine thiolactone) and the polysaccharide was separately

activated with carbonyldiimidazole to form an imidazolylurethane (I) which was susceptible to nucleophilic substitution with a 1,4–butanediamine producing a stable urethane with pendant amine is produced (II). The final activation step was to bromoacetylate the polysaccharide with *p*–nitrophenyl bromoacetate before conjugation under nitrogen (6hr, RT) to the derivatized protein could be achieved [217, 410].

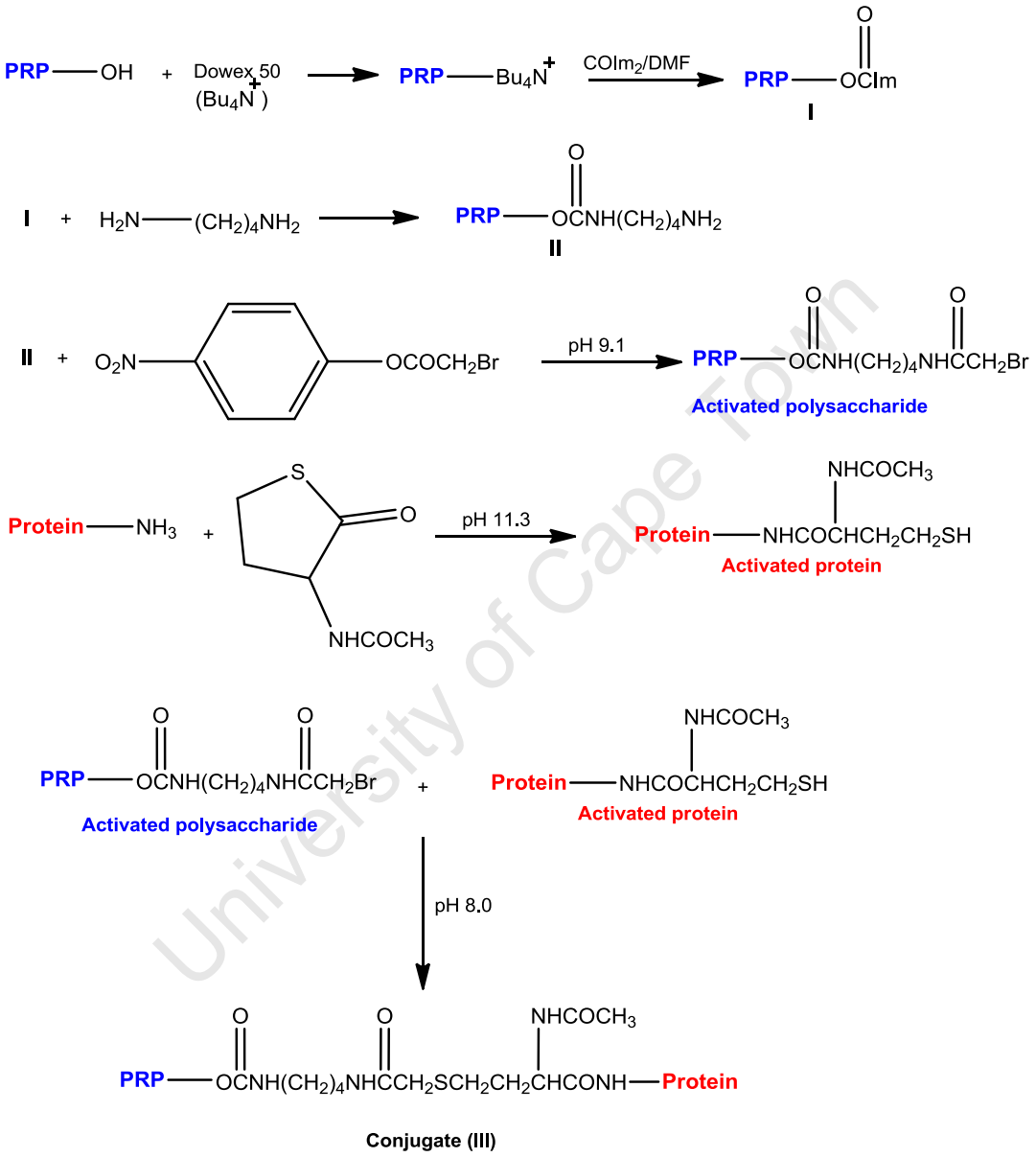

Figure 5.2. Modified representation of the formation of a bigeneric spacer conjugate as used in the conjugate vaccine against Hib (Merck) [410].

Comparison studies on the four main Hib conjugates (Table 5.4) showed that the ProHIBIT conjugate (PRP–DT) was found to be the least immunogenic of the four vaccines [73, 411-413] however, it was found to be highly immunogenic in Finnish children (7 – 24 months old) [414]. The Merck Pedvax vaccine that used OMPC as the carrier protein, was found to stimulate the highest antibody concentration of the four with a 94 % reduction of Hib related

diseases after just a single dose in infants [411, 413]. A study by Schlesinger and Granoff compared the TT, CRM_{197} and OMPC conjugated vaccines and showed that the CRM_{197} vaccine elicited the most antibodies, followed by the vaccine with TT as the carrier protein with the least antibodies against the OMPC conjugated Hib vaccine [415], this was confirmed in 1995 by Lucas and Granoff in rat models where the CRM_{197} vaccine showed a 10–fold higher bactericidal and protective activity than Merck OMPC vaccine [412, 416]. The Hib–TT vaccine gave the highest mean antibodies after 3 doses as well as a greater booster response and higher antibody concentrations in children 2.5 years after immunisation [417].

Table 5.4. Immunogenicity comparison of Hib conjugate vaccines in children at 7 and 15 months (Finland) [409].

Vaccine	GMT (µg/ml)	
	7 months	15 months
PRP–DT	0.68	33.73
PRP–TT	10.59	29.26
PRP–OMPC	1.68	11.16
PRP–CRM_{197}	4.12	58.29

This study showed that it is not only the carrier protein, the type of conjugation chemistry, or the size of polysaccharide that is important in producing an immunogenic conjugate vaccine, rather a combination of many different factors; however there is a clear superiority of the vaccines using TT and CRM_{197} as the carrier proteins.

5.2.2 Meningococcal vaccines

5.2.2.1 Native protein carriers

The second type of conjugate vaccines that employ DT, TT and CRM_{197} as carrier proteins are those that protect against disease caused by *Neisseria meningitides.* In the late 1990s, two CRM_{197} conjugate vaccines, Meningitec, (Wyeth Pharmaceuticals) and Menjugate, (Novartis Vaccines) were developed against meningococcal disease caused by serogroup C. Baxter International licensed the NeisVac–C in 2000 that made use of TT as the protein carrier, also against serogroup C. Both Meningitec and NeisVac–C made use of the same general conjugation chemistry where the polysaccharide was first activated using periodate oxidation and with subsequent coupling directly onto the carrier protein via reductive amination without the need for derivatization [375]. However NeisVac–C was first de–acetylated as it was found that the de–*O*–acetylated conjugate produced higher antibody titres than the acetylated conjugate [418-420]. Menjugate followed a different path with the use of a spacer molecule (*N*–hydroxysuccinimidodiester) between the activated polysaccharide (via acid hydrolysis) and the CRM_{197} protein molecule [375].

A tetravalent vaccine against meningococcal serogroups A, C, W–135, and Y conjugated to DT was first licensed in 2005 (Menactra). CRM_{197} was used in the meningococcal vaccine licensed in 2010 by Novartis (Menveo) and Nimenrix, the tetravalent meningococcal conjugate vaccine licenced by GlaxoSmithKline in 2012 contains TT as the carrier protein. As Menactra was the first licensed tetravalent vaccine, both Menveo and Nimenrix used Menactra as the comparison for non–inferiority in order to be granted licensure.

Non–inferiority was achieved for Menveo in comparison to Menactra where all four serogroups showed higher immunogenicity levels in adolescents and adults when vaccinated with Menveo [421, 422]. The immunogenicity of Nimenrix was compared to Menactra in terms of the percentage of subjects that produced antibody titres above a certain level, with three of the serotypes (MenA, MenW–135 and MenY) showing a superiority with Nimenrix with no statistical difference seen with MenC when compared to Menactra [423]. The comparison, in terms of immunogenicity, of all three tetravalent conjugate vaccines has not yet been published.

5.2.2.2 Derivatized protein carriers

To date there is only one commercially available monovalent conjugate vaccine against meningococcal serogroup A. This vaccine made use of TT as the protein carrier and received WHO prequalification in 2010. The protein was first derivatized with hydrazine in the presence of 20 mM EDC and 0.1 M 2–morpholinoethanesulfonic acid (MES) at a pH of 6.5 [404].

5.2.3 Pneumococcal vaccines

5.2.3.1 Native protein carriers

Until the introduction of Protein D, CRM_{197} held the market share as a protein carrier for *Streptococcus pneumoniae* conjugate vaccines. In 2000, Pfizer developed the first conjugate vaccine protective against *Streptococcus pneumoniae*, Prevnar (PCV7). PCV7 is a conjugate vaccine that consists of the capsular polysaccharide of seven different serotypes individually conjugated to CRM_{197} via reductive amination. In 2009, GSK licensed a 10–valent conjugate vaccine with additional serotypes 1, 5 and F to Pfizer's seven valent. All but one of the serotypes was conjugated to the native Protein D via polysaccharide activation with CDAP [386]. The following year, Pfizer licensed the 13-valent vaccine (serotypes 3, 6A and 19A additional to the 10 serotypes of GSK) Again, CRM_{197} was the choice for protein carrier and the reductive amination conjugation methodology was used [175].

5.2.3.2 Derivatized protein carriers

Of the 10 serotypes found in the GSK conjugate vaccine, only serotype 18C was conjugated to TT (all other serotypes were conjugated to Protein D except 19F which was conjugated to DT). The TT was first derivatized using the ADH/EDC procedure and conjugated to Pn18C using CDAP technology. TT was chosen as the carrier protein for 18C instead of Protein D as the immune response was shown to be much stronger in mice with TT as the protein carrier compared to Protein D (for the same reason, Pn19F was conjugated to DT) [164].

5.2.4 Immune response interference among carrier proteins

In recent years, the efficacy of TT as a protein carrier has been brought into question. TT is itself used as a vaccine against tetanus (lockjaw) as well as being used as a carrier protein in vaccines for Hib, MenC, and pneumonia. Its frequency of use and large dosage amount may overload the immune system, which could result in a higher occurrence of adverse reactions due to pre–existing antibodies in targeted populations [160, 397, 407, 424-426]. Simultaneous immunisations of PRP–TT and pneumococcal–TT vaccines were tested following the standard American infant schedule. As the dosage of the pneumococcal vaccine was increased, the immune response to the Hib vaccine showed decreasing levels that suggested immune interference of the polysaccharide, possibly because of the protein carrier [426].

TT and CRM_{197} were compared for safety and immunogenicity in 2 year old children in the form of a tetravalent pneumococcal conjugate vaccine (making use of serotypes 6A, 14, 19F and 23F). The vaccines used identical conjugation chemistries (reductive amination), and the protein to polysaccharide ratios remained the same at 0.50 ± 0.18. The final vaccine formulation consisted of 50 µg of the carrier protein and approximately 20 µg of total polysaccharide. The children were injected with a mixture of the two vaccines (25 µg of each protein) or either of the two vaccines (containing 50 µg of the carrier). This was followed 2 months later by an identical secondary injection. Sera were taken before each injection as well as 1 month after the second injection and the ELISA IgG serum responses were determined. The results showed that the differences were based on serotypes rather than protein carrier, however the children immunised with the mixture of the two carrier protein vaccines showed higher ELISA responses than those immunised with a single protein carrier [426].

In order to develop an affordable and effective Pn1 conjugate vaccine a suitable protein carrier would have to be determined. The objective of this investigation was to activate a protein carrier, that, when conjugated to pneumococcal serotype 1, would form a conjugate vaccine that could be tested *in vivo* in an animal model. The proteins investigated were BSA,

TT, CRM_{197} and pneumolysoid (PLD). The BSA protein was used as a model carrier protein to investigate whether the conjugation methods were successful as it was readily available, cost effective and of a similar size to the CRM_{197} and PLD proteins. Due to the potential interference of the immune response, TT was investigated as a carrier protein for use in a monovalent conjugate vaccine. As PCV7, PCV13 and PCV15 (in development) make use of CRM_{197} as a carrier protein, conjugation methodologies would have to be performed with CRM_{197} to allow for a direct comparison with the commercially available multivalent vaccines. The added protection offered by PLD (described in Section 5.6) made it an attractive protein carrier to study as a carrier for pneumococcal conjugate vaccines. The relative molecular weights (Mw), number of carboxyls as well as the approximate isoelectric points of each protein investigated are compiled in Table 5.5.

Table 5.5. Comparison of proteins used in this study.

Protein	Molecular Weight (kDa)	Number of amino acid residues	Number of carboxyl groups*	pI (approximate)
BSA	67	606	99	4.7
TT	150	1314	160	5.8
CRM_{197}	58	535	65	5.8
PLD	53	471	64	5.2

*Carboxyl groups from aspartic acid and glutamic acid.

The general derivatization method was modified to suit each of the four proteins tested. The derivatization levels were investigated as each protein would have an optimal level of derivatization for successful conjugation to occur. It was thought that the smaller protein carriers would not have to be derivatized to the higher levels of the larger proteins as too many derivatization sites would result in cross reactions on the protein that would decrease the solubility of the protein in aqueous solutions. Before derivatization, the isoelectric points of the carrier proteins are all below the pH used in subsequent conjugations however derivatization leads to an increase in the pI of the protein. This level of derivatization and ensuing pI change must be monitored as solubility will become an issue if the pI of the derivatized protein corresponds to the pH at which conjugation takes place.

5.3 Bovine Serum Albumin

Bovine serum albumin (BSA) belongs to the class of serum proteins called albumins, which make up about half of the protein in plasma and are the most stable and soluble proteins in plasma. BSA has a molecular weight of 67 kDa and contains 99 carboxyl groups and it is these that are targeted in the derivatization procedure [427, 428].

BSA is one of the most commonly used protein carriers in the laboratory due to its stability, low cost, wide availability and its non–reactivity in a wide range of biochemical reactions.

However, BSA has been known to cross–react immunologically with other serum albumin proteins (found in human serum) and thus is no longer used in vaccines [429-431]. Another reason for not using BSA in clinical trials and vaccines is due to the fact that most albumins are sourced from either human or bovine serum which presents regulatory concerns over blood borne contaminants (mycoplasma, viruses and prions). BSA is generally utilised as a model protein to set up immunoassays in the lab as well as to test the chemistry and biochemistry of a reaction.

According to literature, BSA has been used in conjugations in both its native, underivatized form as well as its ADH derivatized form. Table 5.6 details the reaction conditions used when derivatizing BSA with ADH and EDC. In 1980, Schneerson and Robbins derivatized different proteins, including BSA, with ADH in one of the first licensed uses of a protein carrier in vaccines when they conjugated the derivatized protein to Hib polysaccharide PRP. These conjugates showed an increase in immunogenicity in both mice and rabbits. The proteins were solubilised at a concentration of 25 mg/ml. To these solutions, ADH was added followed by varying concentrations of EDC. The reaction proceeded at room temperature for 3 hours at a constant pH of 4.7 ± 0.2. The derivatized protein was dialysed at 3 – 8 °C against 0.2 M NaCl [114, 432].

In 1997, Kossaczka *et al*. used ADH derivatized BSA as a protein carrier in the conjugation with the Vi polysaccharide of *Salmonella typhi.* Different EDC to protein ratios were tested for the derivatization of BSA but it was found that concentrations of EDC above 0.2 mg per mg of protein did not result in a higher final ratio of ADH to protein [433]. In 2000, the derivatization of BSA with ADH was again published, this time by Shafer *et al*. [434] This derivatized BSA was used to test the 1–cyano–4–methylaminopyridinium tetrafluoroborate (CDAP) conjugation methodology and conjugated to various polysaccharides.

Table 5.6. Hydrazide derivatization details for BSA.

Author	ADH (mg/mg protein)	EDC (mg/mg protein)	pH	Reaction time	Dialysis	Derivatization levels
Schneerson *et al*. [114]	3.45	0.1, 0.3, 0.6	4.7 ±0.2	3 hr.	0.2 M NaCl	n/a*
Kossaczka *et al.* [433]	3.5	0.1	4.9 –5.1	1 hr.	0.15 M NaCl	2.3
Shafer *et al.* [434]	1.8	0.96	5.5	overnight	saline	15.9

*Not available.

5.3.1 Derivatization of BSA

BSA was used as a model protein in developing a proof of concept to test the derivatization chemistry before it was applied to other proteins. BSA was first derivatized with ADH and EDC over a period of four hours and the derivatization levels measured as a percentage of the carboxylic acid substitution (% CS) using the TNBS colorimetric assay (Table 5.7). The derivatized protein was analysed on SEC–HPLC and compared to the native form as shown in Figure 5.3.

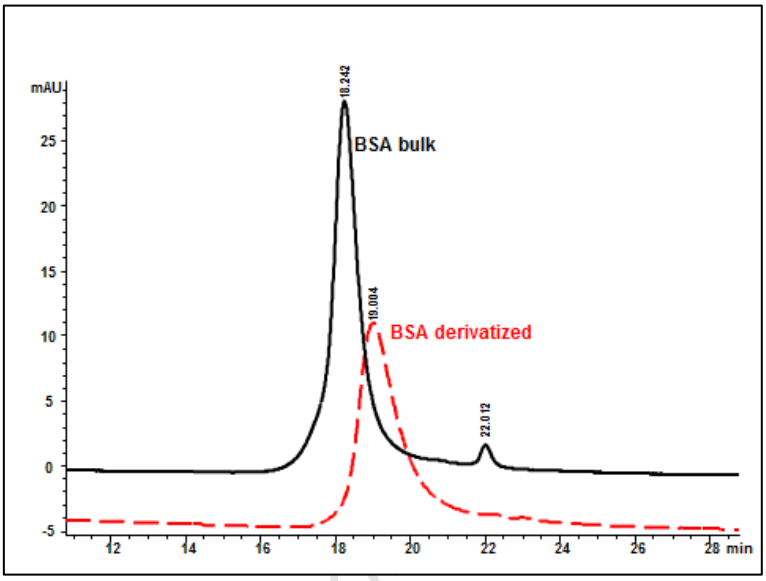

Figure 5.3. SEC–HPLC UV 280 nm chromatogram of BSA (black) and derivatized BSA (red).

A shift in retention time, for the derivatized BSA that eluted at 18.9 min was compared to that of the underivatized protein eluting an apparent smaller molecular weight protein at 18.2 min. It is hypothesised that the free hydrazide group from the ADH molecule interacted with the polyhydroxymethacrylate stationary phase of the columns, resulting in prolonged interaction and retention within the column, and hence a shift to an apparent lower molecular weight was observed.

Table 5.7. Summary of derivatization results of BSA with ADH.

Reaction	Reaction time (hr.)	Protein concentration (mg/ml)	Hydrazide concentration (mM)	Carboxylic acid substitution (%)
1	4	17.94	3.81	20
2	4	10.80	3.61	22
3	1.5	12.25	2.58	14

The pH of the derivatized protein was lowered to 6.5 to determine if the protein was stable at the pH used for conjugation. Aggregation occurred at this pH and was theorised to be due to over derivatization of the protein resulting in a shift of the protein's pI causing the protein to be insoluble at this pH. The derivatization levels of the protein were investigated to see if

lower levels of derivatization would prevent this precipitation occurring at the pH needed for conjugation. This lower level of derivatization was achieved by lowering the reaction time whilst keeping the reactant ratios the same.

By halving the reaction time from 3 hours to 1.5 hours, a decrease was seen in the levels of derivatization from 20 and 22 % to only 14 %. This showed that derivatization levels could be controlled to some effect by controlling the amount of time the reaction is allowed to proceed. However a linear relationship was not found between the levels of derivatization and the reaction time.

5.4 Tetanus Toxoid

Tetanus toxoid is a non–toxic, chemically detoxified (with formaldehyde) tetanus toxin. Tetanus toxin is produced from *Clostridium tetani* bacterium and is composed of 1314 amino acid residues and has a molecular weight of approximately 150 kDa [394]. The toxoid form has been shown to maintain a high degree of secondary and tertiary structure when compared to the native toxin [393]. There are 160 carboxyl groups from the aspartic and glutamic acid residues of the toxoid that are available for derivatization with ADH.

As tabulated in Table 5.2, TT has been used as a carrier protein in conjugate vaccines licensed for a variety of diseases. It has mainly been applied in its underivatized form, although vaccines against meningococcal and pneumococcal diseases have utilised derivatized tetanus toxoid in preparation of conjugates. Underivatized TT was used in the early 1980s by Beuvery *et al.* in the investigation into conjugate vaccines against meningococcal group C [435-437].

TT has been conjugated in its derivatized form as a protein carrier. In 2000, Pawlowski *et al.* used an alternative derivatization method for TT via a bromoacetylation pathway (Figure 5.4) with the *N*–hydroxysuccinimide ester of bromoacetic acid (0.7 mg ester/mg TT). The pH remained at 8.3 and the reaction proceeded for 2 hours at room temperature. This derivatized TT was conjugated to previously thiolated pneumococcal serotypes 14 and 23F [438].

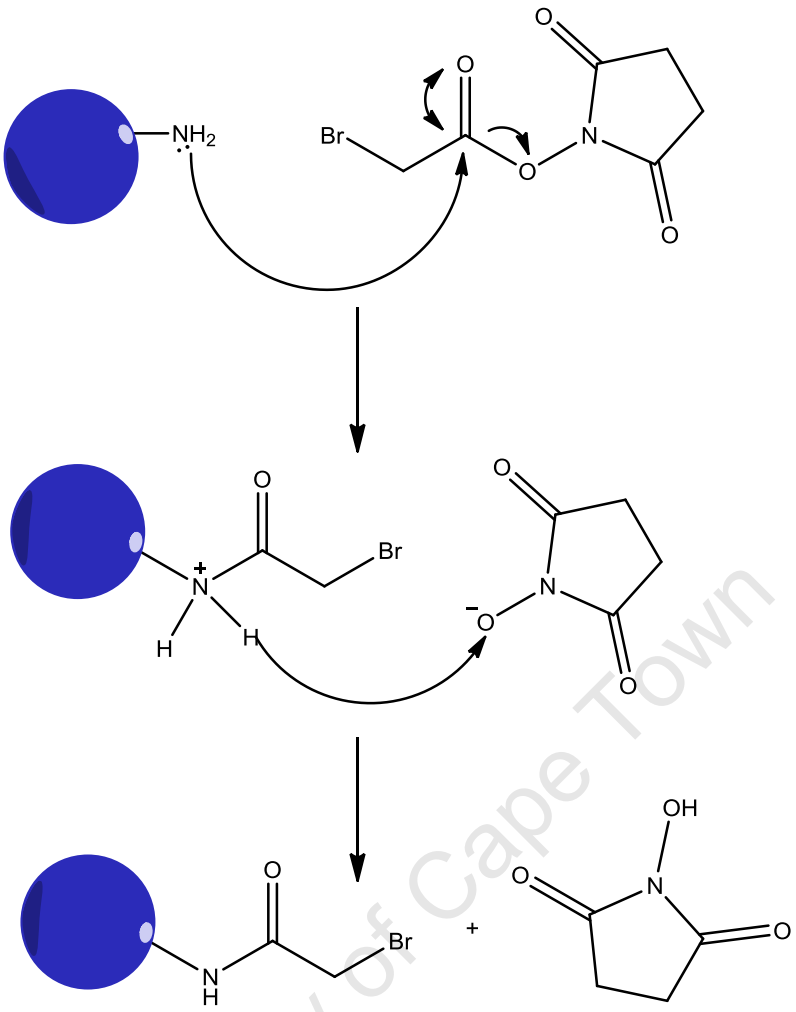

Figure 5.4. Alternative derivatization of TT, via bromoacetylation, described by Pawlowki *et al*. [438].

The majority of the conjugates that utilised derivatized TT as the carrier protein, summarised in Table 5.8, followed the method of Lee and Frasch [390]. The MenA vaccine, licensed in 2009, made use of this chemistry when TT was derivatized with hydrazine and EDC followed by conjugation to an oxidised MenA polysaccharide. GSK also made use of the Lee–Frasch method in their 10 valent pneumococcal vaccine; however it was modified by reacting the protein with ADH for an hour [386]. In 2007, Silveira *et al.* derivatized TT using the hydrazine technology, conjugated it to MenC polysaccharide using reductive amination and tested it in mice [439]. The conjugate gave a 10 to 20–fold rise in immunoglobulin G (IgG) response in mice compared to the pure polysaccharide.

Table 5.8. Reaction conditions for the derivatization of TT for use in conjugate vaccines.

Author	Source of hydrazide	EDC (mM)	pH	Reaction time (hr.)	Dialysis
Lee *et al*. [404]	Hydrazine (0.42 M)	20	6.5	4	30 mM NaCl, 3 mM Na_2CO_3 (pH 10.5)
Biemans *et al.* [386]	ADH (0.2 M)	20	6.2	1	n/a
Silveira et al. [439]	Hydrazine (0.42 M)	20	6.1	4	0.02 M PBS (pH 7.4)

5.4.1 Derivatization of TT

Results from the derivatization of BSA indicated that a decrease in reaction time led to a decrease in derivatization levels. This change in reaction time was applied to TT to determine if these results could be repeated. In previous studies, a 4 hour reaction time led to TT derivatization levels of between 18 and 23 % [440]. Reaction times were decreased from the usual 4 hours to 1.5 hours, before the reaction was quenched with NaOH. Post diafiltration (to remove excess ADH), hydrazide concentration and carboxylic substitution levels were assayed (Table 5.9) and chromatographic profiles were obtained before and after derivatization.

Table 5.9. Summary of derivatization results of TT with ADH.

Reaction time (hr.)	Protein concentration (mg/ml)	Hydrazide concentration (mM)	Carboxylic acid substitution (%)
4	9.26	2.06	21
4	15.81	3.11	18.6
4	17.49	4.26	23
1.5	17.40	1.75	13.4
1.5	17.49	3.07	16.6
1.5	23.48	4.02	16.2
1.5	27.84	4.75	16.1

The UV chromatogram illustrated a shift in retention time between the native and the derivatized TT (Figure 5.5). As with the derivatization of BSA, a shift to an apparent lower molecular weight compound occurred. The derivatization studies confirmed that decreasing the reaction time from 4 hours to 1 hour decreased the derivatization levels; however this decrease was not as large as the difference realised with BSA. Due to Pn1 containing both reactive amino and carboxylic functional groups, it was hypothesised that a lower derivatization level for TT would be more appropriate in order to minimize cross linking and subsequent precipitation.

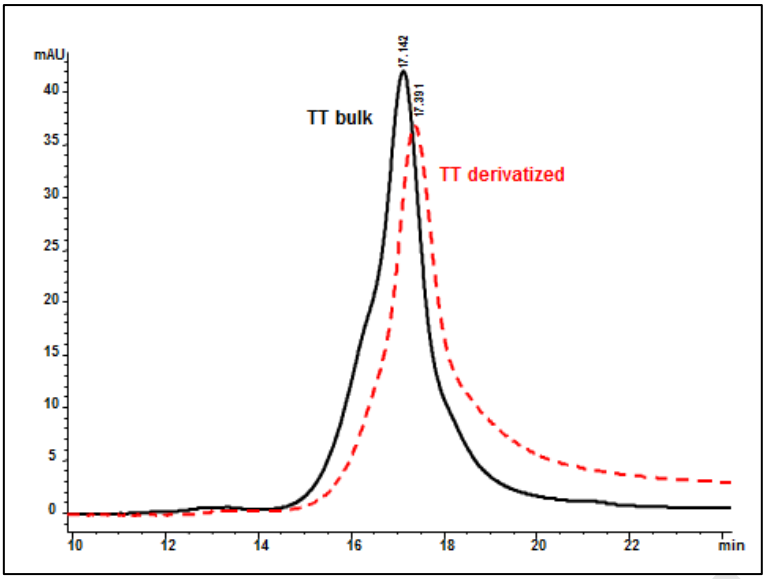

Figure 5.5. SEC–HPLC, UV 280 nm chromatograms of TT (black) and derivatized TT (red) in water.

5.5 CRM_{197}

Different mutant forms of the diphtheria toxin were isolated during the 1 0 's, including the cross–reactive material 197 (CRM_{197}). CRM_{197} is a non–toxic DT mutant that resulted from a single substitution of glycine to glutamic acid at position 52 in the amino acid sequence (Figure 5.6). CRM_{197} shows no enzymatic activity, is therefore nontoxic to humans, and is known to function as an exceptional carrier for polysaccharides in conjugate vaccines [407, 441]. CRM_{197} has a molecular weight of 58 kDa and contains 65 carboxyl groups available for derivatization with ADH [442].

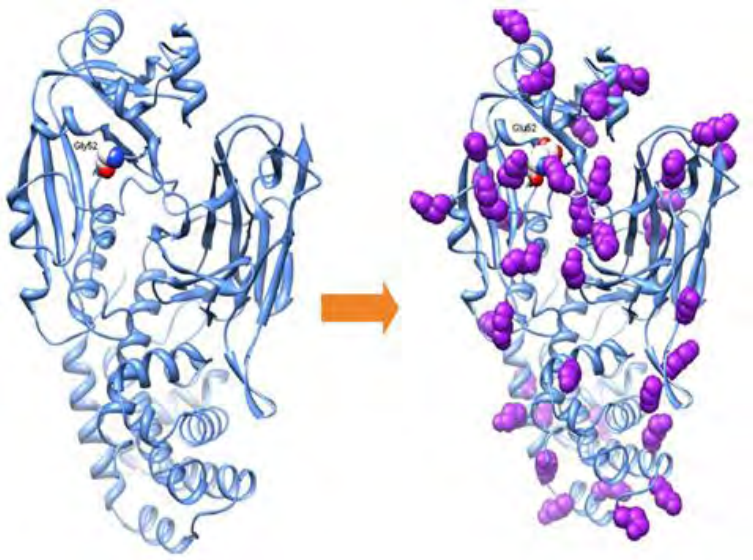

Figure 5.6. Structures of DT (left) and CRM_{197} (right). The accessible lysine residues are highlighted (purple spheres) for CRM_{197} that are available for conjugation. The mutation of the glycine residue in position 52 of DT to the glutamic acid residue at position 55 on CRM_{197} is also depicted [443].

As CRM_{197} is non–toxic, it escapes the need for chemical detoxification that is required for DT (TT is also detoxified, usually by formaldehyde). Chemical detoxification can cause extensive cross linking and epitope modification and may interfere with the immunogenicity of the vaccine [391, 392]. Since detoxification is not required, the lysine residues on the protein are accessible and therefore no derivatization is needed for successful conjugation. At present no conjugate vaccines have been licensed make use of derivatized CRM_{197}, however, as previously described, there are licensed vaccines that contain CRM_{197} as the carrier protein in its native form [443].

A conjugate vaccine against *Salmonella Typhi* under development uses derivatized CRM_{197} as the carrier protein. The derivatization was performed at a higher pH than used with TT in order to minimise protein precipitation, otherwise the method used to derivatize the protein was as per previously described [444].

As the main objective of the investigation was to compare the conjugation chemistries developed against the commercially available conjugate vaccines; a head to head comparison was to be performed. To reduce the number of variables in the comparison, the carrier protein should be kept constant. The decision to investigate the derivatization of CRM_{197} was due to the successful use of the protein in PCV7 and PCV13.

5.5.1 Derivatization of CRM_{197}

The known ADH/EDC method used to activate proteins such as TT and BSA was employed. The derivatization procedure was modified by raising the pH to 6.2 as described by Micoli *et al.* (2011) in order to prevent potential protein aggregation [444]. Reaction times were investigated to provide a range of derivatization levels for evaluation in conjugation reactions.

CRM_{197} was purchased from Pfenex by the Program for Appropriate Technology for Health (PATH) and made available for use in these experiments. A vial of CRM_{197}, containing 20 mg of lyophilized CRM_{197} protein, (other additives included sucrose, sodium phosphate and polysorbate 80), was dissolved in a 60 mM MES buffer, solution pH 6.2, to give a final concentration of 10 mg/ml (0.345 µM). The sample was dialysed against 60 mM 2–(*N*–morpholino)ethane–sulfonic acid (MES) buffer in order to remove the additives. The derivatization reaction procedure followed was the same as previously described (Chapter 2, Section 2.8.1), where ADH was added in a 3.5 mg ADH/mg protein excess at room temperature. Once dissolved, EDC was added to the reaction mixture as an aqueous solution containing a 55 fold molar excess (0.15 mg EDC/mg protein). The reaction proceeded for a defined period of time (Table 5.10) after which the reaction solution was

dialysed against 3 x 2 L solutions of 0.2 M NaCl / 10 mM MES buffer at pH 7.2 using 10 kDa MWCO dialysis cassettes. The derivatized protein was assayed for hydrazide concentration and protein concentration, as well as analysed by SEC–HPLC.

Table 5.10. Summary of derivatization results of CRM_{197} with ADH/EDC.

Reaction	Reaction time (hr.)	Protein concentration (mg/ml)	Hydrazide concentration (mM)	Carboxylic acid substitution (%)
1	1	2.13	0.060	2.5
2	3	2.61	0.176	5.9
3	16	2.84	0.710	24.5
4	16	2.58	0.797	27.1
5	24	2.96	0.802	27

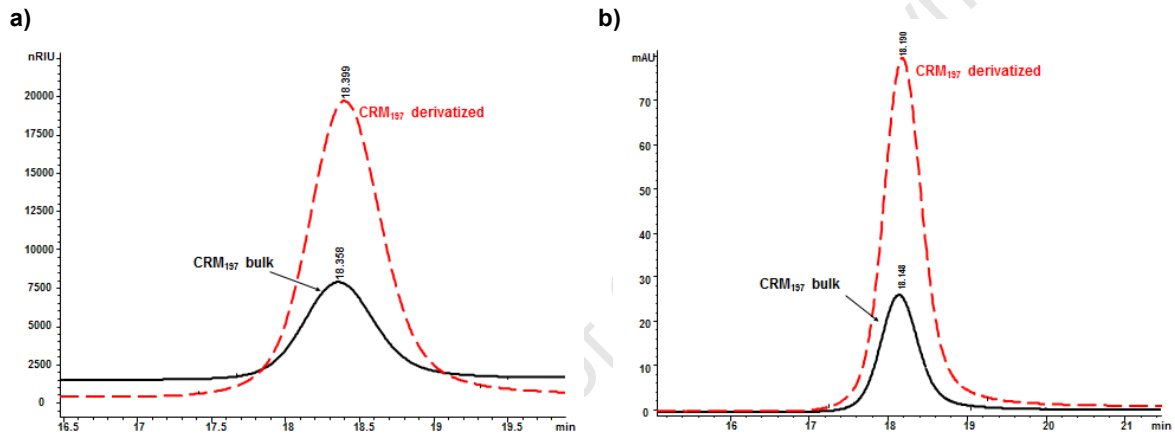

Figure 5.7. SEC–HPLC a) RID and b) UV chromatograms of CRM_{197} before (black) and after (red) derivatization.

Representative chromatograms (Figure 5.7) show the elution time for the native and derivatized protein. No significant shift was seen in either the RID or UV280 signals. The article by Micoli *et al.* also showed that no real difference in retention time was seen before and after derivatization [444]. While Micoli *et al.* used mass spectrometry to determine the level of derivatization, the TNBS assay, was employed in this investigation. By increasing the reaction time from 60 minutes to 3 hours the carboxylic acid substitution more than doubled. However, this percentage derivatization was still low and hence an additional derivatization of 16 hours was performed to increase derivatization levels. An increase in reaction time from 3 hours to 16 hours to 24 hours achieved an increase in percentage carboxylic acid substitution from 6 % to 25 % to 27 % respectively. While 27 % may be over derivatized when using TT as a protein carrier, it was not known what effect this would have on the conjugation of CRM_{197} to polysaccharide.

5.6 Pneumolysoid

Pneumolysin (PLY), a sulfhydryl–activated cytolytic toxin, is produced by all serotypes of *S. pneumoniae* and is assumed to be a virulence factor in pneumococcal infections. Patients with pneumococcal pneumonia have been reported to elicit an antibody response to PLY. Therefore, pneumolysin itself is a potential vaccine candidate to induce species–specific anti–pneumococcal immunity based on anti–PLY antibody and, more importantly, may be a useful protein carrier for the preparation of the conjugate vaccine [445].

The genetically toxoided form of PLY; pneumolysoid (PLD) is used as a carrier protein. Investigations of this protein have been performed extensively with Pn19F polysaccharide. Table 5.11 and Table 5.12 summarise the use of PLD in its native and derivatized form in conjugate investigations. Paton *et al.*, 1991, conjugated activated Pn19F to PLD using EDC coupling through the use of linker, 6–aminocaproic acid [446]. When tested in animal systems, the anti–polysaccharide and anti–pneumolysin titres were significantly higher in immunised mice than non–immunised mice. When the mice were challenged with Pn19F bacteria, the bacteria were eliminated more efficiently from the immunised mice. Survival rates in mice were also higher for the immunised mice [446].

In 1996, Kuo *et al*. patented the conjugation of pneumococcal serotypes Pn14 and Pn18C to PLD [447]. Serotype 14 was first oxidized and conjugated to either ADH–derivatized or non–derivatized PLD. Pn18C was first size–reduced followed by oxidation and conjugated to both underivatized and ADH–derivatized PLD. All conjugations employed reductive amination methodology with cyanoborohydride. PLD was derivatized in 0.1 M potassium phosphate buffer (pH 5.5) by adding a 676 molar excess of ADH, followed by a 614 molar excess of EDC and leaving the solution to react for 3 hours. The derivatized protein was dialysed with 0.1 M potassium phosphate buffer (pH 7.0) to remove any traces of unreacted ADH before being characterised and stored at 4 °C until use [447].

Table 5.11. Use of underivatized PLD in conjugate vaccines.

Author	Pneumococcal serotypes	Modification	Conjugation to PLD
Paton *et al.* [446]	19A	Cyanogen bromide or 6-aminocaproic acid	EDC coupling
Kuo *et al*. [447]	18C	Periodate oxidation	Reductive amination
Michon *et al*. [445]	6B,14,19F,23C	Periodate oxidation	Reductive amination

Table 5.12. Use of derivatized PLD in conjugates.

Author	ADH (w/w)	EDC (w/w)	Reaction time (hr.)	Dialysis	% CS
Kuo *et al*. [447]	2.2	2.2	3	0.1 M potassium phosphate (pH 7.0)	n/a*

Michon *et al.* conjugated four different pneumococcal serotypes, namely 6B, 14, 19F and 23F, to non–derivatized PLD via reductive amination. The four polysaccharides required derivatization with periodate oxidation prior to protein coupling. Mice studies were performed with the monovalent, as well as multivalent conjugates, at two different doses. The lower dose and the multivalent conjugate gave the best responses in the mice. When compared to a TT conjugate vaccine, produced using the same conjugation methodology, the PLD conjugate elicited equivalent or better capsular polysaccharide–specific response. The mice produced high levels of pneumolysin–specific IgG antibodies which have been shown to neutralise pneumolysin induced haemolytic activity *in vitro* [445].

PATH purchased PLD from St Jude's Children's esearch Hospital in the United States and supplied it to The Biovac Institute for investigation as a protein carrier for Pn1. Due to a limited supply of PLD; small–scale (20 mg) derivatizations were performed. The established ADH/EDC derivatization method was applied to PLD, although small changes in ratios and buffers were made according to the Kuo *et al.* [447] paper due to the large difference in the pI between PLD (5.2) and CRM_{197} (5.8) or TT (5.8).

5.6.1 Derivatization of PLD

As it was not made known what additives, if any, were present in the lyophilised pneumolysoid sample, a dialysis step was employed prior to derivatization to remove any excipients that may have been introduced. Two different buffers were tested, namely: 0.1 M potassium phosphate (KH_2PO_4) (pH 5.4) and 0.1 M MES (pH 6.0) as described in Table 5.13. A sample of PLD was dialysed extensively using 5 K MWCO membranes against both buffers before the general method for protein derivatization was applied, i.e. 3.5 mg ADH / mg protein was added followed by 0.11 mg EDC / mg protein. The reaction proceeded for 3 hours at room temperature after which it was extensively dialysed in either 0.1 M KH_2PO_4 (pH 7.0) or 3 mM Na_2CO_3/30 mM NaCl (pH 7.2).

Table 5.13. Dialysis buffers used before and after derivatization of protein PLD. The pH of the buffers is shown.

Reaction	Dialysis buffer before derivatization	Buffer pH	Dialysis buffer after derivatization	Buffer pH
1	0.1 M KH_2PO_4	5.4	0.1 M KH_2PO_4	7.0
2	0.1 M MES	6.0	3 mM Na_2CO_3/30 mM NaCl	7.2

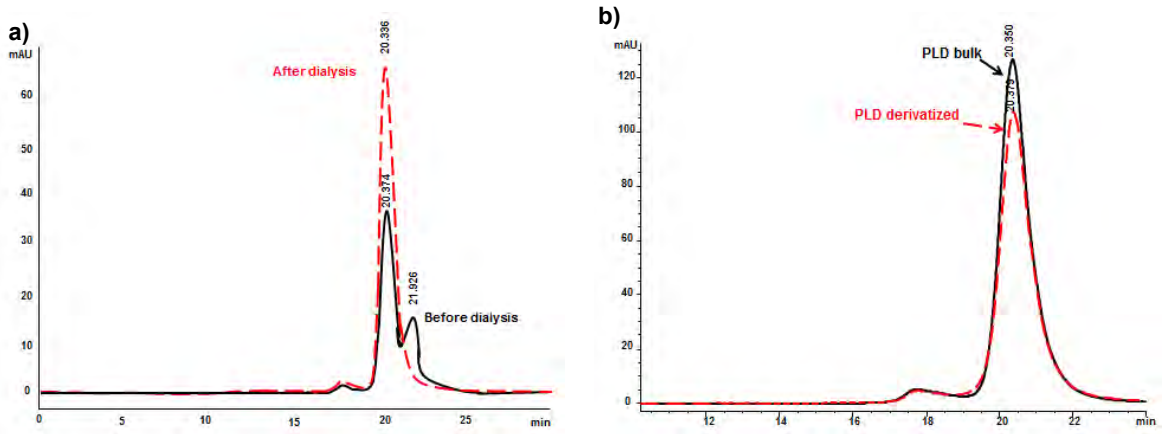

Figure 5.8. SEC–HPLC UV 280 nm chromatograms of a) PLD before (black) and after (red) dialysis with 0.1 M MES buffer and b) PLD before (black) and after (red) derivatization. Dialysis buffer used: 3 mM Na_2CO_3/ 30 mM NaCl.

The derivatized PLD was found to be very unstable in the diafiltration buffer, KH_2PO_4 (pH 7.0), and precipitated out during the three hour reaction. The protein was stable in the Na_2CO_3/NaCl buffer and a sample was analysed on SEC–HPLC as well as being assayed for protein concentration and derivatization levels.

The results of the SEC–HPLC analysis in Figure 5.8 demonstrate that the PLD may have contained an impurity, detected in the UV280 chromatogram, which was removed by means of dialysis. Post derivatization, there seems to be no significant shift in the PLD profile on UV280 which confirmed the findings presented by Kuo *et al.* [447]. Employing the Kuo method for derivatization of PLD gave consistent results of 24 % carboxylic acid substitution with greater than 80 % recoveries.

5.7 Electrophoretic comparison of protein carriers

Three of the four carrier proteins used in the course of the investigation were subjected to sodium dodecyl sulfate polyacrylamide gel electrophoresis (SDS–PAGE) under denaturing conditions to determine the molecular weight of the proteins, and whether the molecular weight of PLD had been maintained post–derivatization. The gel was loaded and run with a two–fold dilution of: (1) BSA, (2) CRM_{197} and (3) PLD (pre–/post–derivatization), starting with a concentration of 400 µg/ml. The gel was stained to allow visualization of the proteins (Figure 5.9).

Figure 5.9. SDS–PAGE (reducing) gel with molecular weight marker (Lane 1); BSA protein (Lane 2, 3); PLD protein (Lane 5, 6); derivatized PLD (Lane 8, 9); and CRM_{197} protein (Lane 11, 12).

The SDS–PAGE gel shows the PLD to be slightly smaller than the BSA and CRM_{197} carrier proteins (56 kDa compared to 64 and 66 kDa respectively). The observed size distribution of the various native proteins is in order with literature. The PLD protein post–derivatization was slightly larger in size than the native PLD and showed no dimerization or trimerization to have occurred during the derivatization process.

5.8 Summary

All four carrier proteins were successfully derivatized using the ADH/EDC derivatization method. For BSA and TT, the SEC–HPLC 280 nm chromatogram revealed a shift in retention time post–derivatization to a lower molecular weight which was hypothesised to be a result of the hydrazides interacting with the column packing. No shift in elution time was seen for either the derivatized CRM_{197} protein or the derivatized PLD protein. Derivatization for all four proteins was confirmed with the colorimetric TNBS assay. Table 5.14 shows the deviations from the Lee, Frasch patent that were successfully used in this investigation. As shown in the BSA experiments, derivatization levels were lowered by decreasing the reaction time of the derivatization procedure. This was confirmed with TT. The reaction times for CRM_{197} had to be extended due to low levels of derivatization seen (below 10 %) after 4 hrs. To achieve derivatization levels of approximately 20 %, a reaction time of between 16 and 24 hours was required. Both derivatizations of PLD gave consistent results with a 24 % carboxylic acid substitution, however the PLD derivatized in KH_2PO_4 (pH 7.0) buffer was found to be unstable and this was substituted with a Na_2CO_3/NaCl buffer at neutral pH. This was shown to stabilise the protein and prevent any aggregation.

Table 5.14. Deviations from the original method for different carrier proteins investigated.

Protein	ADH (w/w)	EDC (w/w)	pH	Reaction time (hr.)	Dialysis	Dialysis pH	% CS
Model	3.5	0.15	4.75	4	30 mM NaCl/ 3 mM Na_2CO_3	10.7	N/A
BSA	3.5	0.15	4.75	1.5	NaCl/Na_2CO_3	10.5	14
TT	3.5	0.15	4.75	1.5	NaCl/Na_2CO_3	10.5	13–17
CRM	3.5	0.15	6.2	16–24	NaCl/ MES	7.2	24–27
PLD	2.5	0.11	6.0	3	NaCl/Na_2CO_3	7.2	24

CHAPTER 6. CONJUGATION

6.1 Introduction

Pn antigens can be converted from a T–cell independent antigen to a T–cell dependent antigen by covalently linking the polysaccharide to a protein. There are many considerations to take into account when producing a conjugate vaccine that is immunogenic: the chemistry used to couple the saccharide to the protein is amongst the most important. The size and functional groups of the saccharide and protein, the type of carrier protein, and the amount of saccharide conjugated to each protein carrier are also aspects that need to be considered to produce a successful conjugate [375, 448, 449].

Conditions such as the time, temperature and pH of the reaction need to be carefully monitored in order to maintain the structural chemistry of the polysaccharide as the creation or destruction of epitopes and the chance of unwanted depolymerisation may lead to a destruction of the saccharide's immunogenicity. The optimised conditions would also prevent cross linking within the saccharide or carrier protein or cross reactivity between conjugates [10, 375, 400].

There are different approaches to the preparation of conjugates, two of which are shown in Figure 6.1. The polysaccharide (either full length or size reduced) can be i) randomly activated, ii) activated at only one terminal, or iii) partially degraded to form activated groups at both terminals. The former is mainly used for the conjugation of large polysaccharides with the latter two being used for oligo– or shorter polysaccharides. The final structure of the conjugate depends on which approach is chosen [375].

Three main functional groups are available for conjugation on the saccharide: the hydroxyl (OH), carboxyl (COOH) and amino (NH_2) groups. However, aldehyde functional groups can be generated via periodate oxidations as well as acid hydrolysis.

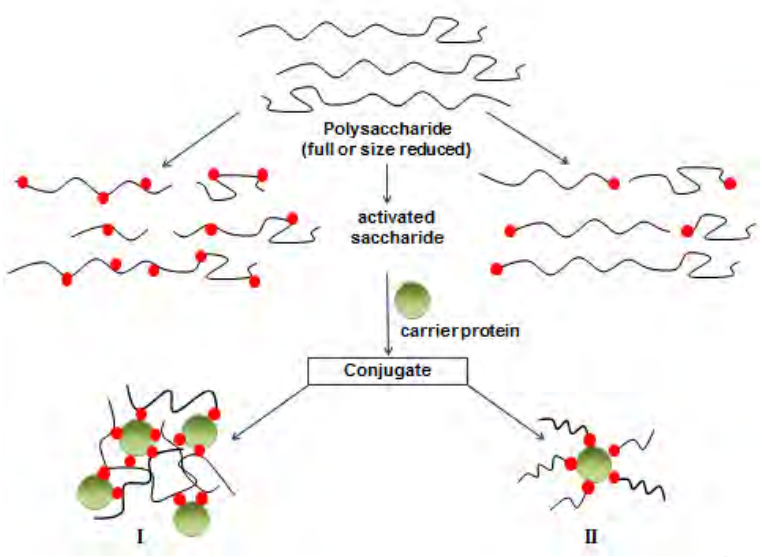

Figure 6.1. Various conjugate structures can be formed depending on how the polysaccharide is activated. I) random activation of the polysaccharide leads to a cross linked lattice type conjugate whereas II) terminal activation produces a single carrier protein with attachment points for each activated polysaccharide.

There are approximately seven different functional groups on a protein that can be considered for conjugations, however due to the number of each of these groups on a protein, the first two groups are the most widely used in conjugation reactions. The seven different groups are:

- Amino groups (lysine) which can be conjugated directly to the carboxyl groups on the saccharide.
- Carboxyl (via aspartic or glutamic acid) which can be conjugated either directly to amino groups or first derivatized with ADH followed by conjugation to the carboxyl groups on the saccharide.
- Hydroxyl groups (threonine, serine tyrosine).
- Sulfhydryl groups (cysteine).
- Imidazole groups found on histidine residues.
- Indole functional groups on tryptophan.
- Guanidine groups found on arginine amino acids [166].

While there are many different chemistries available for conjugations of polysaccharides and proteins only a few different approaches have been used in licensed pneumococcal conjugate vaccines – using the hydroxyl and amine functional groups on the polysaccharide and protein respectively. The general approaches that are used by the manufacturers for the pneumococcal vaccine are based on the same procedures that achieved success with the

licensed Hib conjugate vaccines. In doing so, the manufacturers have a chemistry that has been well defined and they also retain ownership of the proprietary information so as to avoid any intellectual property disputes.

Pfizer used reductive amination chemistry for both the seven and thirteen valent conjugate vaccines [120, 175]. In order for reductive amination to be successful, aldehyde functional groups are needed on the polysaccharide. As the pneumococcal polysaccharides do not contain aldehydes, the saccharides need to be modified; this is usually achieved by oxidising any available diols with sodium periodate (Figure 6.2A). This oxidation usually results in ring opening and could also lead to cleavage of the polymer thus providing simultaneous size reduction and activation of the polysaccharide. In the case of Pn1, there are no available diols so a de–*O*–acetylation step must first take place to remove the *O*–acetyl functional group on the GalA residue to create the diol. Once the aldehydes have been created, they are reacted with the amines on the CRM_{197} carrier protein to form an imine linkage (Figure 6.2B). This process is slow and reversible and an *in situ* reduction with sodium cyanoborohydride to a secondary amine must occur for a stable linkage to form (Figure 6.2C). Any unreacted aldehydes are subsequently reduced with sodium borohydride.

GSK's pneumococcal conjugate vaccine is based on the activation of the hydroxyl groups of the saccharide with 1–cyano–4–dimethylaminopyridium tetrafluoroborate (CDAP) forming a cyanate ester [386]. This activated saccharide can be coupled directly or through a spacer group to the amino group on the carrier protein. Hydroxyl groups themselves do not react spontaneously with CDAP as they have pKas of approximately 12, thus a strong base is needed to transform the stable hydroxyl groups into more reactive alkoxide ions ($–O^-$). These alkoxide ions are more nucleophilic and are able to react with CDAP. However, the use of a strong base has a negative effect as both CDAP and the resultant active cyanate esters are rapidly hydrolysed to inert carbamates, resulting in a lesser amount of active intermediates to efficiently couple to the desired compound. It was determined that instead of increasing the nucleophilicity of the hydroxyl groups; it was more useful to enhance the electrophilicity of CDAP with the addition of a "cyano–transfer" reagent. To this end, as an alternative to NaOH, triethylamine (TEA) was utilised; it reacts with the CDAP forming a *N*–cyanotriethyl–ammonium (CTEA) complex that is more electrophilic than CDAP by itself and is therefore more susceptible to attack by the hydroxyl functional groups (Figure 6.3) [450]. The use of TEA also allowed for the reaction to occur at neutral pH thus avoiding the formation of the inactive carbamate compounds. Table 6.1 shows a comparison of the two conjugation chemistries for Prevnar and Synflorix.

Table 6.1. Comparison of the conjugation chemistries of the three commercially available pneumococcal conjugate vaccines.

	Pfizer	**GlaxoSmithKline**
Licensed vaccine(s)	Prevnar7 and Prevnar13	Synflorix
Carbohydrate activation	Periodate	CDAP
Conjugation	Reductive amination via Schiff's base with sodium cyanoborohydride	Cyanylation via isourea
Quenching	sodium borohydride	glycine

There are many different analytical tools available to show conjugate formation. Size exclusion chromatography can indicate a variance in elution time between the unconjugated and conjugated material due to the shift in molecular weight. SDS–PAGE is another method for depicting conjugate formation and works in a similar fashion to SEC. The large molecular weight conjugate is generally shown as a smear in the high molecular weight region as opposed to the lower molecular weight neat bands seen for most unconjugated proteins [10].

The solution containing conjugate often contains unconjugated polysaccharide and protein present in varying amounts [451]. As it is the conjugate that will directly contribute to the immune response, the unconjugated polysaccharide, protein and any remaining reagents must be removed or at least minimised. This is achieved through conjugate purification. There are various methods available to purify the conjugate including ultrafiltration, chromatographic and precipitation methods. Whilst saccharides can be a few hundred kilodaltons in size, they have an extended structure in solution and thus a large hydrodynamic volume. This apparent large size makes it difficult to separate from the conjugate vaccine using conventional chromatographic techniques, however, by taking advantage of the carrier protein, a method involving the selective precipitation of the conjugate with ammonium sulfate can be utilised [452]. After this separation, the free sugar still present in the conjugate can be quantified by further selective precipitation of the conjugate with deoxycholate [255, 256] followed by either colorimetric or HPAEC–PAD analytical methods [10, 235, 256].

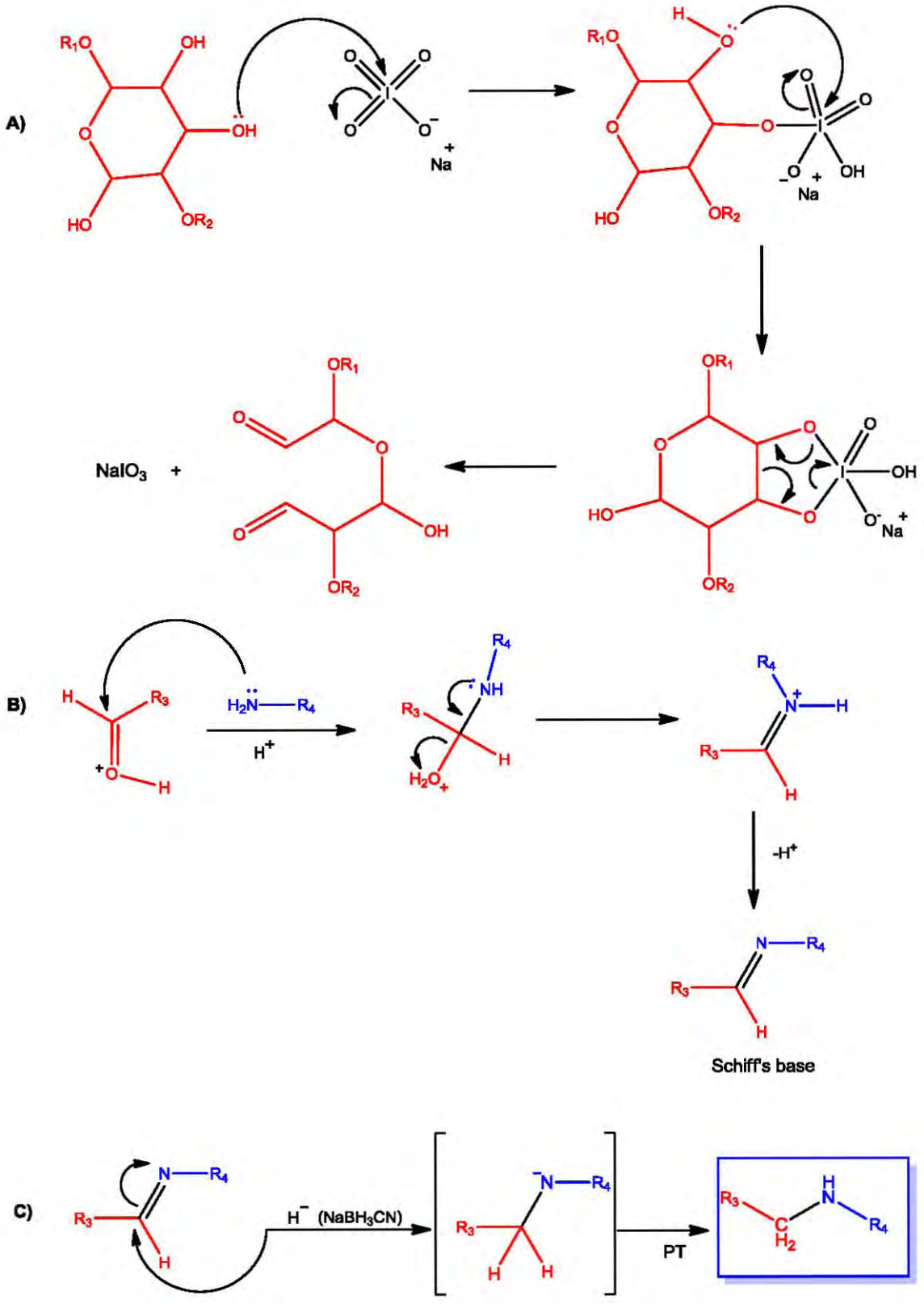

Figure 6.2. Conjugation method used for the production of PCV13. A) Periodate oxidation followed by the formation of a Schiff's base (B) and subsequent reduction (C) to an amine (reductive amination). R1, R2, R3 = remainder of polysaccharide, R4 = protein.

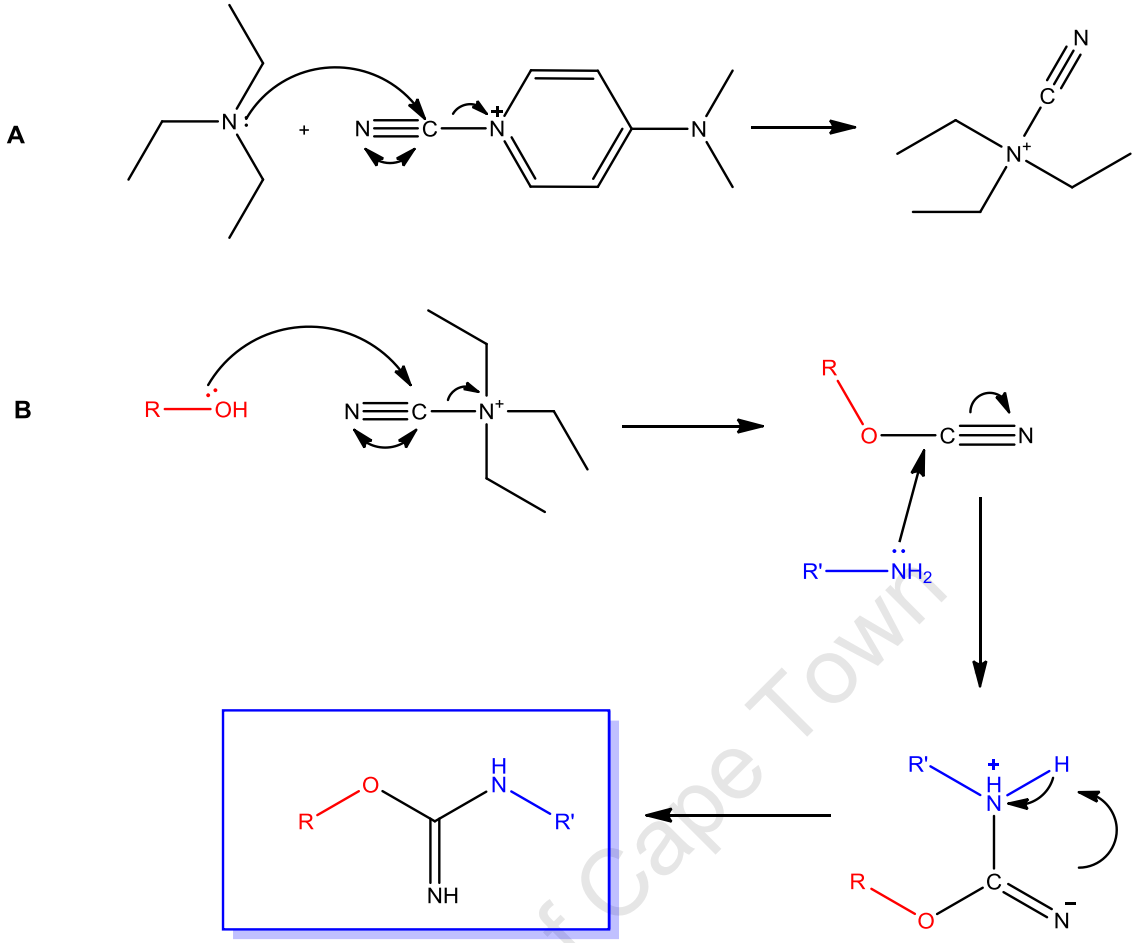

Figure 6.3. Reaction mechanism for CDAP activation of a polysaccharide and subsequent conjugation to a protein.

Both Pfizer and GSK have taken the conjugation approach used for their preparations of the Hib vaccine and applied it to the pneumococcal serotypes, by making use of the hydroxyl and amino groups on the polysaccharide and protein respectively. Several potential issues arise with these conjugation methodologies when applied specifically to the Pn1 PS. The Pfizer conjugation requires diol functional groups available for periodate oxidation to oxidise to aldehydes, hence the Pn1 would need to be de–*O*–acetylated. However, literature indicates the importance of the *O*–acetyl group in terms of its immunogenicity [286, 368, 369], thus modification of this group could potentially lead to a decrease in immunogenicity. GSK's CDAP conjugation methodology activates the hydroxyl functional groups on the polysaccharide; however, the amino group on the AAT saccharide has a greater propensity to react with CDAP than the hydroxyl groups, thus resulting in modification of the amine group. The addition of a strong base in the CDAP conjugation reaction may lead to a loss of the labile groups such as the *O*–acetyl group of the GalA residue which is important for immunogenicity.

As both Pfizer's PCV13 and GSK's PCV10 have only recently been introduced into vaccination programs around the world, information on the efficacy of these vaccines is still being gathered and comparisons cannot yet be determined. It has been revealed in an article by Prymula and Schuerman, in 2009, that the OPA activity against Pn1 had the lowest recorded value at 65.7 % compared to all other serotypes contained in the 10 valent vaccine [164, 165]. The OPA results for Prevnar13 also show Pn1 to have the one of the lowest responses (along with Pn3) [178, 453].

The modification of the *O*–acetyl and amino groups on Pn1 polysaccharide may play a role in the reduced immunogenicity of the serotype in the conjugate vaccines, however, this can only be concluded if a conjugate, prepared using an alternate functional group, resulted in higher immunogenicity levels when compared to the commercial vaccines. One of the unique features of Pn1 PS is the more reactive carboxyl function groups on the GalA residues. With two carboxyl groups available for conjugation on each Pn1 PS repeating unit, random activation of either of these groups and subsequent coupling to a carrier protein could produce a conjugate that is immunogenic in mice studies by virtue of ELISA and OPA assay results. To activate the carboxyl group, the most common reagent 1–ethyl–3–(3–dimethylaminopropyl)carbodiimide (EDC) was investigated. Alternate methods of activation of the carboxyl group were also determined that applied activators; namely HOBt and triazine mediated activation. This activated polysaccharide would subsequently be conjugated to the hydrazide–derivatized protein carriers. The successful conjugates would then be formulated and the chemistries and protein carriers compared to commercial conjugate vaccines.

6.2 EDC Chemistry

Carbodiimides are used to mediate the formation of linkages between amines and either carboxylates (amides) or phosphates (phosphoramides) [454, 455]. Carbodiimides are one of the most widely used zero length cross linkers as they are efficient in forming conjugates between two protein molecules, between a peptide and a protein, between an oligonucleotide and a protein, between a biomolecule and a surface or particle, or any combination of these with small molecules. There are two basic types of carbodiimides: water–soluble and water–insoluble. The water–soluble carbodiimides are the most common choice for biochemical conjugations, because most macromolecules of biological origin are soluble in aqueous buffer solutions. Not only is the carbodiimide itself able to dissolve in the reaction medium, but the by–product of the reaction, an isourea, is also water–soluble, facilitating easy purification [400].

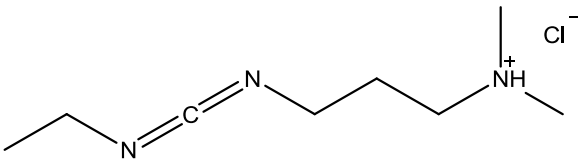

Figure 6.4. Molecular structure of EDC.

EDC (or EDAC; 1–ethyl–3–(3–dimethylaminopropyl)carbodiimide hydrochloride) shown in Figure 6.4 is the most common carbodiimide used for conjugating biological substances containing carboxylates and amines [456]. EDC is water–soluble, which allows for its direct addition to a reaction without prior organic solvent dissolution. Both the reagent itself and the isourea formed as the by–product of the crosslinking reaction are water–soluble and may be easily removed by dialysis or gel filtration [457, 458]. The reagent is, however, labile in the presence of water and therefore the bulk chemical should be stored desiccated at –20 °C. A concentrated solution of EDC in water may be prepared to facilitate the addition of a small molar amount to a reaction, but the stock solution should be dissolved rapidly and used immediately to prevent extensive loss of activity [400]. A variety of chemical conjugates may be formed using EDC, provided one of the molecules contains an amine and the other a carboxylate group. *N*–substituted carbodiimides can react with carboxylic acids to form highly reactive, *O*–acylisourea intermediates (Figure 6.5). Consequently this active species can react with a nucleophile such as a primary amine to form an amide bond [459].

Other nucleophiles are also reactive – oxygen atoms, such as those in water molecules, may act as the attacking nucleophile. In aqueous solutions, hydrolysis by water is the major competing reaction, cleaving off the activated ester intermediate, forming an isourea, and regenerating the carboxylate group [460]. Nakajima and Ikada (1995) investigated EDC amide bond formation in aqueous solution using hydrogels of acrylic acid– or maleic acid–containing polymers and ethylenediamine or benzylamine. Their results indicated that carboxylate activation occurred most effectively with EDC at pH 3.5 – 4.5, while amide bond formation occurred with the highest yield in the range of pH 4 – 6. When working with proteins and peptides, experience indicates that EDC–mediated amide bond formation effectively occurs between pH 4.5 and 7.5. Beyond this pH range, however, the coupling reaction occurs more slowly with lower yields. Most references to the use of EDC describe the optimal reaction medium to be at a pH from 4.7 to 6.0 [461]. However, the carbodiimide reaction occurs effectively up to at least pH 7.5 without significant loss of yield [400]. Conjugations performed under mildly alkaline pH conditions (e.g. pH 8.5) may be conducted to limit the polymerization of proteins, while still facilitating the coupling of a carboxylate–containing molecule at a low substitution level per protein [462]. Some procedures recommend the use of water as the solvent in an EDC reaction, while the pH is maintained

constant by the addition of HCl. Buffered solutions are more convenient, as the pH would not have to be monitored during the course of the reaction.

Table 6.2 details a summary of some of the reactions that make use of EDC as the method of conjugation. Beuvery *et al.*, in 1983, prepared *Neisseria meningitidis* group C polysaccharide–tetanus toxoid conjugates by using high molecular weight polysaccharide and purified tetanus toxoid with EDC as a coupling reagent. It was determined that the composition of the conjugate was not homogeneous and at least 10 % unconjugated polysaccharide was present. The conjugation was performed by the slow addition of a solution of EDC in water to a solution of polysaccharide and protein in equal mass ratios. The EDC was used as the zero length linker between the carboxyl groups on the polysaccharide and the amine functional groups on the carrier protein. The pH was maintained at 4.7 with the addition of HCl and the reaction was stopped after 4 hours with the addition of ethanolamine. The conjugate was dialysed against PBS buffer [435].

Table 6.2. Summary of some conjugations in literature that make use of EDC as a conjugation method.

Author	PS	PS activation	Protein	Protein derivatized (Y/N)	EDC reaction conditions
Beuvery *et al*. [435]	Meningococcal group C	None	TT	N	2.5 mM, 4 hr., pH 4.7
Schneerson *et al*. [115]	Hib, Pn6A	CNBr	TT	N	0.1 M, 3 hr., pH 5.0
Hale *et al*. [463]	Vi	None	rP40	Y	5 mM, 3 hr. pH 5.6–5.9
Cabrera *et al*. [68]	Meningococcal group A, B,C	NaOH	TT	N	0.1 M, 4 hr. pH 5–6
Biemans *et al*. [386]	Pn22F	CDAP/ADH	Protein D	N	1 mg/mg PS, 2.5 hr., pH 5–7

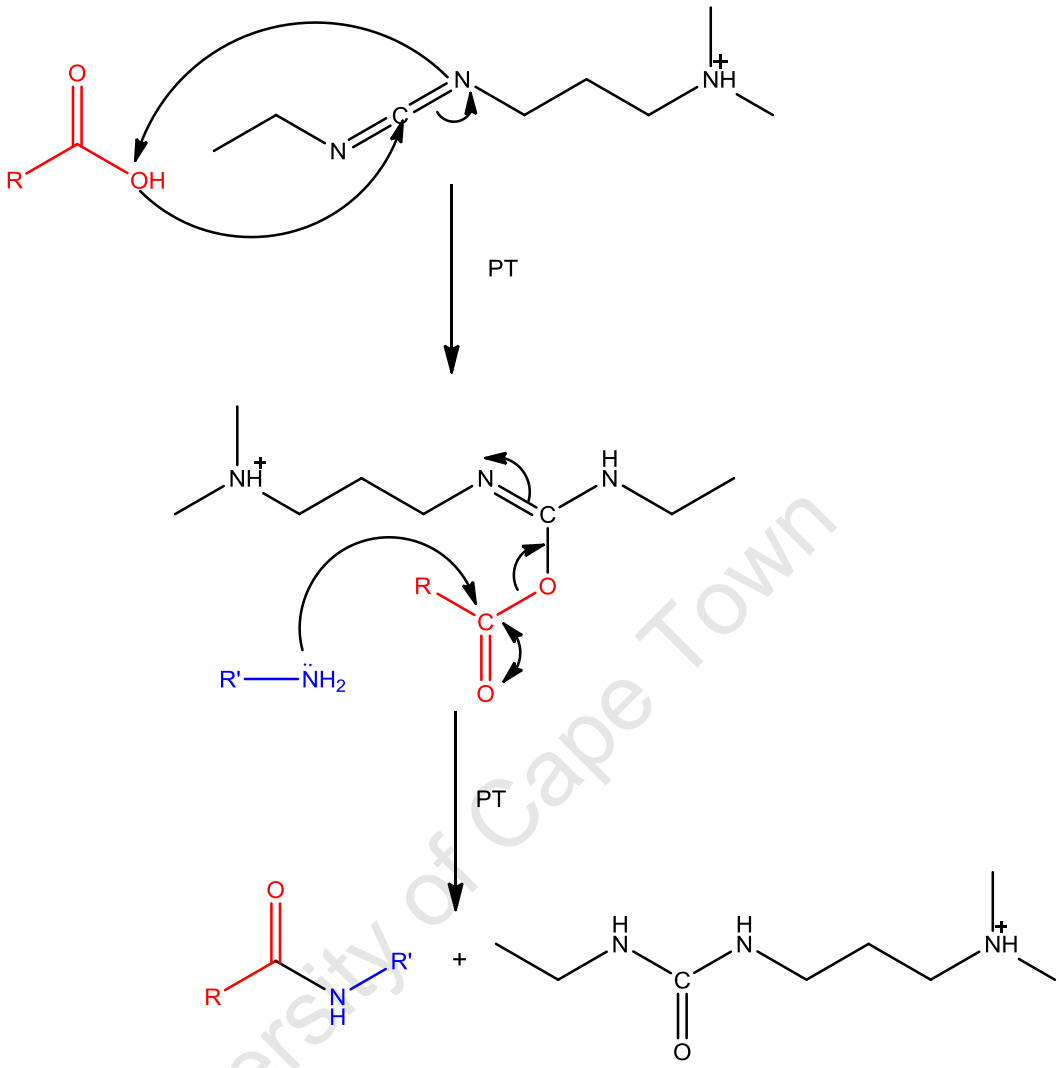

Figure 6.5. Mechanism of the reaction between a carboxyl and an amino functional group with EDC to form a stable amide linkage. A) Reaction between carboxylate functional group with EDC to form active ester intermediate. B) Reaction between active ester intermediate with amine functional group to form amide bond and isourea by–product. Modified from Hermanson [400].

Schneerson *et al.* (1986) used the EDC methodology to couple Pn6A to TT that was injected into human adult volunteers. The hydroxyls on the polysaccharide were first activated with cyanogen bromide (CNBr) and ADH to form the activated PS–ADH compound that was conjugated to TT with EDC at a final concentration of 0.1 M EDC for 3 hours at pH 5.0, before extensive dialysis with 0.2 M NaCl. The Pn6A–TT conjugate elicited an 8 fold increase in antibodies after one injection. A Hib–TT conjugate, produced with the same carbodiimide method was introduced concurrently with the pneumococcal conjugate. A cross reaction was noted with the Pn6A conjugate eliciting Hib antibodies in 13 of 20 volunteers, however, only 4 of 59 volunteers injected with the Hib–TT conjugate produced an increase in Pn6A antibodies [115].

Hale *et al.* (2006) used the carbodiimide–coupling methodology to conjugate carboxyl groups on the capsular polysaccharide of Vi to the ADH–derivatized outer membrane protein of K*lebsiella pneumoniae* (rP40). A final concentration of 5 mM EDC was used in the reaction that proceeded for 3 hours at room temperature within the pH range of 5.6 – 5.9. Immunogenicity studies in mice showed an increase in antibody response compared to the native polysaccharide [463].

Cabrera *et al.* (2006) produced conjugates against *Neisseria meningitides* serogroups A, B, C, *Vibrio cholera* and *Salmonella typhi*, and tested their immunogenicity in mice. These activated saccharides were linked to the carboxyl groups on TT via EDC coupling. The conjugates all elicited higher anti–polysaccharide titres than the unconjugated saccharide [68, 464].

In the investigation by GSK into their 10 valent licensed pneumococcal vaccine, the EDC coupling methodology was evaluated with respect to Pn22F (not used in the vaccine). The polysaccharide was first derivatized with ADH in the presence of CDAP. This ADH–derivatized polysaccharide was conjugated to Protein D using EDC coupling [386] and compared to a Pn22F conjugate prepared using their general CDAP method.

Table 6.3. Comparison of Pn22F–Protein D conjugates using different conjugation methodologies [386].

Polysaccharide	Conjugation	Protein:PS	Free PS (%)
Pn22F	CDAP	0.46	5.8
	EDC	0.27 – 0.23	<1

The conjugates were compared with respect to the ratio of protein to polysaccharide and free polysaccharide levels (Table 6.3) with the EDC conjugate, showing a lower protein–polysaccharide ratio and a much lower percentage of free polysaccharide levels than the CDAP conjugate. The immunogenicity of the polysaccharide and protein were determined in terms of both IgG levels as well as opsonophagocytic titres (Figure 6.6), and revealed that the conjugate prepared with the ADH linker showed superiority over the CDAP conjugate both in the ELISA and in the OPA results [386].

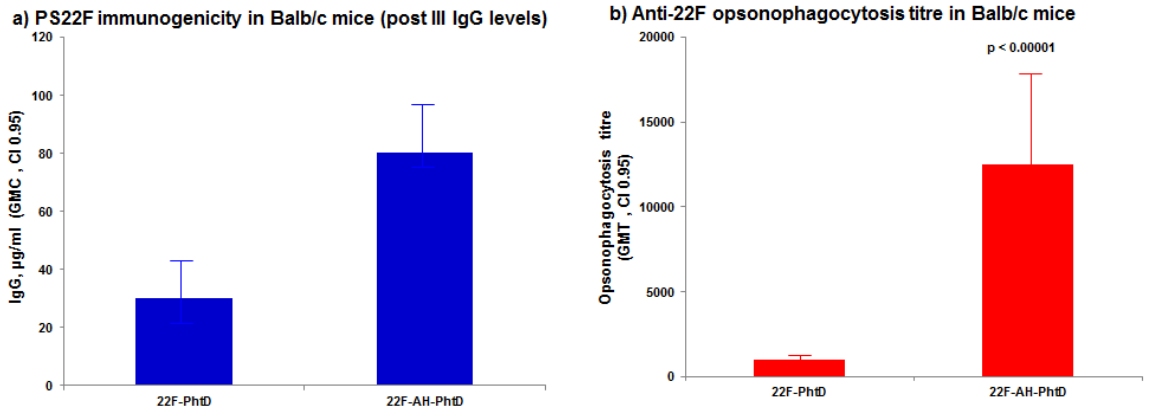

Figure 6.6. Antibody response of Pn22F conjugates prepared using two different conjugation methods modified from Biemans *et al.* [386].

6.2.1 EDC conjugations to BSA

As EDC is one of the most widely used reagents for activating the polysaccharide and subsequent conjugations to protein carriers, it was the first conjugation method to be investigated. BSA was used as a protein carrier to determine if conjugation via EDC coupling was a viable method. The formation of the conjugate was also monitored in two different solutions; NaCl and MES buffer and the results of these investigations could be used as a foundation when alternate protein carriers are used.

In order to determine if conjugation was successful, Pn1 was dissolved in 0.2 M NaCl with a 1:1 molar ratio of derivatized BSA. EDC was added in excess (2 mol EDC for every mol PS) and the reaction was monitored on SEC–HPLC at 30 and 90 min.

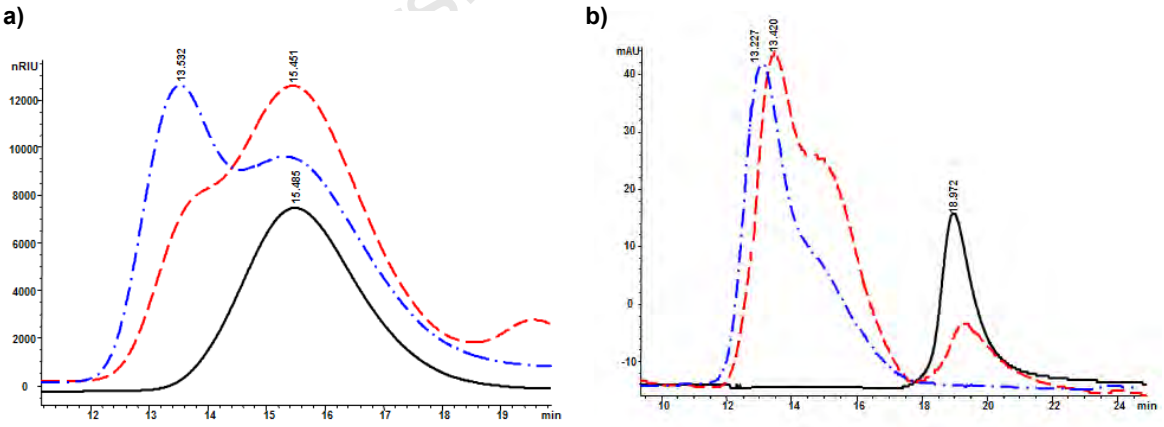

Figure 6.7. SEC–HPLC RID (a) and UV 280 nm (b) chromatograms of Pn1_EDC_BSA in 0.2 M NaCl after 30 (red) and 90 min (blue) compared to Pn1 polysaccharide (a) and BSA (b) (black).

The RID profiles (Figure 6.7a) detail the formation of the conjugate over time. After 30 minutes a shoulder appeared on the higher molecular weight side of the chromatogram where the polysaccharide eluted. After 90 minutes this shoulder had become the major peak at 13.5 min; however, the double humped peak suggested that unconjugated Pn1 may still have been present. The UV signals at 280 nm mimicked the RID signals. At 30 minutes, a

large shift in elution time from the derivatized BSA at 19.0 min to the conjugate peak at 13.4 minutes was shown. This peak was double humped, which in the RID signal suggested that unconjugated saccharide was present, but with the UV signal it was hypothesised that either two different molecular weight conjugates had formed or that the protein or conjugate had aggregated. The smaller molecular weight peak seen in the 30 min chromatogram decreased significantly after 90 minutes confirming that conjugation was still in progress with more saccharide fragments conjugating to the protein. The peak shown at approximately 20 minutes in the 30 minute sample was from unreacted derivatized BSA and disappeared in the 90 minute sample suggesting that all the protein had reacted.

The size exclusion purification method was tested using the Sephacryl S500 packing, on an ÄKTA chromatographic system, to determine if it was a viable method of purification. The resulting chromatogram (Figure 6.8) showed two overlapping peaks, which suggested that the incorrect packing material was used as significant separation could not be obtained. An alternate packing, the Sephacryl S400, was also tested (see molecular weight ranges in Table 6.4) however, the separation did not improve (data not shown). Fractions were collected and analysed on the SEC–HPLC to test for conjugate and unbound saccharide.

Table 6.4. Molecular weight working range for dextrans using Sephacryl size exclusion column packing [465].

Packing	Dextran Mw fractionation range (Da)
S400	$1x10^4 – 2x10^6$
S500	$4x10^4 – 2x10^7$

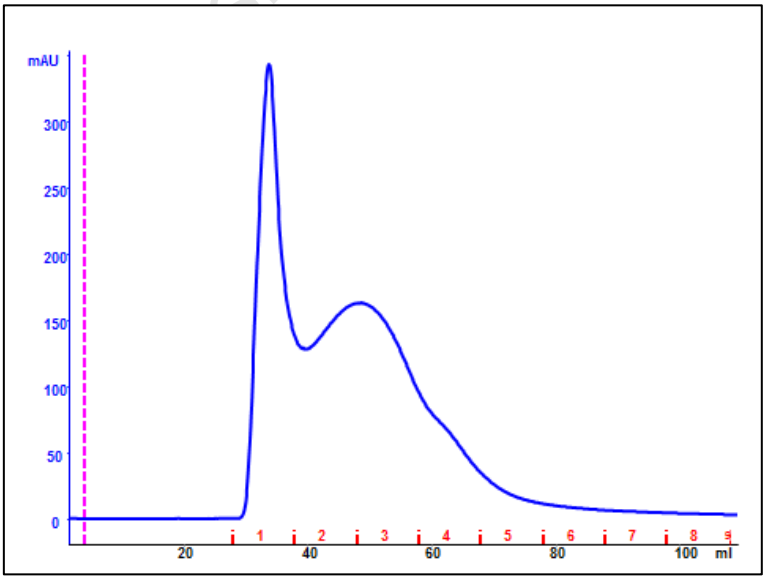

Figure 6.8. UV 280 nm chromatogram of the separation of the Pn1_EDC_BSA conjugate.

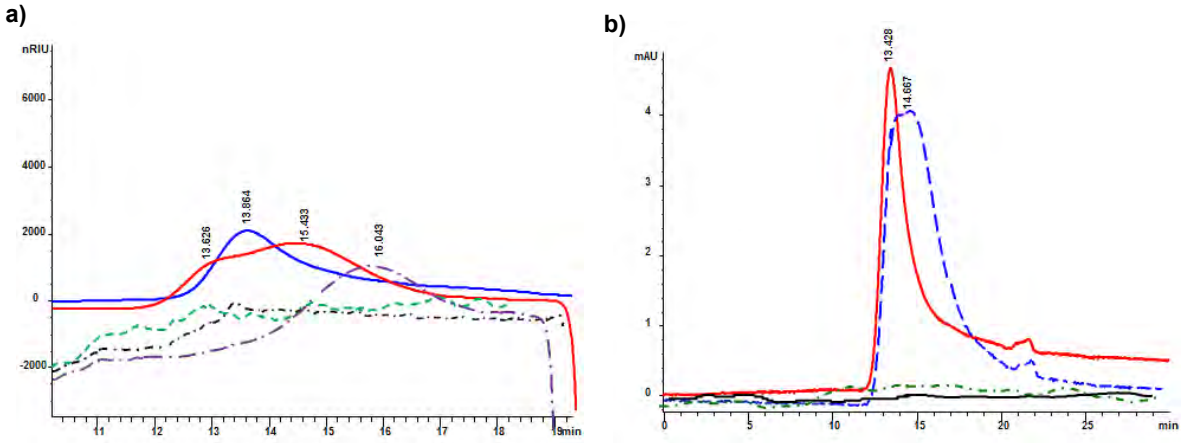

Figure 6.9. SEC–HPLC a) RID and b) UV 280 nm chromatograms of Fractions 1 (black), 2 (blue), 3 (red), 4 (purple) and 5 (green) of Pn1_EDC_BSA conjugate.

Table 6.5. Saccharide and protein content in fractions from Pn1_EDC_BSA.

Fraction number	Total saccharide (mg)	Total protein (mg)
1	1.68	3.96
2	6.39	13.68
3	9.15	17.15
4	3.67	8.80
5	0.23	1.42
Total	21.12	45.00

From the RID chromatogram (Figure 6.9a) the polysaccharide was observed to have eluted in Fractions 2 – 4 with three different molecular weight species. It was observed that only Fractions 2 and 3 contained protein. The colorimetric assays, Table 6.5, gave positive results for saccharide and protein in every fraction. Recoveries of 90 % protein and 42 % polysaccharide were obtained. The low recovery of saccharide could be due to unconjugated Pn1 eluting later on the column or interacting with the N,N'–methylenebisacrylamide found in the column packing thus not eluting. As Pn1 is not UV active, the polysaccharide elution could not be monitored. Table 6.5 confirms the pictorial representation in the chromatograms where Fractions 2 and 3 contained the majority of the polysaccharide and the protein. The protein assay suggested that 17 % of the original amount of protein was found in Fraction 4 although the HPLC chromatogram did not show this. The sample volume injected onto the column was insufficient to allow for full analytical testing.

As conjugation between Pn1 and BSA was shown to be successful, the reaction solution was investigated further to determine whether NaCl or 2–(*N*–morpholino)ethanesulfonic acid (MES) may affect the conjugation reaction.

Two reactions were investigated with ratios of Pn1, BSA and EDC detailed in Table 6.6. The only difference was that the Pn1 was dissolved in either 0.2 M NaCl or 1 M MES. After the reaction was stopped the mixture was centrifuged to pellet out any precipitate and the

supernatant was analysed by SEC–HPLC. Precipitation was observed during both conjugation reactions, however the conjugate in NaCl produced much less visible precipitate than that of the MES buffered reaction.

Table 6.6. Reaction variables for EDC conjugation of Pn1 with derivatized BSA.

Pn1/Protein molar ratio	Reaction solution	Pn1/EDC molar ratio	pH adjustment	Reaction time (hr.)
1:1	0.2 M NaCl	1:2	6.0	2
1:1	1 M MES	1:2	6.0	2

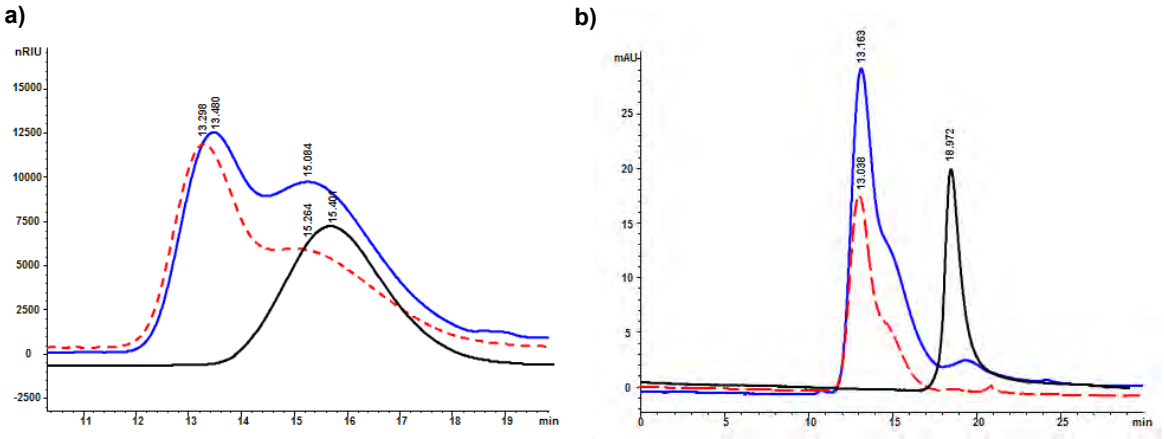

Figure 6.10. SEC–HPLC RID (a) and UV 280 nm (b) chromatograms comparing Pn1 polysaccharide (black) to the Pn1_EDC_BSA conjugate in NaCl (blue) and MES (red) buffer.

The RID profile, Figure 6.10, showed a shift in elution times for both reactions from the Pn1 PS peak at 15.4 min to a higher molecular weight range, eluting at 13.3 min for the NaCl reaction and 13.5 min for the MES conjugate. Both conjugate peaks were double humped, suggesting either that unconjugated saccharide remained in both reactions and/or the presence of two populations of conjugate. The UV chromatograms also showed a large shift in retention time from the derivatized protein at 18.9 min to the new elution time of the conjugate at 13 min. Both conjugate peaks exhibited a slight shouldering that suggested the formation of a lower molecular weight conjugate (as unconjugated saccharide is not UV active). The intensity and area under the conjugate peaks suggested that a greater amount of conjugate was formed in the NaCl solution than in the MES buffer. Both conjugate chromatograms revealed that trace amounts of unconjugated protein remained after the two hour reaction, with a peak elution at 18.9 min.

6.2.2 EDC conjugations to TT

As conjugation to BSA was successful, investigations focussed on the conjugation of Pn1 PS to tetanus toxoid.

Tetanus Toxoid is currently one of the few proteins used clinically as a carrier in commercially available conjugate vaccines as well as in several vaccines undergoing clinical trials. In terms of *Streptococcus pneumoniae,* GSK have used TT as a carrier protein for serotype 18C in their 10 valent conjugate vaccine: Synflorix [386]. TT is also widely used in commercially available Hib vaccines as well as conjugate vaccines against MenC including GSK's tetravalent meningococcal vaccine Nimenrix [407, 423].

With the successful activation of the tetanus toxoid determined (Chapter 5, Section 5.4.1); the EDC conjugation method was applied to the derivatized TT in order to develop a Pn1–TT conjugate.

The conjugation reaction was carried out as described with BSA where size reduced Pn1 and derivatized TT were combined, followed by the addition of EDC. Derivatized TT must be kept at a high pH to avoid precipitation and as such the pH of the PS:protein combination was lowered to 6.85 with 0.1 M HCl (pH 6.85 is at the upper working range of EDC). The conjugation was monitored by SEC–HPLC at 1, 2 and 5 hours. Reaction variables are summarised in Table 6.7.

Table 6.7. Reaction variables for the EDC conjugation of Pn1 and derivatized TT.

Pn1/protein mass ratio	Pn1:TT pH	Pn1/EDC molar ratio	Reaction time (hr.)
1:2	6.85	1:10	5

The RID chromatograms in Figure 6.11 track the conjugation reaction over a period of five hours. Pn1 PS eluted at 14.2 min and the conjugate formation was seen with small shifts in elution time to 13.9, 13.9 and 14.0 minutes seen for the 1 hour, 2 hour and 5 hour reactions respectively, thereby indicating that no significant amounts of conjugation had formed. The peak eluted at 17.7 min in all three conjugate samples corresponded to unreacted TT protein. The UV chromatograms showed a large amount of free protein remaining after a reaction time of 5 hours. A small amount of higher molecular weight compound eluted at 13.3 min. This peak increased in intensity and area over time which was indicative of the slow formation of conjugate. Whilst the species eluted in the range of the conjugate (13 – 14 min) it could not be identified conclusively as conjugate or as aggregated protein without further analysis.

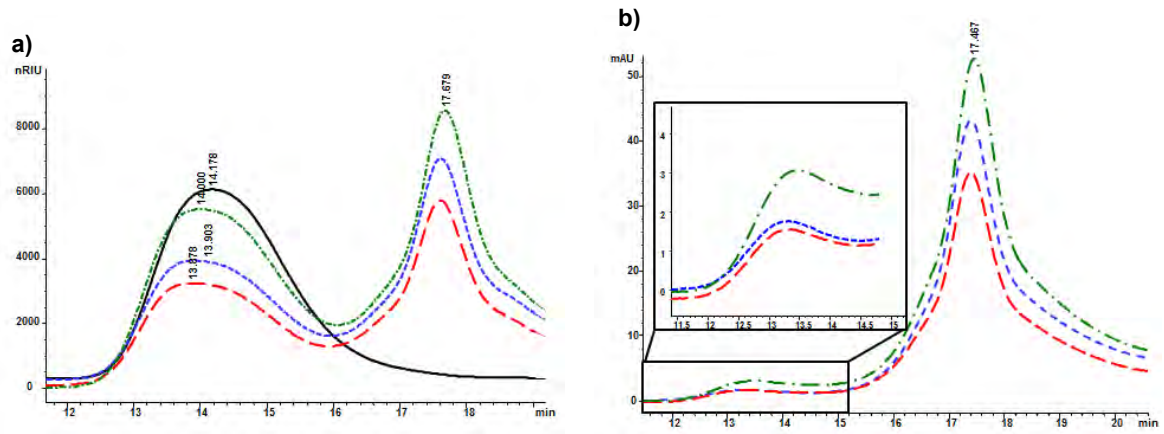

Figure 6.11. SEC–HPLC a) RID and b) UV 280 nm chromatograms of Reaction 2, Pn1_EDC_TT, traced over a period of time: 1 hr. (blue), 2 hr. (red) and 5 hours (green). Pn1 polysaccharide (black) is shown as a comparison in the RID chromatogram.

The conjugate was left to react over 24 hours where a large amount of precipitate was seen to have formed. The sample was centrifuged to pellet out the precipitate and the clear supernatant was analysed by SEC–HPLC. The chromatograms for the supernatant of the overnight conjugate are shown in Figure 6.12. The RID chromatogram compared the conjugate with unconjugated Pn1 PS; a small shift in elution time from the polysaccharide at 14.2 min to 14.0 min occurred, this was suggestive of conjugation, however, a large amount of free protein was present in the RID signal at 17.9 min. The UV profile confirmed the suggestions made in the RID chromatograms; a small peak was seen at 14 min that suggested either a small amount of conjugation had taken place or aggregation of the derivatized protein had occurred. In order to analyse the pellet by SEC–HPLC, different solvents were used to dissolve it; a low pH (0.1 M MES, pH 5.5), pH neutral (water) and high pH buffer (30mM NaCl/3mM Na_2CO_3, pH 10.5) were tested. The pellet was barely soluble in any of the solvents but the high pH buffer partially dissolved the pellet and this was analysed by SEC–HPLC. The RID and UV chromatograms for the pellet in the three different solvents are displayed in Figure 6.12c and d.

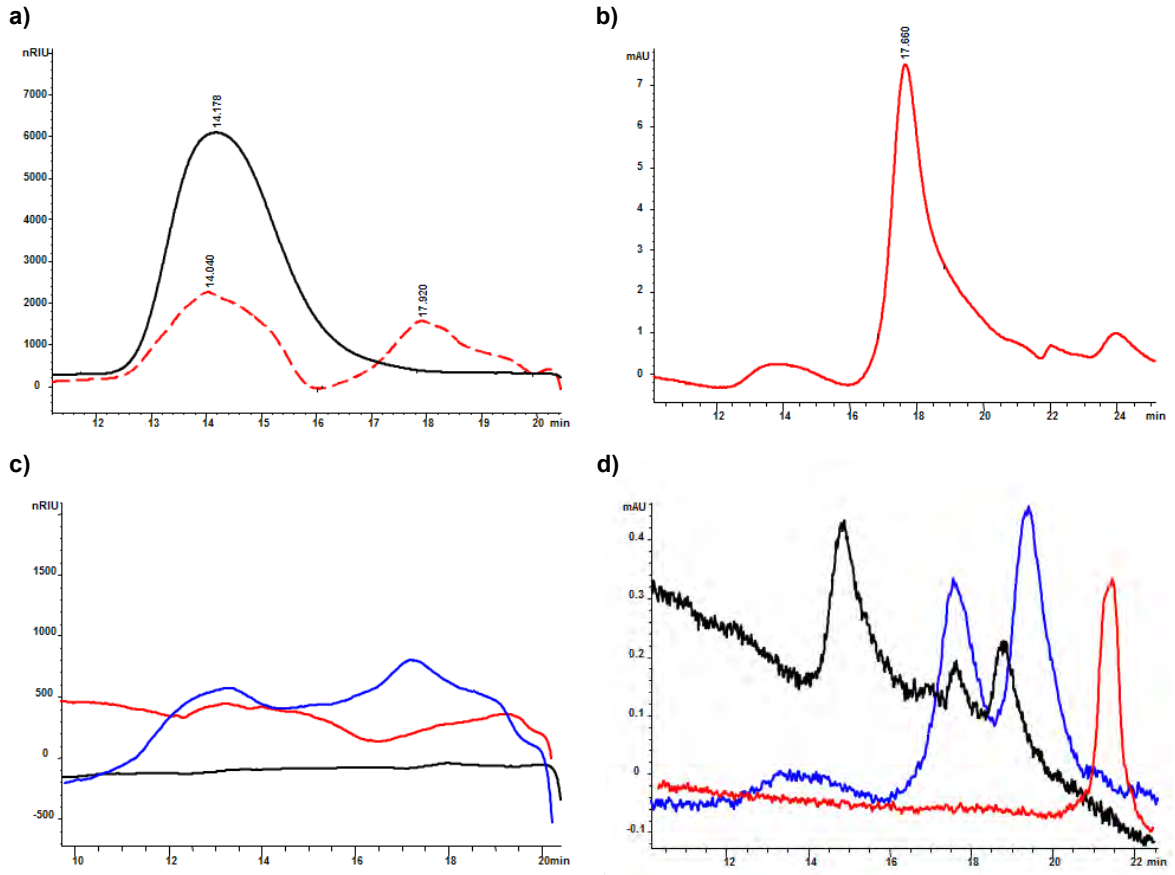

Figure 6.12. SEC–HPLC a) RID and b) UV 280 nm chromatograms of Pn1_EDC_TT supernatant (red) compared to Pn1 polysaccharide (black) as well as the a) RID and b) UV 280 nm chromatograms of pellet dissolved in various buffered solutions. Black–0.1 M MES buffer pH 5.5, blue–in water, and red–30 mM NaCl/3 mM Na_2CO_3 pH 10.5.

The RID chromatograms of the pellet dissolved in the low or high pH buffers showed no trace of polysaccharide or protein. The pellet dissolved in water showed trace amounts of conjugate and unconjugated protein. Minimal conjugate was observed in the UV chromatogram of the MES buffer and trace amounts of protein and reagents were eluted in the additional two solutions.

As seen from the results above, significant conjugation was not achieved with tetanus toxoid as a protein carrier and alternative strategies had to be investigated to achieve a successful conjugation of Pn1 PS and TT.

6.3 Activator chemistry

There are a number of reasons hypothesised as to why EDC was not successful in the TT conjugation reactions:

- Pn1 has both carboxyl and amine groups on its repeating unit and cross linking of the polysaccharide could account for a small amount of precipitation (seen both in the BSA and TT reactions). TT itself has a large number of carboxyl groups and

derivatization is not fully complete, thus carboxyl groups may still be found on the surface of the protein. These groups could react with the amino groups or the derivatized hydrazide groups also found on the protein which will cause the protein to precipitate out.

- The active ester formed by the reaction of the carboxyl group on the polysaccharide with EDC reacts very slowly with amines and can hydrolyse in aqueous solutions [455]. If the amine target is not reacted with the activated carboxylate before it hydrolyses the desired conjugate cannot form. This is especially the case when the amine target is in low concentrations in water as is the case with most protein molecules.
- In addition to reacting with carboxyl groups, EDC is known to form stable complexes with any exposed sulfhydryl groups [466] as well as tyrosine residues, most likely through the phenolate ionized form of its side chain [467].
- Hydrolysis by water is a major competing reaction as it both inactivates the EDC itself and it can also cleave the activated ester thereby forming an isourea and regenerating the carboxylate group [460].

Alternate reaction methodologies were sought in order to circumvent the problems of EDC conjugations. The addition of an activator would produce a more stable active ester as well as generating a better electrophile that is more susceptible to nucleophilic attack by the hydrazide–derivatized protein [400, 456]. The concentration of the added activator is usually much greater than that of the amine containing compound hence the reaction will proceed through the active ester intermediate, however, the final product of this two–step reaction is identical to that obtained with EDC alone in that a stable amide bond is formed between the carboxylate group on one compound with the amine group on another [400].

6.3.1 HOBt activator chemistry

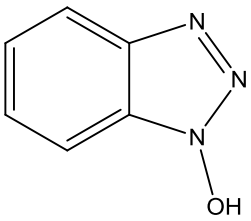

Figure 6.13. Molecular structure of 1–hydroxybenzotriazole (HOBt).

1–Hydroxybenzotriazole (HOBt) (Figure 6.13) is a widely used activating group for the construction of an amide bond during peptide and β–lactam antibiotic synthesis [333, 468, 469]. HOBt works by creating an active ester intermediate of the polysaccharide which would react with the amine groups on a protein carrier creating a conjugate. Active esters of HOBt

have also been employed in the formation of a C–C bond during the preparation of the antibiotic malonomicin [470]. Chan and Cox (2008) determined that the reaction rates of conjugation were independent of HOBt and that the rate limiting step was the reaction between the carboxylic acid group and EDC during the formation of the *O*–acylisourea. However it was determined that a high yields of amide formation was found in the presence of HOBt and very poor conversion rates to the amide in HOBt's absence [468].

The decision to make use of HOBt mediated coupling came from the article by Bulpitt and Aeschlimann (1999) when they used HOBt/EDC to couple hyaluronic acid (HA) to different amines [471]. The degree of derivatization of HA could be controlled and varied in the range of 10 – 70 % depending on the nature of the amine containing nucleophile. The derivatized HA compounds were reacted together to form hydrogels using gluteraldehyde, hydrazide and *N*–hydroxysuccinimide esters to a degree of between 10 % and 25 %. These hydrogels were infiltrated by cells and supported growth factor – induced remodelling in the rat ectopic bone formation. Hydrogels formed with the highly derivatized HA compounds were found to be anti–adhesive to cells and could be used to generate tissue separations and prevent adhesions following surgery [471].

The mechanistic details of a HOBt mediated conjugation (Figure 6.14), begin with the formation of the reactive *O*–acylisourea intermediate is by reacting EDC with the carboxyl functional group on one compound. This intermediate is reacted almost instantaneously with the HOBt to form a HOBt active ester and the EDC by–product. Two different active esters can be formed with HOBt. The two different esters, one being the *O*–acyl derivative and the other the *N*–acyl derivative were investigated by Brink *et al.* [472]. The kinetics of the reaction suggested that the O–acyl active ester is more likely to form and the mixture will isomerise almost completely into the *N*–acyl derivative over time [470]. Sterically hindered molecules also mainly produced the *O*–acyl derivative which suggested that the *N*–acyl isomer has greater steric limitations on its formation, and therefore bulkier substrates would favour the extra atom between the HOBt rings and form the *O*–acyl isomer. The initial formation of the *O*–acyl isomer proposes that the reaction at the oxygen atom goes through a lower activation energy path than the ring nitrogen due to the more available steric approach, while the eventual formation of the more stable *N*–acyl derivative is suggestive of the thermodynamic product [473].

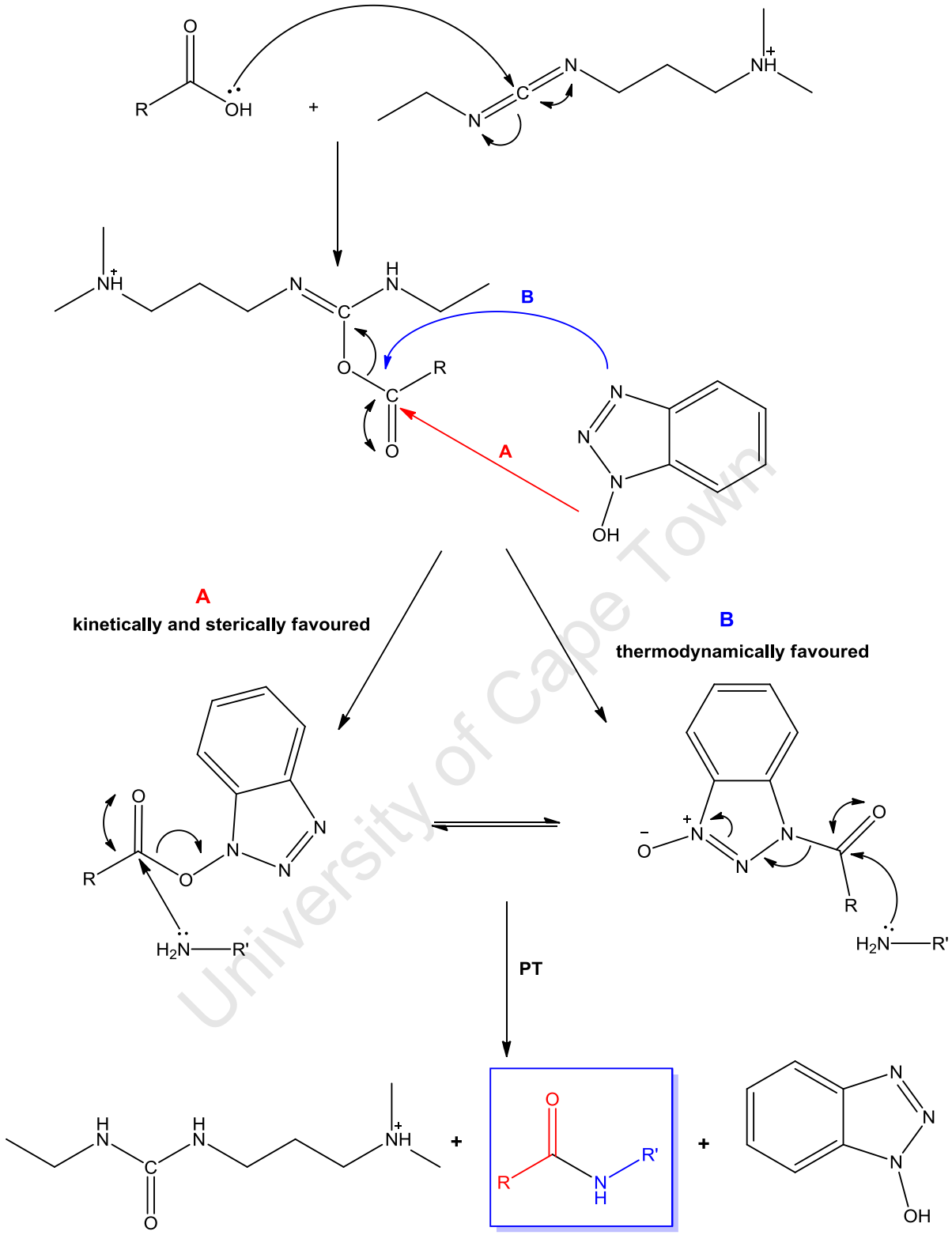

Figure 6.14. Representative reaction steps taken in the HOBt mediated conjugation between a carboxyl and amine group. I) Creation of an *O*–acylisourea intermediate, II) formation of the HOBt active ester, III) creation of the amide bond linkage.

The preference for *O*–acylation corresponds to the change in relative tautomerization of the HOBt nucleophile in solution during the course of the reaction [474]. This is an example of the Curtin–Hammett principle (Figure 6.15) which states that the relative energies of the

transitions states control the selectivity of the reaction rather than the relative energies of the starting materials [472, 475]. It is also theorised that the *O*–acyl derivative is more electrophilic and hence more susceptible to nucleophilic attack than the *N*–acyl derivative [473, 476].

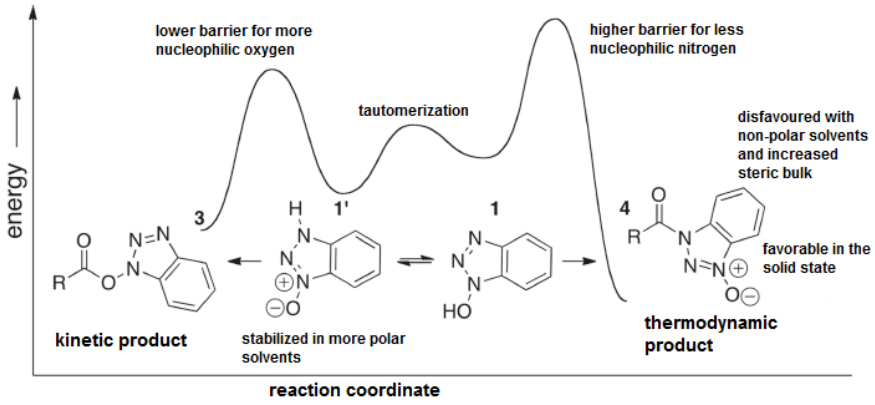

Figure 6.15. The Curtin–Hammett equilibrium of HOBt tautomers and acylated HOBt adducts [472].

With the unsuccessful conjugation of derivatized TT with Pn1 using the EDC coupling technology, an EDC mediated coupling conjugation procedure using HOBt was investigated. As the conjugation with BSA using the EDC coupling technology was successful it was thought that the formation of an active ester with the carboxyl groups found in Pn1 would drive the reaction between an amine group and the active ester intermediate.

Three protein carriers were investigated, i.e. TT, CRM_{197} and PLD; the majority of the reactions were carried out using TT. Most investigations were performed on small scale (25 – 50 mg) and involved establishing whether the use of HOBt would significantly enhance conjugate formation. Once this was established, investigations into the initial polysaccharide and protein mass ratios were performed, the pH of the mixture of Pn1 and protein was optimised to reduce precipitation and the pH of the EDC/HOBt reactant mixture was also optimised to reduce precipitation. Once the process parameters were established with TT as the carrier protein the methodology was applied to other protein carriers with the view of comparing the highest yielding protein carrier with commercially available conjugate vaccines in animal studies.

6.3.1.1 HOBt mediated conjugations to TT

Nine conjugates were prepared using Pn1, TT and EDC/HOBt. Table 6.8 details the process parameters. Derivatized and underivatized protein was compared as well as different polysaccharide to protein ratios, polysaccharide to EDC/HOBt mass ratios and pH adjustments.

Table 6.8. Polysaccharide and protein variables for Reactions 1 – 9 employing HOBt mediated coupling.

Reaction	PS – Protein mass ratio	Protein derivatized (Yes/No)	Protein pH	pH of protein – Pn1 mixture	Pn1/HOBt molar ratio	EDC/HOBt molar ratio	EDC/HOBt pH
1	1:5	No	6.80	n/a	1:6.4	1:1	None
2	1:5	Yes (16.1 %)	6.80	n/a	1:6.4	1:1	None
3	1:3	Yes (17.2 %)	8.00	7.03	1:6.6	1:1	None
4	1:3	Yes (17.2 %)	8.00	7.12	1:12.9	1:1	7.10
5	1:1	Yes	8.5	8.04	1:6.2	1:1	6.70
6	2:1	Yes	8.5	7.84	1:6.2	1:1	6.70
7	0.5:1	Yes	8.5	7.84	1:6.2	1:1	6.70
8	1:1	Yes (16.2 %)	9.62	7.54	1:6.3	1:1	6.80
9	2:1	Yes (16.6 %)	7.56	7.44	1:6.5	1:1.3	6.80

The first two reactions were performed in order to investigate whether the carrier protein could be conjugated to the polysaccharide without protein derivatization. Reactions 1 and 2 were performed using the same process parameters, differing only in the use of native (Reaction 1) and derivatized (Reaction 2) protein. The pH of the derivatized protein was first lowered from 10.5 to 6.8 before addition to the polysaccharide. In a separate reaction vessel EDC and HOBt were dissolved in a 1:1 solution of water and dimethylsulfoxide (DMSO). The EDC and HOBt mixture was added drop–wise to the polysaccharide–protein solution and the reaction was left to proceed overnight with slow, continuous mixing. Small amounts of precipitation were seen during the addition of the reagents. Samples of each reaction were taken for SEC–HPLC analysis before the reactions were dialysed with 0.2 M NaCl.

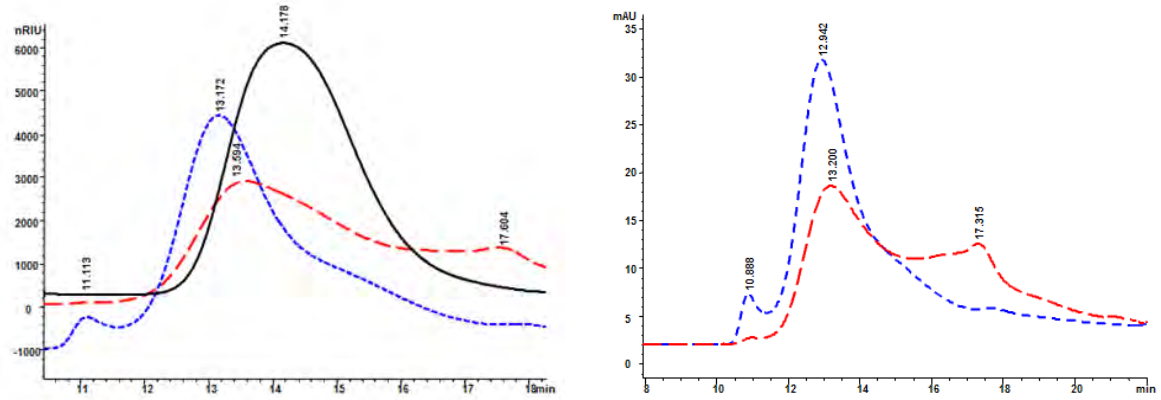

Figure 6.16. SEC–HPLC RID (a) and UV 280 nm (b) chromatograms of Pn1_HOBt_TT using underivatized TT (Reaction 1 – red) and derivatized TT (Reaction 2 – blue). Pn1 polysaccharide (black) is shown for comparison.

The RID profiles of both Reactions 1 and 2 (Figure 6.16a) exhibit a shift in elution time of the Pn1 PS from 14.2 min to 13.6 min and 13.2 minutes for the underivatized and derivatized TT reactions respectively, thus indicating the presence of conjugate. The conjugate prepared using underivatized TT exhibited a broad shoulder to the right that is an indication of the presence of unconjugated saccharide. There was also a peak eluting at 17.8 min which is indicative of unconjugated TT present in the sample. The conjugate prepared with the derivatized protein displayed a much sharper peak eluting at 13.2 min thus suggesting a larger molecular weight conjugate had been formed when compared to that of the underivatized protein. The conjugate peak also displayed a shoulder towards the lower molecular weight range which was suggestive of unconjugated polysaccharide. The peak eluting at 11.1 min seen in the derivatized protein conjugate was considered an artefact as it was not seen in the dialysed sample.

The UV profiles of the conjugates are presented in Figure 6.16b. Both conjugates exhibited a main peak at 13 min corresponding to the conjugate. The conjugate prepared with the underivatized protein (Reaction 1) did indicate the presence of unconjugated protein with a peak seen at 17.3 min. Reaction 2, using the derivatized protein showed a sharp peak at 12.9 with a small shoulder on the low molecular weight (right–hand) side which suggested a lower molecular weight conjugate could have formed. It may also suggest that the reaction had not proceeded to completion. As the Pn1 PS is not UV active this shoulder was not indicative of unconjugated saccharide. Trace amounts of unconjugated protein could be seen at 17.5 min and the peak eluting at 10.89 min was removed with dialysis. SEC–HPLC analysis of these two reactions suggested that higher conjugation efficiencies had occurred using derivatized protein.

The next two reactions were performed to determine whether adjustment of pH of the EDC/HOBt mixture would play a role before addition to the polysaccharide/protein mixture as

well as if the reagents were added in sufficient excess. The water/DMSO solution, which lowered the pH of the EDC/HOBt mixture, has a low pH (± 5.18) and was thought to contribute to the instability of the derivatized TT. Reaction 3 was performed with no adjustment of the reagents' pH where the pH of Reaction 4's reagents was adjusted to pH 7.10 before its addition to the polysaccharide/protein mixture. The reagents in Reaction 4 were added at twice the molar value than in Reaction 3. Full details of the reaction variables are found in Table 6.8.

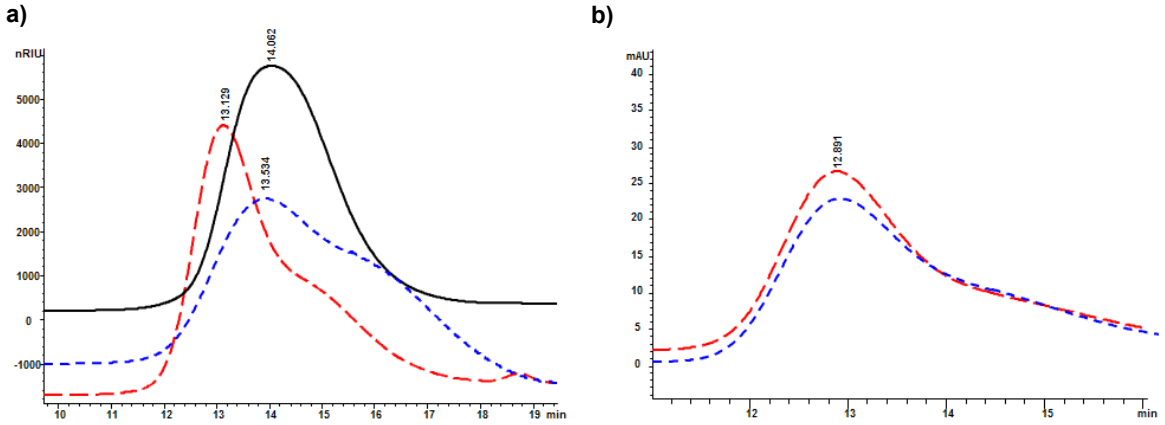

Figure 6.17. SEC–HPLC RID (a) and UV 280 nm (b) chromatograms of Pn1_HOBt_TT conjugates from Reactions 3 (blue) and 4 (red) to determine whether a pH adjustment of the EDC/HOBt mixture was necessary. Pn1 PS (black) is shown for comparison.

Figure 6.17 (a and b) show the RID and UV 280 nm chromatographic signals of Reactions 3 and 4. For Reaction 3 the RID signal showed a slight shift to higher molecular weight material and the UV signal confirmed this with a peak eluting at 12.9 min. The large shoulder on the right of Reaction 3's conjugate peak for the RID signal and the absence of this shoulder in the UV signal suggested that there was unconjugated saccharide or a lower molecular weight conjugate present. A large amount of precipitate was formed during the addition of the reagents as a result of a drop in pH and further analysis was not possible. Reaction 4 displayed a shift in the RID signal to the higher molecular weight range when compared to the Pn1 PS. As with Reaction 3, a shoulder was present on the lower molecular weight side of the conjugate peak which was confirmed to be unconjugated saccharide by the absence of this shoulder in the UV spectrum. The conjugate however, did remain in solution which confirmed that the final pH adjustment of the reaction mixture must be made, after the addition of the activating species.

Purification of Reaction 4 was through a size exclusion S500 column (as performed previously in EDC experiments). Two main peaks eluted in the UV profile of the conjugate (Figure 6.18) which were collected and analysed for conjugated and free saccharide.

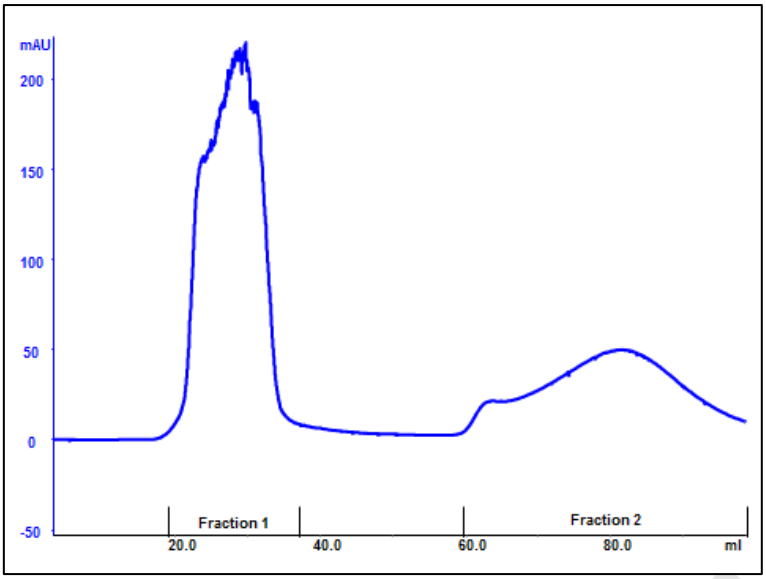

Figure 6.18. Sephacryl S500HR: UV 280 nm chromatogram of Reaction 4. The UV (blue) and conductivity (red) profiles of the conjugate are shown.

Table 6.9. Colorimetric analysis of total and free saccharide levels in Reaction 4.

Peak	Saccharide	
	Total (mg)	Free (mg)
1	8.47	1.52 (18.0 %)
2	1.12	0.53 (47.3 %)

As shown in Table 6.9, the first peak contained the highest percentage of conjugated saccharide with 82 % of the saccharide eluted as conjugated Pn1. The unconjugated saccharide, eluted in the second peak, was determined with the DOC preparation and subsequent uronic acid assay and found to be 47.3 %.

The initial mass ratio of polysaccharide to protein was investigated to determine which initial ratio would result in the optimal polysaccharide–protein ratio. Reactions 5, 6 and 7 were performed in order to create consistency in the reaction conditions and to evaluate the polysaccharide–protein ratio. In Reaction 5, the polysaccharide to protein mass ratio was 1:1, in Reaction 6 this was 2:1 and Reaction 7 had a 0.5:1 polysaccharide protein mass ratio (Table 6.10).

Table 6.10. Initial polysaccharide and protein mass ratios used in Reactions 5,6 and 7.

Reaction	PS – Protein mass ratio
5	1:1
6	2:1
7	0.5:1

The pH of the protein solution (87.5 mg) was lowered from 10.5 to 8.5 before being divided between the three reactions, according to the initial ratio needed, and added to the polysaccharide. In a separate vial the EDC and DMSO were mixed together and the pH of

the collective activating mixture was raised from 5.11 to 6.70 before being added in equal proportions to the three polysaccharide–protein mixtures. The reaction was left at room temperature for 24 hours, followed by dialysis against 0.2 M NaCl to remove any unreacted reagents.

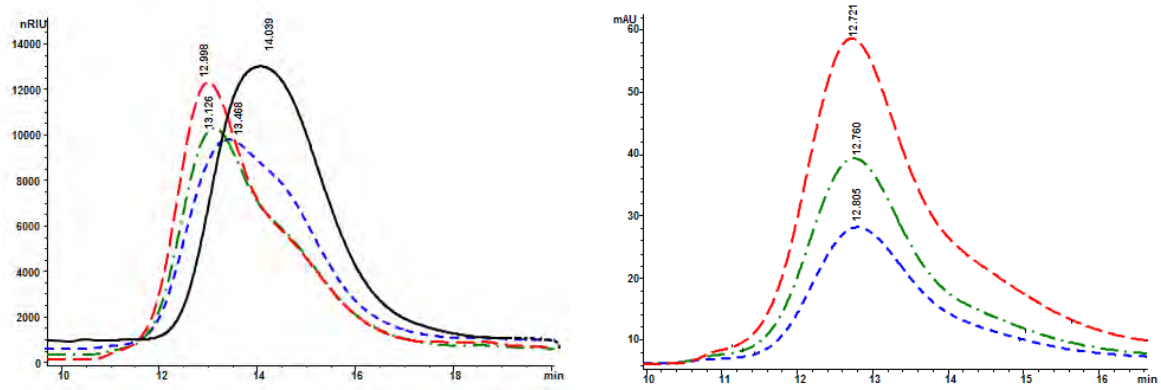

Figure 6.19. SEC–HPLC RID (a) and UV 280 nm (b) chromatograms of Reactions 5 (green), 6 (blue) and 7 (red) producing the Pn1_HOBt_TT conjugates. Pn1 PS (black) serves as a comparison.

The peaks in the RID chromatograms in Figure 6.19 exhibited the formation of the conjugates for all three reactions. They showed a large shift in the elution time compared to the size reduced Pn1 elution. The broad shape of Reaction 6 (2:1 Pn1:TT mass ratio) suggested that either a large quantity of polysaccharide remained unreacted or that the molecular weight range of the conjugate was broad. The peak shapes for Reactions 5 and 7 were identical and a small amount of unconjugated saccharide remained. The peaks displayed in the UV chromatogram at 280 nm all depicted the formation of the conjugate at approximately 12.8 min. The difference in the intensity of the three peaks was due to the concentration of polysaccharide and protein present in each reaction. The peaks all showed similar shapes with a slight broadening suggestive of the formation of a range of different molecular weight conjugates. Purification using a Sephacryl S500 HR column and subsequent saccharide and protein analysis was performed on all three reactions.

The representative elution profile, monitored at 280 nm for the three reactions (Figure 6.20) revealed one large peak of higher molecular weight with a shoulder to the right and one peak of smaller molecular weight. It was previously shown that the small peak was most likely due to unconjugated polysaccharide, and/or unreacted reagents so as a result, Fraction 4 was not subjected to testing. The large, shouldered peak was collected in three fractions and assayed for protein and saccharide composition.

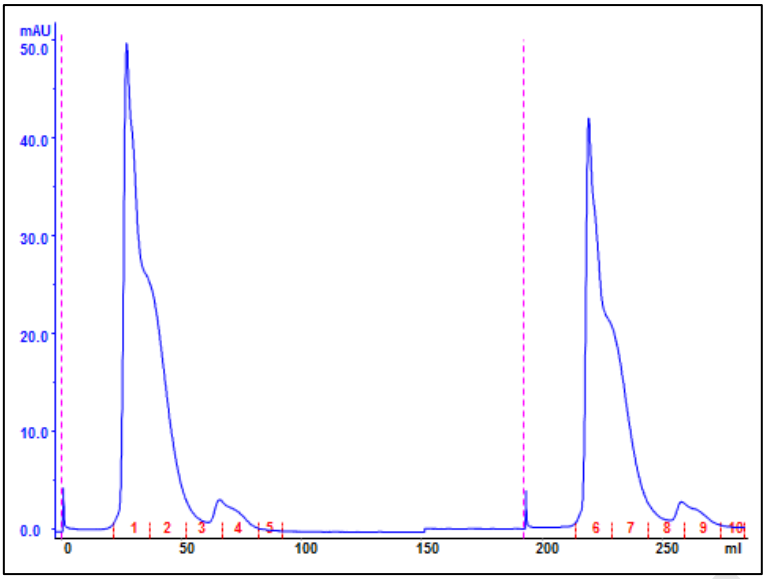

Figure 6.20. Sephacryl S500 HR: UV 280 nm representative profile of Reactions 5 – 7.

Table 6.11. Saccharide and protein results of fractions collected for Reactions 5, 6 and 7.

Reaction	Initial PS:Protein ratio	Fraction	Total saccharide (mg)	Free saccharide	Protein (mg)	PS:Protein ratio
5	1:1	1	2.92	0.45 mg (15 %)	4.14	0.60
		2	4.67	1.34 mg (29 %)	1.78	1.87
		3	0.31	0.23 mg (74 %)	0.24	0.33
6	2:1	1	1.62	0.49 mg (30 %)	2.61	0.43
		2	4.60	1.37 mg (30 %)	0.68	4.75
		3	0.73	0.09 mg (12 %)	0.18	3.56
7	0.5:1	1	3.14	0.25 mg (8 %)	10.41	0.28
		2	5.32	0.54 mg (10 %)	5.63	0.85
		3	0.74	0.34 mg (46 %)	0.95	0.72

The results in Table 6.11 confirmed that the majority of the polysaccharide and protein eluted in the first two fractions for all three reactions with the majority of the protein found in the first fraction and the bulk of the polysaccharide in the second fraction. The levels of free saccharide were also lower in the first two fractions than the third suggesting that the third fraction mainly contained unreacted polysaccharide. A summary of the free saccharide and conjugation efficiencies can be found in Table 6.12. The final protein to polysaccharide ratio of all three reactions were comparable to their initial ratios with Reaction 5 exhibiting a final protein to polysaccharide ratio of 0.95:1, Reaction 6 presenting a final ratio of 1.44:1 and Reaction 7 resulted in a final ratio of 0.47 mg polysaccharide to every mg of protein. In terms of conjugation efficiency, Reaction 7 gave the best conjugation efficiency of 32.3 %, with the lowest efficiency of 20 % resulting from Reaction 6 It is hypothesised that the greater the

amount of polysaccharide, the greater the potential for cross–linking within the saccharide and hence less is available for conjugation to the protein.

Table 6.12. Conjugation efficiencies and final Ps: Protein ratios for Reactions 5, 6 and 7.

Reaction	Ps: Protein ratio (initial)	Total saccharide (mg)	Free saccharide	Protein (mg)	PS:Protein ratio (final)	Conjugation efficiency (%)
5	1:1	7.90	2.02 mg (26 %)	6.16	0.95	23.5
6	2:1	6.95	1.95 mg (28 %)	3.47	1.44	20.0
7	0.5:1	9.20	1.13 mg (12 %)	16.99	0.47	32.3

Reactions 8 and 9 were performed on a larger scale than the preceding reactions in order to investigate the issues with precipitation as well as to confirm that the conjugation reaction was scalable. As the protein supply was limited, a large scale reaction with a polysaccharide to protein ratio of 1:2 was not performed. Reaction 8 was performed on a 1:1 polysaccharide: protein mass scale with both EDC and HOBt added in a 6.3 molar excess. Reaction 9 was performed on a 2:1 polysaccharide–protein mass scale as this was determined to be the optimal ratio used in other conjugation strategies. EDC and HOBt were added in a 5 and 6.5 molar excess respectively and the pH of both activating mixtures was raised to 6.8 before addition to the polysaccharide and protein mixture.

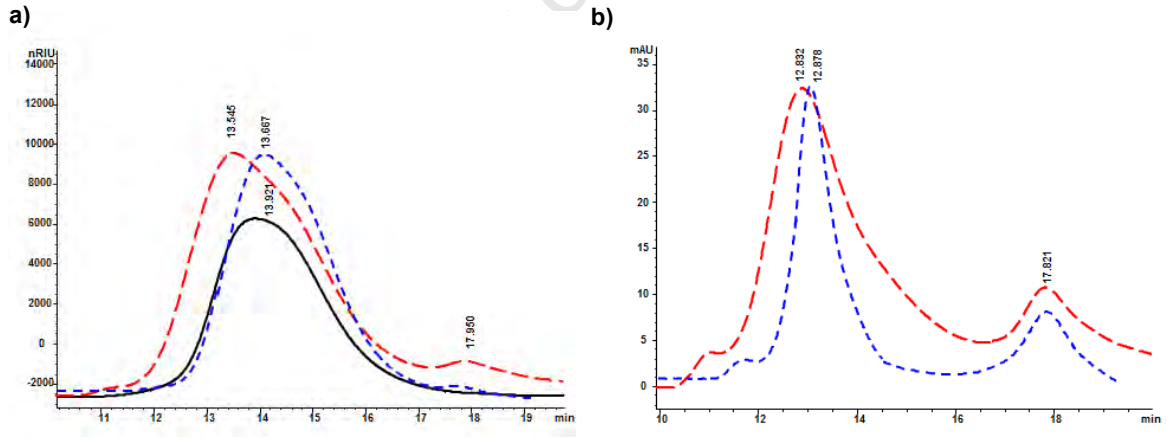

Figure 6.21. SEC–HPLC RID and UV 280 nm chromatograms of the Pn1_HOBt_TT conjugate Reaction 8 (red) compared to Reaction 9 (blue) and the Pn1 PS (black).

The RID profile for Reaction 8 together with the UV280 signal (Figure 6.21) presented a peak at 12.8 min that is attributed to the formation of a conjugate. The results also confirmed that not all the protein had been consumed during the course of the reaction. Reaction 9 contained an initial polysaccharide to protein mass ratio of 2:1 and again, both the RID and UV280 profile revealed the formation of a conjugate peak; the RID elution time slightly later at 13.6 min than the UV280 peak at 12.9 min. The peak at approximately 18 min indicates the presence of free protein. No precipitation was observed and this was attributed to the

reaction conditions employed. The relative small volume of protein at high pH and much larger volume of buffered Pn1 solution at a lower pH, meant that the addition of the two did not lead to a drastic change in pH and hence precipitation of the protein. These results suggest that the precipitate was a result of the smaller scale reactions. Continuous monitoring of the pH must be observed as conjugation is favourable at a pH under 7.

Both reaction products were subjected to purification using the S500 HR packing material connecting to the ÄKTA FPLC system. The UV profile of Reaction 8 (Figure 6.22a) revealed a small peak between 20 – 40 ml and a large peak between 60 – 100 ml. Fractions 2 – 7 were analysed on the SEC–HPLC as well as with colorimetric assays to determine the total protein, total saccharide as well as the percentage free saccharide in each fraction. The UV profile of Reaction 9 (Figure 6.22b) also displayed two peaks, but, due to the intensity of the second peak, the first peak in the chromatogram appears insignificant. Fractions were collected and analysed as per Reaction 8.

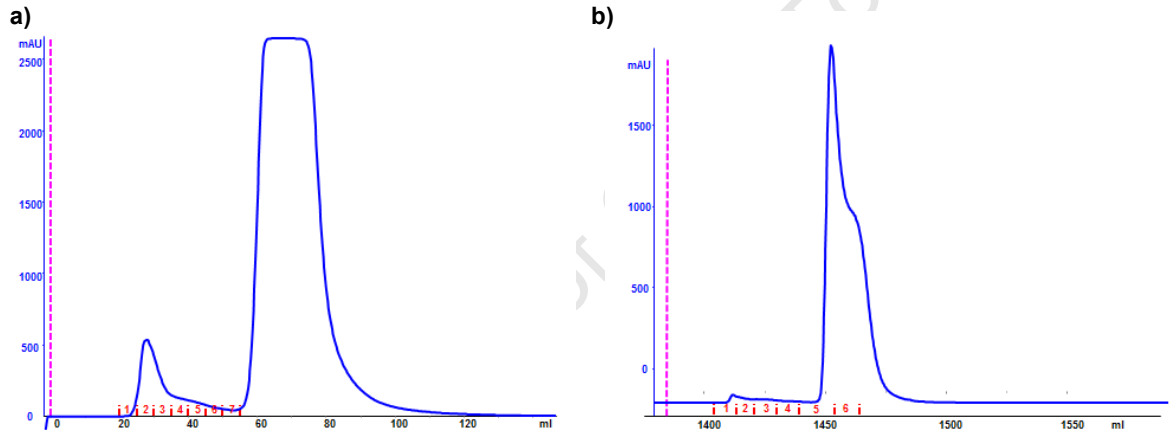

Figure 6.22. Sephacryl S500 HR UV 280 nm elution profile of a) Reaction 8 and b) Reaction 9.

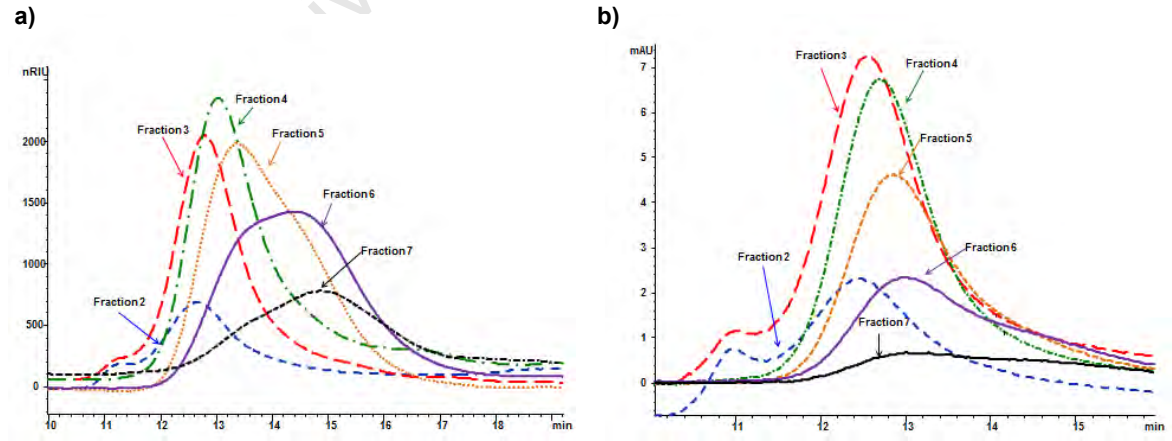

Figure 6.23. SEC–HPLC a) RID and b) UV280 chromatograms of the Fractions 2 (blue), 3 (red), 4 (green), 5 (orange), 6 (purple) and 7 (black) of Reaction 8, collected on Sephacryl S500HR column.

The results of the chromatographic analysis (Figure 6.23) and colorimetric assays (Table 6.13) for Reaction 8 revealed the presence of polysaccharide and protein in all fractions. The highest percentage saccharide concentration was found in Fractions 4, 5 and 6. The protein

concentrations confirm the higher levels of proteins in the first peak. The second peak was theorised to contain a mixture of HOBt and free protein as the protein assay result could not account for the very intense UV peak following S500 purification. The DOC preparation for free saccharide was performed and the resulting assay confirmed the presence of free saccharide in all fractions. Fractions 2 and 3 exhibited a very small amount of free saccharide, with Fractions 4, 5 and 6 each containing a free saccharide percentage of above 30 %.

Table 6.13. Analytical assay results to determine final polysaccharide–protein ratios and conjugation efficiency for Reaction 8.

Fraction	Elution Time (min)		Total saccharide (mg)	Free saccharide (mg)	Protein (mg)	PS:Protein ratio	Conjugation efficiency (%)
	RID	UV					
2	12.76	12.40	8.35	0.40 (5 %)	44.11	0.18	
3	12.85	12.56	14.98	2.53 (17 %)	37.72	0.33	
4	12.92	12.69	22.33	7.09 (32 %)	18.95	0.80	
5	13.37	12.82	33.43	16.34 (49 %)	14.38	1.18	
6	14.18	13.08	33.00	17.99 (55 %)	9.70	1.54	
7	14.83	13.00	17.57	9.78 (56 %)	5.76	1.35	
TOTAL	–		129.66	54.13 (42 %)	130.62*	**	38

*Overestimation as only 100 mg protein used (unreacted matrix interference).
**Not determined as incorrect value for protein calculated.

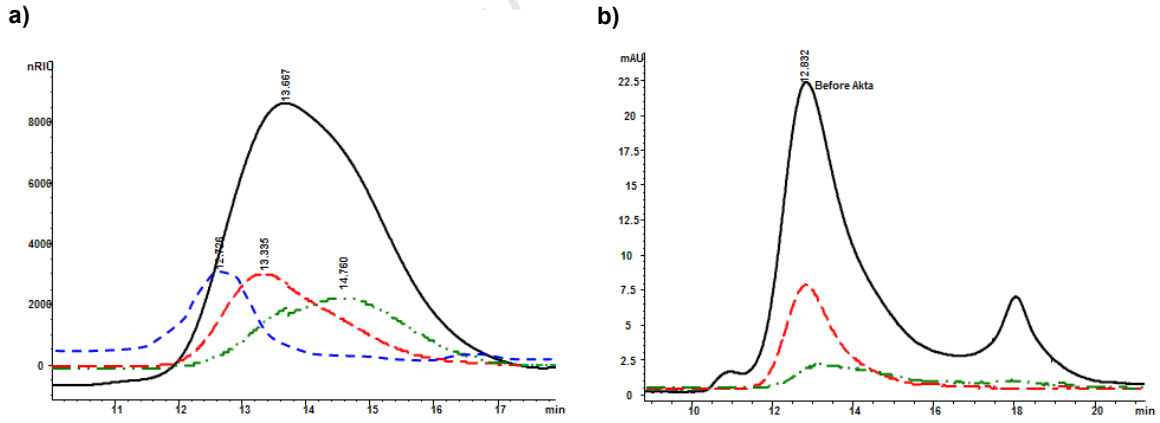

Figure 6.24. SEC–HPLC a) RID and b) UV 280 nm chromatogram of Reaction 9 (black) and the fractions collected after purification on S500 HR. Fraction 1 (blue), Fraction 2 (red) and Fraction 3 (green) are shown.

Figure 6.24 details the SEC–HPLC RID and UV profiles of Reaction 9 as well as the fractions collected after separation on the S500 HR column. Fractions 1, 2 and 3 were the only fractions to show any trace of saccharide or protein where Fraction 1 contained the highest molecular weight material although not enough conjugate was eluted to assay for free and total saccharide content. Fraction 2 was hypothesised to contain most of the conjugate as it had showed a significant elution in both the RID and UV traces.

The results of the colorimetric assays for the two main fractions are tabulated in Table 6.14. Fractions 1 – 3 tested positive for saccharide with no saccharide present in Fractions 4 and 5. The UV chromatogram (absorbance at 279 nm) was positive for all fractions however Fractions 4 and 5 suggest the presence of HOBt. The DOC preparation for free saccharide was performed on Fractions 2 and 3 and the resulting assay confirmed free saccharide in both fractions. The percentage free saccharide in both these fractions was very high. This, along with the HPLC profiles, suggested that the reaction may not have worked. The total conjugation efficiency for this reaction was 27.25 %, however, the final PS:protein ratio was approximately 1.1 which was an optimal conjugation ratio.

Table 6.14. Analytical assays for the collected fractions of Reaction 9, with calculated conjugation efficiency and polysaccharide–protein ratios.

Fraction	Total saccharide (mg)	Free saccharide (mg)	Protein (mg)	PS:Protein ratio	Conjugation efficiency (%)
2	26.82	10.19 (38 %)	14.67	1.13	–
3	24.96	14.34 (58 %)	9.94	1.06	–
Total	51.78	24.53 (48 %)	24.61	1.10	27.25

6.3.1.2 Summary of HOBt conjugations with TT

The conjugations of Pn1 to the TT were successful only when HOBt was added to the EDC conjugation technique. By visual comparison of the chromatograms of the EDC and HOBt reactions a clear shift in retention time in both the RID and UV signals can be seen for the HOBt reactions. It was found that the HOBt/EDC mixture had to be pH controlled as when it was added to the reaction mixture the pH of the reaction mixture was lowered past the isoelectric point of TT resulting in precipitation. When this pH was controlled in the subsequent TT all reactants remained in solution and no precipitate was observed. On the small scale, the optimal reaction (Reaction 7) showed the lowest free saccharide (12 %) and highest conjugation efficiency (32.3 %). The protein to polysaccharide ratio was on the low side (0.47) due to the larger amount of protein used. In the larger scale reactions, the limited amount of protein meant that only two reactions could be performed. Reactions 8 and 9 showed similarities in the free saccharide amount (42 % vs. 48 %) but accurate protein values could not be determined for Reaction 8 due to matrix interferences. The conjugation efficiency of Reaction 8 was 38 %, higher than that of 27 % for Reaction 9 but due to the interferences in Reaction 8, this may be inaccurate. These investigations showed that conjugation of Pn1 to a derivatized carrier protein can be achieved using HOBt mediated EDC coupling technology.

6.3.1.3 *HOBt mediated conjugations to CRM_{197}*

CRM_{197} is licensed for human use in several efficacious conjugate vaccines commercially available [175] and used routinely in children. The HOBt conjugation method proven effective with TT as a protein carrier was applied to CRM_{197}.

The reaction variables for the conjugations of Pn1 and derivatized CRM_{197} using the HOBt mediated conjugation methodology are found in Table 6.15. Reaction 1 was performed with a 2:1 initial polysaccharide to protein mass ratio. The protein was derivatized to a very low level of 2.5 %. Reaction 2 was performed on a 2:1 polysaccharide–protein mass ratio with CRM_{197} derivatized to 24.5 %. Both reactions were allowed to proceed overnight followed by extensive dialysis with 10 mM MES/ 0.2 M NaCl (pH 7.2).

Table 6.15. Reaction variables for the conjugation of Pn1 to derivatized CRM_{197} using the HOBt mediated conjugation methodology.

Reaction	Pn1/Protein mass ratio	CRM_{197} derivatization levels	EDC/HOBt molar ratio	Pn1/HOBt molar ratio
1	2:1	2.5	1:1.1	1:12
2	2:1	24.5	1:1	1:6

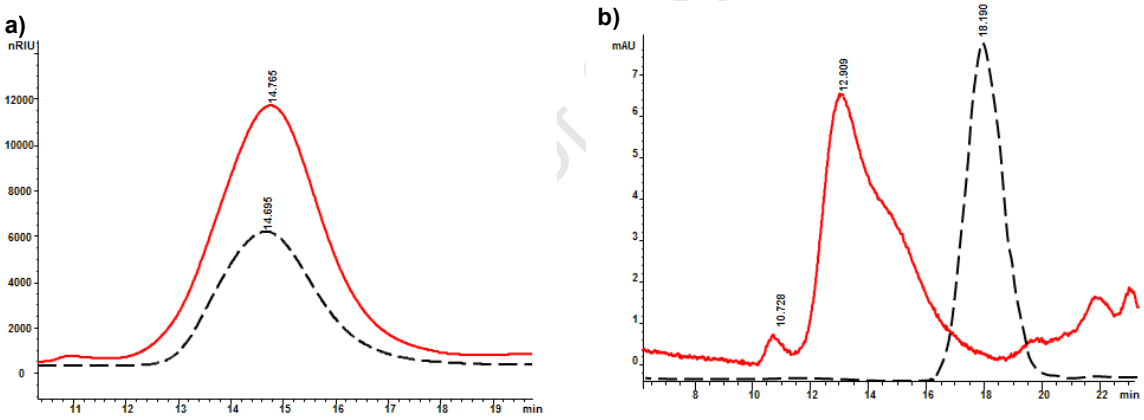

Figure 6.25. SEC–HPLC a) RID and b) UV chromatograms of Pn1 (RID – black) and CRM_{197} (UV – black) and Reaction 1: Pn1_HOBt_CRM_{197} (red).

For Reaction 1 the RID profile in Figure 6.25 did not show a difference in the shift in elution time (and therefore molecular weight) between the polysaccharide and the conjugate. However, a shift was seen in the UV chromatogram with the formation of a conjugate peak at 12.9 min and the disappearance of the peak at 18.1 min. This shift was hypothesised in the TT conjugations to signify successful conjugation. Whilst the disappearance of the peak at 18.3 min is confirmation of the complete consumption of protein, the lack of shift in the RID signal was theorised to be due to unconjugated polysaccharide and required further investigation.

Hydrophobic interaction column (HIC) was investigated as an alternate means of conjugate purification as size exclusion chromatography did not prove to be successful with the TT

conjugations. Underivatized CRM_{197} protein was used in order to explore the optimal conditions for HIC. These investigations are summarised in Table 6.16 (solution A – 1 M $(NH_4)_2SO_4$, and solution B – 0.05 M sodium phosphate buffer (pH 7.0)). Purification of the conjugate was performed on HiTrap 5 ml columns. In the first experiment, step 1 consists of 0.5 M ammonium sulfate but as shown in Figure 6.26a, this was insufficient to successfully bind all of the protein. In the second experiment (Figure 6.26b) 1 M ammonium sulfate binds the protein to the column; this is shown by the absence of the early peak. At a gradient of 50 % B, the protein was released from the column and detected; however, the concentration of the protein (amount loaded) was too small to obtain an adequate profile. The three UV profiles suggest that conditions used in experiment 3, a step–wise elution, reveal the best separation parameters. The initial concentration of ammonium sulfate, determined in experiment 2 to be suitable to allow for binding of the protein to the column, was used. A step–wise elution from 0 to 100 % solution B, was introduced.

Table 6.16. Summary of HIC investigations with solution A: 1 M $(NH_4)_2SO_4$ and solution B: 0.05 M sodium phosphate buffer (pH 7.0). The protein concentration was ~ 2 mg/ml.

Experiment	Step 1		Step 2	Step 3		Injection vol. (µl)
	Solution A	Solution B		Solution A	Solution B	
1	50 %	50 %	Gradient	0 %	100 %	100
2	100 %	0 %	Gradient	0 %	100 %	100
3	100 %	0 %	–	0 %	100 %	500

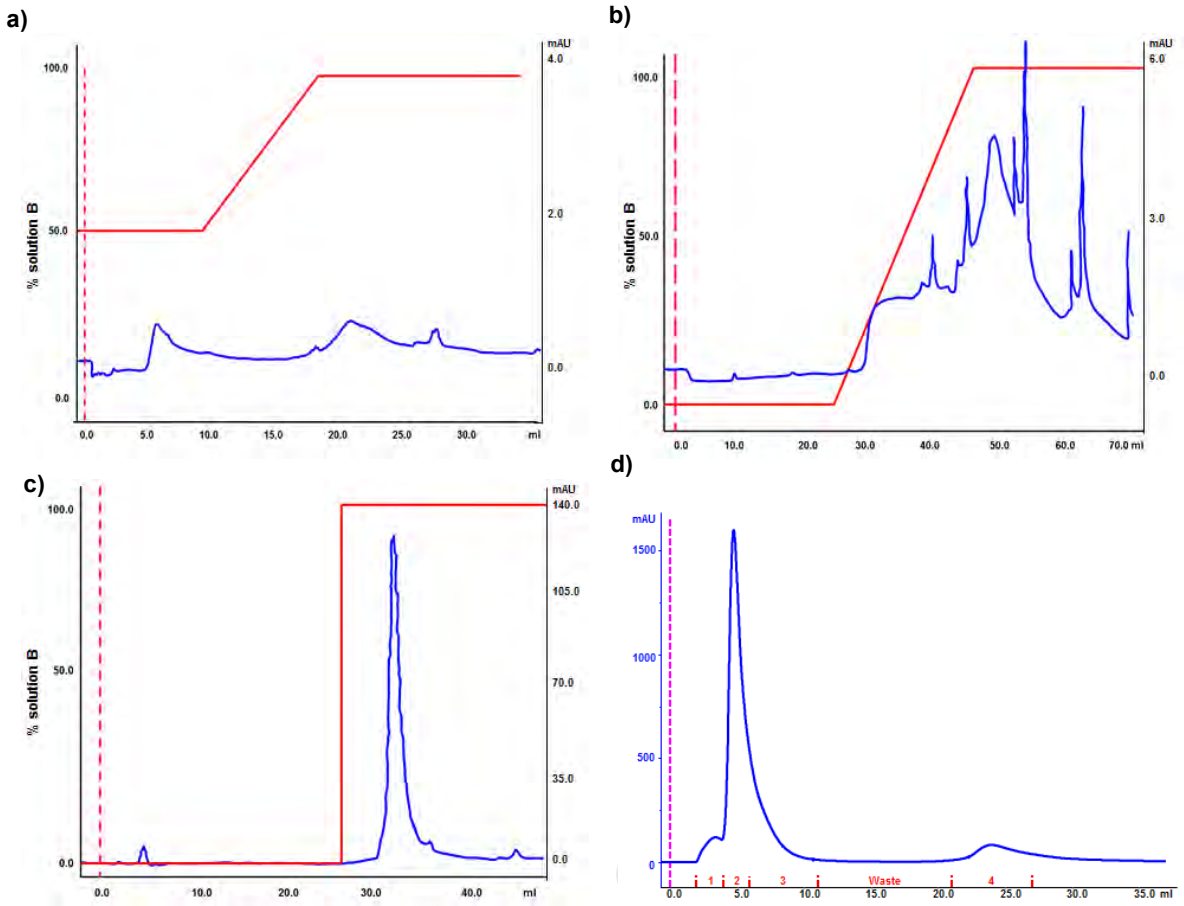

Figure 6.26. UV profile (blue) of HIC experiments 1(a), 2(b) and 3 (c). The red trace shows the gradient elution of solution B. d) the UV profile of the Pn1_HOBt_CRM197 conjugate as well as the fractions collected.

In order to separate sufficient product for further investigation a sample of 1 ml (0.87 mg Pn1) was loaded on the HIC column as shown in Figure 6.26d and the fractions were subsequently analysed for total and free saccharide and protein (Table 6.17).

Table 6.17. Assay results for fractionated Reaction 1 conjugate (1 ml conjugate, 0.87 mg Pn1) showing saccharide and protein results.

Fraction	Total Saccharide (mg)	Free Saccharide	Protein (mg)
1	0.18	77 %	0.200
2	0.19	82 %	0.079
3	0.07	n/a	0.141
4	0.04	n/a	0.189
Total	0.48 (55 %)	62.5 %	0.609

Saccharide and protein were detected in all four fractions collected. Approximately 77 % of the polysaccharide eluted was unconjugated in the first fraction. The large second peak (Fractions 2 and 3) was theorised to contain conjugate with the third peak (Fraction 4) containing only unconjugated protein. The analytical assays revealed that Fraction 4 contained the bulk of the protein with polysaccharide in trace amounts. This indicated that

not all the protein was conjugated, which is in contradiction to the SEC–HPLC chromatogram that proposed that no unconjugated protein was present, although the broadness of the conjugate peak is likely shielding any unconjugated protein. The larger peak contained both polysaccharide and protein although a large amount (82 %) of the polysaccharide eluted was unconjugated.

The profiles (Figure 6.27) of the SEC–HPLC analysis of Reaction 2 show a shift in elution time as previously seen with TT conjugations. The double hump of the conjugate profile in the RID profile indicated either the presence of free saccharide or a bi–modal conjugate of two different molecular weights. The UV profile showed a large shift in elution time from CRM_{197} at 18.12 min to the conjugate at 12.92 min. This served as a further confirmation that conjugation has taken place.

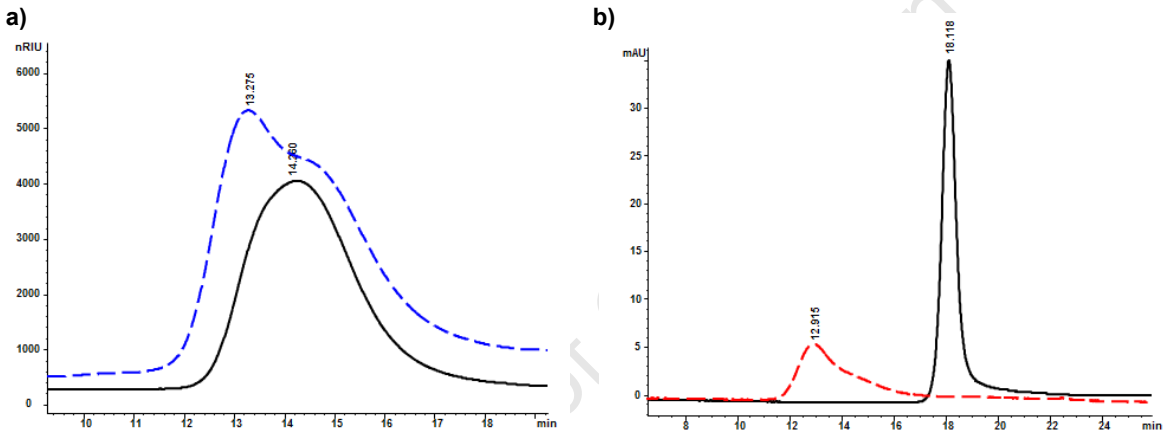

Figure 6.27. SEC–HPLC a) RID and b) UV 280 nm chromatograms of Reaction 2, Pn1_HOBt_CRM_{197} (blue/red) before ammonium sulfate precipitation. Pn1 PS (black) is shown for comparison.

As neither size exclusion (Sephacryl S500 column) nor HI chromatography provided adequate separation of unconjugated and conjugated saccharide, ammonium sulfate precipitation was investigated. It was hypothesised that the conjugate would precipitate in saturated ammonium sulfate if the protein were able to do so without polysaccharide conjugated to it. Two volumes of saturated ammonium sulfate were added to the derivatized CRM_{197} however no precipitation was observed. It was hypothesised that the solution of 1 mg/ml CRM_{197} was too dilute to facilitate precipitation. The derivatized protein was concentrated down approximately 10–fold using a 50 kDa MWCO filter and centrifugation at 4000 rpm (actual concentration not determined due to volume size). Approximately a two volume equivalent of saturated ammonium sulfate was added. A precipitate was observed which confirmed that the conjugate could be precipitated with ammonium sulfate.

A portion of the conjugate formed in Reaction 2 (containing 50 mg polysaccharide and 25 mg protein) was concentrated down to a gel like solution and approximately two volumes of ammonium sulfate were added. The mixture was stirred and left to precipitate overnight at

2 – 8 °C. This mixture was centrifuged to pellet out the conjugate and the clear ammonium sulfate supernatant was discarded. This pelleted conjugate was subjected to a second round of precipitation before being reconstituted in PBS buffer (pH 7.2) and colorimetric analysis for protein as well as free and unconjugated saccharide was performed. The results are shown in Table 6.18.

Table 6.18. Analytical assay results of saccharide and protein content for Reaction 2.

Total saccharide (mg)	Free saccharide (mg)	Total protein (mg)	PS:Protein ratio	Conjugation efficiency (%)
12.80	1.17 (3.6 %)	7.83	1.48	23.4

Low recoveries of saccharide (25.6 %) and protein (31.3 %) were achieved with ammonium sulfate precipitation. As no saccharide was detected in the waste of the concentration step, or in the supernatant following the ammonium sulfate precipitation, it was hypothesised that the conjugate remained on the membrane filters during the concentration step. As the conjugate was concentrated down 10–fold (approximately 1 ml), it was too viscous to analyse for saccharide to determine if any had remained on the membrane filter. The results from the ammonium sulfate precipitation showed that only 3.59 % of the saccharide retained was unconjugated. This is below the minimum of 5 % agreed upon by The Biovac Institute at the beginning of the investigation. A final ratio of 1.48 mg polysaccharide to every mg protein was achieved with a conjugation efficiency of 23.4 %. The conjugation efficiency was calculated by taking the final result of the conjugated polysaccharide (11.63 mg) as a percentage of the total polysaccharide that underwent ammonium sulfate precipitation (50 mg). Due to the loss of polysaccharide and protein during the concentration step, this conjugation efficiency could potentially be a lot higher.

6.3.1.4 Summary of HOBt conjugations to CRM_{197}

Conjugation of Pn1 PS to CRM_{197} carrier protein was effectively performed using HOBt mediated EDC coupling chemistry. The two reactions investigated the derivatization levels of the carrier protein as well as different purification methods. The CRM_{197} with the lower levels of derivatization underwent HIC purification and was found to contain high levels of unconjugated polysaccharide. The conjugate with the higher derivatization levels showed a shift in retention time in the RID signal indicative of conjugation. This conjugate was purified by ammonium sulfate precipitation, and a free saccharide level of less than 5 % was determined. This conjugate was formulated and put forward for *in vivo* mice studies to compare with the triazine conjugate as well as two commercially available vaccines.

The conjugations of Pn1 to both TT and CRM_{197} carrier proteins were found to be successful when using the HOBt mediated conjugation technique. Table 6.19 compares the analytical

results of the conjugates prepared. The free saccharide was determined to be the lowest when CRM_{197} was used as the protein carrier. In terms of conjugation efficiency the TT conjugate was the highest of all three conjugates and the saccharide to protein ratio of the TT conjugate was closest to the ideal value of 0.75 – 1.0.

Table 6.19. Comparison of three different carrier proteins in conjugates prepared using the HOBt methodology.

Derivatized protein	Free saccharide (%)	PS:Protein ratio	Conjugation efficiency (%)
TT	47.4	1.10	27.25
CRM_{197}	3.59	1.48	23.4

6.3.2 Triazine activator conjugations

2–Chloro–4,6–dimethoxy–1,3,5–triazine (CDMT), shown in Figure 6.28, is known to be a useful non–carbodiimide condensing agent for the synthesis of esters and acid anhydrides, especially in the formation of peptide bonds between a carboxylic acid and an amine.

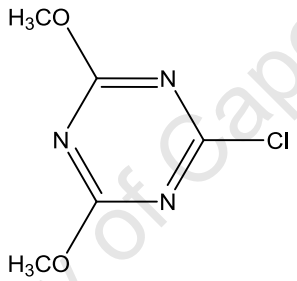

Figure 6.28. Structure of CDMT.

The standard method for making amide bonds using CDMT consists of two main steps; the formation of the activated carboxyl group and the conjugation of the active species to the amino group on the protein. The carboxylic acid on the polysaccharide reacts with the CDMT in the presence of *N*–methylmorpholine (NMM) to form a CDMT–activated intermediate, an active ester depicted in Figure 6.29. The second step involves the coupling of the carboxylic acid to the DMTMM (prepared *in situ*) followed by nucleophilic displacement of the triazine moiety by the amine resulting in the formation of an amide bond. Preliminary studies by Kaminski showed that for the activation of sodium, silver or quaternary ammonium salts of carboxylic acids to successfully occur, the presence of a base was required. This base had to come from a very select group including tetramethylguanidine, *N*–methylmorpholine (NMM), dimethylaminopyridine or pyridine, although the best results were obtained with NMM [477]. The NMM base is used to neutralise the chloride ions which are released from the CDMT during the activation. The activation takes place in a non–polar/polar (acetonitrile and water) solvent as this allows for the dissolution of both the polysaccharide (water) and CDMT (acetonitrile or any solvent less polar than water) to occur. An advantage of using this

non–polar/polar solvent mixture is that both hydrophobic and hydrophilic amines can be used. Once the reaction is completed, Dowex H^+ /Na^+, which are cation exchange resins or a dilute acid, can be used to remove the main morpholinium by–product [478].

When the CDMT was added to the carboxylic acid, followed by the NMM, left to stir for an hour followed by the addition of the amine compound, significant racemization occurred via the formation of a azlactone formed via the cyclization of *N*–acetyl–α–amino acids that contain both a nitrogen and oxygen in the ring where the oxygen is adjacent to a carbonyl. Garret *et al*. (2002) first showed this occurrence when amino acid analogues were coupled with CDMT to create peptide bonds. The coupling took place over 22 hours where the acidic compound was dissolved in ethyl acetate before the addition of 1.45 molar excess of CDMT. This was cooled to 15 °C and a 2.4 fold molar excess of NMM was added. The mixture was warmed to room temperature and left to react overnight. However, the authors noted that the intermediate formed was not the active ester, but instead an azlactone. It was theorised that by adding the amine in the beginning of the reaction as it would prevent the cross–linked azlactone from forming. The authors repeated the experiment but added the amine in the beginning creating a one–step reaction. The amide bond was formed to completion in less than 60 min [479].

The CDMT coupling reaction was first used to prepare hyaluronic acid (HA) conjugates in 2007 when Bergman *et al.* coupled HA to a number of compounds with differing functional groups [478]. The general procedure that was applied to HA is described as follows: HA, containing 0.2 mmol carboxylic acid groups was first dissolved in water. To this acetonitrile was added to a ratio of 3:2 with respect to water. NMM was added in a molar equivalent to the amount of carboxylic acid on the HA. The solution was cooled to 4 °C and CDMT was added and the reaction left to stir for one hour at room temperature. The resulting active ester was mixed with a molar equivalent of the amine and stirred for a further 20 hours at room temperature before 1 ml Dowex H^+ was added to quench the reaction. The reaction mixture was stirred, filtered and dialysed against water. Many methods published before Bergman *et al*. coupled HA in organic solvents, namely DMSO and dimethylformamide but the authors had to change the counter ion on the carboxylic acid groups on the HA from sodium to tetrabutylammonium in order to make the HA soluble in the organic solvents.

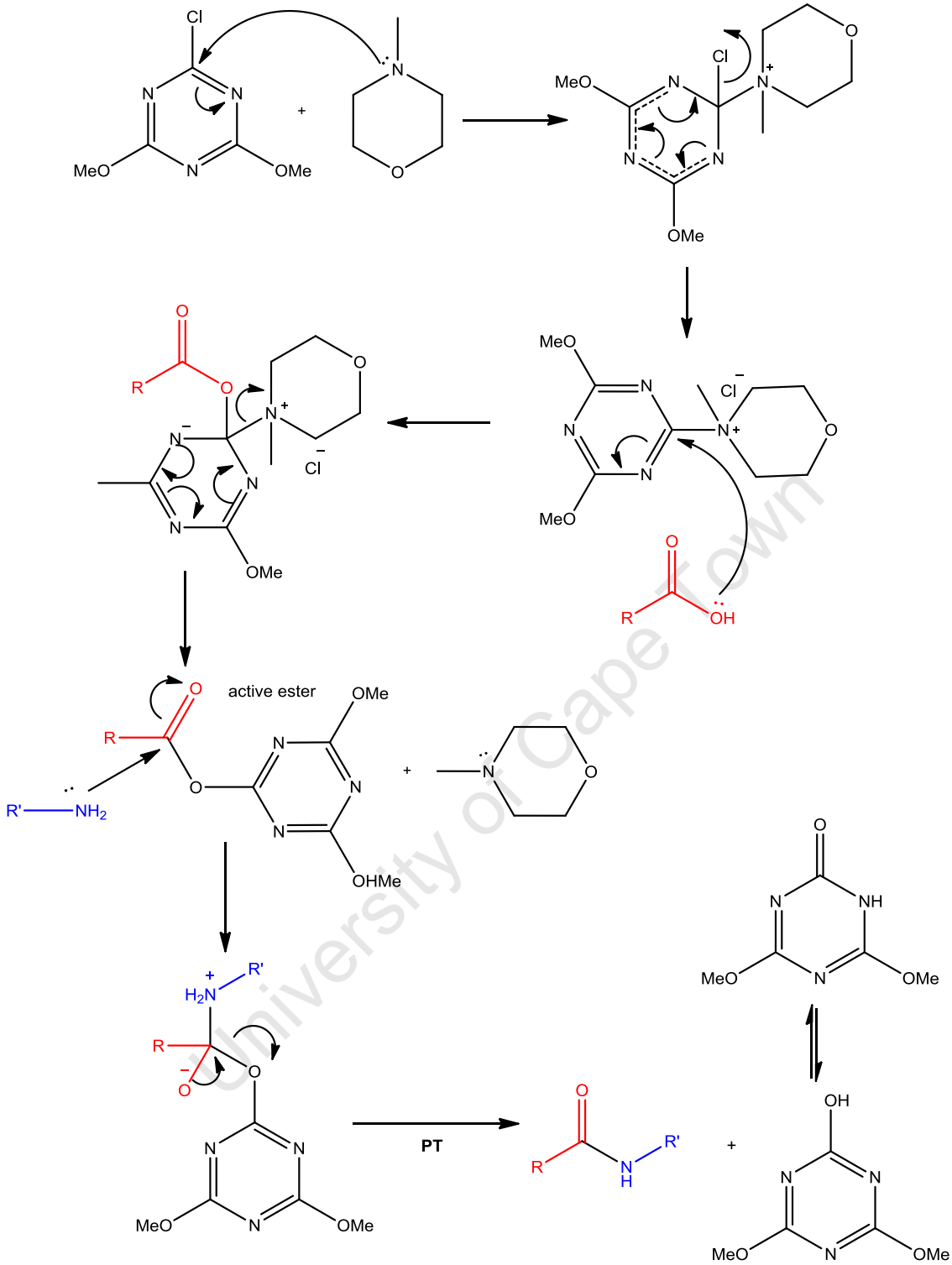

Figure 6.29. Mechanistic detail of the conjugation of a carboxyl group with an amine functional group through the use of CDMT and NMM.

In 2011, Schanté *et al.* compared three HA derivatives synthesised using three different methods. The first was the classic carbodiimide–coupling (EDC) in water; the second was the triazine coupling method in acetonitrile and water, and the third using 2–chloro–1–methylpyridinium iodide (CMPI) in anhydrous DMF. The synthesis of the HA alanine compound using CDMT was adapted from Bergman *et al.* (2007) [478]. The HA sodium salt

was first dissolved in a water–acetonitrile solution (3:2). A 3 molar excess of CDMT was added and the solution was left to react, forming the HA–dimethoxytriazine intermediate, for 1 hour in an ice bath. A 4.5 molar excess of NMM was added along with the alanine derivative and the reaction was left overnight at room temperature with constant stirring. Dowex–H^+ and Dowex–Na^+ were added to remove any excess amines. The results of these three couplings; the EDC, triazine and CMPI reactions, showed that the coupling in the anhydrous DMF solvent gave substitutions of the carboxyl groups of up to 100 % [480, 481]. Whilst this was what the authors were looking for, for the pneumococcal type 1 polysaccharide, lower activation levels are preferable due to the presence of both carboxylic acid and amino groups on the repeating unit that could lead to cross linking.

In 1999, Kunishima synthesised the 4–(4,6–dimethoxy–1,3,5–triazin–2–yl)–4–methyl–morpholinium chloride (DMTMM) salt by reacting CDMT with *N*–methylmorpholine (NMM) in THF at room temperature for 30 minutes [482]. As DMTMM is simply the reaction between CDMT and NMM it reacts with carboxyl groups in the same way. It activates the carboxyl group of the polysaccharide forming a reactive triazinyl ester which is capable of reacting with an amine (or any nucleophile).

The advantages of the DMTMM reagent over the classical CDMT and NMM reagents are numerous. DMTMM is water soluble and is compatible with many other solvents including alcohols, ethyl acetate and diethyl ether. No tertiary amine base is needed as NMM is liberated during the reaction of DMTMM with the carboxylic acid grouping. The main by–product 2–hydroxy–4,6–dimethoxy–1,3,5–triazine which is generated during the reaction as well as any excess reagent can be easily removed and recycled for the manufacture of DMTMM. DMTMM is also reactive over a wide pH range and in some cases pH control is not necessary [483, 484].

Pneumococcal polysaccharides undergoing coupling reactions using the DMTMM salt had previously been reported by Esser and Schlottmann in 2006. The polysaccharides were coupled to Luminex spheres for use in serological assays. A 200 mg/ml solution of DMTMM was added to the polysaccharides and the reaction mixture was left to react at room temperature for between 40 and 60 minutes before purification and subsequent conjugation to the Luminex amino–microspheres. The reaction was left to proceed overnight in the dark after which the pneumococcal polysaccharide microspheres were washed to remove any free polysaccharides before storage in blocking buffer, available for use in serological assays. The conjugation method was found to be reproducible and stable for at least 3 months [485].

The decision to use CDMT and NMM instead of the DMTMM salt in the investigations was made after various factors were considered. Firstly the cost involved: at the time of writing, 5 g of CDMT was nearly one sixth of the cost of the DMTMM salt and NMM was one tenth of the cost of the salt, so it would thus prove cheaper to make the salt than to purchase the salt form. Secondly, it has been reported that the reactions all require longer times to proceed to completion. The formation of the activated ester occurs after 1.5 hours, and the conversion rate of conjugation is much lower with the DMTMMM salt than with that of the classical CDMT/NMM method. The type of carboxylic acid is also limited with DMTMM where only sterically hindered pivalic or benzoic acids with electron withdrawing groups seemed to work successfully with DMTMM [486].

The objective of this study was to develop an alternative method for the conjugation of Pn1 PS other than the known carbodiimide approach. The structural similarities of Pn1 PS and HA support the investigation into triazine conjugations. In the case of Pn1, there are two galacturonic acid residues available for triazine activation which would be coupled to the derivatized protein. The pH and subsequent precipitation issues surrounding EDC conjugations would be avoided as triazine conjugations take place at neutral pH.

The conjugation group at The Biovac Institute investigated this new conjugation methodology with Pn1 polysaccharide. Conjugations of Pn1 and four (derivatized) carrier proteins; BSA, TT, CRM_{197} and PLD were found to be successful when using the triazine methodology. The activating species was formed separately in an organic solvent, before addition to the polysaccharide solution. An initial polysaccharide–protein mass ratio of 2:1 was determined to be the optimum mass ratio needed in order to achieve a final mass ratio in the conjugate of 1. Ammonium sulfate precipitation was the preferred method of removing free saccharide instead of size exclusion chromatography.

Table 6.20. Comparison of the conjugation results between conjugates containing derivatized TT, CRM_{197} and PLD as protein carriers.

Derivatized protein	Free saccharide (%)	Saccharide: protein ratio	Conjugation efficiency (%)
TT	2.1	0.5	21.4
CRM_{197}	7.2	1.32	21.9
PLD	15.8	0.91	32

Table 6.20 compares the analytical results of the conjugates prepared with derivatized TT, CRM_{197} and PLD as protein carriers. The PLD conjugate gave the best polysaccharide–protein final mass ratio of 0.91 compared to 1.32 for the CRM_{197} conjugate and 0.5 for the TT conjugate. The conjugation efficiency of the PLD conjugate was also the highest, followed closely by the CRM_{197} and TT conjugates.

6.4 Formulation with adjuvant

In the current regulatory environment, there is an increasing necessity to develop vaccines that are well defined in molecular terms. The first vaccines available used whole, inactivated pathogens which presented a complex range of antigens, whereas the recent vaccines are based instead on selected antigens which in some cases may be single molecules or fragments thereof which can be derived from bacteria, tumour cells, allergens or an auto–antigen [487]. These molecular vaccines are often poorly immunogenic and an adjuvant is often needed to enhance the cellular and/or humoral immune response to an antigen [192, 488].

The word 'adjuvant' is derived from the Latin verb *adjuvare* which means "towards help" [489]. They were first described as "substances used in combination with a specific antigen that produced a more robust immune response than the antigen alone" by Gaston amon [490]. There are a number of characteristics that the ideal adjuvant should exhibit. Adjuvants should first and foremost be safe, and non–toxic with no occurrences of local or systemic responses. They should be chemically defined, stable in a formulation with the antigen, they should, most importantly, not confer immunity on their own but improve the potency of the immune response when formulated with an antigen in a vaccine, and must be effective in infants and young children [192, 490, 491]. These characteristics of an adjuvant promote an earlier, longer lasting and more potent immunological reaction against the antigen. This advantage leads to the use of reduced quantities of the antigen to elicit the same immunological response [192, 492].

While there are a number of adjuvants in use in clinical studies, the main adjuvant, used in the majority of licensed conjugate vaccines, are the aluminium based adjuvants: aluminium hydroxide and aluminium phosphate. The adjuvant effect of aluminium compounds were first investigated in 1926, when Glenny *et al.* precipitated a diphtheria toxoid with potassium alum ($AlK(SO_4)_2.12H_2O$). When compared in immunological studies in rabbits and guinea pigs, to the toxoid alone, this adjuvanted toxoid produced a significant increase in the immune response [493, 494]. The work by Glenny, led to the thought that for an antigen to produce an immune response it must be adsorbed onto the aluminium adjuvant. This observation led to the hypothesis of the mechanism of action of these adjuvants in that the antigen is slowly released from the adjuvant once injected into physiological fluid, due to the difference in makeup of the physiological fluid from that of the formulated vaccine that would affect the adsorption of the antigen on the adjuvant [192, 494, 495]. The World Health Organization recommends adsorption of 80 % or more of tetanus and diphtheria toxoids to aluminium–

containing adjuvants. The United States Minimum Requirement also specifies that at least 75 % of the diphtheria toxoid be adsorbed by aluminium–containing adjuvants [496, 497].

Aluminium adjuvants are most widely used as they have a very long safety record [498]. Regulatory requirements mean that any new adjuvant must be put through a number of investigations to determine if its benefits of being an adjuvant outweigh any tolerability or safety issues. This long and arduous process has already been performed for the aluminium adjuvants, making the use of these adjuvants much more inviting [499].

There are however, several disadvantages of aluminium adjuvants. They are known to only stimulate the humoral immune response. Another major drawback of these adjuvants is that they cannot be lyophilised nor frozen as both of these processes would destroy the gel–based structure [192].

The major mechanism that allows for the adjuvants to adsorb the antigen is electrostatic interaction. Electrostatic interaction takes advantage of the differences of the isoelectric point of the two aluminium adjuvants. If the isoelectric point of the antigen is known, the adjuvant, with the opposite surface charge, can be used [500]. This was best illustrated by Seeber *et al.* when it was shown that lysozyme, with a high isoelectric point of 11.0 was poorly adsorbed by the aluminium hydroxide adjuvant which also has a high pI, but the lysozyme was adsorbed strongly by the aluminium phosphate adjuvant that has a low pI of 5.5 [501].

Adjuvants are not the only additions to a vaccine formulation. Preservatives, such as phenol, 2–phenoxyethanol and thiomersal (not used in children's' vaccinations due to safety concerns [502]), are added mostly to multi–dose vials to combat the potential risk of contamination [9]. Additives are added in order to buffer, stabilise, and prevent the formulation from aggregating and from sticking to the vial; these can include certain sugars such as sucrose, lactose and sorbitol. Salts, such as sodium chloride and succinic acid, along with surfactants (Tween–80), are also commonly used in formulations not just to buffer the vaccine, but also to reduce the injection pain and to normalise the vaccine with the physiological fluid at a rapid rate, as well as to prevent the vaccine from sticking to the glass vial and stopper [502].

The ionic strength of the formulation will also affect the adsorption of the antigen to the adjuvant. Al–Shakhshir *et al.* investigated this when they monitored the amount of lysozyme adsorbed onto aluminium phosphate at pH 7.4 by varying the salt concentration. It was found that the best adsorption occurred in the presence of 0.06 M NaCl, adsorption was greatly reduced at 0.15 M NaCl and no adsorption was seen with a concentration of 0.25 M NaCl [503]. It is now common practice to keep the ionic strength of the vaccine formulation as low as possible when electrostatic interaction is the mode of adsorption [500].

6.4.1 Formulation study

The devised Pn1 vaccine formulation was based on the Pfizer product utilising in–house methodology for preparing aluminium phosphate *in situ*. A comparison between the proposed formulation and that of Pfizer's is summarised in Table 6.21. The only difference between the components in the formulation was the amount of NaCl added but the amount used was still low enough not to inhibit the adsorption as shown by Al–Shakhshir [503].

Table 6.21. Proposed formulation for the Pn1 experimental conjugates and Pfizer's Prevnar 13 vaccine formulation (volume = 1 000 ml).

Component	Pfizer	Proposed
$AlPO_4$ (as Al^{3+}) (mg)	0.125	0.125
NaCl (mg)	4.250	4.500
Succinic acid (mg)	0.295	0.295
Polysorbate 80 (Tween–80) (mg)	0.100	0.100

The formulation of the conjugates involved the slow formation of aluminium phosphate from aluminium chloride and sodium phosphate. After the aluminium phosphate had formed, the pH was adjusted and the antigen added. Adsorption of the antigen to the aluminium phosphate occurred over a number of hours. Succinate buffer was included to provide pH control and improve the process control. Polysorbate 80 improves the robustness of the manufacturing process [376].

All five conjugates used in the animal studies (two in Round I and three in Round II, described later) were prepared using this formulation, only the type and volume of antigen was changed between formulations. All antigens were formulated to a final concentration of 2 µg/ml. After each formulation was complete, a competition ELISA was performed in order to determine the percentage absorption of the antigen (conjugate) onto the aluminium adjuvant. A 2 µg/ml Pn1 antigen was used as a positive control with a blank formulation (not containing the antigen) used as a negative control. The five conjugates that were prepared are shown in Table 6.22 with specific volumes of each component used is shown in Table 6.23.

Table 6.22. Conjugate formulations in animal studies.

Conjugate formulation number	Protein	Chemistry utilised	Round of animal study
Form001	CRM_{197}	HOBt	I
Form002	CRM_{197}	Triazine*	I
Form003	CRM_{197}	Triazine*	II
Form004	TT	Triazine*	II
Form005	PLD	Triazine*	II

*Triazine conjugates prepared by the conjugation team at The Biovac Institute.

Table 6.23. Specific volumes used in formulations prepared for animal studies.

Formulation	$AlCl_3$ (ml)	Na_3PO_4 (ml)	Succinic acid (ml)	Tween (ml)	NaCl (ml)	Antigen (ml)	WFI (ml)	P/Al	Final pH
Form001	138.20	42.47	25.0	10	63.03	1.54	719.76	1.41	7.02
Form002	138.20	42.47	25.0	10	63.03	1.32	719.98	1.42	7.10
Form003	82.92	29.16	15.0	6	37.82	0.94	428.16	1.31	6.90
Form004	138.20	45.26	25.0	10	63.03	3.26	715.25	1.22	6.76
Form005	138.20	45.86	25.0	10	63.03	1.45	716.46	1.24	6.83

The absorption efficiencies of the antigen onto the adjuvant were determined by quantifying the amount of unbound conjugate in the formulation solution. This is therefore inversely proportional to the amount of conjugate that has been absorbed onto the aluminium phosphate adjuvant. The ATCC Pn1 PS was used as a reference standard. Figure 6.30 displays the ELISA results graphically with both the amount of free conjugate and the amount of conjugate that was absorbed onto the adjuvant.

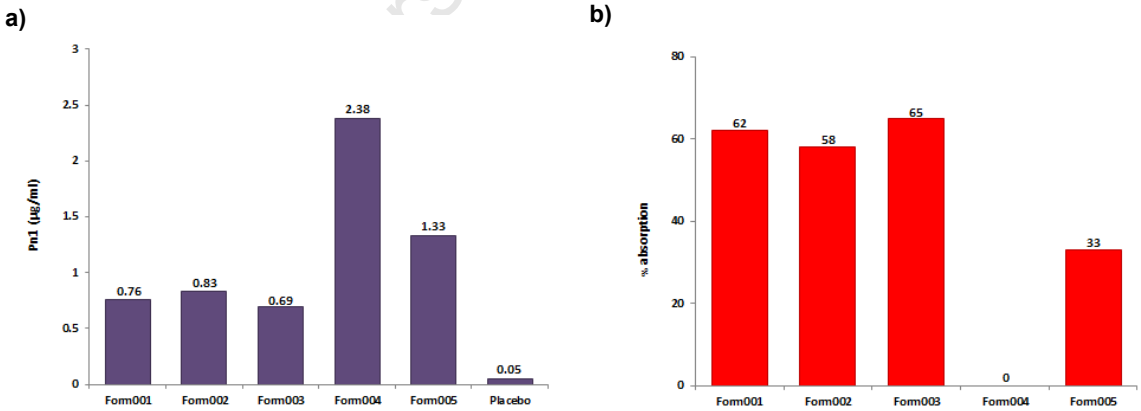

Figure 6.30. Competition ELISA results of all Pn1 formulations quantifying a) the amount of Pn1 polysaccharide and b) the percentage absorption of Pn1.

A variable amount of absorption for all the conjugates was revealed through the ELISA results. The highest absorption values were seen for the conjugates with CRM_{197} as the protein carrier (Form001, Form002 and Form003). Absorptions of between 58 and 65 % were seen for this protein carrier. Pneumolysoid conjugates (Form005) showed much lower

adjuvant absorption of only 33 % and the TT conjugate (Form004) showed no absorption at all. The lack of adsorption of the TT conjugate is hypothesised to be due to a pH issue as Kumar *et al.* suggests that TT absorption onto aluminium phosphate adjuvant is optimal at a pH near 5 and decreases when the pH approaches 6.3 – 7 [504]. However, due to time constraints, this formulation method could not be optimised for each conjugation.

6.5 Animal studies

6.5.1 Animal study design

All animal procedures used were approved and performed by the University of Witwatersrand. Five week old outbred NMRI female mice were obtained from the National Health Laboratory Services (NHLS) animal facility based at the NICD in Johannesburg, South Africa. The study consisted of two different phases (Round I and II). Round I investigated the immunogenicity of the two different conjugation chemistries: EDC mediated and triazine. CRM_{197} was used as the protein carrier for both conjugation chemistries. The prepared conjugates were compared to a commercial vaccine that contained CRM_{197} as the protein carrier so that the only difference in the conjugates was the conjugation chemistry. The conjugation chemistry that presented with the best results was taken to Round II where three protein carriers: CRM_{197}, TT and PLD were conjugated to Pn1 PS using the conjugation chemistry of choice from Round I. These three conjugates were compared to two commercial conjugate vaccines. For each round the body mass of the mice was monitored and recorded on a weekly basis.

Table 6.24. Sample details for Round I of animal studies.

Conjugate/Vaccine	Carrier protein	Conjugation Chemistry
Placebo* Diluent + $AlPO_4$	–	–
Positive control Commercial vaccine I	CRM_{197}	Reductive amination
Form001	CRM_{197}	EDC mediated
Form002	CRM_{197}	Triazine

*Placebo/negative control consisted of the diluent and aluminium phosphate. (Same formulation but no antigen present).

Table 6.25. Sample details for Round II of animal studies.

Conjugate/Vaccine	Carrier Protein	Conjugation Chemistry
Placebo*	n/a	n/a
Diluent + $AlPO_4$ + unconjugated Pn1	PLD unconjugated	n/a
Commercial vaccine I	CRM_{197}	reductive amination
Commercial vaccine II	Protein D	CDAP
Form003	CRM_{197}	preferred chemistry**
Form004	TT	preferred chemistry**
Form005	PLD	preferred chemistry**

* Placebo/negative control consisted of the diluent and aluminium phosphate. (Same formulation but no antigen present).
**Preferred chemistry chosen from Round I

Table 6.24 and Table 6.25 outline the conjugates and samples used in both rounds of animal studies. The negative control I (placebo) used in both rounds of animal studies contained 100 µl of $AlPO_4$ adjuvant. This adjuvant was the same concentration as that used in the conjugate formulations. A second negative control, used in Round II consisted of the $AlPO_4$ adjuvant as well as a mixture of unconjugated Pn1 PS and PLD protein in order to check that immunogenicity levels were not a result of either the polysaccharide or the protein on its own. Two commercially available vaccines were used as positive controls in this study and both of the commercial vaccines employ different conjugation chemistries to the ones tested. One of the vaccines contained CRM_{197} as the protein carrier. The second commercial vaccine contained Pn1 PS conjugated to Protein D, however, both TT and DT are found in this vaccine as carrier proteins for other serotypes. The five conjugates that were investigated in this study were injected in a 100 µl formulated dose consisting of 200 ng of Pn1 conjugate and $AlPO_4$ as adjuvant.

Mice however, do not produce a dose dependent response and are not the ideal animal model for testing conjugates and these results can only provide an indication of the immunogenicity of the conjugates.

6.5.2 Immunoassays

As anticapsular antibodies are used by the immune system to prevent invasive bacterial diseases, measuring the serotype–specific antibody titres as well as the opsonophagocytic (OPA) activities against the serotypes have become the preferred methods to evaluate the immunogenicity of conjugate vaccines [129]. The safety and immunogenicity of new vaccines are determined through clinical studies. The WHO have determined a number of licensure criteria in order to by–pass the difficulties related to clinical efficacy trials [162]. A study will fulfil this criteria if immunological non–inferiority to the licensed conjugate vaccines

can be shown using specific techniques such as enzyme–linked immunosorbent assay (ELISA) and opsonophagocytic (OPA) assays [162, 505].

With a large number of samples, the OPA assay becomes labour intensive and difficult to perform and therefore many laboratories will measure the antibody binding by ELISA alone to form an idea of how the vaccine will perform. Since antibodies to the capsular polysaccharide are the mediators against infection, an assay that can measure the antibody levels can be used as a substitute for the OPA assay, however a correlation between the two assays must first be determined [506].

6.5.2.1 ELISA

The total IgG antibody titres against Pn1 serotype 1 were used to compare the different vaccinated mouse groups and were determined by the method first described by Conception and Wernette in 2001 [506]. This method was modified to enable it to detect mouse IgG. The IgG results were calculated based on an in–house reference serum that was given an arbitrarily value of 100 units/ml. Samples that fell below the detection limits were given a titre value of half of the detection limit. The ELISA assay was optimised and validated for linearity, specificity, sensitivity, background, inter– and intra–assay precision as well as coating concentration [507].

As previously stated, for an ELISA to be used in the place of an OPA assay, there must be a strong correlation between the two titres. It has been suggested that a correlation co–efficient of above 0.8 is a good enough correlation [506]. This was performed during Round II of the animal study when the OPA assay was in place.

6.5.2.2 OPA

Opsonins are antibodies in the blood serum that make the pneumococcal bacteria more susceptible to phagocytosis [10, 508, 509]. These opsonins bind to the capsular polysaccharide and phagocytes bind to these antibodies in order to induce the killing of the cell in what is known as opsonophagocytosis [10]. As opsonophagocytosis is an essential process in the immune system's defence against *S. pneumoniae*, a method that allows for the measurement of the opsonins is a vital tool in determining whether or not the conjugates prepared would be able to illicit an immune response.

At the WHO consultation meeting in 2003 it was decided that the OPA assay used to determine immunogenicity should follow the Romero–Steiner *et al.* method and such was used in the measurement of functional antibodies in his investigation [386, 510]. The functionality of the antibodies in the serum samples was expressed as the opsonophagocytic

titre, which is the reciprocal dilution at which ≥50 bacterial killing occurred in comparison to the control wells [507].

6.5.3 Body weight profiles

One of the variables monitored throughout this investigation was the body weight of all mice. An increase in weight during the investigation is an indication of good health (Figure 6.31). No differences between the placebo and the vaccine mice groups were observed. One mouse, used in the first round of studies did however develop a tumour and was terminated. This mouse belonged to the HOBt (EDC mediated) conjugate group however this was an isolated, adverse event and was not thought to be related to the conjugate vaccine as it has been documented that NMRI mice have a high propensity to develop spontaneous tumours [511-513].

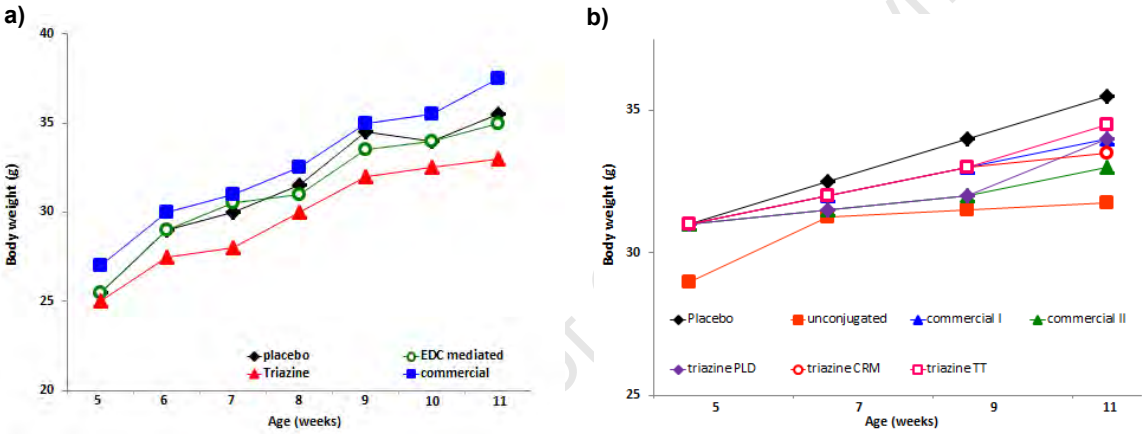

Figure 6.31. Mouse body weight profiles from a) round I and b) round II studies. Body weight curve after mice were vaccinated with conjugate vaccines or placebo. The body weight was recorded weekly for mice. The mean body weight for each group of mice is shown (n =12 per group).

6.5.4 Round I results

The OPA assay had not been fully developed and optimised by the time Round I of the animal studies took place and hence only the ELISA results could be reported. Both the HOBt as well as the triazine mediated conjugates produced significantly higher titres than the commercial vaccine. The data represented graphically in Figure 6.32 detail the values of the ELISA assays for the conjugates. All of the mice in the two conjugate chemistry groups were able to produce a measurable antibody response, with only 11 out of the 12 from the commercial vaccine being able to do the same and as expected, none of the mice from the placebo group were able to produce any antibody titres. The placebo was given an arbitrary value of 0.1 as they fell below the limit of detection of the assay. It was shown that all the values for the commercial vaccine were within the range of 0.1 – 24 µ/ml. Values for the HOBt conjugate fell within a range of 3.4 – 207.5 µ/ml with the triazine ranging between 4.7 – 375.1 µ/ml. A two tailed comparison was performed to determine if there was any

significant difference between the two chemistries but they were found not to be statistically different.

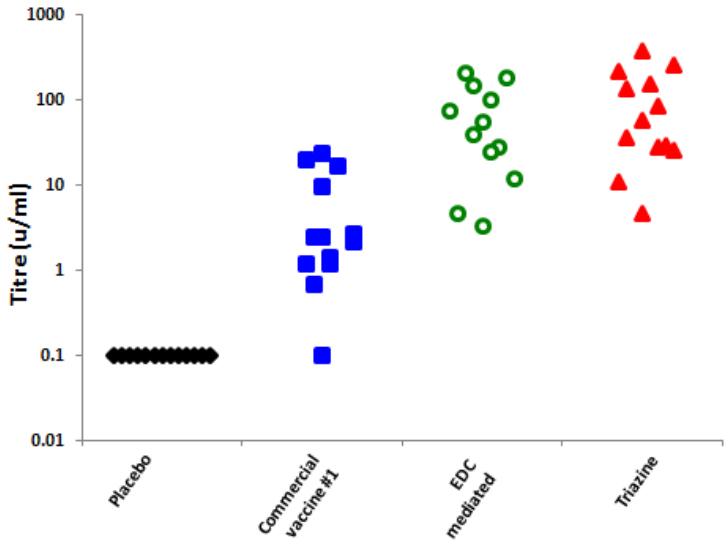

Figure 6.32. Graphical comparison of the ELISA immunogenicity levels of the two experimental conjugate vaccines (Green – HOBt chemistry, and red – triazine chemistry) compared to the commercially available vaccine (blue). The negative control is shown for comparison.

Whilst these results show a large difference between the commercial vaccine and the two conjugates investigated, it must be noted that the commercial vaccine is a multivalent vaccine including more than 10 different serotypes thus the serotype specific host responses of the commercial vaccine may be supressed by the higher antigen load. To date, this has not been further investigated.

6.5.5 Round II

6.5.5.1 Western blot analysis of conjugates

Although there was no significant difference between the results of the carbodiimide mediated and triazine conjugates, the triazine chemical conjugation method was chosen to be the preferred method for Round II animal studies. This round compared three different protein carriers (TT, CRM_{197} and PLD) to the two commercial vaccines to determine 1) if the conjugation chemistry was superior to those techniques used in the commercial vaccines and 2) the superior protein carrier.

Before formulation, all conjugates prepared for Round II of the animal study were subjected to Western blot analysis to demonstrate conjugate formation and to confirm that the structural integrity (epitope) of the protein was retained after conjugation. In separate experiments unconjugated Pn1 and Pn1 conjugated to the three different proteins (CRM_{197}, TT and PLD) were first subjected to SDS–PAGE followed by electrophoretic transfer onto a PVDF membrane and staining.

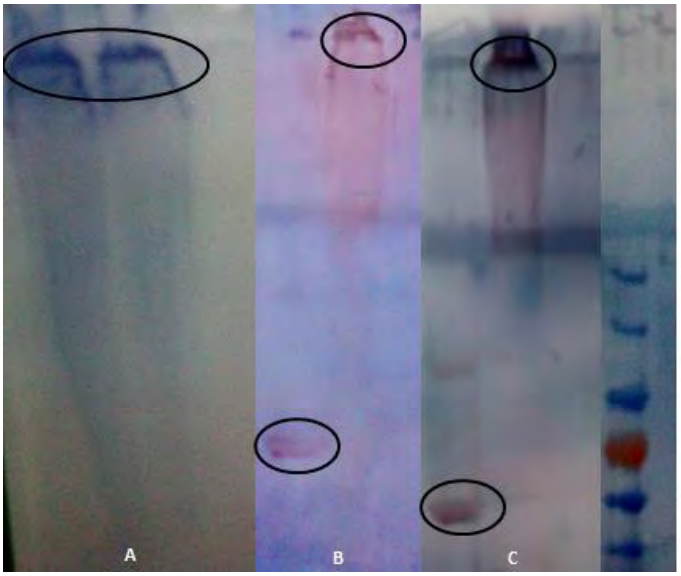

Figure 6.33. Image of PVDF membranes containing A) native TT (lane 1) and Pn1–TT conjugate (lane 2), B) native CRM_{197} (lane 1) and Pn1–CRM_{197} conjugate (lane 2) and C) native PLD (lane 1) and Pn1–PLD (lane 2) post western blot analysis.

The results of the Western blots, (Figure 6.33), demonstrate that antibodies specific to the protein (TT, DT (for CRM_{197}) and PLD) were able to bond to the specific conjugate as shown by the second band in each figure. The first lane in each gel depicts the underivatized and unconjugated protein that acted as positive controls for antibody recognition. From these results it can be concluded that each conjugated protein retained its structural antigenic integrity as it was still recognisable to the antibody post derivatization and conjugation. The lack of free protein (i.e. no band or streaking observed between 55 – 70 kDa) in both the CRM_{197} and PLD conjugation samples confirm good conjugation efficiency. As the TT was run under native (non–reducing) conditions, its tertiary structural conformation prevented it from entering the gel. The conjugates were each formulated onto aluminium phosphate adjuvant, followed by Round II of the animal investigations.

6.5.5.2 Animal results

The immunogenicity of the conjugates was compared to two negative and two positive controls. The ELISA results are graphically displayed in Figure 6.34 with the OPA assay results revealed in Figure 6.35.

Two of the three different protein carriers tested resulted in higher antibody titres to both commercially available vaccines. As with the first round of animal studies, it must be mentioned that the commercial vaccines are both multivalent vaccines of more than 10 different serotypes and the specific host responses for Pn1 in these vaccines may be inhibited by the antigen load.

All of the conjugates exhibited higher antibody titres than those of the two negative controls. For the ELISA results three of the mice injected with the unconjugated Pn1 negative control did show an immune response, and 11 out of the 12 mice injected with commercial vaccine I produced antibody titres. All of the other conjugates showed 100 % conversion rates. The OPA revealed slightly different seroconversion results when one of the 12 mice in the commercial vaccine I and two of the 12 in the PLD conjugate group failed to produce any detectable OPA results and were given a value under that of the detectable limit. The second commercial vaccine as well as the conjugates with TT and CRM_{197} as protein carriers gave 100 % seroconversion rates.

The conjugate that employed TT as the protein carrier gave the highest antibody titres with a geometric mean concentration (GMC) of 357.4 µ/ml with the CRM_{197} conjugates resulting in the second highest levels with a GMC of 141.1 µ/ml. Interestingly, the conjugates with PLD as a carrier protein gave lower titres than one of the commercial vaccines, however, they were found not to be statistically different to either commercial vaccine. As PLD is derived from PLY, a pneumococcal protein, it should have its own immune protective potential and thus, a conjugate with PLD as a protein carrier should have the added advantage of giving a broader protective immunity than the other conjugates. This result does not support the results released by Michon *et al.* in 1998 where the pneumococcal–PLD conjugates produced similar immunogenic results to the results obtained with pneumococcal–TT conjugates, however Michon made use of native, underivatized PLD and used reductive amination as a coupling chemistry [445]. These differences could attest to the difference in immunogenicity as described here.

Significantly higher OPA titres were observed for all conjugate vaccines in comparison to the placebo and unconjugated controls. As with the ELISA assay, the conjugate with PLD resulted in lower titres than one of the commercial vaccines however no significant difference was seen in the titres between both the commercial vaccines and the PLD conjugate. The conjugates using TT and CRM_{197} produced GMC titres of up to 10–fold higher than the commercial vaccines.

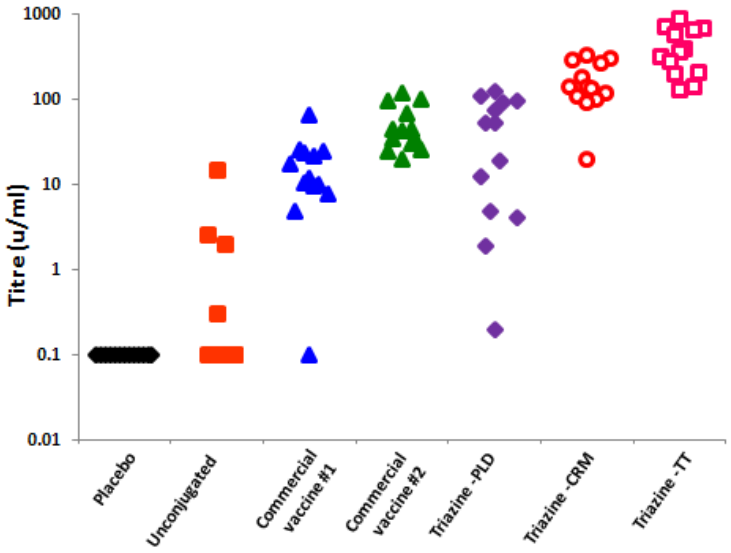

Figure 6.34. Graphical comparison of the ELISA immunogenicity levels in Round II of the animal studies, comparing three different protein carriers (Purple – PLD, red – CRM_{197} and pink – TT) with two commercially available conjugate vaccines (blue and green). The negative controls are shown for comparison.

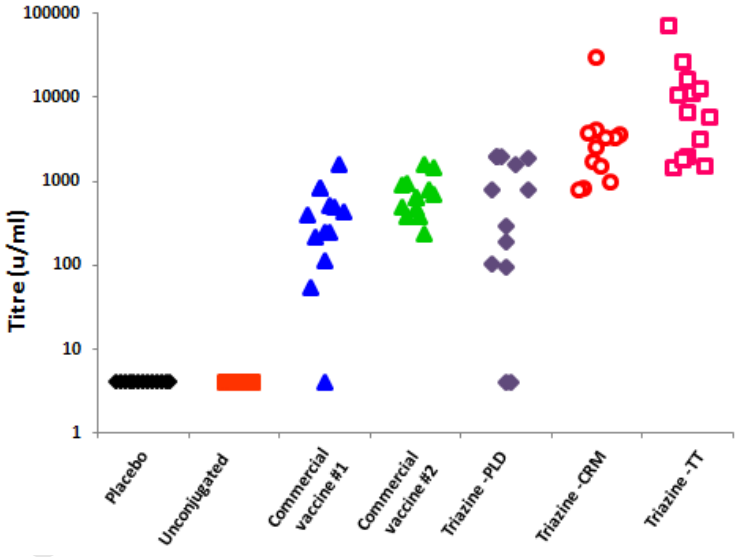

Figure 6.35: Graphical comparison of the OPA functional antibody responses in mice in Round II. Comparisons are made with the three different protein carriers (Purple – PLD, red – CRM_{197} and pink – TT) and two commercially available conjugate vaccines (blue and green). The negative controls are shown for comparison.

6.5.6 Summary of animal results

All new pneumococcal vaccines need to adhere to certain essential conditions – including immunologic non–inferiority to contemporary licensed vaccines. The results demonstrate that when the Pn1 PS was coupled to CRM_{197} using either HOBt or triazine mediated chemistries; both novel protein–polysaccharide conjugation chemistries were capable of generating considerably more effective immune responses than the commercially available vaccines.

It must be taken into account that the prepared conjugate vaccine consisted of only one serotype whereas the commercially available vaccine were multivalent. It is known that whilst combining several different antigens into one vaccine broadens the coverage of the vaccine, it does lead to a reduction in the immunogenicity of a single antigen in the multivalent vaccine. This has been shown to occur in vaccines against viruses such as flu [514], human papillomavirus [515], protein vaccines [516] as well as in pneumococcal conjugate vaccines [517]. In the case of conjugate vaccines, Fattom et al. observed a reduction of between 30 and 90 % in antibody responses to several serotype of a 12–valent *Escherichia coli* conjugate vaccines. The authors also identified a reduction of 30 % in the immunogenicity of *S. aureus* type 8 antibodies when the conjugate vaccine was combined with a type 5 conjugate vaccine.

With the need to overcome the limitation of carrier overload, attention has turned to the use of unique protein carriers. TT and CRM_{197} have shown to be the most frequently employed protein carriers due to their highly immunogenic characteristics and history of safe use within humans. In this study, it was found that the immune response of the conjugate with PLD as a carrier protein was inferior to that of either the TT or CRM_{197} conjugates. The conjugation strategy for PLD conjugates would need to be optimised as the animal results are in opposition to those described by Michon *et al.* in 1998 [445]. Michon used underivatized PLD and reductive amination coupling chemistry which may account for the difference in immunogenicity. Further work on the derivatization levels on PLD as well as optimisation of the conjugation chemistry need to be investigated as well as both the formulation conditions and the stability of the PLD conjugate.

CHAPTER 7. CONCLUSIONS

Pneumonia is the leading cause of death in children worldwide and is estimated to kill 1.6 million children every year. Pneumonia affects children and families everywhere, but is most prevalent in sub–Saharan Africa and South–east Asia. The capsular polysaccharide has been shown to be the most important virulence factor and over 90 pneumococcal serotypes have been recognised. Serotype 1 is responsible for up to 20 % of invasive pneumococcal diseases in developing countries and has been the cause of several outbreaks in the African meningitis belt. It is ranked among the top three serotypes in GAVI–eligible countries and is among the top six ranked serotypes among children under 5 years of age in regions with the highest burden of pneumococcal disease.

The distinctive epidemiology of IPD infections from Pn1, suggested that a monovalent Pn1 conjugate vaccine would be beneficial to developing countries and would have a significant public health value for epidemic control. This led to the aim of the present study: the development of a process and quality control methods for the preparation of an immunogenic conjugate vaccine against *Streptococcus pneumoniae* serotype 1 disease.

The Pn1 polysaccharide was purified following a two–step process utilising a differential filtration with ethanol. Small scale purifications were designed in order to investigate methods of inactivation as well as pH control. The favoured inactivation method was found to be phenol and an optimal pH of 7.8 was needed to ensure the complete precipitation of the PS in its CTA salt form. The optimisations determined in the small scale purifications were applied to larger fermentation batches to show that the purification method could be scaled up to 15 and 30 L batches.

This purified polysaccharide was subjected to a number of analytical tests in order to confirm that the purified polysaccharide batches conformed to the World Health Organisation specifications. These assessments were first optimised and validated and included size analysis, uronic acid composition, O–acetylation patterns and purity.

The viscosity of the purified polysaccharide hampered its detailed characterisation and ease of manipulation in conjugation reactions. Methods of size reduction were investigated and both sonication and microfluidization were successfully applied to model polysaccharides and Pn1. Composition and NMR studies confirmed that mechanical sizing had no impact on the structural integrity of the saccharides. Whilst sonication was able to achieve higher levels of size reduction and maintained the polydispersity of the polysaccharide when compared to microfluidization, the latter was found to be more suited to a GMP environment and was

advantageous in terms of scalability, control and consistency. The structure of the repeating unit of the polysaccharide and size reduced saccharide was fully elucidated by use of 1D and 2D NMR spectroscopy. The NMR study confirmed that the partially *O*–acetylated polysaccharide consisted of a mixture of de–*O*–acetylated Pn1 PS and polysaccharide acetylated at two different positions of GalA. NMR analysis of one specific purified Pn1 PS batch revealed *O*–acetylation in only one position (C2 of GalA, residue B), which indicated that the bacteria *O*–acetylates at one position and the fermentation and purification parameters such as pH and temperature permit migration to the C3 position.

Compositional analysis of the purified polysaccharide was also accomplished by means of hydrolysis and chromatographic methods. Conventional hydrolysis methods reported in the literature were applied but resulted in low recoveries due to the stability of the glycosidic linkage between the two galacturonic acid residues. Therefore alternate means of hydrolysis that utilised microwaves as a source of heat were investigated. Two different microwave–assisted hydrolysis methods were successfully developed, namely TFA hydrolysis and methanolysis, followed by analysis using anion–exchange and gas chromatography. This study showed the potential of microwave–assisted hydrolysis which can be applied to other bacterial polysaccharides that are particularly resistant to acid hydrolysis.

This purified, fully characterised and size–reduced polysaccharide was then successfully conjugated to hydrazide–derivatized protein carriers via the polysaccharide's carboxyl groups. The derivatization of four different protein carriers, BSA, TT, CRM_{197} and PLD, with ADH was successfully achieved. The reaction introduced a highly reactive hydrazide functional group on some of the carboxyl groups on the protein. The four different proteins behaved differently which led to modifications of the derivatization procedure for each protein; TT required a shortened reaction time whereas the reaction with CRM_{197} needed to be lengthened to >16 hours in order to achieve derivatization levels comparable to TT.

In order to conjugate the polysaccharide to the hydrazide–derivatized protein, the widely used carbodiimide methodology was first attempted and found to be successful only when conjugating to the model BSA protein. With the addition of an activating species, two novel conjugation methodologies were studied; one of which made use of a triazine activating compound and the other, 1–hydroxybenzotriazole, increased the electrophilicity of the polysaccharide and enabled conjugation to occur. Two protein carriers; TT and CRM_{197} were successfully conjugated to Pn1 using this HOBt methodology. Precipitation/aggregation was observed during small scale reactions but this was later identified as a pH and volume problem which was resolved in the larger scale reactions. The conjugates were successfully purified by precipitation with ammonium sulfate however further work into the purification of

all the conjugates needs to be investigated as some reactions contained high levels of free/unconjugated polysaccharide. Problems with the precipitation of PLD during conjugation reactions would need to be further investigated with the examination of reaction buffer, reaction time and purification methods.

The successful conjugate vaccine candidates were formulated with an aluminium phosphate adjuvant. Owing to time constraints, optimisation of the formulation did not take place. The adjuvanted conjugates were compared to two commercially available multivalent pneumococcal conjugate vaccines in order to establish non–inferiority. Two separate studies in mice were performed; the first compared the two investigated conjugation methodologies where Pn1 PS was conjugated to the hydrazide–derivatized CRM_{197} carrier protein using either HOBt or triazine methods. These two conjugates were compared to a commercially available conjugate that also used CRM_{197} as the carrier protein and therefore it was only the conjugation chemistry that was compared. No statistical difference between the two candidate vaccines was determined and both conjugates produced much higher ELISA titres than the commercial vaccine.

The second round of studies applied the triazine conjugation method to Pn1 and three different protein carriers (TT, CRM_{197} and PLD) and compared which protein carrier would provide the best immunogenicity data. Comparisons between the three conjugates and two commercial vaccines were performed using both ELISA and OPA data. The results showed, on average, 5–fold and 12 fold increases in the ELISA antibody titre and 7–fold and 15 fold increases for the OPA data for the CRM_{197} and TT conjugates respectively when compared to the two commercially available vaccines. The PLD conjugate did not show any statistical superiority to the commercial vaccines but was shown to be non–inferior.

By targeting the carboxyl functional groups, of the polysaccharide and using a hydrazide–derivatized protein carrier, the conjugate was able to induce high levels of antibodies and a strong killing potential. These levels of immunogenic and functional antibodies produced by the experimental vaccines, as well as the suggested tolerance in mice gave a strong indication of the potential of this new conjugation approach for conjugate vaccines against pneumococcal type 1 disease.

CONFERENCES AND PRESENTATIONS

Parts of this thesis have been presented at conferences:

Oral Presentation (2009): University of Trieste

Talk Entitled: Developing a vaccine against pneumococcal type 1 disease

Oral and Poster Presentation (2012): 26th International Carbohydrate Symposium in Madrid, Spain

Poster and Talk Entitled: Development of a *Streptococcus pneumoniae* conjugate vaccine against serotype 1 disease.

APPENDIX 1: PURIFICATION RESULTS

Batch	**1**	**2**	**3**	**4**	**5**	**6**	**7**	**8**	**9**	**10**
Fermentation mode	Fermentor	Fermentor	Fermentor	Fermentor	Fermentor	Fermentor	Wave	Fermentor	Wave	Fermentor
Fermentation volume (L)	15	15	15	30	15	15	8	15	6	15
Initial pH	7.20	7.32	7.33	7.05	7.05	7.31	7.91	7.21	7.43	7.20
Initial PS concentration (mg/L)	535	550	550	530	500	530	400	365	264	391
Final Analytical Assays										
PS Content (UA assay) (g)	0.45	2.4	5.4	7.3	Purification failed due to improper clarification	Purification failed due to improper clarification	2.3	Purification failed due to improper clarification	1.6	0.71
O–acetylation (mass %)	–	20	20	23			24		23	23
NMR (mol %)	–*	–	–	–			67		80	–
Nucleic acid (%)	1.570	1.000	1.909	2.181			0.004		0.099	2.181
Protein (%)	6.40	0.29	0.28	1.68			0.61		0.28	6.40
CWPS (mol %)	–*	1.4	0.9	1.9			2.2		2.3	1.9
% recovery	**6**	**29**	**65**	**50**	–	–	**72**	–	**99**	**12**

Batch	**11**	**12**	**13**	**14**	**15**	**16**	**17**	**18**	**19**
Fermentation mode	Fermentor	Fermentor	Wave	Wave	Wave	Fermentor	Fermentor	Fermentor	Fermentor
Fermentation volume (L)	15	–	8	8	8.5	–	–	15	15
Initial pH	7.32	–	7.41	7.02	6.75	–	–	7.05	7.09
Initial PS concentration (mg/L)	932	–	642	268	595	–	–	602	341
Final Analytical Assays									
PS Content (UA assay) (g)	3.7	Not purified due to fermentor electronics offline	2.1	1.7	2.5	Not purified due to problem with centrifuge	Not purified due to accident in BSL3 facilities	7.6	4.0
O–acetylation (mass %)	23		21	23	18			0	23
O–acetylation (mol %)	79		77	76	74			0	67
Nucleic acid (%)	1.271		1.061	0.004	0.099			1.200	1.100
Protein (%)	0.13		0.86	0.10	1.05			3.10	1.70
CWPS (mol %)	1.5		1.5	2.0	1.4			1.2	1.9
% recovery	**27**	–	**41**	**79**	**49**	–	–	**43**	**51**

* NMR not performed

REFERENCES

1. Austrian, R., *Pneumococcal otitis media and pneumococcal vaccines, a historical perspective.* Vaccine, 2001. **19**: p. S71-S77.
2. Schranz, J., *Pneumococcal conjugate vaccines: what do we know and what do we need?* Procedia in Vaccinology, 2009. **1** (1): p. 189-205.
3. *Pneumonia and diarrhoea: Tackling the deadliest diseases for the world's poorest children*, 2012. UNICEF.
4. *WHO World Health Statistics 2012. Global health indicators*, 2012.
5. *WHO/Unicef. Pneumonia: The forgotten killer of children*. 2006. http://www.unicef.org/mdg/mortalitymultimedia/Pneumonia_The_Forgotten_Killer_of_Children.pdf [Accessed on: 12 December 2012].
6. Guo, Z. and Boons, G.-J. *Carbohydrate-based vaccines and immunotherapies*. Wiley Series in Drug Discovery and Development, ed. Wang, B. 2009. John Wiley and Sons: New Jersey.
7. *Pneumococcal Disease*, in *Epidemiology and Prevention of Vaccine-Preventable Diseases: The Pink Book: Course Textbook* 2012. CDC.
8. Austrian, R., *The first one hundred years.* Reviews of Infectious Diseases, 1981. **3** (2): p. 183-189.
9. Plotkin, S.A. and Orenstein, W.A., *Vaccines*. 4 ed 2004. Saunders.
10. Siber, G.R., Klugman, K.P., and Makela, P.H. *Pneumococcal Vaccines: The impact of conjugate vaccines*. 2008. ASM Press: Washington DC.
11. Lopez, R., *Pneumococcus: the sugar coated bacteria.* International Microbiology, 2006. **9**: p. 179-190.
12. Lund, E. and Henrichsen, J., *Laboratory diagnosis, serology and epidemiology of Streptococcus pneumoniae*, in *Methods in Microbiology*, Norris, J.R. 1978. Academic Press: London. p. 241-262.
13. Bahler, B., Lee, T.-S., Lotvin, J.A., Ruppen, M.E., and Charbonneau, P. for Wyeth. *Separation of contaminants from Streptococcus pneumoniae polysaccharide by pH manipulation*. 2006. Organisation, W.I.P. PCT/US2006/12134. WO 2006/110352 A2.
14. Bahler, B., Lee, T.-S., Lotvin, J.A., Ruppen, M.E., and Charbonneau, P. for Wyeth LLC. *Separation of contaminants from Streptococcus pneumoniae polysaccharides by pH manipulation.* 2010. Office, U.S.P. 11/396108. US 7718791 B2.
15. AlonsoDeVelasco, E., Verheul, A.F., Verhoef, J., and Snippe, H., *Streptococcus pneumoniae: Virulence factors, pathogenesis and vaccines.* Microbiological Reviews, 1995. **59** (4): p. 591-603.
16. Lloyd, A.J., Gilbey, A.M., Blewett, A.M., De Pascale, G., El Zoeiby, A., Levesque, R.C., Catherwood, A.C., Tomasz, A., Bugg, T.D., Roper, D.I., and Dowson, C.G., *Characterization of tRNA-dependent peptide bond formation by MurM in the synthesis of Streptococcus pneumoniae peptidoglycan.* Journal of Biological Chemistry, 2008. **283** (10): p. 6402-6417.
17. Tillet, W.S., Goebel, W.F., and Avery, O.T., *Chemical and immunological properties of a species specific carbohydrate of pneumococci.* Journal of Experimental Medicine, 1930. **52** (6): p. 895-900.
18. Jennings, H.J., Lugowski, C., and Young, N.M., *Structure of the complex polysaccharide C-substance from Streptococcus pneumoniae type 1.* Biochemistry, 1980. **19**: p. 4712-4719.
19. Austrian, R., *Some observations on the pneumococcus and current status of pneumococcal disease and its prevention.* Reviews of Infectious Diseases, 1981. **3** (Supplement): p. S1-S17.

20. Rodgers, G.L. and Klugman, K.P., *The future of pneumococcal disease prevention.* Vaccine, 2011. **29** (Supplement 3): p. C43-C48.

21. Henrichsen, J., *Six newly recognized types of Streptococcus pneumoniae.* Journal of Clinical Microbiology, 1995. **33** (10): p. 2759-2763.

22. Henrichsen, J., *Typing of Streptococcus pneumoniae: Past, present, and future.* American Journal of Medicine, 1999. **107** (Supplement 1A): p. S50-S54.

23. Dochez, A.R. and Avery, O.T., *The elaboration of specific soluble substance by pneumococcus during growth.* The Journal of Experimental Medicine, 1917. **26** (4): p. 477-493.

24. Heidelberger, M. and Avery, O.T., *The soluble specific substance: First paper.* Journal of Experimental Medicine, 1923. **38** (1): p. 73-79.

25. Tomasz, A., *Surface components of Streptococcus pneumoniae.* Reviews of Infectious Diseases, 1981. **3** (2): p. 190-211.

26. Weinberger, D. ., Trzciński, K., Lu, Y.-J., Bogaert, D., Brandes, A., Galagan, J., Anderson, P.W., Malley, R., and Lipsitch, M., *Pneumococcal Capsular Polysaccharide Structure Predicts Serotype Prevalence.* PLoS Pathogens, 2009. **5** (6): p. e1000476.

27. Paton, J.C., Hansman, D.J., Boulnois, G.J., Andrew, P.W., Mitchell, T.J., and Walker, J.A. for *Pneumolysin mutants and pneumococcal vaccines made therefrom* 2004. Office, U.S.P. 08/378 213. US 6716432.

28. *Pneumococcal vaccines WHO position paper.* World Health Organization Weekly Epidemiological record, 2012. **87** (12): p. 129-144.

29. Mehr, S. and Wood, N., *Streptococcus pneumoniae – a review of carriage, infection, serotype replacement and vaccination.* Paediatric Respiratory Reviews, 2012. **13** (4): p. 258-264.

30. Lloyd-Evans, N., O'Dempsey, T.J.D., I., B., Secka, O., Demba, E., Todd, J.E., McArdle, T.F., Banya, W.S., and Greenwood, B., *Nasopharyngeal carriage of pneumococci in Gambian children and in their families.* The Pediatric Infectious Disease Journal, 1996. **15**: p. 866-871.

31. Dagan, R., Melamed, R., Muallem, M., Piglansky, L., and Yagupsky, P., *Nasopharyngeal colonization in Southern Israel with antibiotic-resistant pneumococcci during the first 2 years of life: Relation to serotypes likely to be included in pneumococcal conjugate vaccines.* The Journal of Infectious Diseases, 1996. **174** (6): p. 1352-1355.

32. Cardozo, D.M., Nascimento-Carvalho, C.M., Andrade, A.L., Silvany-Neto, A.M., Daltro, C.H., Brandao, M.A., Brandao, A.P., and Brandileone, M.C., *Prevalence and risk factors for nasopharyngeal carriage of Streptococcus pneumoniae among adolescents.* Journal of Medical Microbiology, 2008. **57** (Pt 2): p. 185-189.

33. Gray, B.M., Converse III, G.M., and Dillon Jr., H.C., *Epidemiologic studies of Streptococcus pneumoniae in infants: Acquisition, carriage, and infection during the first 24 months of life.* The Journal of Infectious Diseases, 1980. **142** (6): p. 923-933.

34. Vives, M., Garcia, M.E., Saentz, P., Mora, M., Mata, L., Sabharwal, H., and Svanborg, C., *Nasopharyngeal colonization in Costa Rican children during the first year of life.* The Pediatric Infectious Disease Journal, 1997. **16**: p. 852-858.

35. Bravo, L.C., *Overview of the disease burden of invasive pneumococcal disease in Asia.* Vaccine, 2009. **27** (52): p. 7282-7291.

36. Basarab, M., Ihekweazu, C., George, R., and Pebody, R., *Effective management in clusters of pneumococcal disease: a systematic review.* The Lancet Infectious Diseases, 2011. **11** (2): p. 119-130.

37. Davidson, M., Parkinson, A.J., Bulkow, L.R., Fitzgerald, M.A., Peters, H.V., and Parks, D.J., *The Epidemiology of Invasive Pneumococcal Disease in Alaska, 1986-1990: Ethnic Differences and Opportunities for Prevention.* The Journal of Infectious Diseases, 1994. **170** (2): p. 368-376.

38. Pletz, M.W., Maus, U., Krug, N., Welte, T., and Lode, H., *Pneumococcal vaccines: mechanism of action, impact on epidemiology and adaption of the species.* International Journal of Antimicrobial Agents, 2008. **32** (3): p. 199-206.

39. Kilpi, T., Herva, E., Kaijalainen, T., Syrjanen, R., and Takala, A.K., *Bacteriology of acute otitis media in a cohort of Finnish children followed for the first two years of life.* The Pediatric Infectious Disease Journal, 2001. **20** (7): p. 654-662.

40. Eskola, J., Kilpi, T., Palmu, A., Jokinen, J., Haapakoski, J., Herva, E., Takala, A.K., Kayhty, H., Karma, P., Kohberger, R., Siber, G.R., and Makela, P.M., *Efficacy of a pneumococcal conjugate vaccine against acute otitis media.* New England Journal of Medicine, 2001. **344**: p. 403-409.

41. Teele, D.W., Klein, J.O., and Rosner, B., *Epidemiology of otitis media during the first seven years of life in children in greater Boston: A prospective, cohort study.* The Journal of Infectious Diseases, 1989. **160** (1): p. 83-94.

42. Pitsiou, G.G. and Kioumis, I.P., *Pneumococcal vaccination in adults: does it really work?* Respiratory Medicine, 2011. **105** (12): p. 1776-1783.

43. *Meningitis - pneumococcal*. National Center for Biotechnology Information. Available from: http://www.ncbi.nlm.nih.gov/pubmedhealth/PMH0001632/. [Accessed on:12 September 2012].

44. Baraff, L.J., Lee, S.I., and Schriger, D.L., *Outcomes of bacterial meningitis in children: a meta-analysis. .* The Pediatric Infectious Disease Journal, 1993. **12**: p. 389-394.

45. Musher, D.M., *Infections caused by Streptococcus pneumoniae: clinical spectrum, pathogenesis, immunity and treatment.* Clinical Infectious Diseases, 1992. **14**: p. 801-809.

46. Greenberg, D., Givon-Lavi, N., Newman, N., Bar-Ziv, J., and Dagan, R., *Nasopharyngeal carriage of individual Streptococcus pneumoniae serotypes during pediatric pneumonia as a means to estimate serotype disease potential.* The Pediatric Infectious Disease Journal, 2011. **30** (3): p. 227-233.

47. Poolman, J., Kriz, P., Feron, C., Di-Paolo, E., Henckaerts, I., Miseur, A., Wauters, D., Prymula, R., and Schuerman, L., *Pneumococcal serotype 3 otitis media, limited effect of polysaccharide conjugate immunisation and strain characteristics.* Vaccine, 2009. **27** (24): p. 3213-3222.

48. Hausdorff, W.P., Bryant, J., Klock, C., Paradiso, P., and Siber, G.R., *The contribution of specific pneumococcal serogroups to different disease manifestations: Implications for conjugate vaccine formulation and use. Part II.* Clinical Infectious Diseases, 2000. **30** (1): p. 122-140.

49. Alanee, S.R., McGee, L., Jackson, D., Chiou, C.C., Feldman, C., Morris, A.J., Ortqvist, A., Rello, J., Luna, C.M., Baddour, L.M., Ip, M., Yu, V.L., and Klugman, K.P., *Association of serotypes of Streptococcus pneumoniae with disease severity and outcome in adults: an international study.* Clinical Infectious Diseases, 2007. **45** (1): p. 46-51.

50. Kisakye, A., Makumbi, I., Nansera, D., Lewis, R., Braka, F., Wobudeya, E., Chaplain, D., Nalumansi, E., Mbabazi, W., and Gessner, B.D., *Surveillance for Streptococcus pneumoniae meningitis in children aged <5 years: implications for immunization in Uganda.* Clinical Infectious Diseases, 2009. **48** (Supplement 2): p. S153-S161.

51. O'Brien, K.L., Wolfson, L.J., Watt, J., Henkle, E., Deloria-Knoll, M., McCall, N., Lee, E., Mulholland, E.K., Levine, O.S., and Cherian, T., *Burden of disease caused by Streptococcus pneumoniae in children younger than 5 years: global estimates.* The Lancet, 2009. **374**: p. 893-902.

52. Zar, H.J. and Madhi, S.A., *Pneumococcal conjugate vaccine - a health priority.* South African Medical Journal, 2008. **98** (6): p. 463-467.

53. Nunes, M.C. and Madhi, S.A., *Safety, immunogenicity and efficacy of pneumococcal conjugate vaccine in HIV-infected individuals.* Human Vaccines & Immunotherapeutics, 2012. **8** (2): p. 161-173.

54. Hausdorff, W.P., *The roles of pneumococcal serotypes 1 and 5 in paediatric invasive disease.* Vaccine, 2007. **25** (13): p. 2406-2412.

55. *Pneumococcal regional serotype distribution for pneumococcal AMC TPP*, 2008. GAVI PneumoADIP.

56. Liu, L., Johnson, H.L., Cousens, S., Perin, J., Scott, S., Lawn, J.E., Rudan, I., Campbell, H., Cibulskis, R., Li, M., Mathers, C., and Black, R.E., *Global, regional, and national causes of child mortality: an updated systematic analysis for 2010 with time trends since 2000.* The Lancet, 2012. **379** (9832): p. 2151-2161.

57. Hausdorff, W.P., Bryant, J., Paradiso, P., and Siber, G.R., *Which pneumococcal serogroups cause the most invasive disease: Implications for conjugate vaccine formulation and use. Part I.* Clinical Infectious Diseases, 2000. **30** (1): p. 100-121.

58. Gessner, B.D., Mueller, J.E., and Yaro, S., *African meningitis belt pneumococcal disease epidemiology indicates a need for an effective serotype 1 containing vaccine, including for older children and adults.* BMC Infectious Diseases, 2010. **10**.

59. Weir, D.M., *Immunology - an outline for students of medicine and biology*. 4 ed 1977. Edinburgh: Churchill Livingstone.

60. *Immune System*. National Institute of Health. Available from: http://www.niaid.nih.gov/topics/immunesystem/Pages/default.aspx. [Accessed on:12 November 2012].

61. Janeway, C.A., Travers, P., Walport, M., and Shlomchik, M.J. *Immunobiology: The Immune System in Health and Disease.* . Garland Science. Available from: http://www.ncbi.nlm.nih.gov/books/NBK27156/. [Accessed on:12 November 2012].

62. Wars, D.W., *Host defense against Streptococcus pneumoniae: The role of the spleen.* Reviews of Infectious Diseases, 1981. **3** (2): p. 299-309.

63. Zandvoort, A. and Timens, W., *The dual function of the splenic marginal zone: essential for initiation of anti-TI-2 responses but also vital in the general first-line defense against blood-borne antigens.* Clinical and Experimental Immunology, 2002. **130**: p. 4-11.

64. Klosterman, L., *Immune system* 2009. Marshall Cavendish Benchmark.

65. Mond, J.J., Vos, Q., Lees, A., and Snapper, C.M., *T cell independent antigens.* Current Opinion in Immunology, 1995. **7**: p. 349-354.

66. Rijkers, G.T., Sanders, E.A.M., Breukels, M.A., and Zegers, B.J.M., *Infant B cell responses to polysaccharide determinants.* Vaccine, 1998. **16** (14/15): p. 1396-1400.

67. Klein Klouwenberg, P. and Bont, L., *Neonatal and infantile immune responses to encapsulated bacteria and conjugate vaccines.* Clinical and Developmental Immunology, 2008. **2008**: p. e628963.

68. Cabrera, O., Cuello, M., Soto, C.R., Martínez, M.E., del Campo, J.M., Pérez, O., Infante, J.F., and Sierra, G., *New method for obtaining conjugated vaccines.* Vaccine, 2006. **24** (Supplement): p. S76-S78.

69. Rappuoli, R. and De Gregorio, E., *A sweet T cell response.* Nature Medicine, 2011. **17** (12): p. 1551-1552.

70. Pomat, W.S., Lehmann, D., Sanders, R.C., Lewis, D.J., Wilson, J., Rogers, S., Dyke, T., and Alpers, M.P., *Immunoglobulin G antibody responses to polyvalent pneumococcal vaccine in children in the highlands of Papua New Guinea.* Infection and Immunity, 1994. **62** (5): p. 1848-1854.

71. Laferriere, C., *The immunogenicity of pneumococcal polysaccharides in infants and children: a meta-regression.* Vaccine, 2011. **29** (40): p. 6838-6847.

72. Gonzalez-Fernandez, A., Faro, J., and Fernandez, C., *Immune responses to polysaccharides: lessons from humans and mice.* Vaccine, 2008. **26** (3): p. 292-300.

73. Kelly, D.F., Moxon, E.R., and Pollard, A.J., *Haemophilus influenzae type b conjugate vaccines.* Immunology, 2004. **113** (2): p. 163-174.

74. Avci, F.Y. and Kasper, D.L., *How bacterial carbohydrates influence the adaptive immune system.* Annual Review of Immunology, 2010. **28**: p. 107-130.

75. Avci, F.Y., Li, X., Tsuji, M., and Kasper, D.L., *A mechanism for glycoconjugate vaccine activation of the adaptive immune system and its implications for vaccine design.* Nature Medicine, 2011. **17** (12): p. 1602-1609.

76. de Quandros, C.A. *Vaccines: preventing disease and protecting health*. 2003. Pan American Health Organization: Washington, D.C.

77. Cobb, B.A., Wang, Q., Tzianabos, A.O., and Kasper, D.L., *Polysaccharide processing and presentation by the MHCII pathway.* Cell, 2004. **117** (5): p. 677-687.

78. Cobb, B.A. and Kasper, D.L., *Zwitterionic capsular polysaccharides: thenew MHCII-dependent antigens.* Cellular Microbiology, 2005. **7** (10): p. 1398-1403.

79. Tzianabos, A.O., Onderdonk, A.B., Rosner, B., R.L., C., and Kasper, D.L., *Structural features of polysaccharides that induce intra-abdominal abcesses.* Science, 1993. **262** (5132): p. 416-419.

80. Tzianabos, A.O., Kasper, D.L., and Onderdonk, A.B., *Structure and function of bacteroides fragilis capsular polysaccharides: Relationship to induction and preventionn of abscesses.* Clinical Infectious Diseases, 1995. **20** (Supplement): p. S132-S140.

81. Duan, J., Avci, F.Y., and Kasper, D.L., *Microbial carbohydrate depolymerization by antigen-presenting cells: deamination prior to presentation by the MHCII pathway.* Proceedings of the National Academy of Sciences, USA, 2008. **105** (13): p. 5183-5188.

82. Mertens, J., Fabri, M., Zingarelli, A., Kubacki, T., Meemboor, S., Groneck, L., Seeger, J., Bessler, M., Hafke, H., Odenthal, M., Bieler, J.G., Kalka, C., Schneck, J.P., Kashkar, H., and Kalka-Moll, W.M., *Streptococcus pneumoniae serotype 1 capsular polysaccharide induces CD8CD28 regulatory T lymphocytes by TCR crosslinking.* PLoS Pathogens, 2009. **5** (9): p. e1000596.

83. Truck, J., Lazarus, R., Clutterbuck, E.A., Bowman, J., Kibwana, E., Bateman, E.A.L., and Pollard, A.J., *The zwitterionic type I Streptococcus pneumoniae polysaccharide does not induce memory B cell formation in humans.* Immunobiology, 2013. **218** (3): p. 368-372.

84. Brodie, W.H., Rogers, W.G., and Hamilton, E.T.E., *A contribution to the pathology of infection by the pneumococcus.* South African Medical Journal, 1899. **6**: p. 258-264.

85. Nathan, E.A., *A report on pneumonia at the Premier Diamond Mine.* The Transvaal Medical Journal, 1907. **2**: p. 154-159.

86. Wright, A.E., Parry Morgan, W.P., Colebrook, L., and Dodgson, R.W., *Observations on prophylactic inoculation against pneumococcus infections, and on the results which have been achieved with it.* The Lancet, 1914. **1**: p. 1-10.

87. Rijkers, G.T., van Mens, S.P., and van Velzen-Blad, H., *What do the next 100 years hold for pneumococcal vaccination.* Expert Review of Vaccines, 2010. **9** (11): p. 1241-1244.

88. Lister, F.S., *An experimental study of prophylactic inoculation against pneumococcal infection in the rabbit and in man.* Publications of the South African Institute for Medical Research, 1916. **8**: p. 231-287.

89. Heidelberger, M., MacLeod, C.M., Kaiser, S.J., and Robinson, B., *Antibody formation in volunteers following injection of pneumococci or their type-specific polysaccharides.* Journal of Experimental Medicine, 1946. **83** (4): p. 303-320.

90. Tillet, W.S. and Francis, T., *Cutaneous reactions to the polysaccharides and proteins of pneumococcus in lobar pneumonia.* Journal of Experimental Medicine, 1929. **50** (5): p. 687-701.

91. Finland, M. and Sutliff, W.D., *Specific cutaneous reactions and circulating antibodies in the course of lobar pneumonia. I. Cases receiving no serum therapy. .* Journal of Experimental Medicine, 1931. **54**: p. 637-642.

92. MacLeod, C.M., Hodges, R., Heidelberger, M., and Bernhard, W.G., *Prevention of pneumococcal pneumonia by immunization with specific capsular polysaccharides.* Journal of Experimental Medicine, 1945. **82**: p. 445-465.

93. Heidelberger, M., MacLeod, C.M., and Di Lapi, M.M., *The human antibody response to simultaneous injection of six specific polysaccharides of pneumococcus.* Journal of Experimental Biology, 1948. **88** (3): p. 369-372.

94. Austrian, R. and Gold, J., *Pneumococcal bacteremia with especial reference to bacteremic pneumococcal pneumonia.* Annals of Internal Medicine, 1964. **60** (5): p. 759-776.

95. Austrian, R., Douglas, R.M., Schiffman, G., Coetzee, A.M., Koornhof, H.J., Hayden-Smith, S., and Reid, R.D., *Prevention of pneumococcal pneumonia by vaccination.* Transactions of the Association of American Physicians, 1976. **89**: p. 184-194.

96. Klugman, K.P., Hayden-Smith, S., and Koornhof, H.J., *Evidence that prevention of carriage by pneumococcal capsular vaccines may be the mechanism of protection from pneumococcal pneumonia.* South African Journal of Epidemiology and Infection, 2011. **26** (4): p. 221-224.

97. Butler, J.C., Shapiro, E.D., and Carlone, G.M., *Pneumococcal vaccines: History, current status, and future directions.* American Journal of Medicine, 1999. **107** (Supplement 1A): p. S69-S76.

98. Robbins, J.B., Austrian, R., Lee, C.J., Rastogi, S.C., Schiffman, G., Henrichsen, J., Mäkelä, P.H., Broome, C.V., Facklam, R.R., Tiesjema, R.H., and Jr, J.C.P., *Considerations for Formulating the Second-Generation Pneumococcal Capsular Polysaccharide Vaccine with Emphasis on the Cross-Reactive Types within Groups.* The Journal of Infectious Diseases, 1983. **148** (6): p. 1136-1159.

99. Parkinson, A.J., Davidson, M., Fitzgerald, M.A., Bulkow, L.R., and Parks, D.J., *Serotype distribution and antimicrobial resistance patterns of invasive isolates of Streptococcus pneumoniae: Alaska 1986-1990.* The Journal of Infectious Diseases, 1994. **170** (2): p. 461-464.

100. Hedlund, J., Svenson, S.B., Kalin, M., Henrichsen, J., Olsson-Liljequist, B., Möllerberg, G., and Källenius, G., *Incidence, Capsular Types, and Antibiotic Susceptibility of Invasive Streptococcus pneumoniae in Sweden.* Clinical Infectious Diseases, 1995. **21** (4): p. 948-953.

101. Lee, C.J., Banks, S.D., and Li, J.P., *Virulence, immunity, and vaccine related to Streptococcus pneumoniae.* Critical Reviews in Microbiology, 1991. **18**: p. 89-114.

102. Rozenbaum, M.H., Boersma, C., Postma, M.J., and Hak, E., *Observed differences in invasive pneumococcal disease epidemiology after routine infant vaccination.* Expert Review of Vaccines, 2011. **10** (2): p. 187-199.

103. Ortqvist, A., Henckaerts, I., Hedlund, J., and Poolman, J., *Non-response to specific serotypes likely cause for failure to 23-valent pneumococcal polysaccharide vaccine in the elderly.* Vaccine, 2007. **25** (13): p. 2445-2450.

104. Grabenstein, J.D. and Manoff, S.B., *Pneumococcal polysaccharide 23-valent vaccine: Long-term persistence of circulating antibody and immunogenicity and safety after revaccination in adults.* Vaccine, 2012. **30** (30): p. 4435-4444.

105. Moberley, S., Krause, V., Cook, H., Mulholland, K., Carapetis, J., Torzillo, P., and Andrews, R., *Failure to vaccinate or failure of vaccine? Effectiveness of the 23-valent pneumococcal polysaccharide vaccine program in Indigenous adults in the Northern Territory of Australia.* Vaccine, 2010. **28** (11): p. 2296-2301.

106. *Pneumococcal conjugate vaccine for childhood immunization - WHO position paper.* World Health Organization Weekly Epidemiological record, 2007. **82** (12): p. 93-104.

107. Jones, C., *Vaccines based on the cell surface carbohydrates of pathogenic bacteria.* Annals of the Brazilia Academy of Sciences, 2005. **77** (2): p. 293-324.

108. Goebel, W.F. and Avery, O.T., *Chemo-immunological studies on conjugated carbohydrate proteins: IV The synthesis of the p-aminobenzyl ether of the soluble specific substance of type III pneumococcus and its coupling with proteins.* Journal of Experimental Medicine, 1931. **54** (3): p. 431-436.

109. Avery, O.T. and Goebel, W.F., *Chemo-immunological studies on conjugated carbohydrate proteins: II Immunological specificity of synthetic sugar-protein antigens.* Journal of Experimental Medicine, 1929. **50** (4): p. 533-550.

110. Goebel, W.F. and Avery, O.T., *Chemo-immunological studies on conjugated carbohydrate proteins: I. The synthesis of p-aminophenol b-glucoside, p-aminophenol b-galactoside, and their coupling with serum globulin* Journal of Experimental Medicine, 1929. **50** (4): p. 521-531.

111. Goebel, W.F., Avery, O.T., and Babers, F.H., *Chemo-immunological studies on conjugated carbohydrate proteins: IX The specificity of antigens prepared by combining the p-aminophenol glycosides of disaccharides with proteins.* Journal of Experimental Medicine, 1934. **60** (5): p. 599-617.

112. Goebel, W.F., Babers, F.H., and Avery, O.T., *Chemo-immunological studies on conjugated carbohydrate-proteins: VI The synthesis of p-aminophenol a-glucoside and its coupling with protein.* Journal of Experimental Medicine, 1932. **55** (5): p. 761-767.

113. Avery, O.T. and Goebel, W.F., *Chemo-immunological studies on conjugated carbohydrate proteins: V The immunological specificity of an antigen prepared by combining the capsular polysaccharide of type III pneumococcus with foreign protein.* Journal of Experimental Medicine, 1931. **54** (3): p. 437-447.

114. Schneerson, R., Barrera, O., Sutton, A., and Robbins, J.B., *Preparation, characterization and immunogenicity of Haemophilus influenzae type b polysaccharide-protein conjugates.* The Journal of Experimental Medicine, 1980. **152**: p. 361-376.

115. Schneerson, R., Robbins, J.B., J.C., P.J., Bell, C., Schlesselman, J.J., Sutton, A., Wang, Z., Schiffman, G., Karpas, A., and Shiloach, J., *Quantitative and qualitative analyses of serum antibodies elicited in adults by Haemophilus influenzae type b and pneumococcus type 6A capsular polysaccharide-tetanus toxoid conjugates.* Infection and Immunity, 1986. **52** (2): p. 519-528.

116. *Countries having introduced Hib vaccine and infant Hib coverage - WHO/IVB database, September 2011*. World Health Organization. Available from: http://www.who.int/nuvi/hib/decision_implementation/en/index1.html. [Accessed on:24 September 2012].

117. Dinleyici, E.C., *Current status of pneumococcal vaccines: lessons to be learned and new insights.* Expert Review of Vaccines, 2010. **9** (9): p. 1017-1022.

118. Rennels, M.B., Edwards, K.M., Keyserling, H.L., Reisinger, K.S., Hogerman, D.A., Madore, D.V., Chang, I., Paradiso, P.R., Malinoski, F.J., and Kimura, A., *Safety and immunogenicity of heptavalent pneumococcal vaccine conjugated to CRM197 in United States infants. .* Pediatrics, 1998. **101** (4): p. 604-611.

119. Dinleyici, E.C. and Yargic, Z.A., *Pneumococcal conjugated vaccines: impact of PCV-7 and new achievements in the postvaccine era.* Expert Review of Vaccines, 2008. **7** (9): p. 1367-1394.

120. Anderson, P.W. and Eby, R. for The University of Rochester. *Immunogenic conjugates of Streptococcus pneumonial capsular polymer and toxin or in toxiad*. 1994. Office, U.S.P. 819305. 5360897.

121. Dagan, R. and Poland, G., *World Pneumonia Day: fighting pneumonia with safe and affordable vaccines.* Vaccine, 2010. **28** (48): p. 7577-7578.

122. Black, S., Shinefield, H.R., Fireman, B., Lewis, E., Ray, P., Hansen, J.B., Elvin, L., Ensor, K.M., Hackell, J., Siber, G.R., Malinoski, F.J., Madore, D.V., Chang, I., Kohberger, R., Watson, W., Austrian, R., and Edwards, K.M., *Efficacy, safety and immunogeniicty of heptavalent pneumococcal conjugate vaccine in children.* The Pediatric Infectious Disease Journal, 2000. **19** (3): p. 187-196.

123. O'Brien, K.L., Moulton, L.H., Reid, R., Weatherholtz, R., Oski, J., Brown, L., Kumar, G., Parkinson, A.J., Hu, D., Hackell, J., Kohberger, R., Siber, G.R., and Santosham, M., *Efficacy and safety of seven-valent conjugate pneumococcal vaccine in American Indian children: group randomised trial.* The Lancet, 2003. **362**: p. 355-361.

124. Prymula, R., Motlova, J., and Kriz, P., *Comparison of Streptococcus pneumoniae serotypes causing acute otitis media and invasive disease in young children in the Czech Republic.* Indian Journal of Medical Research, 2004. **119**: p. 168-170.

125. Hansen, J., Black, S., Shinefield, H., Cherian, T., Benson, J., Fireman, B., Lewis, E., Ray, P., and Lee, J., *Effectiveness of heptavalent pneumococcal conjugate vaccine in children younger than 5 years of age for prevention of pneumonia: updated analysis using World Health Organization standardized interpretation of chest radiographs.* The Pediatric Infectious Disease Journal, 2006. **25** (9): p. 779-781.

126. Black, S.B., Shinefield, H.R., Ling, S., Hansen, J., Fireman, B., Spring, D., Noyes, J., Lewis, E., Ray, P., Lee, J., and Hackell, J., *Effectiveness of heptavalent pneumococcal conjugate vaccine in children younger than five years of age for prevention of pneumonia.* The Pediatric Infectious Disease Journal, 2002. **21** (9): p. 810-815.

127. Adamkiewicz, T.V., Silk, B.J., Howgate, J., Baughman, W., Strayhorn, G., Sullivan, K., and Farley, M.M., *Effectiveness of the 7-valent pneumococcal conjugate vaccine in children with sickle cell disease in the first decade of life.* Pediatrics, 2008. **121** (3): p. 562-569.

128. Kourtis, A.P., Ellington, S., Bansil, P., Jamieson, D.J., and Posner, S.F., *Hospitalizations for invasive pneumococcal disease among human immunodeficiency virus-1 infected children, adolescents and young adults in the United States in the era of highly active antiretroviral therapy and the conjugate pneumococcal vaccine.* The Pediatric Infectious Disease Journal, 2010. **29** (6): p. 561-563.

129. Moffitt, K.L. and Malley, R., *Next generation pneumococcal vaccines.* Current Opinion in Immunology, 2011. **23** (3): p. 407-413.

130. Black, S., Shinefield, H., Baxter, R., Austrian, R., Bracken, L., Hansen, J., Lewis, E., and Fireman, B., *Postlicensure Surveillance for Pneumococcal Invasive Disease After Use of Heptavalent Pneumococcal Conjugate Vaccine in Northern California Kaiser Permanente.* The Pediatric Infectious Disease Journal, 2004. **23** (6): p. 485-489.

131. Hsu, K.K., Shea, K.M., Stevenson, A.E., and Pelton, S.I., *Changing serotypes causing childhood invasive pneumococcal disease: Massachusetts, 2001-2007.* The Pediatric Infectious Disease Journal, 2010. **29** (4): p. 289-293.

132. Singleton, R.J., Hennessy, T.W., L.R., B., Hammitt, L.L., Zulz, T., Hurlburt, D.A., Butler, J.C., Rudolph, K., and Parkinson, A.J., *Invasive pneumococcal disease caused by nonvaccine serotypes among alaska native children with high levels of 7-valent pneumococcal conjugate vaccine coverage.* The Journal of the American Medical Association, 2007. **297** (16): p. 1784-1792.

133. Hausdorff, W.P., van Dyke, M.K., and Effelterre, v., *Serotype replacement after pneumococcal vaccination.* The Lancet, 2012. **379** (9824): p. 1387-1388.

134. Weinberger, D.M., Malley, R., and Lipsitch, M., *Serotype replacement in disease after pneumococcal vaccination.* The Lancet, 2011. **378** (9807): p. 1962-1973.

135. Jacobs, M.R., Good, C.E., Bajaksouzian, S., and Windau, A.R., *Emergence of Streptococcus pneumoniae serotypes 19A, 6C, and 22F and serogroup 15 in Cleveland, Ohio, in relation to introduction of the protein-conjugated pneumococcal vaccine.* Clinical Infectious Diseases, 2008. **47** (11): p. 1388-1395.

136. Krishnamurthy, T., Lee, C.J., Henrichsen, J., Carlo, D.J., Stoudt, T.M., and Robbins, J.B., *Characterization of the cross reaction between type 19F (19) and 19A (57) pneumococcal capsular polysaccharides: Compositional anallysis and immunological relation determined with rabbit typing antisera.* Infection and Immunity, 1978. **22** (3): p. 727-735.

137. Pichichero, M.E. and Casey, J.R., *Emergence of a multiresistant serotype 19A pneumococcal strain not included in the 7-valent conjugate vaccine as an otophaogen in children.* The Journal of the American Medical Association, 2007. **298** (15): p. 1772-1778.

138. Kaplan, S.L., Barson, W.J., Lin, P.L., Stovall, S.H., Bradley, J.S., Tan, T.Q., Hoffman, J.A., Givner, L.B., and Mason, E.O., Jr., *Serotype 19A Is the most common serotype causing invasive pneumococcal infections in children.* Pediatrics, 2010. **125** (3): p. 429-436.

139. Hoberman, A., Paradise, J.L., Shaikh, N., Greenberg, D.P., Kearney, D.H., Colborn, D.K., Rockette, H.E., Kurs-Lasky, M., McEllistrem, M.C., Zoffel, L.M., Balentine, T.L., Barbadora, K.A., and Wald, E.R., *Pneumococcal resistance and serotype 19A in Pittsburgh-area children with acute otitis media before and after introduction of 7-valent pneumococcal polysaccharide vaccine.* Clinical Pediatrics, 2011. **50** (2): p. 114-120.

140. Picazo, J., Ruiz-Contreras, J., Hernandez, B., Sanz, F., Gutierrez, A., Cercenado, E., Meseguer, M.A., Delgado-Iribarren, A., Rodriguez-Avial, I., and Mendez, C., *Clonal and clinical profile of Streptococcus pneumoniae serotype 19A causing pediatric invasive infections: a 2-year (2007-2009) laboratory-based surveillance in Madrid.* Vaccine, 2011. **29** (9): p. 1770-1776.

141. Choi, E.H., Kim, S.H., Eun, B.W., Kim, S.J., Kim, N.H., Lee, J., and Lee, H.J., *Streptococcus pneumoniae serotype 19A in children, South Korea.* Emerging Infectious Diseases, 2008. **14** (2): p. 275-282.

142. Lee, H.J., Park, S.E., and Kim, K.H., *Immune response to 19A serotype after immunization of 19F containing pneumococcal conjugate vaccine in Korean children aged 12-23 months.* Korean Journal of Pediatrics, 2011. **54** (4): p. 163-168.

143. *What is the Pneumococcus - powerpoint presentation*. PneumoAction. Available from: http://www.preventpneumo.org/data-tools/slides.cfm. [Accessed on:15 June 2012].

144. Hausdorff, W.P., Feikin, D.R., and Klugman, K.P., *Epidemiological differences among pneumococcal serotypes.* The Lancet Infectious Diseases, 2005. **5** (2): p. 83-93.

145. Aguiar, S.I., Brito, M.J., Goncalo-Marques, J., Melo-Cristino, J., and Ramirez, M., *Serotypes 1, 7F and 19A became the leading causes of pediatric invasive pneumococcal infections in Portugal after 7 years of heptavalent conjugate vaccine use.* Vaccine, 2010. **28** (32): p. 5167-5173.

146. Brueggemann, A.B. and Spratt, B.G., *Geographic distribution and clonal diversity of Streptococcus pneumoniae serotype 1 Isolates.* Journal of Clinical Microbiology, 2003. **41** (11): p. 4966-4970.

147. Saha, S.K., Naheed, A., El Arifeen, S., Islam, M., Al-Emran, H., Amin, R., Fatima, K., Brooks, W.A., Breiman, R.F., Sack, D.A., and Luby, S.P., *Surveillance for invasive Streptococcus pneumoniae disease among hospitalized children in Bangladesh: antimicrobial susceptibility and serotype distribution.* Clinical Infectious Diseases, 2009. **48** (Supplement 2): p. S75-S81.

148. Romney, M.G., Hull, M.W., Gustafson, R., Sandhu, J., Champagne, S., Wong, T., Nematallah, A., Forsting, S., and Daly, P., *Large community outbreak of Streptococcus pneumoniae serotype 5 invasive infection in an impoverished, urban population.* Clinical Infectious Diseases, 2008. **47** (6): p. 768-774.

149. Leimkugel, J., Forgor, A.A., Gagneux, S., Pfluger, V., Flierl, C., Awine, E., Neegeli, M., Dangy, J.-P., Smith, T., Hodgson, A., and Plusch, G., *An outbreak of serotype 1 Streptococcus pneumoniae meningitis in Northern Ghana with features that are characteristic of Neisseria meningitidis meningitis epidemics.* The Journal of Infectious Diseases, 2005. **19** (192-198).

150. Imohl, M., Reinert, R.R., Ocklenburg, C., and van der Linden, M., *Association of serotypes of Streptococcus pneumoniae with age in invasive pneumococcal disease.* Journal of Clinical Microbiology, 2010. **48** (4): p. 1291-1296.

151. Ruckinger, S., von Kries, R., Siedler, A., and van der Linden, M., *Association of serotype of Streptococcus pneumoniae with risk of severe and fatal outcome.* The Pediatric Infectious Disease Journal, 2009. **28** (2): p. 118-122.

152. Madhi, S.A. and Klugman, K.P., *A role for Streptococcus pneumoniae in virus-associated pneumonia.* Nature Medicine, 2004. **10** (8): p. 811-813.

153. Klugman, K.P., Madhi, S.A., Huebner, R.E., Kohberger, R., Mbelle, N., and Pierce, N., *A trial of a 9-valent pneumococcal conjugate vaccine in children with and those without HIV infection.* New England Journal of Medicine, 2003. **349** (14): p. 1341-1348.

154. Cutts, F.T., Zaman, S.M.A., Enwere, G., Jaffar, S., Levine, O.S., Okoko, J.B., Oluwalana, C., Vaughan, A., Obaro, S.K., Leach, A., McAdam, K.P., Biney, E., Saaka, M., Onwuchekwa, U., Yallop, F., Pierce, N.F., Greenwood, B.M., and Adegbola, R.A., *Efficacy of nine-valent pneumococcal conjugate vaccine against pneumonia and invasive pneumococcal disease in The Gambia: randomised, double-blind, placebo-controlled trial.* The Lancet, 2005. **365** (9465): p. 1139-1146.

155. Saaka, M., Okoko, B.J., Kohberger, R.C., Jaffar, S., Enwere, G., Biney, E.E., Oluwalana, C., Vaughan, A., Zaman, S.M., Asthon, L., Goldblatt, D., Greenwood, B.M., Cutts, F.T., and Adegbola, R.A., *Immunogenicity and serotype-specific efficacy of a 9-valent pneumococcal conjugate vaccine (PCV-9) determined during an efficacy trial in The Gambia.* Vaccine, 2008. **26** (29-30): p. 3719-3726.

156. Prymula, R., Peeters, P., Chrobok, V., Kriz, P., Novakova, E., Kaliskova, E., Kohl, I., Lommel, P., Poolman, J., Prieels, J.-P., and Schuerman, L., *Pneumococcal capsular polysaccharides conjugated to protein D for prevention of acute otitis media caused by both Streptococcus pneumoniae and non-typable Haemophilus influenzae: a randomised double-blind efficacy study.* The Lancet, 2006. **367** (9512): p. 740-748.

157. Schuerman, L., Prymula, R., Henckaerts, I., and Poolman, J., *ELISA IgG concentrations and opsonophagocytic activity following pneumococcal protein D conjugate vaccination and relationship to efficacy against acute otitis media.* Vaccine, 2007. **25** (11): p. 1962-1968.

158. Lucero, M.G., Nohynek, H., Williams, G., Tallo, V., Simoes, E.A., Lupisan, S., Sanvictores, D., Forsyth, S., Puumalainen, T., Ugpo, J., Lechago, M., de Campo, M., Abucejo-Ladesma, E., Sombrero, L., Nissinen, A., Soininen, A., Ruutu, P., Riley, I., and Makela, H.P., *Efficacy of an 11-valent pneumococcal conjugate vaccine against radiologically confirmed pneumonia among children less than 2 years of age in the Philippines: a randomized, double-blind, placebo-controlled trial.* The Pediatric Infectious Disease Journal, 2009. **28** (6): p. 455-462.

159. Ugpo, J., Lucero, M., Williams, G., Lechago, M., Nillos, L., Tallo, V., and Nohynek, H., *Reactogenicity and tolerability of a non-adjuvanted 11-valent diphtheria-tetanus toxoid pneumococcal conjugate vaccine in Filipino children.* Vaccine, 2009. **27** (20): p. 2723-27239.

160. Dagan, R., Goldblatt, D., Maleckar, J.R., Yaich, M., and Eskola, J., *Reduction of antibody response to an 11-valent pneumococcal vaccine coadministered with a vaccine containing acellular pertussis components.* Infection and Immunity, 2004. **72** (9): p. 5383-5391.

161. *Expert committee on biological standardization:* , in *Recommendations to assure the quality, safety and efficacy of pneumococcal conjugate vaccines.* 2009. World Health Organization Relacement of TRS 927 Annex 2.

162. *Annex 2: Recommendations for the production and control of pneumococcal conjugate vaccines*, 2005. World Health Organization WHO technical report series no 927.

163. Jódar, L., Butler, J., Carlone, G., Dagan, R., Goldblatt, D., Käyhty, H., Klugman, K., Plikaytis, B., Siber, G., Kohberger, R., Chang, I., and Cherian, T., *Serological criteria for evaluation and licensure of new pneumococcal conjugate vaccine formulations for use in infants.* Vaccine, 2003. **21** (23): p. 3265-3272.

164. *Assessment report for Synflorix*, 2009. European Medicines Agency Procedure no: EMEA/H/C/000973.

165. Prymula, R. and Schuerman, L., *10 valent pneumococcal nontypeable Haemophilus influenzae PD conjugate vaccine: Synflorix.* Expert Review of Vaccines, 2009. **8** (11): p. 1479-1500.

166. Biemans, R.L., Denoel, P., Poolman, J., and Prieels, J.P. for GlaxoSmithKline. *Vaccine*. 2007. Organization, W.I.P. PCT/EP2007/053412. WO 2007/116028 A2.

167. Nurkka, A., Joensuu, J., Henckaerts, I., Peeters, P., Poolman, J., Kilpi, T., and K??yhty, H., *Immunogenicity and Safety of the Eleven Valent Pneumococcal Polysaccharide-Protein D Conjugate Vaccine in Infants.* The Pediatric Infectious Disease Journal, 2004. **23** (11): p. 1008-1014.

168. Vesikari, T., Wysocki, J., Chevallier, B., Karvonen, A., Czajka, H., Arsene, J.P., Lommel, P., Dieussaert, I., and Schuerman, L., *Immunogenicity of the 10-valent pneumococcal non-typeable Haemophilus influenzae protein D conjugate vaccine (PHiD-CV) compared to the licensed 7vCRM vaccine.* The Pediatric Infectious Disease Journal, 2009. **28** (Supplement 4): p. S66-S76.

169. Wysocki, J., Tansey, S., Brachet, E., Baker, S., Gruber, W., Giardina, P., and Arora, A., *Randomised, controlled trial of concomitant pneumococcal and meningococcal conjugate vaccines.* Vaccine, 2010. **28** (49): p. 7779-7786.

170. Wysocki, J., Tejedor, J.C., Grunert, D., Konior, R., Garcia-Sicilia, J., Knuf, M., Bernard, L., Dieussaert, I., and Schuerman, L., *Immunogenicity of the 10-valent pneumococcal non-typeable Haemophilus influenzae protein D conjugate vaccine (PHiD-CV) when coadministered with different neisseria meningitidis serogroup C conjugate vaccines.* The Pediatric Infectious Disease Journal, 2009. **28** (Supplement 4): p. S77-S88.

171. Bermal, N., Szenborn, L., Chrobot, A., Alberto, E., Lommel, P., Gatchalian, S., Dieussaert, I., and Schuerman, L., *The 10-valent pneumococcal non-typeable Haemophilus influenzae protein D conjugate vaccine (PHiD-CV) coadministered with DTPw-HBV/Hib and poliovirus vaccines: assessment of immunogenicity.* The Pediatric Infectious Disease Journal, 2009. **28** (Supplement 4): p. S89-S96.

172. Knuf, M., Pankow-Culot, H., Grunert, D., Rapp, M., Panzer, F., Kollges, R., Fanic, A., Habib, A., Borys, D., Dieussaert, I., and Schuerman, L., *Induction of immunologic memory following primary vaccination with the 10-valent pneumococcal nontypeable Haemophilus influenzae protein D conjugate vaccine in infants.* The Pediatric Infectious Disease Journal, 2012. **31** (1): p. 31-36.

173. Vesikari, T., Karvonen, A., Lindblad, N., Korhonen, T., Lommel, P., Willems, P., Dieussaert, I., and Schuerman, L., *Safety and immunogenicity of a booster dose of the 10-valent pneumococcal nontypeable Haemophilus influenzae protein D conjugate vaccine coadministered with measles-mumps-rubella-varicella vaccine in children aged 12 to 16 months.* The Pediatric Infectious Disease Journal, 2010. **29** (6): p. 47-56.

174. Kim, C.H., Kim, J.S., Cha, S.H., Kim, K.N., Kim, J.D., Lee, K.Y., Kim, H.M., Kim, J.H., Hyuk, S., Hong, J.Y., Park, S.E., Kim, Y.K., Kim, N.H., Fanic, A., Borys, D., Ruiz-Guinazu, J., Moreira, M., Schuerman, L., and Kim, K.H., *Response to primary and booster vaccination with 10-valent pneumococcal nontypeable Haemophilus influenzae protein D conjugate vaccine in Korean infants.* The Pediatric Infectious Disease Journal, 2011. **30** (12): p. 235-243.

175. Hausdorff, W.P., Siber, G.R., Paradiso, P., and Prasad, A.K. for Wyeth. *Multivalent pneumococcal polysaccharide-protein conjugate composition*. 2007. Office, U.S.P. 11/644207. US2007/0184072 A1.

176. Scott, D.A., Komjathy, S.F., Hu, B.T., Baker, S., Supan, L.A., Monahan, C.A., Gruber, W., Siber, G.R., and Lockhart, S.P., *Phase 1 trial of a 13-valent pneumococcal conjugate vaccine in healthy adults.* Vaccine, 2007. **25** (33): p. 6164-6166.

177. Scott, D., Ruckle, J., Dar, M., Baker, S., Kondoh, H., and Lockhart, S., *Phase 1 trial of 13-valent pneumococcal conjugate vaccine in Japanese adults.* Pediatrics International, 2008. **50** (3): p. 295-299.

178. Kieninger, D.M., Kueper, K., Steul, K., Juergens, C., Ahlers, N., Baker, S., Jansen, K.U., Devlin, C., Gruber, W.C., Emini, E.A., and Scott, D.A., *Safety, tolerability, and immunologic noninferiority of a 13-valent pneumococcal conjugate vaccine compared to a 7-valent pneumococcal conjugate vaccine given with routine pediatric vaccinations in Germany.* Vaccine, 2010. **28** (25): p. 4192-4203.

179. Yeh, S.H., Gurtman, A., Hurley, D.C., Block, S.L., Schwartz, R.H., Patterson, S., Jansen, K.U., Love, J., Gruber, W.C., Emini, E.A., and Scott, D.A., *Immunogenicity and safety of 13-valent pneumococcal conjugate vaccine in infants and toddlers.* Pediatrics, 2010. **126** (3): p. 493-505.

180. Kellner, J.D., Halperin, S., Scheifele, D., Connor, D.D., Dionne, M., McDonald, J.C., Meekison, W.G., Predy, G., Rubinstein, E., Tapiero, B., Zickler, P., Pride, M., Patterson, S., Girgenti, D., Gruber, W., Emini, E.A., and Scott, D. *Immunogenicity and safety of a 13-valent pneumococcal conjugate vaccine in healthy infants and toddlers given with routine pediatric vaccinations in Canada*. in *7th Internation Symposium on Pneumococci and Pneumococcal Diseases*. 2010. Israel.

181. Vanderkooi, O.G., Scheifele, D.W., Girgenti, D., Halperin, S.A., Patterson, S.D., Gruber, W.C., Emini, E.A., Scott, D.A., and Kellner, J.D., *Safety and immunogenicity of a 13-valent pneumococcal conjugate vaccine in healthy infants and toddlers given with routine pediatric vaccinations in Canada.* The Pediatric Infectious Disease Journal, 2012. **31** (1): p. 72-77.

182. Cooper, D., Yu, X., Sidhu, M., Nahm, M.H., Fernsten, P., and Jansen, K.U., *The 13-valent pneumococcal conjugate vaccine (PCV13) elicits cross-functional opsonophagocytic killing responses in humans to Streptococcus pneumoniae serotypes 6C and 7A.* Vaccine, 2011. **29** (41): p. 7207-7211.

183. Nunes, M.C. and Madhi, S.A., *Review on the immunogenicity and safety of PCV-13 in infants and toddlers.* Expert Review of Vaccines, 2011. **10** (7): p. 951-980.

184. Skinner, J.M., Indrawati, L., Cannon, J., Blue, J., Winters, M., Macnair, J., Pujar, N., Manger, W., Zhang, Y., Antonello, J., Shiver, J., Caulfield, M., and Heinrichs, J.H., *Pre-clinical evaluation of a 15-valent pneumococcal conjugate vaccine (PCV15-CRM197) in an infant-rhesus monkey immunogenicity model.* Vaccine, 2011. **29** (48): p. 8870-8876.

185. Musey, L. *Safety, Tolerability, and Immunogenicity of 15-Valent Pneumococcal Conjugate Vaccine (PCV15) in Healthy Adults*. in *Infectious Diseases Society of America*. 2011. Boston.

186. Sobanjo, A., Vesikari, T., Malacaman, E., Shapiro, S., Dallas, M., Hoover, P., McFetridge, R., Marchese, R.D., Watson, W., and Musey, L. *Safety, tolerability, and immunogenicity of 15-valent pneumococcal conjugate vaccine (PCV15) in toddlers previously immunized with 7-valent pneumococcal conjugate vaccine (PCV7)*. in *European Society for Pediatric Infectious Diseases*. 2011. The Haugue, Netherlands.

187. Croucher, N.J., Harris, S.R., Fraser, C., Quail, M.A., Burton, J., van der Linden, M., McGee, L., von Gottberg, A., Song, J.H., Ko, K.S., Pichon, B., Baker, S., Parry, C.M., Lambertsen, L.M., Shahinas, D., Pillai, D.R., Mitchell, T.J., Dougan, G., Tomasz, A., Klugman, K.P., Parkhill, J., Hanage, W.P., and Bentley, S.D., *Rapid pneumococcal evolution in response to clinical interventions.* Science, 2011. **331** (6016): p. 430-434.

188. Moffitt, K.L., Yadav, P., Weinberger, D.M., Anderson, P.W., and Malley, R., *Broad antibody and T cell reactivity induced by a pneumococcal whole-cell vaccine.* Vaccine, 2012. **30** (29): p. 4316-4322.

189. Antonio, M., Hakeem, I., Awine, T., Secka, O., Sankareh, K., Nsekpong, D., Lahai, G., Akisanya, A., Egere, U., Enwere, G., Zaman, S.M., Hill, P.C., Corrah, T., Cutts, F., Greenwood, B.M., and Adegbola, R.A., *Seasonality and outbreak of a predominant Streptococcus pneumoniae serotype 1 clone from The Gambia: expansion of ST217 hypervirulent clonal complex in West Africa.* BMC Microbiology, 2008. **8**: p. 198-204.

190. Mehiri-Zghal, E., Decousser, J.W., Mahjoubi, W., Essalah, L., El Marzouk, N., Ghariani, A., Allouch, P., and Slim-Saidi, N.L., *Molecular epidemiology of a Streptococcus pneumoniae serotype 1 outbreak in a Tunisian jail.* Diagnostic Microbiology and Infectious Disease, 2010. **66** (2): p. 225-227.

191. Klugman, K.P., Madhi, S.A., Adegbola, R.A., Cutts, F., Greenwood, B., and Hausdorff, W.P., *Timing of serotype 1 pneumococcal disease suggests the need for evaluation of a booster dose.* Vaccine, 2011. **29** (18): p. 3372-3373.

192. Walsh, G., *Biopharmaceuticals - Biochemistry and Biotechnology*. 2 ed 2003. England: Wiley and Sons Ltd.

193. *Wave Bioreactor Catalog 2006*, 2006. Wave Europe Pvt. Ltd.

194. Liveyns, R., Gilles, D., and Arickx, M. for SmithKline *Process for the preparation of purified bacterial capsular antigenic polysaccharides, the obtained products and their use.* 1983. Office, E.P. EP19820107154 19820807. EP0072513.

195. Field, L.D., Sternhell, S., and Kalman, J.R. *Organic structures from spectra*. 4 ed. 2008. John WIley and Sons Ltd.: England.

196. Dische, Z., *A new specific color reaction for hexuronic acids.* The Journal of Biological Chemistry, 1946. **167**: p. 189-199.

197. Dische, Z., *A modification of the carbazole reaction of hexuronic acids for the study of polyuronides.* The Journal of Biological Chemistry, 1949. **183**: p. 489-195.

198. Bitter, T. and Muir, H.M., *A modified uronic acid carbazole reaction.* Analytical Biochemistry, 1962. **4** (4): p. 330-334.

199. Hestrin, S., *The reaction of acetylcholine and other carboxylic acid derivatives with hydroxylamine and its analytical application.* The Journal of Biological Chemistry, 1949. **180** (1): p. 249-262.

200. Aksnes, G., *The complex between hydroxamic acids and ferric ions, and the use of the complex for quantitative determination of hydroxamic acids, acyl derivatives and ferric salts.* Acta Chemica Scandinavica, 1957. **11**: p. 710-716.

201. Walker, J.M. *The protein protocols handbook*. 2 ed., ed. Mezzina, D. 2002. Humans Press.

202. Goldfarb, A.R., Saidel, L.J., and Mosovich, E., *The ulltraviolet absorption spectra of proteins.* The Journal of Biological Chemistry, 1951. **193**: p. 397-404.

203. Creighton, T.E., *Proteins: structures and molecular properties*. 2 ed 1993. W.H. Freeman. 207.

204. *Instructions for Coomassie (Bradford) protein assay kit*, 2011. Thermo Scientific.

205. *Protein Assay: Technical handbook*, 2005. Pierce Biotechnology.

206. Snyder, S.L. and Showalter, P.Z., *An improved 2,4,6-trinitrobenzenesulfonic acid method for the determination of amines.* Analytical Biochemistry, 1975. **64**: p. 284-288.

207. Qi, X.-Y., Keyhani, N.O., and Lee, Y.C., *Spectroscopic determination of hydrazine, hydrazides, and their mixtures with trinitrobenzenesulfonic acid.* Analytical Biochemistry, 1988. **175**: p. 139-144.

208. Stramski, D. and Piskozub, J., *Estimation of scattering error in spectroscopic measurements of light absorption by aquatic particles from three-dimensional radiative transfer simulations.* Applied Optics, 2003. **42** (18): p. 3634-3647.

209. *Instructions: TNBSA*, 1999. Pierce Chemical Company.

210. Manz, A., Pamme, N., and Iossifidis, D., *Bioanalytical Chemistry* 2004. London: Imperial College Press.

211. Mikkelsen, S.R. and Corton, E., *Bioanalytical Chemistry* 2004. New Jersey: Wiley-Interscience.

212. Gault, V.A. and McClenaghan, N.H., *Understanding Bioanalytical Chemistry: Principles and Applications* 2009. Wiley-Blackwell.

213. Wilson, K. and Walker, J. *Principles and techniques of biochemistry and molecular biology*. 7 ed. 2010. Cambridge University Press: Cambridge, United Kingdom.

214. O'Dell, J.W., *Determination of turbidity by nephelometry: Method 180.1*, Agency, U.S.E.p., Editor 1993. Revision 2.0.

215. Sadar, M., *Introduction to laser nephelometry: an alternative to conventional particulate analysis methods*, 2005.

216. Labtech, B., *NEPHELOstar plus: Laser based microplate nephelometer that measures light scattering*, 2012.

217. Marburg, S., Tolman, R.L., Kniskern, P.J., Miller, W.J., Hagopian, A., Ip, C.C., Hennessey Jr, J.P., Kubek, D.J., and Burke, P.D. for Merck & Co Inc. *Pneumococcal polysaccharide conjugate vaccine*. 1997. Office, U.S.P. 246394. 5623057.

218. Lee, C.-J., *Quality control of polyvalent pneumococcal polysaccharide-protein conjugate vaccine by nephelometry.* Biologicals, 2002. **30** (2): p. 97-103.

219. Frokjaer, S. and Hovgaard, L. *Pharmaceutical formulation: Develoment of peptides and proteins*. 2000.

220. BIO-RAD, *Criterion precast gels: Instruction manual and application guide*, 2011. Bio-Rad Laboratories Document number: 4110001 Rev F.

221. BIO-RAD, *Criterion XT precast gel instruction guide*, Bio-Rad Revision B.

222. BIO-RAD, *Protein Blotting guide: A guide to transfer and detection*, Bio-Rad.

223. BIO-RAD, *Immun-Blot PVDF membrane for protein blotting: Instruction manual,* Bio-Rad.

224. Davey, J. and Lord, M., *Gel electrophoresis of proteins*, in *Cell structure: A practical approach* 2003. Oxford University Press. p. 197-268.

225. *Protein Blotting Handbook* 2012. Millipore Application Note: TP001ENEU. Available from: http://www.millipore.com/publications.nsf/a73664f9f981af8c852569b9005b4eee/bdd070ddcbe9b90385257a95005ce13e/$FILE/TP001ENEU,_MM.pdf. [Accessed on: 12 December 2012].

226. Gunzler, H. and Williams, A. *Handbook of Analytical Techniques*. 2002. Wiley-VCH: Germany.

227. Amersham, *Gel Filtration: Principles and methods*, 2002. Amersham Biosciences.

228. Lee, Y.C., *High-performance anion-exchange chromatography for carbohydrate analysis.* Analytical Biochemistry, 1990. **189** (2): p. 151-162.

229. Hardy, M.R., Townsend, R.R., and Lee, A., *Monosaccharide analysis of glycoconjugates by anion exchange chromatography with pulsed amperometric detection.* Analytical Biochemistry, 1970. **170**: p. 54-62.

230. Townsend, R.R., Hardy, M.R., Hindsgaul, O., and Lee, Y.C., *High-performance anion-exchange chromatography of oligosaccharides using pellicular resins and pulsed amperometric detection.* Analytical Biochemistry, 1988. **174** (2): p. 459-470.

231. *Analysis of carbohydrates by high performance anion exchange chromatography with pulsed amperometric detection (HPAE-PAD)*, 2000. Dionex Corporation: United States.

232. *Product manual for CarboPac Ma1, CarboPac PA1, CarboPac PA10 and CarboPac PA100*, 2010. Dionex Corporation Document number: 031824. Revision: 8.

233. Liang, C. and Lucy, C.A., *Characterization of ion chromatography columns based on hydrophobicity and hydroxide eluent strength.* Journal of Chromatography A, 2010. **1217** (52): p. 8154-8160.

234. Cataldi, T.R.I., Campa, C., and De Benedetto, G.E., *Carbohydrate analysis by high-performance anion-exchange chromatography with pulsed amperometric detection: The potential is still growing.* Fresenius Journal of Analytical Chemistry, 2000. **368**: p. 739-758.

235. Talaga, P., Vialle, S., and Moreau, M., *Development of a high-performance anion-exchange chromatography with pulsed-amperometric detection based quantification assay for pneumococcal polysaccharides and conjugates.* Vaccine, 2002. **20**: p. 2474-2484.

236. Martin, A.J.P. and Synge, R.L.M., *A new form of chromatogram employing two liquid phases.* Biochemical Journal, 1941. **35**: p. 1358-1368.

237. James, A.T. and Martin, A.J.P., *Gas-liquid partition chromatography: The separation and micro-estimation of volatile fatty acids from formic acid to dodecanoic acid.* Biochemical Journal, 1952. **50**: p. 679-690.

238. Golay, M.J.E. for *Vapor Fractometer column*. 1960. Office, U.S.P. 2920478.

239. Condon, R.D., *Design considerations of a gas chromatography system employing high efficiency Golay columns.* Analytical Chemistry, 1959. **31** (9): p. 1717-1722.

240. Ettre, L., *Evolution of capillary columns for gas chromatography.* LC-GC The Magazine of Separation Science, 2001. **19** (1): p. 48-56.

241. Fox, A., Wright, L., and Fox, K., *Gas chromatography-tandem mass spectrometry for trace detection of muramic acid, a peptidoglycan chemical marker, in organic dust.* Journal of Microbiological Methods, 1995. **22**: p. 11-26.

242. Kim, J.S., Laskowich, E.R., Arumugham, R.G., Kaiser, R.E., and MacMichael, G.J., *Determination of saccharide content in pneumococcal polysaccharides and conjugate vaccines by GC-MSD.* Analytical Biochemistry, 2005. **347** (2): p. 262-274.

243. Tsai, C.S., *Biomacromolecules: Introduction to Struture Function and Informatics* 2007. New Jersey: Wiley-Liss.

244. Purcell, E.M., Torrey, H.C., and Pound, R.V., *Resonance Absorption by Nuclear Magnetic Moments in a Solid.* Physical Review, 1946. **69** (1-2): p. 37-38.

245. Bloch, F., Hansen, W.W., and Packard, M., *Nuclear Induction.* Physical Review, 1946. **70** (7-8): p. 460-474.

246. Lindley, D. *Landmarks: NMR-Grandmother of MRI*. Physical Review Focus, 2006. **18**, DOI: 10.1103/PhysRevFocus.18.18 http://physics.aps.org/story/v18/st18 [Accessed on: 14 August 2012].

247. Balci, M., *Basic ^{1}H- and ^{13}C-NMR Spectroscopy* 2005. The Netherlands: Elsevier.

248. Vialle, S., Sepulcri, P., Dubayle, J., and Talaga, P., *The teichoic acid (C-polysaccharide) synthesized by Streptococcus pneumoniae serotype 5 has a specific structure.* Carbohydrate Research, 2005. **340** (1): p. 91-96.

249. Melander, W., *Salt effect on hydrophobic interactions in precipitation and chromatography of proteins: an interpretation of the lyotropic series.* Archives of Biochemistry and Biophysics, 1977. **183** (1): p. 200-215.

250. O'Farrell, P.A., *Hydrophobic interaction chromatography*, in *Protein purification protocols*, Cutler, P. 2004. Humana Press: New Jersey. p. 133-138.

251. Dennison, C., *A Guide to Protein Isolation* 2003. The Netherlands: Kluwer Academic Publ.

252. Zhang, Y. and Cremer, P.S., *Interactions between macromolecules and ions: The Hofmeister series.* Current Opinion in Chemical Biology, 2006. **10** (6): p. 658-663.

253. Lyklema, J., *Simple Hofmeister series.* Chemical Physics Letters, 2009. **467** (4-6): p. 217-222.

254. Vlachy, N., Jagoda-Cwiklik, B., Vacha, R., Touraud, D., Jungwirth, P., and Kunz, W., *Hofmeister series and specific interactions of charged headgroups with aqueous ions.* Advances in Colloid and Interface Science, 2009. **146** (1-2): p. 42-47.

255. Guo, Y.-Y., Anderson, R., McIver, J., Gupta, R.K., and Siber, G.R., *A simple and rapid method for measuring unconjugated capsular polysaccharide (PRP) of Haemophilus influenzae type b in PRP-tetanus toxoid conjugate vaccine.* Biologicals, 1998. **26**: p. 33-38.

256. Lei, Q.P., Lamb, D.H., Heller, R., and Pietrobon, P., *Quantitation of low level unconjugated polysaccharide in tetanus toxoid-conjugate vaccine by HPAEC/PAD following rapid separation by deoxycholate/HCl.* Journal of Pharmaceutical and Biomedical Analysis, 2000. **21**: p. 1087-1091.

257. Cui, S.W., *Structural analysis of polysaccharides*, in *Food Carbohydrates: Chemistry, physical properties and applications*, Cui, S.W. 2005. Taylor and Francis: Florida.

258. *Annex 1: Recommendations for the production and control of Haemophilus influenzae type b conjugate vaccines*, 2000. World Health Orgaization Technical Report Series No 897.

259. *Recommendations to assure the quality, safety and efficacy of Group A meningococcal conjugate vaccines*, 2006. World Health Organization WHO/BS/06.2041.

260. Karamanos, N.K., Hjerpe, A., Tsegenidis, T., Engfeldt, B., and Antonopoulos, C.A., *Determination of iduronic acid and glucuronic acid in glycosaminoglycans after stoichiometric reduction and depolymerization using high-performance liquid chromatography and ultraviolet detection.* Analytical Biochemistry, 1988. **172**: p. 410-419.

261. Brudin, S.S., Shellie, R.A., Haddad, P.R., and Schoenmakers, P.J., *Comprehensive two-dimensional liquid chromatography: ion chromatography x reversed-phase liquid chromatography for separation of low-molar-mass organic acids.* Journal of Chromatography A, 2010. **1217** (43): p. 6742-6746.

262. Albersheim, P., Nevins, D.J., English, P.D., and Karr, A., *A method for the analysis of sugars in plant cell-wall polysaccharides by gas-liquid chromatography.* Carbohydrate Research, 1967. **5** (3): p. 340-345.

263. Bleton, J., P., M., Sansoulet, J., Goursaud, S., and Tchapla, A., *Characterization of neutral sugars and uronic acids after methanolysis and trimethylsilylation for recognition of plant gums.* Journal of Chromatography A, 1996. **720**: p. 27-49.

264. Nygren, Y., Fredriksson, S.-A., and Nilsson, B., *Identification of sialic acid and related acids as acetylated lactones by gas chromatography/mass spectrometry.* Journal of Mass Spectrometry, 1996. **31**: p. 267-274.

265. Rumpel, C. and Dignac, M.-F., *Gas chromatographic analysis of monosaccharides in a forest soil profile: Analysis by gas chromatography after trifluoroacetic acid hydrolysis and reduction–acetylation.* Soil Biology and Biochemistry, 2006. **38** (6): p. 1478-1481.

266. Sassaki, G.L., Souza, L.M., Serrato, R.V., Cipriani, T.R., Gorin, P.A., and Iacomini, M., *Application of acetate derivatives for gas chromatography-mass spectrometry: novel approaches on carbohydrates, lipids and amino acids analysis.* Journal of Chromatography A, 2008. **1208** (1-2): p. 215-222.

267. Martens, D.A. and Frankenberger Jr., W.T., *Determination of saccharides in biological materials by high-performance anion-exchange chromatography with pulsed amerometric detection.* Journal of Chromatography, 1991. **546**: p. 293-309.

268. Cataldi, T.R.I., Campa, C., and Casella, I.G., *Study of sugar acids separation by high-performance anion-exchange chromatography-pulsed amperometric detectio using alkaline eluents spiked with Ba, Sr, or Ca as acetate or nitrate salts.* Journal of Chromatography A, 1999. **848**: p. 71-81.

269. Somme, R., *Degradation of glucuronic acid-containing exopolysaccharides from Rhizobium by the hakomori methylation procedure.* Carbohydrate Research, 1986. **152**: p. 237-241.

270. Renard, C.M.G.C. and Jarvis, M.C., *Acetylation and methylation of homogalacturonans 1: optimisation of the reaction and characterisation of the products.* Carbohydrate Polymers, 1999. **39**: p. 201-207.

271. Kim, J.S., Reuhs, B.L., Michon, F., Kaiser, R.E., and Arumugham, R.G., *Addition of glycerol for improved methylation linkage analysis of polysaccharides.* Carbohydrate Research, 2006. **341** (8): p. 1061-1064.

272. Kim, J.S., Laskowich, E.R., Michon, F., Kaiser, R.E., and Arumugham, R.G., *Monitoring activation sites on polysaccharides by GC-MS.* Analytical Biochemistry, 2006. **358** (1): p. 136-142.

273. Toukach, F.V., Kocharova, N.A., Maszewska, A., Shashkov, A.S., Knirel, Y.A., and Rozalski, A., *Structure of the O-polysaccharide of Providencia alcalifaciens O8 containing (2S,4R)-2,4-dihydroxypentanoic acid, a new non-sugar component of bacterial glycans.* Carbohydrate Research, 2008. **343** (15): p. 2706-2711.

274. Hellerqvist, C.G., Hoffman, J., Lindberg, B., Pilotti, A., and Lindberg, A.A., *Anomeric nature of the D-mannose residues in the Salmonella typhi and S. strasbourg lipopolysaccharides.* Acta Chemica Scandinavica, 1971. **25** (4): p. 1512-1513.

275. Hoffman, J., Lindberg, B., and Svensson, S., *Determination of the anomeric configuration of sugar residues in cetylated oligo- and polysaccharides by oxidation with chromium trioxide in acetic acid.* Acta Chemica Scandinavica, 1972. **26**: p. 661-666.

276. Laine, R.A. and Renkonen, O., *Analysis of anomeric configurations in glyceroglycolipids and glycosphingolipids by chromium trioxide oxidation.* Journal of Lipid Research, 1975. **16**: p. 102-106.

277. Itasaka, O., Sugita, M., Yoshizaki, H., and Hori, T., *Determination of the anomeric configurations of Corbicula ceramide di- and trihexose by chromium trioxide oxidation.* Journal of Biochemistry, 1976. **80**: p. 935-936.

278. Kochetkov, N.K., Chizhov, O.S., and Shashkov, A.S., *Dependence of ^{13}C chemical shifts on the spatial interactions of protons and its application in structural and conformational studies of oligo- and polysaccharides.* Carbohydrate Research, 1984. **133**: p. 173-185.

279. Backman, I., Jansson, P.E., and Kenne, L., *Synthesis, NMR and conformational studies of some 1,4-linked disaccharides.* Journal of the Chemical Society, Perkin Transactions 1, 1990. (5): p. 1383-1388.

280. Bush, C.A. and Martin-Pastor, M., *Structure and conformation of complex carbohydrates of glycoproteins, glycolipids and bacterial polysaccharides.* Annual Review of Biophysics and Biomolecular Structure, 1999. **28**: p. 269-293.

281. Abeygunawardana, C., Williams, T.C., Sumner, J.S., and Hennessey, J.P., Jr., *Development and validation of an NMR-based identity assay for bacterial polysaccharides.* Analytical Biochemistry, 2000. **279** (2): p. 226-240.

282. Wormald, M.R., Petrescu, A.J., Pao, Y.-L., Glithero, A., Elliot, T., and Dwek, R.A., *Conformational studies of oligosaccharides and glycopeptides: Complementarity of NMR, X-ray crystallography and molecular modelling.* Chemical Reviews (Washington, D. C.), 2002. **102**: p. 371-386.

283. Clement, M.J., Imberty, A., Phalipon, A., Perez, S., Simenel, C., Mulard, L.A., and Delepierre, M., *Conformational studies of the O-specific polysaccharide of Shigella flexneri 5a and of four related synthetic pentasaccharide fragments using NMR and molecular modeling.* Journal of Biological Chemistry, 2003. **278** (48): p. 47928-47936.

284. Fehér, K., Pristovšek, P., Szilágyi, L., Ljevaković, Đ., and Tomašić, J., *Modified glycopeptides related to cell wall peptidoglycan: conformational studies by NMR and molecular modelling.* Bioorganic & Medicinal Chemistry, 2003. **11** (14): p. 3133-3140.

285. Aubin, Y., Jones, C., and Freedberg, D.I., *Using NMR Spectroscopy to obtain the higher order structure of biopharmaceutical products.* BioPharm International, 2010. (Supplement): p. 28-38.

286. Heidelberger, M., Goebel, W.F., and Avery, O.T., *The soluble specific substance of pneumococcus: Third paper.* Journal of Experimental Medicine, 1925. **42** (5): p. 727-745.

287. Avery, O.T. and Goebel, W.F., *Chemoimmunological studies on the soluble specific substance of pneumococcus: I The isolation and properties of the acetyl polysaccharide of pneumococcus type I.* Journal of Experimental Medicine, 1933. **58** (6): p. 731-755.

288. Heidelberger, M., Kendall, F.E., and Scherp, H.W., *The specific polysaccharides of types I, II and III pneumococcus.* Journal of Experimental Medicine, 1936. **64** (4): p. 559-572.

289. Alberty, R.A. and Heidelberger, M., *Fractionation and physical-chemical studies of a commercial preparation of the specific polysaccharide of type I pneumococcus.* Journal of the American Chemical Society, 1948. **70** (1): p. 211-213.

290. Smith, E.E.B., Galloway, B., and Mills, G.T., *The purification and composition of type I pneumococcal capsular polysaccharide.* Biochemical Journal, 1960. **76**: p. 35P.

291. Guy, R.C.E., How, M.J., Stacey, M., and Heidelberger, M., *Capsular polysaccharide of type 1 pneumococcus: I Purification and chemical modification.* The Journal of Biological Chemistry, 1967. **212** (21): p. 5106-5111.

292. Lindberg, B., Lindqvist, B., Lonngren, J., and Powell, D.A., *Structural studies of the capsular polysaccharide from Streptococcus pneumoniae type 1.* Carbohydrate Research, 1980. **78**: p. 111-117.

293. Stroop, C.J.M., Xu, Q., Retzlaff, M., Abeygunawardana, C., and Bush, C.A., *Structural analysis and chemical depolymerization of the capsular polysaccharide of Streptococcus pneumoniae type 1.* Carbohydrate Research, 2002. **337**: p. 335-344.

294. *European Pharmacopoeia*. 6 ed 2007. Strasbourg: Council of Europe.

295. *Guidance for Industry: Q2B validation of analytical procedures: methodology*, 1996. FDA.

296. Riley, C.M. and Rosanske, T.W. *Development and Validation Of Analytical Methods*. Progress in Pharmaceutical and Biomedical Analysis, ed. Riley, C.M. and Fell, A.F. Vol. 3. 1996. Elsevier Science.

297. *Guideline for Industry: Text on validation of analytical procedures*, 1995. FDA ICH-Q2A.

298. Bowness, J.M., *5-Formylfuroic acid and the carbazole reaction for uronic acids and acidic polysaccharides.* Biochemical Journal, 1958. **70** (1): p. 107-111.

299. Li, J., Kisara, K., Danielsson, S., Lindstrom, M.E., and Gellerstedt, G., *An improved methodology for the quantification of uronic acid units in xylans and other polysaccharides.* Carbohydrate Research, 2007. **342** (11): p. 1442-1449.

300. *Recommendations for the production and control of pneumococcal conjuugate vaccines*, 2003. World Health Organization.

301. Hestrin, S. and Mager, J., *Color test for identification of glucose.* Analytical Chemistry, 1947. **19** (12): p. 1032-1035.

302. Guzowski Jnr., J.P., Golanoski, C., and Montgomery, E.R., *A gas chromatographic method for the indirect determination of hydroxylamine in pharmaceutical preparations: conversion into nitrous oxide.* Journal of Pharmaceutical and Biomedical Analysis, 2003. **33**: p. 963-974.

303. Chaplin, M.F. and Kennedy, J. *Carbohydrate Analysis: A practical approach*. 2 ed. The Practical Approach Series, ed. Rickwood, D. and Hames, B.D. 2003. Oxford University Press.

304. Brummer, Y. and Cui, C., *Understanding carbohydrate analysis*, 2005. Taylor and Francis.

305. Englyst, H.N. and Cummings, J.H., *Simplified method for the measurement of total non-starch polysaccharides by gas-liquid chromatography of constituent sugars as alditol acetates.* The Analyst, 1984. **109** (7): p. 937-942.

306. Garna, H., Mabon, N., Nott, K., Wathelet, B., and Paquot, M., *Kinetic of the hydrolysis of pectin galacturonic acid chains and quantification by ionic chromatography.* Food Chemistry, 2006. **96** (3): p. 477-484.

307. Chambers, R.E. and Clamp, J.R., *An assessment of methanolysis and other factors used in the analysis of carbohydrate-containing materials.* Journal of Biochemistry (Great Britain), 1971. **125**: p. 1009-1018.

308. Yu Ip, C.C., Manam, V., Hepler, R., and Hennessey Jr, J.P., *Carbohydrate composition analysis of bacterial polysaccharides: Optimized acid hydrolysis conditions for HPAEC-PAD analysis.* Analytical Biochemistry, 1992. **201**: p. 343-349.

309. Arnous, A. and Meyer, A.S., *Quantitative prediction of cell wall polysaccharide composition in grape (Vitis vinifera L.) and apple (Malus domestica) skins from acid hydrolysis monosaccharide profiles.* Journal of Agricultural & Food Chemistry, 2009. **57** (9): p. 3611-3619.

310. Fengel, D. and Wegener, G., *Hydrolysis of cellulose: mechanisms of enzymatic and acid catalysis*, in *Advances in Chemistry* 1979. American Chemical Society. p. 145-158.

311. De Ruiter, G.A., Schols, H.A., Voragen, G.J., and Rombouts, F.M., *Carbohydrate analysis of water-soluble uronic acid-containing polysaccharides with high-performance anion-exchange chromatography using methanolysis combined with TFA hydrolysis is superior to four other methods.* Analytical Biochemistry, 1992. **207**: p. 176-185.

312. Boons, G.-J., Lee, Y.C., Suruki, A., Taniguchi, N., and Voragen, A.G.J. *Comprehensive glycoscience: From chemistry to systems biology*. ed. Kamerling, J.P. 2007. Elsevier: The Netherlands.

313. Talaga, P., Bellamy, L., and Moreau, M., *Quantitative determination of C-polysaccharide in Streptococcus pneumoniae capsular polysaccharides by use of high-performance anion-exchange chromatography with pulsed amperometric detection.* Vaccine, 2001. **19**: p. 2987-2994.

314. Manzi, A.E., *Total compositional analysis by high-performance liquid chromatography or gas-liquid chromatography*, in *Current Protocols in Molecular Biology* 2000. John Wiley and Sons.

315. Willför, S., Pranovich, A., Tamminen, T., Puls, J., Laine, C., Suurnäkki, A., Saake, B., Uotila, K., Simolin, H., Hemming, J., and Holmbom, B., *Carbohydrate analysis of plant materials with uronic acid-containing polysaccharides–A comparison between different hydrolysis and subsequent chromatographic analytical techniques.* Industrial Crops and Products, 2009. **29** (2-3): p. 571-580.

316. Sweeley, C.C. and Walker, B., *Determination of carbohydrates in glycolipides and gangliosides by gas chromatography.* Analytical Chemistry, 1964. **36** (8): p. 1461-1466.

317. Jeanloz, R.W. and Jeanloz, D.A., *The degradation of hyaluronic acid by methanolysis.* Biochemistry, 1964. **3** (1): p. 121-123.

318. Quemener, B., Lehave, M., and Metro, F., *Assessment of methanolysis for the determination of composite sugars of gelling carrageenans and agarose by HPLC.* Carbohydrate Research, 1995. **266**: p. 53-64.

319. Quemener, B., Marot, C., Mouillet, L., Da Riz, V., and Diris, J., *Quantitative analysis of hydrocolloids in food systems by methanolysis coupled to reverse HPLC. Part 2. Pectins, alginates and xanthan.* Food Hydrocolloids, 2000. **14**: p. 19-28.

320. Bertaud, F., Sundberg, A., and Holmbom, B., *Evaluation of acid methanolysis for analysis of wood hemicelluloses and pectins.* Carbohydrate Polymers, 2002. **48**: p. 319-324.

321. Poxton, I.R., Tarello, E., and Baddiley, J., *The structure of C-polysaccharide from the walls of Streptococcus pneumoniae.* Biochemical Journal, 1978. **175**: p. 1033-1042.

322. Gedye, R., Smith, F., Westaway, K., Ali, H., Baldisera, L., Laberge, L., and Rousell, J., *The use of microwave ovens for rapid organic synthesis.* Tetrahedron Letters, 1986. **27** (3): p. 279-282.

323. Lidstrom, P., Tierney, J., Wathey, B., and Westman, J., *Microwave assisted organic synthesis - a review.* Tetrahedron 2001. **57**: p. 9225-9283.

324. Loupy, A., Perreux, L., Liagre, M., Burle, K., and Moneuse, M., *Reactivity and selectivity under microwaves in organic chemistry. Relation with medium effects and reaction mechanisms.* Pure and Applied Chemistry, 2001. **73** (1): p. 161-166.

325. Corsaro, A., Chiacchio, U., Pistara, V., and Romeo, G., *Microwave-assisted chemistry of carbohydrates.* Current Organic Chemistry, 2004. **8**: p. 511-538.

326. Hayes, B., *Recent Advances in Microwave-assisted synthesis.* Aldrichimica ACTA, 2004. **37** (2): p. 66-76.

327. de la Hoz, A., Diaz-Ortiz, A., and Moreno, A., *Microwaves in organic synthesis. Thermal and non-thermal microwave effects.* Chemical Society Reviews, 2005. **34** (2): p. 164-178.

328. Kappe, C.O. and Stadler, A. *Microwaves in Organic and Medicinal Chemistry*. Wiley-VCH. Available from: http://onlinelibrary.wiley.com/book/10.1002/3527606556. [Accessed on:05 June 2012].

329. Wiesbrock, F. and Schubert, U.S., *Microwaves in chemistry: the success story goes on.* Chemistry Today, 2006. **24** (3): p. 30-33.

330. Horikoshi, S. and Serpone, N., *Photochemistry with microwaves.* Journal of Photochemistry and Photobiology C: Photochemistry Reviews, 2009. **10** (2): p. 96-110.

331. Richel, A., Laurent, P., Wathelet, B., Wathelet, J.-P., and Paquot, M., *Microwave-assisted conversion of carbohydrates. State of the art and outlook.* Comptes Rendus Chimie, 2011. **14** (2-3): p. 224-234.

332. Margolis, S.A., Jassie, L., and Kingston, H.M., *The hydrolysis of proteins by microwave energy.* Journal of Automatic Chemistry, 1991. **13** (3): p. 93-95.

333. Fara, M.A., Díaz-Mochón, J.J., and Bradley, M., *Microwave-assisted coupling with DIC/HOBt for the synthesis of difficult peptoids and fluorescently labelled peptides—a gentle heat goes a long way.* Tetrahedron Letters, 2006. **47** (6): p. 1011-1014.

334. Paolini, I., Nuti, F., de la Cruz Pozo-Carrero, M., Barbetti, F., Kolesinska, B., Kaminski, Z.J., Chelli, M., and Papini, A.M., *A convenient microwave-assisted synthesis of N-glycosyl amino acids.* Tetrahedron Letters, 2007. **48** (16): p. 2901-2904.

335. Engelhart, W.G., *Microwave hydrolysis of peptides and proteins for amino acid analysis.* Am. Biotechnol. Lab, 1990. **15**: p. 31-34.

336. Bornaghi, L.F. and Poulsen, S.-A., *Microwave-accelerated Fischer glycosylation.* Tetrahedron Letters, 2005. **46** (20): p. 3485-3488.

337. de Paula, V.C., Pinheiro, I.O., Lopes, C.E., and Calazans, G.C., *Microwave-assisted hydrolysis of Zymomonas mobilis levan envisaging oligofructan production.* Bioresource Technology, 2008. **99** (7): p. 2466-2470.

338. Singh, V., Tiwari, A., Tripathi, D.N., and Malviya, T., *Microwave promoted methylation of plant polysaccharides.* Tetrahedron Letters, 2003. **44** (39): p. 7295-7297.

339. Hirose, T., Kopek, B.G., Wang, Z.H., Yusa, R., and Baldwin, B.W., *Microwave oven synthesis of esters promoted by imidazole.* Tetrahedron Letters, 2003. **44**: p. 1831-1833.

340. Soderholm, S.L., Damm, M., and Kappe, C.O., *Microwave-assisted derivatization procedures for gas chromatography/mass spectrometry analysis.* Molecular Diversity, 2010. **14** (4): p. 869-888.

341. Lamble, K.J. and Hill, S.J., *Microwave digestion procedures for environmental matrices.* The Analyst, 1998. **123**: p. 103-133.

342. Cheng, M.-C., Wang, K.-T., Inoue, S., Inoue, Y., Khoo, K.-H., and Wu, S.-H., *Controlled acid hydrolysis of colominic acid under microwave irradiation.* Analytical Biochemistry, 1999. **267**: p. 287-293.

343. Singh, V., Sethi, R., Tewari, A., Srivastava, V., and Sanghi, R., *Hydrolysis of plant seed gums by microwave irradiation.* Carbohydrate Polymers, 2003. **54** (4): p. 523-525.

344. Xing, R., Liu, S., Yu, H., Guo, Z., Wang, P., Li, C., Li, Z., and Li, P., *Salt-assisted acid hydrolysis of chitosan to oligomers under microwave irradiation.* Carbohydrate Research, 2005. **340** (13): p. 2150-2153.

345. Orozco, A., Ahmad, M., Rooney, D., and Walker, G., *Dilute acid hydrolysis of cellulose and cellulosic bio-waste using a microwave reactor system.* Process Safety and Environmental Protection, 2007. **85** (5): p. 446-449.

346. Zhao, J. and Monteiro, M.A., *Hydrolysis of bacterial wall carbohydrates in the microwave using trifluoroacetic acid.* Carbohydrate Research, 2008. **343** (14): p. 2498-2503.

347. Chhatbar, M., Meena, R., Prasad, K., and Siddhanta, A.K., *Microwave assisted rapid method for hydrolysis of sodium alginate for M/G ratio determination.* Carbohydrate Polymers, 2009. **76** (4): p. 650-656.

348. Allard, B. and Derenne, S., *Microwave assisted extraction and hydrolysis: An alternative to pyrolysis for the analysis of recalcitrant organic matter? Application to a forest soil (Landes de Gascogne, France).* Organic Geochemistry, 2009. **40** (9): p. 1005-1017.

349. Zhang, Z. and Zhao, Z.K., *Solid acid and microwave-assisted hydrolysis of cellulose in ionic liquid.* Carbohydrate Research, 2009. **344** (15): p. 2069-2072.

350. Yoshida, T., Tsubaki, S., Teramoto, Y., and Azuma, J.I., *Optimization of microwave-assisted extraction of carbohydrates from industrial waste of corn starch production using response surface methodology.* Bioresource Technology, 2010. **101** (20): p. 7820-7826.

351. Dřímalová, E., Velebný, V., Sasinková, V., Hromádková, Z., and Ebringerová, A., *Degradation of hyaluronan by ultrasonication in comparison to microwave and conventional heating.* Carbohydrate Polymers, 2005. **61** (4): p. 420-426.

352. Bezáková, Z., Hermannová, ., Dřímalová, E., a lovíková, A., Ebringerová, A., and Velebný, V., *Effect of microwave irradiation on the molecular and structural properties of hyaluronan.* Carbohydrate Polymers, 2008. **73** (4): p. 640-646.

353. Choi, J.-i., Kim, J.-K., Kim, J.-H., Kweon, D.-K., and Lee, J.-W., *Degradation of hyaluronic acid powder by electron beam irradiation, gamma ray irradiation, microwave irradiation and thermal treatment: A comparative study.* Carbohydrate Polymers, 2010. **79** (4): p. 1080-1085.

354. *Microwave Chemistry: How it all works*. CEM Corporation. Available from: http://cem.com/page130.html. [Accessed on:20 December 2011].

355. Giguere, R.J., Bray, T.L., Duncan, S.M., and Majetich, G., *Application of commercial microwave ovens to organic synthesis.* Tetrahedron Letters, 1986. **27** (41): p. 4945-4948.

356. Kunlan, L., Lixin, X., Jun, P., Guoying, C., and Zuwei, X., *Salt assisted acid hydrolysis of starch to D-glucose under microwave irradiation.* Carbohydrate Research, 2001. **331**: p. 9-12.

357. Chang, M., Meyers, H.V., Nakanishi, K., Ojika, M., Park, J.H., Park, M.H., Takeda, R., Vazquez, J.T., and Wiesler, W.T., *Microscale structure determination of oligosaccharides by the exciton chirality method.* Pure and Applied Chemistry, 1989. **61** (7): p. 1193-1200.

358. Itonori, S., Takahashi, M., Kitamura, T., Aoki, K., Dulaney, J.T., and Sugita, M., *Microwave-mediated analysis for sugar, fatty acid, and sphingoid compositions of glycosphingolipids.* Journal of Lipid Research, 2004. **45** (3): p. 574-581.

359. Khan, M.U. and Williams, J.P., *Microwave-mediated methanolysis of lipids and activation of thin-layer chromatographic plates.* Lipids, 1993. **28**: p. 953-955.

360. Oigman, S.S., de Souza, R.O., Dos Santos Junior, H.M., Hovell, A.M., Hamerski, L., and Rezende, C.M., *Microwave-assisted methanolysis of green coffee oil.* Food Chemistry, 2012. **134** (2): p. 999-1004.

361. Larsson, K. and Petersson, G., *Methanolysis of galacturonic acid. Dimethyl acetals.* Carbohydrate Research, 1974. **34**: p. 323-329.

362. Petersson, G., Samuelson, O., Anjou, K., and von Sydow, E., *Mass spectrometric identification of aldolactones as trimethylsilyl ethers.* Acta Chemica Scandinavica, 1967. **21**: p. 1251-1256.

363. Jones, C. and Mulloy, B., *The application of nuclear magnetic resonance to structural studies of polysaccharides*, in *Methods in Molecular Biology*, Jones, C. and Mulloy, B. 1993. Humana Press Inc.

364. Watson, M.J. and Baddiley, J., *The action of nitrous acid on C-teichoic acid (C-substance) from the walls of Diplococcus pneumoniae.* Journal of Biochemistry (Great Britain), 1974. **137**: p. 399-404.

365. Kulakowska, M., Brisson, J.-R., Griffith, D.W., Young, N.M., and Jennings, H.J., *High resolution NMR spectroscopic analysis of the C-polysaccharide of Streptococcus pneumoniae.* Canadian Journal of Chemistry, 1993. **71** (5): p. 644-648.

366. Karlsson, C., Jansson, P.E., and Sorenson, U., *The pneumococcal common antigen C-polysaccharide occurs in different forms.* European Journal of Biochemistry, 1999. **265**: p. 1091-1097.

367. Kniskern, P.J., Ip, C.C., Hagopian, A., Hennessey Jr, J.P., Miller, W.J., Kubek, D.J., Burke, P.D., Marburg, S., and Tolman, R.L. for Merck & Co Inc. *Pneumococcal polysaccharide conjugate vaccine*. 2010. Office, E.P. 92300655.5. EP 0497525B2.

368. Enders, J.F. and Wu, C.-Y., *An immunological study of the A substance or acetyl polysaccharide of pneumococcus type I.* Journal of Experimental Medicine, 1934. **60** (2): p. 127-147.

369. Chow, B.F., *Immunological studies on a new preparation of type specific polysaccharide from pneumococcus type I.* Journal of Experimental Medicine, 1936. **64** (6): p. 843-854.

370. Jansson, P.-E., Kenne, L., and Schweda, E., *Nuclear magnetic resonance and conformational studies on monoacetylated methyl D-gluco- and D-galacto-pyranosides.* Journal of the Chemical Society, Perkin Transactions 1, 1987. p. 377-383.

371. Kapre, S. and Jana, S.K. for Serum Institute of India Ltd. *Purification of capsular polysaccharides*. 2011. Organization, W.I.P. PCT/IN2011/000332. WO 2011/145108 A2.

372. Goncalves, V.M., Takagi, M., Carmo, T.S., Lima, R.B., Ferreira, F., Albani, S.M., Pinto, F.R., Zangirolami, T.C., Giordano, R.C., Tanizaki, M.M., and Cabrera-Crespo, J., *Simple and efficient method of bacterial polysaccharides purification for vaccines production using hydrolytic enzymes and tangential flow ultrafiltration*, in *Communicating Current Research and Educational Topics and Trends in Applied Microbiology*, Mendez-Vilas, A. 2007. p. 450-457.

373. Gonçalves, V.M., Zangirolami, T.C., Giordano, R.L.C., Raw, I., Tanizaki, M.M., and Giordano, R.C., *Optimization of medium and cultivation conditions for capsular polysaccharide production by Streptococcus pneumoniae serotype 23F.* Applied Microbiology & Biotechnology, 2002. **59** (6): p. 713-717.

374. Yuan, Y., Ruppen, M.E., Sun, W., Chu, L., Simpson, J., Patch, J., Charbonneau, P., and Moran, J.K. for Wyeth. *Shortened purification process for the production of capsular streptococcus pneumoniae polysaccharides*. 2012. Office, E.P. 11194173.8. EP 2436700 A1.

375. Ravenscroft, N. and Feavers, I.M., *Conjugate Vaccines*, in *Meningococcal Disease. Pathogenicity and Prevention*, Frosch, M. and Maiden, M. 2006. Wiley-VCH Verlag GmbH & Co KGaA: Weinheim. p. 343-369.

376. *Assessment report for Prevenar 13*, 2009. European Medicines Agency Procedure No: EMEA/H/C/001104.

377. Pawlowski, A. and Svenson, S.B., *Electron beam fragmentation of bacterial polysaccharides as a method of producing oligosaccharides for the preparation of conjugate vaccines.* FEMS Microbiology Letters, 1999. **174**: p. 255-263.

378. Svenson, S.B. and Lindberg, A.A., *Oligosaccharide-protein conjugate: a novel approach for making Salmonella O-antigen immunogens.* FEMS Microbiology Letters, 1977. **1**: p. 145-148.

379. Svenson, S.B. and Lindberg, A.A., *Coupling of acid labile Salmonella specific oligosaccharides to macromolecular carriers.* Journal of Immunological Methods, 1979. **25**: p. 232-335.

380. Anderson, P.W., Pichichero, M.E., Stein, E.C., Porcelli, S., Betts, R.F., Connuck, D.M., Korones, D., Insel, R.A., Zahradnik, J.M., and Eby, R., *Effect of oligosaccharide chain length, exposed terminal group, and hapten loading on the antibody response of human adults and infants to vaccines consisting on Haemophilus influenzae type b capsular antigen uniterminally coupled to the diphtheria protein CRM197.* The Journal of Immunology, 1989. **142** (7): p. 2464-2468.

381. Paoletti, L.C., Kasper, D.L., Michon, F., DiFabio, J., Jennings, H.J., Tosteson, T.D., and Wessels, M.R., *Effects of chain length on the immunogenicity in rabbits of group Streptococcus type III oligosaccharide-tetanus toxoid conjugates.* Journal of Clinical Investigation, 1992. **89**: p. 203-209.

382. Kabat, E.A. and Bezer, A.E., *The effect of variation in molecular weight on the antigenicity of dextran in man.* Archives of Biochemistry and Biophysics, 1958. **78**: p. 306-318.

383. Brandt, B.L., Artenstein, M.S., and Smith, C.D., *Antibody responses to meningococcal polysaccharide vaccines.* Infection and Immunity, 1973. **8**: p. 590-596.

384. Martin, D.G., Jarvis, F.G., and Milner, K.C., *Physicochemical and biological properties of sonically treated Vi antigen.* Journal of Bacteriology, 1967. **94**: p. 1411-1416.

385. MacNair, J.E., Desai, T., Teyral, J., Abeygunawardana, C., and Hennessey, J.P., Jr., *Alignment of absolute and relative molecular size specifications for a polyvalent pneumococcal polysaccharide vaccine (PNEUMOVAX 23).* Biologicals, 2005. **33** (1): p. 49-58.

386. Biemans, R.L., Garcon, N.M.-J., Hermand, P., Poolman, J., and Van Mechellen, M.P. for GlaxoSmithKline Biologicals *Vaccine comprising Streptococcus pneumoniae capsular polysaccharide conjugates*. 2009. Office, U.S.P. 12/097631. US2009/0017059 A1.

387. Czechowska-Biskup, R., Rokita, B., Lotfy, S., Ulanski, P., and Rosiak, J.M., *Degradation of chitosan and starch by 360-kHz ultrasound.* Carbohydrate Polymers, 2005. **60** (2): p. 175-184.

388. Cook, E.J. and Lagace, A.P. for Biotechnology Development Corporation. *Apparatus for forming emulsions*. 1985. Office, U.S.P. 581568. 4533254.

389. Zon, G., Szu, S., Egan, W., Robbins, J.D., and Robbins, J.B., *Hydrolytic stability of pneumococcal group 6 (type 6A and 6B) capsular polysaccharides.* Infection and Immunity, 1982. **37** (1): p. 89-103.

390. Lee, C.H. and Frasch, C.E. for The Government of the United States of America. *Polysaccharide-protein conjugate vaccines*. 2005. Organization, W.I.P. PCT/US2004/025477. WO 2005/014037 A2.

391. Alouf, J.E. and Popoff, M.R. *The comprehensive sourcebook of bacterial protein toxins*. 2006. Academic Press.

392. Lavelle, E.C., Leavy, O., and Mills, K.H.G., *Modified Bacterial Toxins*, Hackett, C.J. and Harn, D.A. 2006. Humana Press.

393. Robinson, J.P., Picklesimer, J.B., and Puett, D., *Tetanus Toxin.* The Journal of Biological Chemistry, 1975. **250** (18): p. 7435-7442.

394. Bizzini, B., Blass, J., Turpin, A., and Raynaud, M., *Chemical characterization of tetanus toxin and toxoid.* European Journal of Biochemistry, 1970. **17**: p. 100-105.

395. *Diphtheria toxin, diphtheria toxoid, CRM mutant*, 1994. List Biological Laboratories Inc.

396. Vliegenthart, J.F., *Carbohydrate based vaccines.* FEBS Letters, 2006. **580** (12): p. 2945-2950.

397. Pollabauer, E.M., Petermann, R., and Ehrlich, H.J., *The influence of carrier protein on the immunogenicity of simultaneously administered conjugate vaccines in infants.* Vaccine, 2009. **27** (11): p. 1674-1679.

398. *Peptides for immunization*, 2008. Thermo Fisher Scientific Application note: TI-PEP06-0908.

399. Inman, J.K. and Dintzis, H.M., *The derivatisation of cross-linked polyacrylamide beads. Controlled introduction of functional groups for the preparation of special purpose, biochemical adsorbants.* Biochemistry, 1969. **8** (10): p. 4074-4082.

400. Hermanson, G.T., *Bioconjugate Techniques* 2008. United Kingdon: Academic Press.

401. *NeisVac-C Product monograph: Suspension for injection in pre-filled syringe Meningococcal group C polysaccharide conjugate vaccine (adsorbed)*, 2009. Baxter International Inc.

402. Verez Bencomo, V., Fernandez Santana, V., Hardy, E., Toledo, M.E., Rodriguez, M.C., Heynngnezz, L., Rodriguez, A., Baly, A., Herrera, L., Izquierdo, M., Villar, A., Valdes, Y., Cosme, K., Deler, M.L., Montane, M., Garcia, E., Ramos, A., Aguilar, A., Medina, E., Torano, G., Sosa, I., Hernandez, I., Martinez, R., Muzachio, A., Carmenates, A., Costa, L., Cardoso, F., Campa, C., Diaz, M., and Roy, R., *A synthetic conjugate polysaccharide vaccine against Haemophilus influenze type b.* Science, 2004. **305**: p. 522-525.

403. Fernandez Santana, V., Peña Icart, L., Beurret, M., Costa, L., and Verez Bencomo, V., *Glycoconjugate vaccines against Haemophilus influenzae type b.* Methods in Enzymology, 2006. **415**: p. 153-163.

404. Lee, C.H., Kuo, W.C., Beri, S., Kapre, S., Joshi, J.S., Bouveret, N., LaForce, F.M., and Frasch, C.E., *Preparation and characterization of an immunogenic meningococcal group A conjugate vaccine for use in Africa.* Vaccine, 2009. **27** (5): p. 726-732.

405. Pace, D., Pollard, A.J., and Messonier, N.E., *Quadrivalent meningococcal conjugate vaccines.* Vaccine, 2009. **27** (Supplement 2): p. B30-B41.

406. *WHO prequalified vaccines: Filterable search for prequalified vaccines with product detail*. World Health Organization. Available from: http://www.who.int/immunization_standards/vaccine_quality/PQ_vaccine_list_en/en/. [Accessed on:08 July 2012].

407. Knuf, M., Kowalzik, F., and Kieninger, D., *Comparative effects of carrier proteins on vaccine-induced immune response.* Vaccine, 2011. **29** (31): p. 4881-4890.

408. Ada, G. and Isaacs, D., *Carbohydrate-protein conjugate vaccines.* Clinical Microbiology and Infection, 2003. **9** (2): p. 79-85.

409. Eskola, J., *Use of conjugate vaccines to prevent meningitis caused by Haemophilus influenzae type b or Streptococcus pneumoniae.* Journal of Hospital Infection, 1995. **30**: p. 313-321.

410. Marburg, S., Jorn, D., Tolman, R.L., Arison, B., McCauley, J., Kniskern, P.J., Hagopian, A., and Vella, P.P., *Bimolecular chemistry of macromolecules: Synthesis of bacterial polysaccharide conjugates with Neuisseria meningitidis membrane protein.* Journal of the American Chemical Society, 1986. **108**: p. 5282-5287.

411. Eskola, J., *Foresight in medicine: current challenges with Haemophilus influenzae type b conjugate vaccines.* Journal of Internal Medicine, 2010. **267** (3): p. 241-250.

412. Ladhani, S.N., *Two decades of experience with the Haemophilus influenzae serotype b conjugate vaccine in the United Kingdom.* Clinical Therapeutics, 2012. **34** (2): p. 385-399.

413. Ward, J.I., Brenneman, G., Letson, G.W., and Heyward, W.L., *Limited efficacy of a Haemophilus influenzae type b conjugate vaccine in Alaska native infants.* New England Journal of Medicine, 1990. **323** (20): p. 1393-1401.

414. Eskola, J., Kayhty, H., Takala, A.K., McVerry, P.H., and Makela, P.H., *A randomised, prospective field trial of a conjugate vaccine in the protection of infants and young children against invasive Haemophilus influenzae type b disease.* New England Journal of Medicine, 1990. **232** (20): p. 1381-1387.

415. Schlesinger, Y. and Granoff, D.M., *Avidity and bactericidal activity of antibody elicited by different Haemophilus influenzae type b conjugate vaccines.* The Journal of the American Medical Association, 1992. **267**: p. 1489-1494.

416. Lucas, A.H. and Granoff, D.M., *Functional differences in idiotypically defined IgG1 anti-polysaccharide antibodies elicited by vaccination with Haemophilus influenzae type B polysaccharide-protein conjugates.* The Journal of Immunology, 1995. **154** (8): p. 4195-4202.

417. Decker, M.D., Edwards, K.M., Bradley, M., and Palmer, P., *Comparitive trial in infants of four conjugate Haemophilus influenzae type b vaccines.* Journal of Pediatrics, 1992. **120**: p. 184-189.

418. Richmond, P., Borrow, R., Findlow, J., Martin, S., Thornton, C., Cartwright, K., and Miller, E., *Evaluation of De-O-acetylated meningococcal C polysaccharide-tetanus toxoid conjugate vaccine in infancy: reactogenicity, immunogenicity, immunologic priming, and bactericidal activity against O-acetylated and De-O-acetylated serogroup C strains.* Infection and Immunity, 2001. **69** (4): p. 2378-2382.

419. Fusco, P.C., Farley, E.K., Huang, C.H., Moore, S., and Michon, F., *Protective meningococcal capsular polysaccharide epitopes and the role of O acetylation.* Clinical and Vaccine Immunology, 2007. **14** (5): p. 577-584.

420. Peltola, H., Safary, A., Kayhty, H., Karanko, V., and Andre, F.E., *Evaluation of two tetravalent (ACYW135) meningococcal vaccines in infants and small children: A clinical study comparing immunogenicity of O-acetyl-negative and O-acetyl-positive group C polysaccharides.* Pediatrics, 1985. **76**: p. 91-96.

421. *Assessment report for Menveo*, 2008. European Medicines Agency Procedure No: EMEA/H/C/001095.

422. Cooper, B., DeTora, L., and Stoddard, J., *Menveo: a novel quadrivalent meningococcal CRM197 conjugate vaccine against serogroups A, C, W-135 and Y.* Expert Review of Vaccines, 2011. **10** (1): p. 21-33.

423. *Assessment report for Nimenrix*, 2012. European Medicines Agency Procedure no: EMEA/H/C/002226.

424. Dagan, R., Poolman, J., and Siegrist, C.A., *Glycoconjugate vaccines and immune interference: A review.* Vaccine, 2010. **28** (34): p. 5513-5523.

425. Dagan, R., Eskola, J., Leclerc, C., and Leroy, O., *Reduced response to multiple vaccines sharing common protein epitopes that are administered simultaneously to infants.* Infection and Immunity, 1998. **66** (5): p. 2093-2098.

426. Anderson, P., Treanor, J., Porcelli, S., and Pichichero, M., *Non-interference between two protein carriers when used with the same polysaccharide for pneumococcal conjugate vaccines in 2-year-old children.* Vaccine, 2003. **21** (13-14): p. 1554-1559.

427. Murayama, K. and Tomida, M., *Heat-induced secondary structure and conformation change of bovine serum albumin investigated by Fourier transform infrared spectroscopy.* Biochemistry, 2004. **43** (36): p. 11526-11532.

428. Weijers, R.N.M., *Amino acid sequence in bovine serum albumin.* Clinical Chemistry, 1977. **23** (7): p. 1361-1362.

429. Benjamin, D.C., *Evidence for specific suppression in the maintenance of immunologic tolerance.* Journal of Experimental Medicine, 1975. **141**: p. 635-647.

430. Ruoslahti, E. and Engvall, E., *Immunological crossreaction between alpha-fetoprotein and albumin.* Proceedings of the National Academy of Sciences, USA, 1976. **73** (12): p. 4641-4644.

431. Vicente-Serrano, J., Caballero, M.L., Rodríguez-Pérez, R., Carretero, P., Pérez, R., Blanco, J.G., Juste, S., and Moneo, I., *Sensitization to serum albumins in children allergic to cow's milk and epithelia.* Pediatric Allergy and Immunology, 2007. **18** (6): p. 503-507.

432. Robbins, J.B. and Schneerson, R., *Polysaccharide-protein conjugates: A new generation of vaccines.* The Journal of Infectious Diseases, 1990. **161** (5): p. 821-832.

433. Kossaczka, Z., Bystricky, S., Bryla, D., Shiloach, J., Robbins, J.B., and Szu, S., *Synthesis and immunological properties of Vi and Di-O-acetyl pectin protein conjugates with adipic acid dihydrazide as the linker.* Infection and Immunity, 1997. **65** (6): p. 2088-2093.

434. Shafer, D.E., Toll, B., Schuman, R.F., Nelson, B.L., Mond, J.J., and Lees, A., *Activation of soluble polysaccharides with 1-cyano-4-dimethylaminopyridium tetrafluoroborate (CDAP) for use in protein-polysaccharide conjugate vaccines and immunological reagents. II. Selective crosslinking of proteins to CDAP-activated polysaccharides.* Vaccine 2000. **18**: p. 1273-1281.

435. Beuvery, E.C., Miedema, F., van Delft, R., and Haverkamp, J., *Preparation and immunochemical characterization of meningococcal group C polysaccharide-tetanus toxoid conjugates as a new generation of vaccines.* Infection and Immunity, 1983. **40** (1): p. 39-45.

436. Beuvery, E.C., Roy, R., Kanhai, V., and Jennings, H.J., *Characteristics of two types of meningococcal group C polysaccharide conjugates using tetanus toxoid as carrier protein.* Developments in Biological Standardization, 1986. **65**: p. 197-204.

437. Beuvery, E.C., Speijers, G.J.A., Lutz, B.I.G., Freudenthal, D., Kanhai, V., Haagmans, B., and Derks, H., *Analytical, toxicological and immunological consequences of the use of N-ethyl-N'-(3-dimethylaminopropyl) carbodiimide as coupling reagent for the preparation of meningococcal group C polysaccharide-tetanus toxoid conjugate as vaccine for human use.* Developments in Biological Standardization, 1986. **63**: p. 117-128.

438. Pawlowski, A., Kallenius, G., and Svenson, S.B., *Preparation of pneumococcal capsular polysaccharide-protein conjugate vaccines utilizing new fragmentation and conjugation technologies.* Vaccine, 2000. **18**: p. 1873-1885.

439. Silveira, I.A., Bastos, R.C., Neto, M.S., Laranjeira, A.P., Assis, E.F., Fernandes, S.A., Leal, M.L., Silva, W.C., Lee, C.H., Frasch, C.E., Peralta, J.M., and Jessouroun, E., *Characterization and immunogenicity of meningococcal group C conjugate vaccine prepared using hydrazide-activated tetanus toxoid.* Vaccine, 2007. **25** (41): p. 7261-7270.

440. Wilson, S., *R&D Process Development Report No: CBP005 - Development of a conjugate process for the manufacture of a Hib PRP:TT conjugate vaccine*, Cape Biologicals. p. 1-59.

441. Malito, E., Bursulaya, B., Chen, C., Lo Surdo, P., Picchianti, M., Balducci, E., Biancucci, M., Brock, A., Berti, F., Bottomley, M.J., Nissum, M., Costantino, P., Rappuoli, R., and Spraggon, G., *Structural basis for lack of toxicity of the diphtheria toxin mutant CRM197.* Proceedings of the National Academy of Sciences, USA, 2012. **109** (14): p. 5229-5234.

442. Giannini, G., Rappuoli, R., and Ratti, G., *The amino acid sequence of two non toxic mutants of diphtheria toxin: CRM45 and CRM197.* Nucleic Acids Research, 1984. **12** (10): p. 4063-4069.

443. Bröker, M., Dull, P.M., Rappuoli, R., and Costantino, P., *Chemistry of a new investigational quadrivalent meningococcal conjugate vaccine that is immunogenic at all ages.* Vaccine, 2009. **27** (41): p. 5574-5580.

444. Micoli, F., Rondini, S., Pisoni, I., Proietti, D., Berti, F., Costantino, P., Rappuoli, R., Szu, S., Saul, A., and Martin, L.B., *Vi-CRM 197 as a new conjugate vaccine against Salmonella Typhi.* Vaccine, 2011. **29** (4): p. 712-720.

445. Michon, F., Fusco, P.C., Minetti, C.A., Laude-Sharp, M., Uitz, C., Huang, C.-H., D'Ambra, A.J., Moore, S., Remeta, D.P., Heron, I., and Blake, M.S., *Multivalent pneumococcal capsular polysaccharide conjugate vaccines employing genetically detoxified pneumolysin as a carrier protein.* Vaccine, 1998. **16** (18): p. 1732-1741.

446. Paton, J.C., Lock, R.A., Lee, C.-J., Li, J.P., Berry, A.M., Mitchell, T.J., Andrew, P.W., Hansman, D., and Boulnois, G.J., *Purification and immunogenicity of genetically obtained pneumolysin toxoids and their conjugation to Streptococcus pneumonia type 19F polysaccharide* Infection and Immunity, 1991. **59** (7): p. 2297-2304.

447. Kuo, J.S.-C. and Ree, H.K. for American Cyanamid Company. *Pneumococcal polysaccharide recombinant pneumolysin conjugate vaccines for immunisation against pneumococcal infections*. 1996. Office, U.S.P. 295305. 5565204.

448. Weintraub, A., *Immunology of bacterial polysaccharide antigens.* Carbohydrate Research, 2003. **338** (23): p. 2539-2547.

449. Makela, P.H. and Kayhty, H., *Evolution of conjugate vaccines.* Expert Review of Vaccines, 2002. **1** (4): p. 399-410.

450. Kohn, J. and Wilchek, M., *A new approach (cyano-transfer) for cyanogen bromide activation of sepharose at neutral pH, which yields activated resins, free of interfering nitrogen derivatives.* Biochemical and Biophysical Research Communications, 1982. **107** (3): p. 7.

451. Peeters, C.C.A.M., Tenbergen-Meekes, A.-M.J., Poolman, J.T., Zegers, B.J.M., and Rijkers, G.T., *Immunogenicity of a Streptococcus pneumoniae type 4 polysaccharide-protein conjugate vaccine is decreased by admixture of high doses of free saccharide.* Vaccine, 1992. **10** (12): p. 833-840.

452. McMaster, R.P. for Connaught Laboratories. *Purification of polysaccharide-protein conjugate vaccines by ultrafiltration with ammonium sulfate solutions*. 2000. Organization, W.I.P. PCT/US99/30109. WO 00/38711.

453. Gadzinowski, J., Albrecht, P., Hasiec, B., Konior, R., Dziduch, J., Witor, A., Mellelieu, T., Tansey, S.P., Jones, T., Sarkozy, D., Emini, E.A., Gruber, W.C., and Scott, D.A., *Phase 3 trial evaluating the immunogenicity, safety, and tolerability of manufacturing scale 13-valent pneumococcal conjugate vaccine.* Vaccine, 2011. **29** (16): p. 2947-2955.

454. Ghosh, S.S., Kao, P.M., McCue, A.W., and Chappelle, H.L., *Use of maleimide-thiol coupling chemistry for efficientt synthesis of oligonucleotide-enzyme conjugate hybridization probes.* Bioconjugate Chemistry, 1990. **1**: p. 71-76.

455. Hoare, D.G. and Koshland, D.E., *A procedure for the selective modification of carboxyl groups in proteins.* Journal of the American Chemical Society, 1967. **88** (9): p. 2057-2058.

456. Ulrich, H., *Chemistry and technology of carbodiimides* 2007. United Kingdom: John Wiley and Sons Ltd.

457. Sheehan, J.C., Cruickshank, P.A., and Boshart, G.L., *A convenient synthesis of water soluble carbodiimides.* Journal of Organic Chemistry, 1961. **26**: p. 2525-2528.

458. Sheehan, J.C., Preston, J., and Cruickshank, P.A., *A rapid synthesis of oligonucleotide derivatives without isolation of intermediates.* Journal of the American Chemical Society, 1965. **87**: p. 2492-2493.

459. Williams, A. and Ibrahim, I.T., *A new mechanism involving cyclic tautomers for the reaction with nucleophiles of the water soluble peptide coupling reagent 1-ethyl-3-(3-(dimethylamino)propyl)carbodiimide (EDC).* Journal of the American Chemical Society, 1981. **103**: p. 7090-7095.

460. Gilles, M.A., Hudson, A.Q., and Borders, C.L., *Stability of water soluble carbodiimides in queous solution.* Analytical Biochemistry, 1990. **184**: p. 244-248.

461. *Carbodiimides Pamphlet*, 2011. Uptima: France.

462. Nakajima, N. and Ikada, Y., *Mechanism of amide formation by carbodiimides for bioconjugation in aqueous media. .* Bioconjugate Chemistry, 1995. **6**: p. 123-130.

463. Hale, C., Bowe, F., Pickard, D., Clare, S., Haeuw, J.F., Powers, U., Menager, N., Mastroeni, P., and Dougan, G., *Evaluation of a novel Vi conjugate vaccine in a murine model of salmonellosis.* Vaccine, 2006. **24** (20): p. 4312-4320.

464. Cabrera Blanco, O., Cuello Perez, M., Sierra Gonzalez, V.G., Soto Rodriguez, C.R., and Martinez Pozo, M.E. for *Method of obtaining conjugate vaccines and vaccine compositions containing same*. 2005. Office, E.P. 03773443.1. EP1582217 A1.

465. *Instructions - Gel filtration media*, 2006. GE Healthcare Instruction code: 56-1190-98 AE.

466. Carraway, K.L. and Triplett, R.B., *Reaction of carbodiimides with protein sulfhydryl groups.* Biochimica et Biophysica Acta, 1970. **200**: p. 564-566.

467. Carraway, K.L. and Koshland Jr, D.E., *Reaction of tyrosine residues in proteins with carbodiimide reagents.* Biochimica et Biophysica Acta, 1968. **160**: p. 272-274.

468. Chan, L.C. and Cox, B.G., *Kinetics of amide formation through carbodiiimide/N-hydroxybenzotriazole (HOBt) couplings.* Journal of Organic Chemistry, 2007. **72**: p. 8863-8869.

469. Li, P. and Xu, J.-C., *HOBt and HOAt-derived immonium salts: new and highly efficient coupling reagents for peptide synthesis.* Tetrahedron Letters, 2000. **41**: p. 721-724.

470. Singh, J., Fox, R., Wong, W., Kissick, T.P., and Moniot, J.L., *The structures of alkoxycarbonyl, acyl and sulfonate derivatives of 1-hydroxybenzotriazole: N- vs O-substitution.* Journal of Organic Chemistry, 1988. **53** (1): p. 205-209.

471. Bulpitt, P. and Aeschlimann, D., *New strategy for chemical modification of hyaluronic acid preparation of functionalised derivatives and their use in the formation of novel biocompatible hydrogels* Journal of Biomedical Materials Research, 1999. **47**: p. 152-169.

472. Brink, B.D., DeFrancisco, J.R., Hillner, J.A., and Linton, B.R., *Curtin-Hammett and steric effects in HOBt acylation regiochemistry.* Journal of Organic Chemistry, 2011. **76** (13): p. 5258-5263.

473. Anders, E., Katritzky, A.R., Malhotra, N., and Stevens, J., *A MO theoretical study on the rearrangement of 1-hydroxy- and 1-(acyloxy)-1,2,3,-triazoles and their benzotriazole analogues: Comparison of ab initio and semiempirical calculations.* Journal of Organic Chemistry, 1992. **57**: p. 3698-3705.

474. Boyle, F.T. and Jones, R.A.Y., *Azole N-oxides. Part I. The tautomerism of benzotriazole 1-oxide and its 4- and 6-nitro-derivatives with the corresponding 1-hydroxybenzotriazole.* Journal of the Chemical Society, Perkin Transactions 2, 1973. **0** (2): p. 160-164.

475. Clayden, J., Greeves, N., Warren, S., and Wothers, P., *Organic Chemistry* 2001. New York: Oxford University Press.

476. McCarthy, D.G., Hegarty, A.F., and Hathaway, B.J., *N-hydroxy-compounds as acyl transfer agents. Part 1. Kinetics and mechanism of nucleophilic displacements on 1-hydroxybenzotriazole esters and crystal and molecular structure of 1-benzoyloxybenzotriazole.* Journal of the Chemical Society, Perkin Transactions 2, 1977. (2): p. 224-231.

477. Kaminski, Z.J., Paneth, P., and Rudinkski, J., *A Study on the activation of carboxylic acids by means of 2-chloro-4,6-dimethoxy-1,3,5-triazine and 2-chloro-4,6-diphenoxy-1,3,5-triazine.* Journal of Organic Chemistry, 1998. **63**: p. 4245-4255.

478. Bergman, K., Elvingson, C., Hilborn, J., Svensk, G., and Bowden, T., *Hyaluronic Acid Derivatives Prepared in Aqueous Media by Triazine-Activated Amidation.* Biomacromolecules, 2007. **8** (7): p. 2190-2195.

479. Garrett, C.E., Jiang, X., Prasad, K., and e pič, O., *New observations on peptide bond formation using CDMT.* Tetrahedron Letters, 2002. **43**: p. 4161-4165.

480. Schanté, C., Zuber, G., Herlin, C., and Vandamme, T.F., *Synthesis of N-alanyl-hyaluronamide with high degree of substitution for enhanced resistance to hyaluronidase-mediated digestion.* Carbohydrate Polymers, 2011. **86** (2): p. 747-752.

481. Schanté, C.E., Zuber, G., Herlin, C., and Vandamme, T.F., *Chemical modifications of hyaluronic acid for the synthesis of derivatives for a broad range of biomedical applications.* Carbohydrate Polymers, 2011. **85** (3): p. 469-489.

482. Kunishima, M., Kawachi, C., Iwasaki, F., Terao, K., and Tani, S., *Synthesis and characterization of 4-(4,6-dimethoxy-1,3,5-triazin-2-yl)-4-methylmorpholinium chloride.* Tetrahedron Letters, 1999. **40**: p. 5327-5330.

483. Shieh, W.-C., Chen, Z., Xue, S., McKenna, J., Wang, R.- ., Prasad, K., and ep ič, O., *Synthesis of sterically-hindered peptidomimetics using 4-(4,6-dimethoxy-1,3,5-triazine-2-yl)-4-methyl-morpholinium chloride.* Tetrahedron Letters, 2008. **49** (37): p. 5359-5362.

484. Kaminski, Z.J., *Triazine-based condensing reagents.* Biopolymers, 2000. **55**: p. 140-164.

485. Schlottmann, S.A., Jain, N., Chirmule, N., and Esser, M.T., *A novel chemistry for conjugating pneumococcal polysaccharides to Luminex microspheres.* Journal of Immunological Methods, 2006. **309** (1-2): p. 75-85.

486. Kunishima, M., Kawachi, C., Morita, J., Terao, K., Iwasaki, F., and Tani, S., *4-(4,6-dimethoxy-1,3,5-triazin-2-yl)-4-methylmorpholinium chloride: An efficient condensing agent leading to the formation of amides and esters.* Tetrahedron, 1999. **55**: p. 13159-13170.

487. Moingeon, P., De Taisne, C., and Almond, A., *Delivery technologies for human vaccines.* British Medical Bulletin, 2002. **62**: p. 29-44.

488. Dekker, C.L., Gordon, L., and Klein, J., *Dose optimization strategies for vaccines: the role of adjuvants and new technologies*, 2008. National Vaccine Advisory Committee.

489. *Oxford Dictionaries*. Oxford University Press. Available from: http://oxforddictionaries.com/definition/english/adjuvant?q=adjuvant. [Accessed on:24 September 2012].

490. Dey, A.K. and Srivastava, I.K., *Novel adjuvants and delivery systems for enhancing immune responses induced by immunogens.* Expert Review of Vaccines, 2011. **10** (2): p. 227-251.

491. *Committee for medicinal products for human use: Guideline on adjuvants in vaccines for human use.*, 2005. EMEA: London, United Kingdom.

492. Vogel, F.R., *Improving vaccine performance with adjuvants.* Clinical Infectious Diseases, 2000. **30** (Supplement 3): p. S266-S270.

493. Lindblad, E.B., *Aluminium compounds for use in vaccines.* Immunology and Cell Biology, 2004. **82**: p. 497-505.

494. Romero Mendez, I.Z., Shi, Y., HogenEsch, H., and Hem, S.L., *Potentiation of the immune response to non-adsorbed antigens by aluminum-containing adjuvants.* Vaccine, 2007. **25** (5): p. 825-833.

495. Jiang, D., Morefield, G.L., HogenEsch, H., and Hem, S.L., *Relationship of adsorption mechanism of antigens by aluminum-containing adjuvants to in vitro elution in interstitial fluid.* Vaccine, 2006. **24** (10): p. 1665-1669.

496. Heimlich, J.M., Regnier, F.E., White, J.L., and Hem, S.L., *The in vitro displacement of adsorbed modedl antigens from aluminium-containing adjuvants by interstitial proteins.* Vaccine, 1999. **17**: p. 2873-2881.

497. *Immunological adjuvants.*, 1976. World Health Organization: Geneva World Health Organization Technical Report Series No. 595.

498. Jendrek, S., Little, S.F., Hem, S., Mitra, G., and Giardina, S., *Evaluation of the compatibility of a second generation recombinant anthrax vaccine with aluminum-containing adjuvants.* Vaccine, 2003. **21** (21-22): p. 3011-3018.

499. Petrovsky, N. and Cooper, P.D., *Carbohydrate-based immune adjuvants.* Expert Review of Vaccines, 2011. **10** (4): p. 523-537.

500. Singh, M. *Vaccine adjuvants and delivery systems*. 2007. Wiley Interscience: New Jersey.

501. Seeber, S.J., White, J.L., and Hem, S.L., *Predicting the adsorption of proteins by aluminium-containing adjuvants.* Vaccine, 1991. **9**: p. 201-203.

502. Derek, O.Ä. and Mahesh, C., *Excipients Used in Vaccines*, in *Excipient Development for Pharmaceutical, Biotechnology, and Drug Delivery Systems* 2006. Informa Healthcare. p. 333-340.

503. Al-Shakhshir, R.H., Lee, A.L., White, J.L., and Hem, S.L., *Interactions in model vaccines composed of mixtures of aluminum-containing adjuvants.* Journal of Colloid and Interface Science, 1995. **169** (1): p. 197-203.

504. Kumar, S., Kumar, A., Gupta, P., Maheshwari, S.C., and Sokhey, J., *Standardization for optimum adsorption of tetanus toxoid on adjuvant and its relationship with potency.* Indian Journal of Microbiology, 2001. **41** (4): p. 293-296.

505. Henckaerts, I., Durant, N., De Grave, D., Schuerman, L., and Poolman, J., *Validation of a routine opsonophagocytosis assay to predict invasive pneumococcal disease efficacy of conjugate vaccine in children.* Vaccine, 2007. **25** (13): p. 2518-2527.

506. Concepcion, N.F. and Frasch, C.E., *Pneumococcal type 22F polysaccharide absorption improves the specificity of a pneumococcal-polysaccharide enzyme-linked immunosorbent assay.* Clinical and Diagnostic Laboratory Immunology, 2001. **8** (2): p. 266-272.

507. Adrian, P., *Immune response of different polysaccharide-protein conjugates against Streptococcus pneumoniae type 1*, 2012. Research Report for The Biovac Institute.

508. Fleck, R.A., Romero-Steiner, S., and Nahm, M.H., *Use of HL-60 cell line to measure opsonic capacity of pneumococcal antibodies.* Clinical and Diagnostic Laboratory Immunology, 2005. **12** (1): p. 19-27.

509. Romero-Steiner, S., Frasch, C.E., Carlone, G., Fleck, R.A., Goldblatt, D., and Nahm, M.H., *Use of opsonophagocytosis for serological evaluation of pneumococcal vaccines.* Clinical and Vaccine Immunology, 2006. **13** (2): p. 165-169.

510. Romero-Steiner, S., Libutti, D., Pais, L.B., Dykes, J., Anderson, P., Whitin, J.C., Keyserling, H.L., and Carlone, G., *Standardization of an opsonophagocytic assay for the measurement of functional antibody activity against Streptococcus pneumoniae using differentiated HL-60 cells.* Clinical and Diagnostic Laboratory Immunology, 1997. **4** (4): p. 415-422.

511. Rehm, S., Sommer, R., and Deerberg, F., *Spontaneous nonneopastic gastric lesions in female Han:NMRI mice and influence of food restriction throughout life.* Veterinary Pathology Online, 1987. **21**: p. 216-224.

512. Deerberg, F. and Gleichmann, H., *The occurrence of spontaneous immune-complex glomerulonephritis in Han: NMRI mice.* Contributions to Nephrology, 1980. **19**: p. 88-94.

513. Löhrke, H., Hesse, B., and Goerttler, K., *Spontaneous tumors and lifespan of female NMRI mice of the outbred stock sut: NMRT during a lifetime study.* Journal of Cancer Research and Clinical Oncology, 1984. **108** (2): p. 192-196.

514. Gruber, W., Kirschner, K., Tollefson, S., Thompson, J., Reed, G., Edwards, K.M., and Wright, P.F., *Comparison of monovalent and trivalent live attenuated influenza vaccines in young children.* The Journal of Infectious Diseases, 1993. **168** (1): p. 53-60.

515. Garland, S.M., Steben, M., Hernandez-Avila, M., Koutsky, L.A., Wheeler, C.M., Perez, G., Harper, D.M., Leodolter, S., Tang, G.W., Ferris, D.G., Esser, M.T., Vuocolo, S.C., Nelson, M., Railkar, R., Sattler, C., and Barr, E., *Noninferiority of antibody response to human papillomavirus type 16 in subjects vaccinated with monovalent and quadrivalent L1 virus-like particle vaccines.* Clin Vaccine Immunol, 2007. **14** (6): p. 792-795.

516. de Kleijn, E.D., De Groot, R., Lafeber, A.B., Labadie, J., van Limpt, K.C.J.P., Visser, J., Berbers, G.A.M., van Alphen, L., and Rumke, H.C., *Immunogenicity and safety of monovalent P1.7th,4 meningococcal outer membrane vesicle vaccine in toddlers: comparison of two vaccination schedules and two vaccine formulations.* Vaccine, 2001. **19**: p. 1141-1148.

517. Fattom, A., Cho, Y.H., Chu, C., Fuller, S., Fries, L., and Naso, R., *Epitopic overload at the site of injection may result in suppression of the immune response to combined capsular polysaccharide conjugate vaccines.* Vaccine, 1999. **17**: p. 126-133.